A molecular approach to the assessment of peat organic matter – investigating ecosystem-driven differences in chemical composition

Inauguraldissertation

zur

Erlangung der Würde eines Doktors der Philosophie

vorgelegt der

Philosophisch-Naturwissenschaftlichen Fakultät

der Universität Basel

von

Jennifer Kristin Klein

Basel, 2022

Genehmigt von der Philosophisch-Naturwissenschaftlichen Fakultät

auf Antrag von

PD Dr. Jens Leifeld (Erstbetreuer)

Prof. Dr. Christine Alewell (Zweitbetreuerin)

Prof. Dr. Tim Moore (Externer Experte)

Basel, den 19 Oktober, 2021

Prof. Dr. Marcel Mayor
(Dekan)

Table of Contents

Summary

Peatlands contain massive stores of organic carbon (OC), which are vulnerable to loss following drainage and aerobic decomposition. To protect these sensitive C stores in a warming world, research has been increasingly invested in strategies for peatland restoration. While restoration projects can have many aims (re-establishment of biodiversity, biogeochemical function, etc.), baseline measurements and monitoring targets are greatly needed – particularly for rewetting projects seeking to restore peatland C sequestration services (i.e., an excess of net primary productivity relative to decomposition in the ecosystem).

The main objectives of this thesis were to investigate changes in peatland decomposition status through the use of different biogeochemical analysis tools. This objective was achieved through the identification of differences in peat organic matter (OM) chemical composition with changing hydrological status and depth – primarily using pyrolysis gas chromatography mass spectrometry (Py-GC/MS) chemical characterization techniques. This research thus describes the use of high-resolution Py-GC/MS "fingerprinting," as an indicator for degradative conditions.

Before the experimental objectives were approached, the versatility and utility of the method were investigated. As no comprehensive compilation of Py-GC/MS studies on peat had previously been done, an extensive review was conducted of previous work using the method for peat OM chemical characterization. The review investigated peatland plant and microbial biomarkers analyzable by Py-GC/MS, as well as the chemical environment where typical OM components and proxies might occur within the ecosystem – with a focus on natural vs drained peat. It was noted that while plant biomarkers were well represented in the literature, microbial biomarkers were more limited.

Further, to confirm whether Py-GC/MS OM characterizations are a useful proxy for overall peat composition, peat samples were first investigated exclusively by pyrolysis to determine to what degree the volatilized OM entering the analysis instrument (GC/MS) was representative of the original sample. This study found that percent OM volatilized (pyrolysis efficiency) by Py-GC/MS was highly reproducible, and relatively insensitive to changing parameters such as instruments, settings, sample mass or composition (from an organic carbon standpoint). Moreover, a reference baseline for successful pyrolysis efficiency (in terms of percent OM volatilized successfully onto the analytical instrument) was established for researchers using the method for peat.

For the primary experimental objective, two peatland research sites were selected, each with contrasting hydrological management occurring in the same ecosystem (Lakkasuo drained and undrained; Degerö Stormyr undrained and rewetted). OM composition was investigated using Py-GC/MS pyrolysis

products in both a broader exploration of its composition (through the relative abundance of OM chemical classes such as phenols, polysaccharides, lipids, N compounds, etc), and by a more targeted biomarker approach (e.g., lignin pyrolysis products and the *Sphagnum* biomarker *p*-isopropenylphenol). Principal component analysis separated the complex dataset into different environmental influences on peat OM chemistry.

In Lakkasuo, peat drainage for forestry in 1961 resulted in significant differences in peat OM chemical composition in the drainage-affected cores. Decreased relative abundance in phenols and polysaccharides were reflective of the aerobic decomposition of OM originating from previously deposited *Sphagnum*, and increased abundance of guaiacyl-derived lignin, N compounds, C-29 triterpenoid sterols, and sesquiterpenes were reflective of the *Pinus silvestris* onsite. In the Degerö rewetted site, the high phenol abundance in the surface peat corresponded well with the established *Sphagnum riparium* onsite, indicating that phenols are an early sensitive indicator for rewetted conditions in *Sphagnum* peatlands. However, altered chemical composition remained visible in the rewetted site both in surface samples (continued increased abundance in lignin, N compounds, benzenes, lipids, and polyaromatic hydrocarbons (PAHs) – despite the shift in vegetation composition), and in the formerly drained parts of the profile. Peat OM recovery after rewetting may therefore continue to be subject to residual impacts originating from the (permanently) degraded OM below – underscoring the importance of protecting this vulnerable OM from further decomposition.

Overall, this work demonstrates not only that peat OM chemical composition is an effective tool to assess degradative status (and is thus a good proxy for its estimation), but also that hydrology serves as a strong driver for changes in peat chemical composition. The sensitivity of the Py-GC/MS method permits meaningful changes to be detected in OM compounds that are both reflective of changes in environmental influences and also present in very low abundance - allowing for improved source identification and discernment of dominant degradation mechanisms. It is expected that these findings will be particularly useful to those seeking to identify indicators in ecosystems most likely to benefit from rewetting mitigation practices.

Part A: Chapter 1 - Synopsis

Introduction

Climate change, peatlands, and carbon storage

Anthropogenic release of greenhouse gases has resulted in average global temperatures exceeding 1.1 °C above pre-industrial global average levels, and the effects of this warming have already tangibly altered ecological processes (IPCC, 2021). Warming-induced sea level rise (Storlazzi, Elias, & Berkowitz, 2015), extreme weather events (Ummenhofer & Meehl, 2017), biodiversity loss (Bond & Grasby, 2017), and infectious disease transmission (Altizer, Ostfeld, Johnson, Kutz, & Harvell, 2013) are predicted to increase in global influence - with harmful consequences to human populations. For example, without mitigation to limit the current warming trends to less than 1.5°C, there is evidence that equatorial regions may become uninhabitable in the approaching decades (Sherwood & Huber, 2010; Y. Zhang, Held, & Fueglistaler, 2021).

As the most widespread wetland type in the world, peatlands cover ca. 3% of global terrestrial area, and play a vital role in the global carbon (C) cycle currently driving warming global temperatures (Xu, Morris, Liu, & Holden, 2018). Due to their slow organic matter (OM) mineralization rates relative to net primary productivity (NPP), peatlands store roughly 600 gigatonnes (Gt) of C (Yu et al., 2011; Yu, Loisel, Brosseau, Beilman, & Hunt, 2010). In addition to this large C storage capacity, intact peatlands provide ecosystem benefits that range from recreation opportunities, preservation of unique biodiversity and fragile palaeo-environmental archives, and water purification and flooding control (Bonn et al., 2014; Kimmel & Mander, 2010).

The massive C stores contained within peatlands are vulnerable due to their sensitivity to changes in temperature, moisture, nutrient input and litter quality - particularly at higher latitudes (>45°) (Loisel et al., 2014; McGuire et al., 2009). As peatlands degrade, OM stored within them is exposed to increasingly oxic conditions. This, in turn, leads to increased aerobic decomposition, and shifts C storage functions of impacted peatland ecosystems from C sink to source. Anthropogenic drainage of peatland ecosystems has been fairly commonplace since at least the Middle Ages (Van Dam, 2001). Currently, degradation for agriculture and forestry have led to the loss of as much as 50% of natural peatlands in Europe (Joosten, 2009). At present, peatland degradation has resulted in the current estimated global release of almost two Gt CO_2-eq. annually (Leifeld & Menichetti, 2018). As the peatland C balance is projected to shift globally from C sink to source within the next hundred years (Loisel et al., 2021), understanding the contribution of peatlands to global C storage has never been more vital.

Peatland restoration

To ensure that these vital ecosystem services continue to function in the future, international efforts are underway to develop comprehensive strategies for the promotion of peatland restoration and preservation. Examples of targets include biodiversity and habitat (e.g., reintroduction of native species or removal of invasive species or correction of habitat fragmentation), biogeochemical parameters (e.g., restoration of previous pH, addressing eutrophication issues), and hydrological function restoration (canal or ditch blocking/infilling, or re-establishment of open water features (Andersen et al., 2017; Dohong, Aziz, & Dargusch, 2018; Lamers et al., 2015; Rochefort, Quinty, Campeau, Johnson, & Malterer, 2003; Verhoeven, 2014). The success or failure of these measures largely depend on the type of peatland ecosystem – for instance, tropical ecosystems require specific restoration methods tailored to the needs of these regions (Dohong et al., 2018). Moreover, depending on the intended restoration goal, the effects of different restoration measures are not necessarily additive; for instance, maximizing peatland C sequestration may also result in lower overall botanical biodiversity in the ecosystem (Lamers et al., 2015).

While research has been increasingly invested in peatland restoration, in many cases, projects lack clear restoration goals, baseline measurements, and monitoring targets (Andersen et al., 2017). In example, to restore peatland C sequestration ecological services, systems should return to an excess of NPP relative to decomposition (Andersen, Grasset, Thormann, Rochefort, & Francez, 2010) – a goal generally targeted through rewetting. However, the results of restoration projects with this aim have been somewhat inconsistent (Moreno-Mateos, Power, Comín, & Yockteng, 2012). Studies focusing on peatland rewetting activities (and effects of water table manipulation on OM) generally reflect ecosystem changes from the last 100-200 years, making short vs long-term shifts in ecosystem C budgets difficult to interpret, as peat accumulation generally occurs over millennia (Laiho, 2006). Further, while degraded (oxidized, heavily decomposed) and un-degraded (intact vegetation, undecomposed) parts of a restored peatland can sometimes be distinguished macroscopically, it is not always possible to clearly distinguish changing ecosystem conditions on a purely visual basis, as plant macrofossils are often insufficiently preserved in the profile. The degree to which OM stability (and thus C stability) is regained in rewetted peatlands is an area urgently requiring further study: degraded peat under oxic conditions has been found to contain less stable OM than natural undrained peat (Heller & Zeitz, 2012).

The importance of OM chemistry in peatlands

In order to argue the effectiveness of peatland restoration programs (particularly with regards to stakeholders) (Glenk & Martin-Ortega, 2018), a diverse analytical toolkit is needed to assess peatland degradation status and the subsequent impacts on C sequestration. While from a C sequestration

perspective, the most important metric is net peat growth (Lucchese et al., 2010), this proxy cannot be considered in isolation, as similar quantities of OM can store differing quantities of OC – depending on its composition. Moreover, while many of the current tools available to assess net peat growth (micrometeorological tools, *etc*.) are highly effective, they often require expensive long-term infrastructure and permanent onsite staff in remote locations. Molecular characterizations are complementary to the measurements derived from such tools (e.g., flux measurements for CO_2, CH_4, N_2O), as the information obtained from these characterizations can better constrain the relationship between OM most vulnerable to decomposition and subsequent greenhouse gas emissions. In particular, the ability to compare the degradation status of a peatland through time, such as through profile cores, is especially useful in helping to determine whether a peatland is growing (accumulating C), stable, or degrading (losing C). As most peat greenhouse gas emissions originate from aerobic microbial mineralization of stored OM, and the rates of mineralization are constrained not only by hydrologic factors, but also the composition of the OM itself, it is essential to understand the chemical factors and degradative interactions influencing the chemical composition of peat.

As a characteristic example, it has been previously suggested that one enzyme, phenol oxidase, was able to degrade otherwise highly recalcitrant plant-derived phenolic compounds common in peat ecosystems (Freeman, Ostle, & Kang, 2001). However, the mechanisms of action for phenol oxidase require molecular oxygen (O_2), despite the enzyme's persistence in anaerobic conditions. It was proposed that the depressed O_2 content in intact peatlands results in depressed enzymatic activity of phenol oxidase, allowing for subsequent accumulation of phenolic compounds and further depressed activity of other anaerobic biodegradative enzymes (Freeman, Ostle, Fenner, & Kang, 2004; Freeman et al., 2001). A logical consequence of this process is that where aerobic conditions have taken hold, the reverse process may occur; allowing for decomposition to become more active both in the oxic layers, but also potentially in the anoxic layers. Furthermore, the possibility thereby arises to screen for a shift from predominant anaerobic to aerobic decomposition processes (or *vice versa*) through changing relative abundance of phenolic compounds.

Overview of general organic chemistry in northern peatlands

To understand the origin of chemical changes occurring in peat, a general overview of a typical peatland ecosystem, including contributing species (and their dominant chemical contributions to deposited OM) is useful (**Figure 1**). Peat formation occurs where water-saturated conditions lead to anoxic conditions in deposited OM (whether vegetation, animal, or microbial-derived), permitting the rate of OM accumulation to exceed the rate of loss from decomposition processes (Clymo, 1987). Localized hydrology influences the predominant botanical community, whose depositional accumulation contributes to an overall molecular "signature" (e.g., *Sphagnum* moss, or deeper rooting vascular plants),

that can be used to reconstruct previous environmental conditions (McClymont et al., 2011; Schellekens, Bradley, et al., 2015; Schellekens, Buurman, Fraga, & Martínez-Cortizas, 2011). Interactions between deposited vegetative OM and the water table also influence decomposition dynamics, which change with depth in accordance with the dominant microbial community (aerobic vs anaerobic), and serve as a driver for changes in OM chemistry in the peatland profile. These interactions are further controlled by temperature, whether the overall system is rainwater or groundwater fed (ombrotrophic vs minerotrophic), and other biogeochemical influences (pH, nutrient deposition).

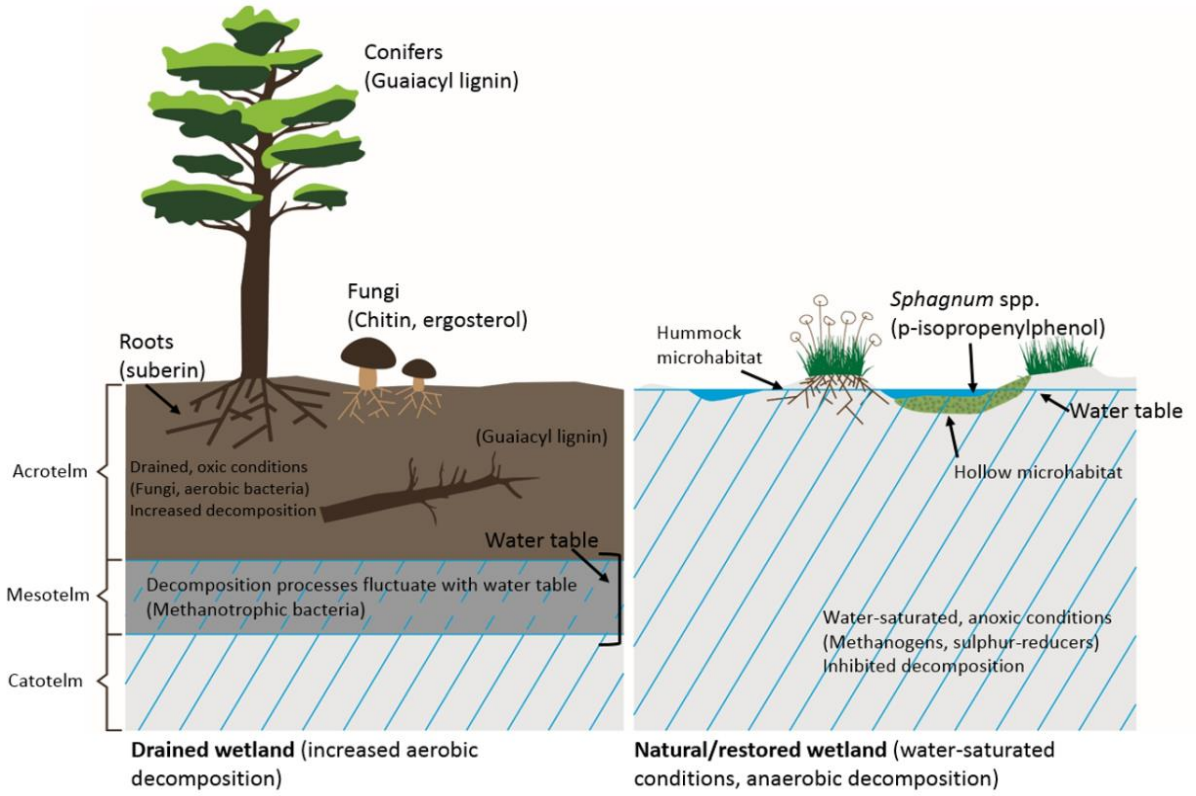

Figure 1. Schematic of typical observable community structure and example associated proxy biomarkers amenable to Py-GC/MS in boreal peatlands, with drained (left) and natural (right) ecosystems depicted. From (Klein, Gross-Schmölders, Alewell, & Leifeld, 2021).

Decomposition in peatlands is generally considered to be a non-linear process (Clymo, 1984), where the degree of decomposition activity is largely dependent on the location within the profile. The highest rates of decomposition occur in the acrotelm – the aerated upper horizons of the profile where recently deposited litter is rapidly degraded by the aerobic microbial community (Clymo, 1984). With depth and increased water saturation, decomposition processes slow as conditions shift from the aerobic horizons to the anaerobic catotelm (Belyea & Clymo, 2001). Between these two horizons lies the mesotelm, where the greatest water table fluctuation generally occurs, and obligate and facultative microbial communities generally display higher biodiversity (Groß-Schmölders et al., 2020).

Peatland chemistry is also highly localized - both spatially (laterally, e.g., through hummock and hollow complexes) and temporally (with depth and progressive decomposition). As the primary focus of the OM chemical characterization conducted for this research was on boreal ecosystems dominated by *Sphagnum*, their general ecological characteristics are highlighted here, with a focus on differentiation between natural and degraded (and rewetted) ecosystems. In the case of peatlands in other ecological regions (e.g., tropical ecosystems), peatland chemistry may vary according to the dominant plant species (Ronkainen, McClymont, Väliranta, & Tuittila, 2013).

"Natural" peatlands (undrained)

As "pristine" undrained peatlands generally feature water-saturated conditions, vegetation must be adapted to this environment. Depending on the primary hydrological source (rainwater, groundwater), plant species may also need to be adapted to nutrient-poor or nutrient-limited conditions. Aerobic decomposition occurs in the uppermost horizons of undrained peat; thereafter, decomposition processes are primarily anaerobic and occur at a substantially reduced rate (Clymo, 1984, 1987). In higher latitudes (>45°N), dominant cover with *Sphagnum* moss is common (Gunnarsson, 2005). *Sphagnum* is particularly important in the development and structure of the overall ecosystem, because its morphology and biochemical properties actively contribute to peat formation (Joosten & Clarke, 2002; Rochefort, 2000). As a result, *Sphagnum* serve as "ecosystem engineers" in peat; driving both the formation and chemical composition of accumulating OM in boreal ecosystems (Palozzi & Lindo, 2017).

This influence can be observed in the chemical composition of *Sphagnum*-dominated OM. *Sphagnum* moss generally demonstrate high phenol content (Zeh et al., 2020), which then accumulates in peatland OM with water-logged anaerobic conditions (Freeman et al., 2001). The *Sphagnum* biomarker *p*-isopropenylphenol is highly organism-specific and undergoes rapid degradation in aerobic peatland conditions, making it a generally reliable indicator for hydrological changes (McClymont et al., 2011; Schellekens, Bindler, et al., 2015). Further, *Sphagnum* produce an abundance of structural hemicellulose polysaccharides known as Sphagnan (Hájek, Ballance, Limpens, Zijlstra, & Verhoeven, 2011). Polysaccharides are comparatively labile and undergo rapid microbial degradation; thus, in intact bogs, abundant and diverse polysaccharides generally derive from "fresh" plant material (Schellekens & Buurman, 2011). While polysaccharides are preferentially degraded over phenols in aerobic conditions in *Sphagnum* bogs, anaerobic conditions inhibit further microbial degradation of either compound class, allowing both phenols and polysaccharides to achieve somewhat stable abundances in the deeper water-saturated catotelm depths.

Degraded peatlands (drained)

In contrast to undrained systems, the aerobic horizon of drained peatlands extends much deeper into the profile. This permits increased growth of vascular plants, which typically require drained conditions for effective growth. On the one hand, drainage can allow the establishment of deep-rooting, long-lived vegetation (shrubs, trees), which can also result in increased OM C/N ratios (Beaulne, Garneau, Magnan, & Boucher, 2021; Minkkinen & Laine, 1998; Minkkinen, Vasander, Jauhiainen, Karsisto, & Laine, 1999). However, the longevity and overall OC stability (and subsequent C emissions) of this increased C stock is still poorly understood (Schimmel, Braun, Subke, Amelung, & Bol, 2021), due to the faster decomposition of lignin in aerobic environments (Dungait, Hopkins, Gregory, & Whitmore, 2012).

Due to the difference in habitat suitability between *Sphagnum* bryophytes and vascular plants in peat, an increase in establishment and dominance of vascular plants in the peatland ecosystem can be used as an indicator for drained conditions. It is important to note that in addition to species that occupy upper margin habitats of hummock/hollow ecosystems, some vascular species are also adapted to intact peatlands, and grow alongside *Sphagnum* moss in water-saturated conditions, (*Vaccinium* spp., *Ericaceae* spp., *Scheuchzeria palustris*). However, the phreatophytic root systems of most non-wetland-adapted vascular plants generally necessitate drained conditions; therefore, they are useful as biomarkers for this purpose. Lignin-derived phenols derive a near exclusive origin from terrestrial vascular plants (Martin, Saiz-Jimenez, & Gonzalez-Vila, 1979), and arise from the polymerization of three primary phenylpropane alcohol precursors: *trans*-coniferyl (guaiacyl-derived lignin), *trans*-sinapyl (syringyl-derived lignin), and *trans-p*-coumaryl (4-vinylphenol). The proportion of these precursors varies by taxa (e.g., gymnosperms typically display a lower syringyl/guaiacyl ratio than angiosperms), which can be further used to identify the primary contributing vascular plant source (Hedges & Mann, 1979). Lignin is more slowly degraded than polysaccharides or *Sphagnum*-derived phenols; allowing for its relative accumulation with depth in intact peat (Schellekens, Buurman, et al., 2015). However, it is vulnerable to decomposition in aerobic environments (Feng, Simpson, Wilson, Williams, & Simpson, 2008; Z. Zhang et al., 2019).

Other chemical changes indicative of increased aerobic decomposition processes are also visible in drained peat ecosystems. While not source specific, low molecular weight benzene compounds such as toluene and styrene are associated with degraded OM in Py-GC/MS studies (Carr, Boom, Chase, Roberts, & Roberts, 2010; Schellekens, Buurman, & Pontevedra-Pombal, 2009), and are in generally higher abundance in drained or degraded peat. Moreover, a higher abundance of N-containing compounds can also be associated with increased decomposition in peatlands. With the exception of indole, which has been associated with un-decomposed plant material (Buurman, Nierop, Pontevedra-Pombal, & Martínez Cortizas, 2006; Vancampenhout et al., 2012), N pyrolysates can be sourced

primarily to amide N, likely from proteinaceous material (Knicker, 2004). Plant-derived proteins are rapidly degraded upon introduction to OM, thus the majority of this proteinaceous material can be assumed to be of microbial origin, and thus in greater abundance in ecosystems undergoing higher rates of microbial mineralization. (Kögel-Knabner & Amelung, 2014). Further, lipids (fats and waxes including but not limited to *n*-alkanes, *n*-alkenes, methylketones, terpenoids) are typically more abundant in vascular plants (Naafs et al., 2019).

Molecular tools for the characterization of peat OM

While broader chemical classes display general differences in abundance in natural vs drained/degraded peat, individual compounds may have specific sources and divergent behavior from other compounds in the same class (catechol phenols, for instance). Molecular biomarkers are effective proxies precisely for this reason; as they are source-specific and informative about the environmental conditions present during deposition (McClymont et al., 2011; Pancost, Baas, van Geel, & Damsté, 2002; Schellekens, Bradley, et al., 2015). As multiple processes occur simultaneously on the same OM (increased dominance of vascular plants in the ecosystem results in increased deposition of lignin-derived OM and decreased deposition of *Sphagnum* phenols and polysaccharides, all of which is then subjected to aerobic decomposition processes), sensitive analytical tools with the capacity to disentangle concurrent effects on OM chemistry are especially useful.

Multiple biogeochemical tools currently exist for assessing peatland chemistry. Due to challenges associated with obtaining an informative overview of peat OM molecular composition and risks of data over-interpretation, it is also increasingly common to employ a multi-proxy approach (Biester, Knorr, Schellekens, Basler, & Hermanns, 2014; Krüger, Alewell, Minkkinen, Szidat, & Leifeld, 2016). In example, bulk elemental analysis provides a rapid estimate of organic stoichiometric composition in OM (C, H, N, O), and can be used to determine C/N atomic ratios and molar ratios (O:C, H:C, N:C) as a general measure of degradation (Leifeld, Klein, & Wüst-Galley, 2020; Moore, Large, Talbot, Wang, & Riley, 2018). Further, preferential microbial respiration of lighter ^{12}C and ^{14}N in peat leads to enrichment of ^{13}C and ^{15}N stable isotopes in the remaining OM, making increased enrichment of heavier isotopes ($\delta^{13}C$, $\delta^{15}N$) a useful indicator for degradation (Alewell, Giesler, Klaminder, Leifeld, & Rollog, 2011; Krüger, Leifeld, Glatzel, Szidat, & Alewell, 2015). As older C stored in deeper parts of the profile is also depleted in ^{14}C (as this radioisotope is taken up only by living organisms), radiocarbon ($F^{14}C$) abundance can be used to obtain calibrated peat age assessments (Trumbore, 2000; Wang et al., 2021). In studies where obtaining peat age estimates is not the primary goal, these measurements are also useful in raw form to validate depth-based comparisons of different OM profiles potentially impacted by subsidence (Klein et al., *in review,* 2021).

Pyrolysis gas chromatography-mass spectrometry (Py-GC/MS) has already been extensively utilized for description of peat chemical composition and decomposition processes (Biester et al., 2014; Buurman et al., 2006; González et al., 2003; Huang et al., 1998; Kaal et al., 2007; Kuder, Kruge, Shearer, & Miller, 1998; Kuder & Kruge, 1998; McClymont et al., 2011; Schellekens, Barberá, & Buurman, 2013; Schellekens, Bindler, et al., 2015; Schellekens, Bradley, et al., 2015; Schellekens & Buurman, 2011; Schellekens et al., 2011; Schellekens, Buurman, & Kuyper, 2012; Schellekens, Buurman, et al., 2015; Schellekens et al., 2009; Schellekens, Horák-Terra, Buurman, Silva, & Vidal-Torrado, 2014; Van Smeerdijk & Boon, 1987; Zeh et al., 2020; Z. Zhang et al., 2019). Py-GC/MS enhances sensitive analysis capabilities offered by GC/MS techniques through prior thermal degradation of high molecular weight organic compounds into characteristic smaller fragments (pyrolysis products) prior to introduction to the analysis instrument - thus permitting volatilization of insoluble biomacromolecules (>600 Daltons) that would otherwise be too large for effective GC/MS characterization (White, Garland, Beyer, & Yoshikawa, 2004). Pyrolysis parameters (i.e., temperature, heating rate) can be tightly controlled, allowing for reproducible analyses. Further, chemical pretreatments are generally not necessary for peat samples, though they are sometimes employed when improved extractions of specific target compounds are desired (Blokker, Yeloff, Boelen, Broekman, & Rozema, 2005; Hoyos-Santillan et al., 2016). This technique can obtain a broader snapshot of compound classes typically found in peat (phenols, polysaccharides, lignin, N-containing compounds, lipids), while also offering high-resolution structural detail of individual pyrolysis products. Due to these advantages, Py-GC/MS-derived pyrolysis products, such as lignin-derived products or biomarker compounds such as *p*-isopropenylphenol (*Sphagnum*), have been proposed as screening tools for overall bulk peat composition (McClymont et al., 2011). Beyond peat, Py-GC/MS analytical applications are wide-ranging, from investigation of shipwreck wood preservation (Traoré, Kaal, & Cortizas, 2017), to the search for organic compounds on Mars (Williams et al., 2020).

Objectives

The main aims of this thesis are to evaluate changes in peatland degradation status (or peatland restoration) using different biogeochemical tools through identification of chemical differences in peat OM composition. This work is divided into the following main research themes as presented in **Chapters 2-5**: i. a review of peat plant and microbial biomarkers analyzable via Py-GC/MS (**Chapter 2**), ii. an investigation of the overall representativeness of pyrolyzed sample of the original OM (**Chapter 3**), iii. high-resolution comparisons of chemical differences in peatlands undergoing contrasting hydrological management; between natural and drained peat (**Chapter 4**), and natural and rewetted peat (**Chapter 5**).

Chapter 2 focuses on a broad-spectrum review of the current molecular proxies available for peat using Py-GC/MS techniques. At the time of this research, no reviews had yet been conducted on the topic, so a comprehensive compilation of Py-GC/MS-derived studies characterizing molecular composition of peat was needed. This chapter investigated the chemical environment present in peatland OM as a function of changes in the ecosystem (e.g., chemical differences with increased drainage and aerobic decomposition) (**Figure 1**), reviewed plant and microbial biomarkers analyzable via Py-GC/MS for peat ecosystems, associated challenges, and future applications of the technique.

As a systematic method approach, **Chapter 3** investigated to what degree pyrolyzed samples were representative of the original sample OM. One notable issue for all Py-GC/MS studies is that the pyrolysis process is not 100 percent efficient, as a carbonaceous residue of unknown composition is left behind as char (Uden, 1993). Moreover, a baseline for "successful" pyrolysis efficiency (in terms of reproducibility and representativeness of the original sample matrix) had not yet been established for peat. To investigate the representativeness of pyrolyzed peat OM of the original sample matrix, OM volatilization (%) (defined as "pyrolysis efficiency" or PyE) of ten diverse peat samples (**Table 1**) were compared across different pyrolysis temperatures, heating rates, sample masses, and original OC and N content (measured by bulk elemental analysis) using a 10-part mineral dilution study. Volatilization was monitored through the determination of sample mass loss primarily using a thermogravimetric (TG) pyrolysis instrument, where the heating rate was strictly controlled and changes in physical properties of the OM were traced as a function of temperature through percent mass loss over time. However, a "flash" instrument was also investigated, where samples were "dropped" into a pre-heated helium-flushed furnace.

The remaining chapters focus on a high-resolution Py-GC/MS analysis of pyrolysis products for selected boreal peatland ecosystems (**Figure 2**). **In Chapter 4**, peatland OM was compared in natural and drained parts of the same Finnish boreal mire (Lakkasuo) to investigate ecosystem-driven differences in chemical composition with drainage and depth. Natural and drained peatlands have been compared by Py-GC/MS methods previously (Kuder et al., 1998; Z. Zhang et al., 2019), as well as other chemical characterization techniques such as FTIR (Harris, Moore, Roulet, & Pinsonneault, 2020; Heller, Ellerbrock, Roßkopf, Klingenfuß, & Zeitz, 2015). However, Py-GC/MS chemical characterization had not yet been conducted from natural and drained sites from the same ecosystem, and thus similar temporal and spatial scales. This study provided a detailed "fingerprint" of peat OM chemical composition with depth at each site, both via sample resolution (3 core replicates per site, 4 cm resolution per core depth profile), and by analyses conducted (108 pyrolysis quantified per sample). Results from the Py-GC/MS study were also compared with molar ratios determined from bulk elemental analysis (N:C, O:C) and $F^{14}C$. Principal component analysis (PCA) was used to separate the environmental influences on peatland chemistry with drainage and depth, which resulted in the identification of four

primary environmental "processes" reflecting botanical contribution *(Sphagnum* vs vascular plants), aerobic and anaerobic decomposition processes, and origin of vascular contribution (Pine vs *Eriophorum*).

Chapter 5 applied the high-resolution methodological approach developed in **Chapter 4** to a minerotrophic boreal mire (Degerö, Sweden) –where one of the two sites had been recently rewetted. To determine initial changes in chemical composition that could serve as possible chemical indicators for rewetting, 105 pyrolysis products representing seven different chemical classes were investigated with depth in the natural and rewetted sites (3 core replicates per site, 2-4 cm resolution), and compared with bulk elemental composition (C/N ratios, H:C/O:C atomic van Krevelen ratios). PCA differentiated the influences on the chemical composition in the natural and rewetted sites both by site, and by the present vs the historical drainage period – the effects of which were visible in the entire profile.

Materials and Methods

Peat Py-GC/MS reference materials (Chapter 2, 4-5)

To compile the existing knowledge available for Py-GC/MS analysis of peat, **Chapter 2** employed an extensive literature review of previously published studies. For pyrolysis product identification and integration (**Chapter 4-5**), chromatography analysis was performed using Agilent ChemStation software. Pyrolysis product mass spectra were compared with data reported in the National Institute of Standards and Technology (NIST 2014) mass spectral library.

Peat vegetation reference materials

To evaluate the most current ecological conditions in the research site, a plant species assessment was conducted onsite for both Lakkasuo and Degerö Stormyr at the time of the June 2017 sampling event (Pascal von Sengbusch). This included an assessment of the current hydrological conditions, dominant botanical species, and the identification of species that served as indicators for the current ecosystem conditions (e.g., facultative vs obligate wetland vegetation, species reflecting ombrotrophic vs minerotrophic conditions). A macrofossil analysis was also conducted on two cores (ON1, OD2) from Lakkasuo (**Chapter 4**), and used to investigate the relationship between Py-GC/MS findings and present vs historical vegetation.

Field samples (Chapter 3-5)

The PyE study (**Chapter 3**) required a selection of different peatland OM samples to determine whether original OM chemistry influenced the pyrolysis process (**Table 1**). The ten peat samples chosen for PyE investigation were selected both because of their diverse origins, and the availability of data from the same samples in a prior analysis using other biogeochemical techniques for comparison (bulk chemical composition from EA and ^{13}C NMR) (Leifeld et al., 2018). Samples representative of various depths and degradation status were investigated, rather than analysis of whole cores.

For the Lakkasuo and Degerö Stormyr sites (**Chapter 4-5**), six peat cores (three replicates from each of the paired sites), were collected to 1 m depth using a Russian peat corer in a June 2017 sampling event. Peat cores were stored at 2°C prior to processing, cut into 2 cm sections, oven-dried at 40 °C for 72 hours, and homogenized using a mixer mill for three minutes at 25 Hz. Samples from each site were denoted by their site source (using nomenclature from previous and parallel studies for consistency) (Groß-Schmölders et al., 2020; J. P. Krüger, 2016). Lakkasuo sites were distinguished by (natural=ON, drained=OD), and Degerö sites distinguished by (natural=NM, drained/rewetted=DC). Site names were followed by core number (1-3), and profile section depth in cm.

Analytical instruments

For the PyE study (**Chapter 3**), an "offline" Netzsch Simultaneous Thermal Analyzer STA 449 equipped with TG-DSC sample carrier (Type S) was used, as well as a double shot pyrolyzer (Frontier laboratories 2020i) operating in single shot mode – both in an inert helium atmosphere. To compare original and post pyrolysis C and N content, an elemental analyzer (EuroEA 3000, Hekatech) was used in dry combustion mode.

A high-resolution Py-GC/MS method was applied as the primary methodological framework of the two ecosystem-driven peatland pairwise comparison studies (**Chapter 4-5**). Both studies utilized the same instrumental programming and setup: the double shot pyrolyzer (Frontier laboratories 2020i) was connected to an Agilent GC/MS system (GC 7890, MSD 5977B). Before Py-GC/MS analysis, samples were dried in 2 cm sections and homogenized in a mixer mill (Retsch MM 400) for 3 minutes (25 hz). Samples from both studies were also measured for C, H, N, and O content using an elemental analyzer (EuroEA 3000).

Three depths in each of the six Lakkasuo cores (8-10, 48-50, 80-82 cm) were measured for fraction ^{14}C ($F^{14}C$) abundances via accelerator mass spectrometry (Oeschger Centre for Climate Change Research, Department of Chemistry and Biochemistry, University of Bern).

Bulk stable $\delta^{13}C$, $\delta^{15}N$ isotope measurements

For validation of the findings obtained by Py-GC/MS, bulk stable isotope abundances ($\delta^{13}C$, $\delta^{15}N$) measured on the same peat cores in parallel research conducted at the University of Basel were correlated to PCA sample pyrolysis product scores in the Lakkasuo and Degerö studies (**Chapters 4-5**) (Groß-Schmölders et al., 2020).

Statistics

Statistical analysis for **Chapter 3** was conducted using Microsoft Excel statistics software. Data analysis for **Chapters 4-5** was conducted using Python (version 3.8.2), with collaborative plots made using Statistica software. Statistical significance for all studies was set at $\boldsymbol{p<0.05}$.

Generally, simpler statistical procedures such as independent t-tests, ANOVA, regression analysis, and coefficients of variation (Pearson) were effective at describing the data in **Chapter 3**. However, the multi-dimensional dataset generated by the large number of pyrolysis products analyzed for **Chapters 4-5** required multivariate statistical tools. To disentangle the shared variation of all pyrolysis products and determine the effect of ecosystem-driven processes on pyrolysis products, PCA was used (Schellekens, Buurman, et al., 2015). Pyrolysis product PCA loadings reflected all shared variation of the investigated pyrolysis products, and loadings on each PC were used to interpret the environmental "processes" (PCs) influencing peat OM chemistry. PCA scores were projected onto individual core depth profiles and reflected the relative influence of each PC in the samples.

Investigated methods not included in this thesis

Compound specific Py-GC/MS (Py-CSIA) is an emerging analytical tool permitting the measurement of isotopic ratios directly to individual pyrolysis products (González-Pérez, Jiménez-Morillo, de la Rosa, Almendros, & González-Vila, 2016; Jiménez-Morillo, Cabrita, Dias, González-Vila, & González-Pérez, 2020; Jiménez Morillo, Rosa Arranz, González-Vila, & González-Pérez, 2015), and its application as an additional methodology was explored. Pyrolysis products from a small subset of the Lakkasuo core samples were measured using Py-CSIA for $\delta^{13}C$ abundance at the stable isotopes laboratory at the Instituto de Recursos Naturales y Agrobiología de Sevilla (IRNAS-CSIC) in Seville, Spain in October 2019.

Study sites

Samples from twelve different peatland sites were used for analysis. Ten of these sites were used as representative samples in the PyE study (**Chapter 3**), where the focus was on pyrolysis-induced volatilization rather than a detailed chemical characterization (**Table 1**). The remaining two peatland sites (Lakkasuo, Degerö Stormyr) were the focus of the high-resolution chemical characterizations (**Chapter 4-5**) serving as the primary objective of this thesis. Both peatlands are examples of vulnerable boreal ecosystems, and incorporate long-running research sites where studies incorporating a variety of methods and goals have previously been conducted (Jaatinen, Fritze, Laine, & Laiho, 2007; Krüger et al., 2016; Minkkinen et al., 1999; Nilsson et al., 2008). Due to their central role in this work, a brief overview of these two sites and their general characteristics is provided.

Table 1. Overview of sampling sites, peatland type, current land use, sample depths, original OC and N content, pH, and degradation status (Chapter 2). From (Klein, Gross-Schmölders, De la Rosa, Alewell, & Leifeld, 2020).

Sample		Site	Coordinates	Peatland type*	Current land use	Sample depth (cm)	OC %	N %	Soil pH**	Status
S-1	P4a 83-85	Paulinenaue	52·69°N, 12·72°E	fen	GL	83-85	10.52	0.6	5.8	Degraded
S-2	Seeboden-Alp5	Seeboden-Alp	47·06°N, 8·46°E	bog	N	32-36	55.67	1.53	3.1	Degraded
S-3	P247D 83-86	Paulinenaue	52·69°N, 12·72°E	fen	GL	83-86	46.57	2.6	5.8	Degraded
S-4	GRC 186-189	Gruyere	47·24°N, 7·05°E	bog	N	186-189	55.49	1.42	4.5	Intact
S-5	HMC 180-183	Hagenmoos	47·24°N, 8·52°E	bog	FL	180-183	56.96	1.56	5.3	Degraded
S-6	Staatswald 80-95	Witzwil	46·98°N, 7·05°E	fen	FL	80-95	50.6	1.96	4	Degraded
S-7	GE1 80-82 BE-1734	Ahlen-Falkenberg	53·41°N, 8·49°E	bog	GL	80-82	50.08	0.9	3.4	Intact
S-8	P33 5-15	Witzwil	46·98°N, 7·05°E	fen	CL	Mai.15	28.13	1.89	6.8	Degraded
S-9	GI-1 80-82 BE-1743	Ahlen-Falkenberg	53·41°N, 8·49°E	bog	GL	80-82	52.38	1.53	3.3	Intact
S-10	Parzelle Spring	Witzwil	46·98°N, 7·05°E	fen	CL	45-55	40.33	2.4	5.1	Degraded

*before drainage

CL=cropland; GL=grassland; FL=forest; N=natural;

** 0.01 M CaCl2

Lakkasuo mire covers an extensive area, and its overall ecology has previously been thoroughly surveyed (Laine et al., 2004). While the larger mire also contains a minerotrophic part, only samples from the southern ombrotrophic part of the mire were investigated (**Figure 2, c-d**). Both parts of the mire have sections that were drained for forestry, and sections that remained undrained and intact. Samples were collected from the margins of the ombrotrophic part of Lakkasuo (61°48'N, 24°19'E), which is *Sphagnum*-dominated, and has been accumulating peat for approximately the last 3-5K years. Ditches were installed in Lakkasuo for forestry purposes in 1961 (depth 70 cm, spacing 40-60 m). The ditch installation and subsequent drainage affected approximately 50% of the mire. Due to hydrologic separation between the ditches (Murphy, Laiho, & Moore, 2009), it was possible for the undrained and drained sites to be sampled in relatively close proximity to each other (15 m), permitting a pairwise comparison of natural and drained cores (**Chapter 4**) from the same ecosystem.

Degerö Stormyr (Northern Sweden 64°11'N, 19°33'E) is an acidic mire with minerotrophic conditions (poor fen) that has been accumulating peat for roughly the last 8K years (**Figure 2, a-b**). Degerö

Figure 2. Overview of the boreal peatland ecosystems selected for Py-GC/MS analysis, with photos from the 2017 sampling event depicting core sites. For Degerö-Stormyr in Northern Sweden, three cores each were sampled from the undrained natural mire (NM, a) and a site near the drainage channel (DC, b). For Lakkasuo in Finland, three cores each were sampled from the undrained (ON, c) and drained (OD, d) areas of the ombrotrophic part of the mire. Photos courtesy of Pascal von Sengbusch. Sampling sites are discussed in further detail in their corresponding chapters; for Lakkasuo (Chapter 4), and for Degerö-Stormyr (Chapter 5).

underwent historical drainage activities, where ditches were installed sometime in the early 20th century (Malmström, 1923). The research site of Degerö contains three different sampling areas: an undrained "natural" part (NM) towards the center of the mire, and two drier sites – one near a glacial ridge, and the other near the historic drainage channel (DC). The DC site demonstrated evidence of rewetting through water-saturated conditions during the site visit in 2017, changes in botanical composition (established *Sphagnum riparium* - a strong indicator for wet minerotrophic conditions), and a subsequent tree ring analysis that reflected a sharp decrease in growth as early as the 1970s. To investigate the influence of rewetting, core replicates were sampled for pairwise comparison (**Chapter 5**) from the area near the drainage channel (DC), and from the natural site (NM).

Results and Discussion

Compilation of Py-GC/MS research

As a comprehensive compilation of peat OM chemical components (including biomarkers) amenable to Py-GC/MS had not yet been conducted, **Chapter 2** sought to provide a "state of the science" for peatland studies incorporating the method. While plant-based studies were well represented, it was noted that fewer organism-specific microbial biomarkers have been identified. Further, several key areas of emerging questions were described in peatland OM research where a detailed chemical characterization could be informative. These key areas included: improved characterization of OM associated with palaeo-fire identification in the peatland profile; incorporation of Py-CSIA techniques to determine primary molecular sources of shifting isotope signals; improved latitudinal OM comparisons to identify whether differences in tropical peat OM renders them more (or less) susceptible to C loss; and potential applications to C cycling models.

Optimization of pyrolysis parameters (PyE)

Chapter 3 sought to explore the reliability of Py-GC/MS results by focusing first on the representativeness of the pyrolyzed material before it entered the analysis instrument (GC/MS). This strategic investigation of the method offers new quality control mechanisms for Py-GC/MS studies by providing an overall estimate for the representativeness of pyrolyzed peat. C PyE (45.1-51.6% volatilization across all samples) was relatively insensitive to instrumental parameters, and not significantly influenced by increase in temperature, sample mass, or by the instrument used (though a significant increase in C PyE was observed when the heating rate was increased from the lowest heating rate settings (10 K/min) to higher heating rate settings (20-50K/min). This finding was in agreement with the results generally reported in biochar studies, which have the opposite goal (maximizing char), and require lower settings to improve yield (Gheorghe, Marculescu, Badea, Dinca, & Apostol, 2009; Zhao et al., 2018).

Despite the much lower initial sample concentrations, N PyE (56.7-75.8% volatilization across all samples) was significantly higher than C PyE ($p<0.05$), and more heavily influenced by instrumental parameters, including temperature and heating rate. Moreover, a strong logarithmic relationship was observed between N PyE and original sample N content ($r=0.83$, $p<0.01$) – where N PyE sharply decreased with low original N concentration, suggesting that N can be expected undergo preferential volatilization in higher temperatures. For acceptable pyrolysis of representative N compounds (>65%), original sample N content >0.5% would be required. Because N serves an outsized role in nutrient-

limited ombrotrophic peatlands (Larmola et al., 2013), this potential for stoichiometric selectivity in Py-GC/MS studies is important to consider – especially for those seeking to characterize the molecular composition of N-containing peat OM.

While C PyE across the different instrumental parameters demonstrated overall robustness and reproducibility of the method, **Chapter 3's** findings illustrated the influence of original sample chemical composition on the pyrolysis process via greater sensitivity to N-containing compounds. The PyE range provided by the study may provide an estimated range for pyrolysis efficiency (and thus, representativeness of the analyzed sample of the original OM matrix) of peat samples measured by Py-GC/MS. For studies focused on the investigation of OC, different pyrolysis parameters – whether temperatures, instrument type ("flash" or ramped), sample mass, or original chemical composition - can be reasonably expected not to have a substantial inhibitory effect on volatilization (as long as exceptionally slow heating rates are not used). However, while C PyE was relatively insensitive to instrumental parameters, N PyE was more likely to be volatilized at very high temperatures and heating rates than might be otherwise appropriate for OC. These results suggest that for those interested in N characterization, original sample N content is required to be >0.5% to achieve sufficient successful volatilization of representative compounds.

Py-GC/MS chemical fingerprinting and peat degradation status

In Lakkasuo, aerobic conditions in the drained site demonstrated a strong influence on OM peat chemistry through significant reductions in phenols and polysaccharides (indicative of "fresh" *Sphagnum*), accompanied by the relative accumulation of higher molecular weight, "recalcitrant" polysaccharides such as levoglucosan and 1,6-anhydro-β-D-glucofuranose. Increased abundance in guaiacyl-derived lignin, benzenes, C-29 triterpenoids, and sesquiterpenes were consistent with the increased presence of *Pinus sylvestris* onsite established for forestry purposes. Notably, these results suggested that short-term, "moderate" changes in peat hydrology (<60 years, and <30 cm historical decrease in the drained water table) strongly influenced peat chemical composition.

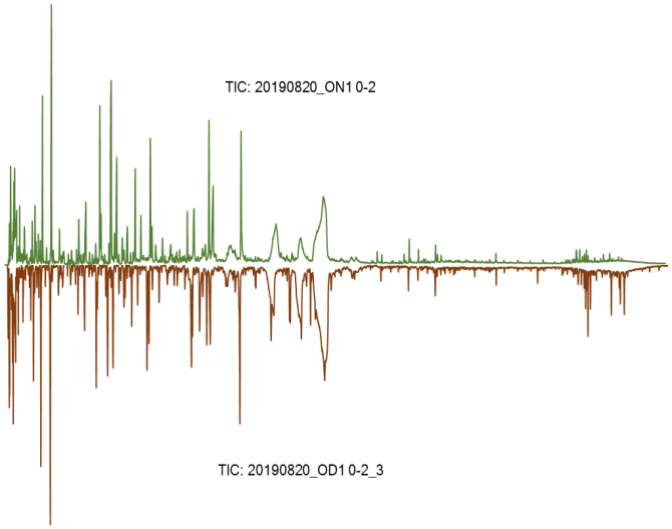

Figure 3. Total ion current (TIC) for natural core ON1 0-2 (green, top) and drained core OD1 0-2 (brown bottom).

In Degerö Stormyr, rewetting resulted in rapid initial changes in OM composition reflecting the changes in vegetation in the surface peat (even after >80 years of drainage). Phenol compounds increased rapidly in abundance in the rewetted surface samples – suggesting that phenol abundance is a sensitive indicator for transitioning rewetted conditions in *Sphagnum* peat. However, the formerly drained peat also continued to display altered chemical characteristics from the natural site that remained visible both in surface samples (continued higher abundance in lignin, N compounds, benzenes, lipids and PAHs – despite the mature growth of *Sphagnum riparium*), and as a "fingerprint" through the entire depth profile. These findings suggested that recovery of accumulating peat OM after rewetting may occur at a time scale beyond a few decades, due to residual impacts originating from the "permanently" altered OM in the underlying drained peat.

Generally, the interpretation of the pyrolysis products between the two peatland sites showed good agreement when similar ecological conditions were present (intact vs drained/historically drained). The chemistry observed in the Lakkasuo site, due to its known history and relatively short length of time since drainage (since 1961), was considered to behave almost in a "textbook" example of chemical differences in response to drainage (higher phenols in natural site, higher lignin, N compounds, benzenes, lipids in drained site) (**Figure 3**). However, unlike Lakkasuo, most peats worldwide were drained in the more distant past. Chemical effects are therefore more likely to be convoluted by simultaneous influences of multiple processes on the same OM over time (periodic changes in climate/precipitation patterns, aerobic processes, anaerobic processes, etc).

Degerö, which is an older peatland with a longer history of drainage, serves as a characteristic example of this. Chemical behavior of the depth profiles generally displayed higher variability in Degerö than in Lakkasuo– particularly in the rewetted site. Moreover, some of the depth trends of specific pyrolysis products in Lakkasuo were not observed as clearly for Degerö. For example, PCA strongly separated the influence of guaiacyl- and syringyl-derived lignin in Lakkasuo, whereas this distinction was less prevalent in Degerö. This could be due to differences in the vegetative composition (as Degerö was not known to be extensively utilized for forestry like Lakkasuo, and thus lignin dominance in Lakkasuo may have been a clearer indicator for drained conditions), or also overall differences in chemistry driven by groundwater source. However, the higher abundance of pyrolysis products associated with vascular plants (lignin, N compounds, benzenes, lipids, PAHs) in the rewetted surface samples, despite the visible renewed growth of *Sphagnum* (and corresponding response in the phenol compound class) may also suggest a permanent "fingerprint" of the historical drained conditions, or residual impacts on the more recently deposited OM originating from the older peat below (Stewart, Moturi, Follett, & Halvorson, 2015). These findings suggest that while rewetting is clearly beneficial in altering the course of C loss through the recovery of peat building vegetation (*Sphagnum*), residual effects on the previously drained

OM remain in the deeper peat, thus highlighting the importance of protecting this vulnerable OM from further degradation.

In Lakkasuo, correlation of the Py-GC/MS data with similar data using other proxies on the same samples (O:C, N:C molar ratios, $\delta^{13}C$, $\delta^{15}N$ stable isotopes) supported the differences observed in peat chemical composition with drainage. Plant biomarkers (*p*-isopropenylphenol, guaiacyl- and syringyl-derived lignin) in the depth profile conformed to general expectations set forth by the plant macrofossil assessment provided for two of the Lakkasuo cores, indicating that the molecular fingerprinting assessment holds true not only with differences in drainage/degradation, but also with increased time since original peat deposition. In Degerö, C/N ratios remained significantly higher in the natural site than the rewetted site in surface samples (0-10 cm, $p<0.05$), lending further support to the argument that the OM in the rewetted surface peat, while transitioning towards recovery, has not yet had sufficient time to chemically respond to the rewetting.

Conclusions

This thesis provides high-resolution chemical comparison of peat OM, demonstrating differences in OM content between natural, drained, and rewetted peatlands. Findings outlined here could be applied in the future to the establishment of chemical "metrics" used to improve descriptions of peatland degradation status – with important implications to those communicating with stakeholders about rewetting restoration projects.

The pyrolysis process is robust and reproducible, and can reasonably be expected to volatilize a representative portion of the sample OM onto the analysis instrument. Moreover, this work provides an estimated range (C PyE 45.1-51.6%, N PyE 56.7-75.8%) for sample volatilization that can be used as a reference by those working with the method for peat. The chemical "fingerprints" generated by Py-GC/MS are good proxy for overall peat composition, and are informative about changes not only in vegetation, but also predominating decomposition processes (i.e., aerobic/anaerobic) with depth. However, while plant-derived components are well characterized in contributing molecular sources to peat OM, more research is needed to identify chemical components contributed by microbial organisms.

Overall, this work demonstrates that peat degradation status can be effectively traced in the depth profile through the investigation of OM. Even short-term and moderate hydrological changes strongly influence the chemical composition of peat OM, and thus are an effective tool to assess degradative status. Interpretation of the chromatograms generated by Py-GC/MS analysis can be somewhat complex; however, the method is well-suited for an equally complex OM matrix, and is highly sensitive to even small changes in chemical composition. Multivariate analyses such as PCA provide a useful means to

separate simultaneous influences, so that the primary origin of individual pyrolysis products can be disentangled and interpreted. Meaningful changes can be detected in compounds present in very low abundance (lignin, individual polysaccharide pyrolysis products), and can be tied to environmental changes in the overall ecosystem at the time the OM was deposited. Py-GC/MS peat depth profiles studies such as those presented in this thesis are likely to be a useful tool across peat ecology disciplines – both for studies focused on palaeo-environmental applications and those focused on the relationship between OM decomposition and greenhouse gas emissions.

Outlook

The application and comparison of multiple biogeochemical proxies (Py-GC/MS derived chemical classes and molecular biomarkers, bulk elemental analysis-derived stoichiometric ratios, $F^{14}C$ depth comparisons) has permitted a high-resolution analysis of the chemical behavior of peat with drainage, depth, and rewetting. This thesis has provided new insights about the behavior of both chemical classes and individual compounds affected by peat degradation processes. In the future, these insights could be applied to rewetting ecosystems undergoing restoration activities to confirm successful responses to mitigation practices.

The findings presented in this work are not representative of all types of peat (fen, bog, boreal, temperate, tropical). Peat OM composition can be quite heterogeneous. An important goal of this research has also been to pinpoint composition aspects that could be used in future studies to assess degradation status across a diverse selection of different peatland types. Further, in order to improve our understanding of how changing peatland OM chemistry impacts greenhouse gas emissions, a logical consequence of this research is to connect such degradative peat indicators as outlined as part of this work to flux measurements (CO_2, N_20, CH_4) (Alm et al., 2007), to investigate the correlation between OM composition and greenhouse gas emissions.

It is also anticipated that relevant findings from this thesis could also be used to improve models currently used to simulate greenhouse gas emissions. For example, model C and N stoichiometry could be improved by more precise peatland OM chemical composition - particularly to better constrain comparisons of simulated C pools to experimental measurements of OC. Improved estimates of the peat OC stock composition will also help to better constrain feedback mechanisms occurring between peatlands, the OC they contain, and climate.

References

Alewell, C., Giesler, R., Klaminder, J., Leifeld, J., & Rollog, M. (2011). Stable carbon isotopes as indicators for environmental change in palsa peats. *Biogeosciences, 8*(7), 1769-1778.

Alm, J., Shurpali, N. J., Tuittila, E.-S., Laurila, T., Maljanen, M., Saarnio, S., & Minkkinen, K. (2007). Methods for determining emission factors for the use of peat and peatlands flux measurements and modelling.

Altizer, S., Ostfeld, R. S., Johnson, P. T., Kutz, S., & Harvell, C. D. (2013). Climate change and infectious diseases: from evidence to a predictive framework. *Science, 341*(6145), 514-519.

Andersen, R., Farrell, C., Graf, M., Muller, F., Calvar, E., Frankard, P., . . . Anderson, P. (2017). An overview of the progress and challenges of peatland restoration in Western Europe. *Restoration Ecology, 25*(2), 271-282.

Andersen, R., Grasset, L., Thormann, M. N., Rochefort, L., & Francez, A.-J. (2010). Changes in microbial community structure and function following Sphagnum peatland restoration. *Soil Biology and Biochemistry, 42*(2), 291-301.

Beaulne, J., Garneau, M., Magnan, G., & Boucher, É. (2021). Peat deposits store more carbon than trees in forested peatlands of the boreal biome. *Scientific Reports, 11*(1), 1-11.

Belyea, L. R., & Clymo, R. (2001). Feedback control of the rate of peat formation. *Proceedings of the Royal Society of London B: Biological Sciences, 268*(1473), 1315-1321.

Biester, H., Knorr, K.-H., Schellekens, J., Basler, A., & Hermanns, Y.-M. (2014). Comparison of different methods to determine the degree of peat decomposition in peat bogs. *Biogeosciences, 11*(10), 2691-2707.

Blokker, P., Yeloff, D., Boelen, P., Broekman, R. A., & Rozema, J. (2005). Development of a proxy for past surface UV-B irradiation: a thermally assisted hydrolysis and methylation py-GC/MS method for the analysis of pollen and spores. *Analytical chemistry, 77*(18), 6026-6031.

Bond, D. P., & Grasby, S. E. (2017). On the causes of mass extinctions. *Palaeogeography, Palaeoclimatology, Palaeoecology, 478*, 3-29.

Bonn, A., Reed, M. S., Evans, C. D., Joosten, H., Bain, C., Farmer, J., . . . Artz, R. (2014). Investing in nature: Developing ecosystem service markets for peatland restoration. *Ecosystem Services, 9*, 54-65.

Buurman, P., Nierop, K. G. J., Pontevedra-Pombal, X., & Martínez Cortizas, A. (2006). Chapter 10 Molecular chemistry by pyrolysis–GC/MS of selected samples of the Penido Vello peat

deposit, Galicia, NW Spain. In I. P. Martini, A. Martínez Cortizas & W. Chesworth (Eds.), *Developments in Earth Surface Processes* (Vol. 9, pp. 217-240): Elsevier.

Carr, A. S., Boom, A., Chase, B. M., Roberts, D. L., & Roberts, Z. E. (2010). Molecular fingerprinting of wetland organic matter using pyrolysis-GC/MS: an example from the southern Cape coastline of South Africa. *Journal of Paleolimnology, 44*(4), 947-961.

Clymo, R. (1984). The limits to peat bog growth. *Philosophical Transactions of the Royal Society of London. B, Biological Sciences, 303*(1117), 605-654.

Clymo, R. (1987). The ecology of peatlands. *Science Progress, 71*, 593-614.

Dohong, A., Aziz, A. A., & Dargusch, P. (2018). A review of techniques for effective tropical peatland restoration. *Wetlands, 38*(2), 275-292.

Dungait, J. A., Hopkins, D. W., Gregory, A. S., & Whitmore, A. P. (2012). Soil organic matter turnover is governed by accessibility not recalcitrance. *Global Change Biology, 18*(6), 1781-1796.

Feng, X., Simpson, A. J., Wilson, K. P., Williams, D. D., & Simpson, M. J. (2008). Increased cuticular carbon sequestration and lignin oxidation in response to soil warming. *Nature Geoscience, 1*(12), 836.

Freeman, C., Ostle, N., Fenner, N., & Kang, H. (2004). A regulatory role for phenol oxidase during decomposition in peatlands. *Soil Biology and Biochemistry, 36*(10), 1663-1667.

Freeman, C., Ostle, N., & Kang, H. (2001). An enzymic'latch'on a global carbon store. *Nature, 409*(6817), 149.

Gheorghe, C., Marculescu, C., Badea, A., Dinca, C., & Apostol, T. (2009). *Effect of pyrolysis conditions on bio-char production from biomass.* Paper presented at the Proceedings of the 3rd WSEAS Int. Conf. on RENEWABLE ENERGY SOURCES.

Glenk, K., & Martin-Ortega, J. (2018). The economics of peatland restoration. *Journal of Environmental Economics and Policy, 7*(4), 345-362.

González-Pérez, J. A., Jiménez-Morillo, N. T., de la Rosa, J. M., Almendros, G., & González-Vila, F. J. (2016). Compound-specific stable carbon isotopic signature of carbohydrate pyrolysis products from C3 and C4 plants. *Journal of the Science of Food and Agriculture, 96*(3), 948-953.

González, J. A., González-Vila, F. J., Almendros, G., Zancada, M. C., Polvillo, O., & Martín, F. (2003). Preferential accumulation of selectively preserved biomacromolecules in the humus

fractions from a peat deposit as seen by analytical pyrolysis and spectroscopic techniques. *Journal of Analytical and Applied Pyrolysis, 68*, 287-298.

Groß-Schmölders, M., Sengbusch, P. v., Krüger, J. P., Klein, K., Birkholz, A., Leifeld, J., & Alewell, C. (2020). Switch of fungal to bacterial degradation in natural, drained and rewetted oligotrophic peatlands reflected in δ 15 N and fatty acid composition. *SOIL, 6*(2), 299-313.

Gunnarsson, U. (2005). Global patterns of Sphagnum productivity. *Journal of Bryology, 27*(3), 269-279.

Hájek, T., Ballance, S., Limpens, J., Zijlstra, M., & Verhoeven, J. T. A. (2011). Cell-wall polysaccharides play an important role in decay resistance of Sphagnum and actively depressed decomposition in vitro. *Biogeochemistry, 103*(1), 45-57. doi: 10.1007/s10533-010-9444-3

Harris, L. I., Moore, T. R., Roulet, N. T., & Pinsonneault, A. J. (2020). Limited effect of drainage on peat properties, porewater chemistry, and peat decomposition proxies in a boreal peatland. *Biogeochemistry, 151*(1), 43-62.

Hedges, J. I., & Mann, D. C. (1979). The characterization of plant tissues by their lignin oxidation products. *Geochimica et Cosmochimica Acta, 43*(11), 1803-1807.

Heller, C., Ellerbrock, R., Roßkopf, N., Klingenfuß, C., & Zeitz, J. (2015). Soil organic matter characterization of temperate peatland soil with FTIR-spectroscopy: effects of mire type and drainage intensity. *European Journal of Soil Science, 66*(5), 847-858.

Heller, C., & Zeitz, J. (2012). Stability of soil organic matter in two northeastern German fen soils: the influence of site and soil development. *Journal of Soils and Sediments, 12*(8), 1231-1240.

Hoyos-Santillan, J., Lomax, B. H., Large, D., Turner, B. L., Boom, A., Lopez, O. R., & Sjögersten, S. (2016). Quality not quantity: Organic matter composition controls of CO2 and CH4 fluxes in neotropical peat profiles. *Soil Biology and Biochemistry, 103*, 86-96.

Huang, Y., Stankiewicz, B., Eglinton, G., Snape, C., Evans, B., Latter, P., & Ineson, P. (1998). Monitoring biomacromolecular degradation of Calluna vulgaris in a 23 year field experiment using solid state 13C-NMR and pyrolysis-GC/MS. *Soil Biology and Biochemistry, 30*(12), 1517-1528.

IPCC. (2021). Climate Change 2021: The Physical Science Basis. Contribution of Working Group I to the Sixth

Assessment Report of the Intergovernmental Panel on Climate Change In V. [Masson-Delmotte, P. Zhai, A. Pirani, S. , C. P. L. Connors, S. Berger, N. Caud, Y. Chen, L. Goldfarb, M. I. Gomis,

M. Huang, K. Leitzell, E. Lonnoy, J. B. & T. K. M. R. Matthews, T. Waterfield, O. Yelekçi, R. Yu and B. Zhou (eds.)]. (Eds.): Cambridge University Press. In Press.

Jaatinen, K., Fritze, H., Laine, J., & Laiho, R. (2007). Effects of short-and long-term water-level drawdown on the populations and activity of aerobic decomposers in a boreal peatland. *Global Change Biology, 13*(2), 491-510.

Jiménez-Morillo, N. T., Cabrita, M. J., Dias, C. B., González-Vila, F. J., & González-Pérez, J. A. (2020). Pyrolysis-compound-specific hydrogen isotope analysis (δ2H Py-CSIA) of Mediterranean olive oils. *Food Control, 110*, 107023.

Jiménez Morillo, N. T., Rosa Arranz, J. M., González-Vila, F. J., & González-Pérez, J. A. (2015). Direct Compound Specific Isotopic Analysis (CHON) of complex samples using analytical pyrolysis (Py-CSIA).

Joosten, H. (2009). The Global Peatland CO2 Picture: peatland status and drainage related emissions in all countries of the world. Wageningen, The Netherlands: Wetlands International.

Joosten, H., & Clarke, D. (2002). Wise use of mires and peatlands. *International Mire Conservation Group and International Peat Society, 304*.

Kaal, J., Baldock, J. A., Buurman, P., Nierop, K. G., Pontevedra-Pombal, X., & Martínez-Cortizas, A. (2007). Evaluating pyrolysis–GC/MS and 13C CPMAS NMR in conjunction with a molecular mixing model of the Penido Vello peat deposit, NW Spain. *Organic Geochemistry, 38*(7), 1097-1111.

Kimmel, K., & Mander, Ü. (2010). Ecosystem services of peatlands: Implications for restoration. *Progress in Physical Geography, 34*(4), 491-514.

Klein, K., Gross-Schmölders, M., Alewell, C., & Leifeld, J. (2021). Chapter Three - Heating up a cold case: Applications of analytical pyrolysis GC/MS to assess molecular biomarkers in peat. In D. L. Sparks (Ed.), *Advances in agronomy* (Vol. 165, pp. 115-159): Academic Press.

Klein, K., Gross-Schmölders, M., De la Rosa, J. M., Alewell, C., & Leifeld, J. (2020). Investigating the influence of instrumental parameters and chemical composition on pyrolysis efficiency of

peat. *Communications in soil science and plant analysis, 51*(12), 1572-1581. doi: 10.1080/00103624.2020.1784916

Knicker, H. (2004). Stabilization of N-compounds in soil and organic-matter-rich sediments—what is the difference? *Marine Chemistry, 92*(1-4), 167-195.

Kögel-Knabner, I., & Amelung, W. (2014). 12.7 - Dynamics, Chemistry, and Preservation of Organic Matter in Soils. In H. D. Holland & K. K. Turekian (Eds.), *Treatise on Geochemistry (Second Edition)* (pp. 157-215). Oxford: Elsevier.

Krüger, Alewell, C., Minkkinen, K., Szidat, S., & Leifeld, J. (2016). Calculating carbon changes in peat soils drained for forestry with four different profile-based methods. *Forest Ecology and Management, 381*, 29-36.

Krüger, Leifeld, J., Glatzel, S., Szidat, S., & Alewell, C. (2015). Biogeochemical indicators of peatland degradation-a case study of a temperate bog in northern Germany. *Biogeosciences, 12*, 2861-2871.

Krüger, J. P. (2016). *Peatland degradation indicated by stable isotope depth profiles and soil carbon loss.* University_of_Basel.

Kuder, T., Kruge, M., Shearer, J., & Miller, S. (1998). Environmental and botanical controls on peatification—a comparative study of two New Zealand restiad bogs using Py-GC/MS, petrography and fungal analysis. *International Journal of Coal Geology, 37*(1-2), 3-27.

Kuder, T., & Kruge, M. A. (1998). Preservation of biomolecules in sub-fossil plants from raised peat bogs — a potential paleoenvironmental proxy. *Organic Geochemistry, 29*(5), 1355-1368. doi: https://doi.org/10.1016/S0146-6380(98)00092-8

Laiho, R. (2006). Decomposition in peatlands: Reconciling seemingly contrasting results on the impacts of lowered water levels. *Soil Biology and Biochemistry, 38*(8), 2011-2024.

Laine, J., Komulainen, V., Laiho, R., Minkkinen, K., Rasinmäki, A., Sallantaus, T., . . . Tuittila, E. (2004). Lakkasuo: a guide to mire ecosystem. *Lakkasuo: a guide to mire ecosystem.*

Lamers, L. P., Vile, M. A., Grootjans, A. P., Acreman, M. C., van Diggelen, R., Evans, M. G., . . . Roelofs, J. G. (2015). Ecological restoration of rich fens in Europe and North America: from trial and error to an evidence-based approach. *Biological Reviews, 90*(1), 182-203.

Larmola, T., Bubier, J. L., Kobyljanec, C., Basiliko, N., Juutinen, S., Humphreys, E., . . . Moore, T. R. (2013). Vegetation feedbacks of nutrient addition lead to a weaker carbon sink in an ombrotrophic bog. *Global Change Biology, 19*(12), 3729-3739.

Leifeld, J., Alewell, C., Bader, C., Krüger, J. P., Mueller, C. W., Sommer, M., . . . Szidat, S. (2018). Pyrogenic carbon contributes substantially to carbon storage in intact and degraded northern peatlands. *Land Degradation & Development, 29*(7), 2082-2091.

Leifeld, J., Klein, K., & Wüst-Galley, C. (2020). Soil organic matter stoichiometry as indicator for peatland degradation. *Scientific Reports, 10*(1), 1-9.

Leifeld, J., & Menichetti, L. (2018). The underappreciated potential of peatlands in global climate change mitigation strategies. *Nature communications, 9*(1), 1071.

Loisel, J., Gallego-Sala, A., Amesbury, M., Magnan, G., Anshari, G., Beilman, D., . . . Charman, D. (2021). Expert assessment of future vulnerability of the global peatland carbon sink. *Nature Climate Change, 11*(1), 70-77.

Loisel, J., Yu, Z., Beilman, D. W., Camill, P., Alm, J., Amesbury, M. J., . . . Barber, K. (2014). A database and synthesis of northern peatland soil properties and Holocene carbon and nitrogen accumulation. *The Holocene, 24*(9), 1028-1042.

Lucchese, M., Waddington, J., Poulin, M., Pouliot, R., Rochefort, L., & Strack, M. (2010). Organic matter accumulation in a restored peatland: Evaluating restoration success. *Ecological Engineering, 36*(4), 482-488.

Malmström, C. (1923). Degerö stormyr.

Martin, F., Saiz-Jimenez, C., & Gonzalez-Vila, F. (1979). Pyrolysis-gas chromatography-mass spectrometry of lignins. *Holzforschung, 33*(6), 210-212.

McClymont, E. L., Bingham, E. M., Nott, C. J., Chambers, F. M., Pancost, R. D., & Evershed, R. P. (2011). Pyrolysis GC–MS as a rapid screening tool for determination of peat-forming plant composition in cores from ombrotrophic peat. *Organic Geochemistry, 42*(11), 1420-1435.

McGuire, A. D., Anderson, L. G., Christensen, T. R., Dallimore, S., Guo, L., Hayes, D. J., . . . Roulet, N. (2009). Sensitivity of the carbon cycle in the Arctic to climate change. *Ecological Monographs, 79*(4), 523-555.

Minkkinen, K., & Laine, J. (1998). Long-term effect of forest drainage on the peat carbon stores of pine mires in Finland. *Canadian Journal of Forest Research, 28*(9), 1267-1275.

Minkkinen, K., Vasander, H., Jauhiainen, S., Karsisto, M., & Laine, J. (1999). Post-drainage changes in vegetation composition and carbon balance in Lakkasuo mire, Central Finland. *Plant and Soil, 207*(1), 107-120. doi: 10.1023/a:1004466330076

Moore, T. R., Large, D., Talbot, J., Wang, M., & Riley, J. L. (2018). The stoichiometry of carbon, hydrogen, and oxygen in peat. *Journal of Geophysical Research: Biogeosciences, 123*(10), 3101-3110.

Moreno-Mateos, D., Power, M. E., Comín, F. A., & Yockteng, R. (2012). Structural and functional loss in restored wetland ecosystems. *PLoS Biol, 10*(1), e1001247.

Murphy, M., Laiho, R., & Moore, T. R. (2009). Effects of water table drawdown on root production and aboveground biomass in a boreal bog. *Ecosystems, 12*(8), 1268-1282.

Naafs, B., Inglis, G., Blewett, J., McClymont, E., Lauretano, V., Xie, S., . . . Pancost, R. (2019). The potential of biomarker proxies to trace climate, vegetation, and biogeochemical processes in peat: A review. *Global and Planetary Change, 179*, 57-79.

Nilsson, M., Sagerfors, J., Buffam, I., Laudon, H., Eriksson, T., Grelle, A., . . . Lindroth, A. (2008). Contemporary carbon accumulation in a boreal oligotrophic minerogenic mire–a significant sink after accounting for all C-fluxes. *Global Change Biology, 14*(10), 2317-2332.

Palozzi, J. E., & Lindo, Z. (2017). Boreal peat properties link to plant functional traits of ecosystem engineers. *Plant and Soil, 418*(1), 277-291. doi: 10.1007/s11104-017-3291-0

Pancost, R. D., Baas, M., van Geel, B., & Damsté, J. S. S. (2002). Biomarkers as proxies for plant inputs to peats: an example from a sub-boreal ombrotrophic bog. *Organic Geochemistry, 33*(7), 675-690.

Rochefort, L. (2000). Sphagnum: a keystone genus in habitat restoration. *The Bryologist, 103*(3), 503-508.

Rochefort, L., Quinty, F., Campeau, S., Johnson, K., & Malterer, T. (2003). North American approach to the restoration of Sphagnum dominated peatlands. *Wetlands Ecology and Management, 11*(1), 3-20.

Ronkainen, T., McClymont, E. L., Väliranta, M., & Tuittila, E.-S. (2013). The n-alkane and sterol composition of living fen plants as a potential tool for palaeoecological studies. *Organic Geochemistry, 59*, 1-9.

Schellekens, J., Barberá, G. G., & Buurman, P. (2013). Potential vegetation markers–analytical pyrolysis of modern plant species representative of Neolithic SE Spain. *Journal of Archaeological Science, 40*(1), 365-379.

Schellekens, J., Bindler, R., Martínez-Cortizas, A., McClymont, E. L., Abbott, G. D., Biester, H., . . . Buurman, P. (2015). Preferential degradation of polyphenols from Sphagnum – 4-Isopropenylphenol as a proxy for past hydrological conditions in Sphagnum-dominated peat. *Geochimica et Cosmochimica Acta, 150*, 74-89. doi: https://doi.org/10.1016/j.gca.2014.12.003

Schellekens, J., Bradley, J. A., Kuyper, T. W., Fraga, I., Pontevedra-Pombal, X., Vidal-Torrado, P., . . . Buurman, P. (2015). The use of plant-specific pyrolysis products as biomarkers in peat deposits. *Quaternary Science Reviews, 123*, 254-264.

Schellekens, J., & Buurman, P. (2011). n-Alkane distributions as palaeoclimatic proxies in ombrotrophic peat: the role of decomposition and dominant vegetation. *Geoderma, 164*(3-4), 112-121.

Schellekens, J., Buurman, P., Fraga, I., & Martínez-Cortizas, A. (2011). Holocene vegetation and hydrologic changes inferred from molecular vegetation markers in peat, Penido Vello (Galicia, Spain). *Palaeogeography, Palaeoclimatology, Palaeoecology, 299*(1-2), 56-69.

Schellekens, J., Buurman, P., & Kuyper, T. W. (2012). Source and transformations of lignin in Carex-dominated peat. *Soil Biology and Biochemistry, 53*, 32-42.

Schellekens, J., Buurman, P., Kuyper, T. W., Abbott, G. D., Pontevedra-Pombal, X., & Martínez-Cortizas, A. (2015). Influence of source vegetation and redox conditions on lignin-based

decomposition proxies in graminoid-dominated ombrotrophic peat (Penido Vello, NW Spain). *Geoderma, 237*, 270-282.

Schellekens, J., Buurman, P., & Pontevedra-Pombal, X. (2009). Selecting parameters for the environmental interpretation of peat molecular chemistry–a pyrolysis-GC/MS study. *Organic Geochemistry, 40*(6), 678-691.

Schellekens, J., Horák-Terra, I., Buurman, P., Silva, A. C., & Vidal-Torrado, P. (2014). Holocene vegetation and fire dynamics in central-eastern Brazil: Molecular records from the Pau de Fruta peatland. *Organic Geochemistry, 77*, 32-42.

Schimmel, H., Braun, M., Subke, J.-A., Amelung, W., & Bol, R. (2021). Carbon stability in a Scottish lowland raised bog: potential legacy effects of historical land use and implications for global change. *Soil Biology and Biochemistry, 154*, 108124.

Sherwood, S. C., & Huber, M. (2010). An adaptability limit to climate change due to heat stress. *Proceedings of the National Academy of Sciences, 107*(21), 9552-9555.

Stewart, C. E., Moturi, P., Follett, R. F., & Halvorson, A. D. (2015). Lignin biochemistry and soil N determine crop residue decomposition and soil priming. *Biogeochemistry, 124*(1), 335-351.

Storlazzi, C. D., Elias, E. P., & Berkowitz, P. (2015). Many atolls may be uninhabitable within decades due to climate change. *Scientific Reports, 5*(1), 1-9.

Traoré, M., Kaal, J., & Cortizas, A. M. (2017). Potential of pyrolysis-GC–MS molecular fingerprint as a proxy of Modern Age Iberian shipwreck wood preservation. *Journal of Analytical and Applied Pyrolysis, 126*, 1-13.

Trumbore, S. (2000). Age of soil organic matter and soil respiration: radiocarbon constraints on belowground C dynamics. *Ecological applications, 10*(2), 399-411.

Uden, P. C. (1993). Nomenclature and terminology for analytical pyrolysis (IUPAC Recommendations 1993). *Pure and applied chemistry, 65*(11), 2405-2409.

Ummenhofer, C. C., & Meehl, G. A. (2017). Extreme weather and climate events with ecological relevance: a review. *Philosophical Transactions of the Royal Society B: Biological Sciences, 372*(1723), 20160135.

Van Dam, P. J. (2001). Sinking Peat Bogs: Enviornmental Change Holland, 1350-1550. *Environmental history*, 32-45.

Van Smeerdijk, D. G., & Boon, J. J. (1987). Characterisation of subfossil Sphagnum leaves, rootlets of Ericaceae and their peat by pyrolysis-high-resolution gas chromatography-mass spectrometry. *Journal of Analytical and Applied Pyrolysis, 11*, 377-402.

Vancampenhout, K., De Vos, B., Wouters, K., Swennen, R., Buurman, P., & Deckers, J. (2012). Organic matter of subsoil horizons under broadleaved forest: Highly processed or labile and plant-derived? *Soil Biology and Biochemistry, 50*, 40-46.

Verhoeven, J. T. (2014). Wetlands in Europe: perspectives for restoration of a lost paradise. *Ecological Engineering, 66*, 6-9.

Wang, Y., Paul, S. M., Jocher, M., Espic, C., Alewell, C., Szidat, S., & Leifeld, J. (2021). Soil carbon loss from drained agricultural peatland after coverage with mineral soil. *Science of the Total Environment*, 149498.

White, D. M., Garland, D. S., Beyer, L., & Yoshikawa, K. (2004). Pyrolysis-GC/MS fingerprinting of environmental samples. *Journal of Analytical and Applied Pyrolysis, 71*(1), 107-118.

Williams, A. J., Eigenbrode, J. L., Williams, R. H., Buch, A., Teinturier, S., Millan, M., . . . Mahaffy, P. R. (2020). *The Search for Fatty Acids on Mars: Results from the First In Situ Thermochemolysis Experiment at Gale Crater, Mars*. https://ui.adsabs.harvard.edu/abs/2020AGUFMP070...05W

Xu, J., Morris, P. J., Liu, J., & Holden, J. (2018). PEATMAP: Refining estimates of global peatland distribution based on a meta-analysis. *Catena, 160*, 134-140.

Yu, Z., Beilman, D., Frolking, S., MacDonald, G. M., Roulet, N. T., Camill, P., & Charman, D. (2011). Peatlands and their role in the global carbon cycle. *Eos, Transactions American Geophysical Union, 92*(12), 97-98.

Yu, Z., Loisel, J., Brosseau, D. P., Beilman, D. W., & Hunt, S. J. (2010). Global peatland dynamics since the Last Glacial Maximum. *Geophysical Research Letters, 37*(13).

Zeh, L., Igel, M. T., Schellekens, J., Limpens, J., Bragazza, L., & Kalbitz, K. (2020). Vascular plants affect properties and decomposition of moss-dominated peat, particularly at elevated temperatures. *Biogeosciences, 17*(19), 4797-4813.

Zhang, Y., Held, I., & Fueglistaler, S. (2021). Projections of tropical heat stress constrained by atmospheric dynamics. *Nature Geoscience, 14*(3), 133-137.

Zhang, Z., Wang, J., Lyu, X., Jiang, M., Bhadha, J., & Wright, A. (2019). Impacts of land use change on soil organic matter chemistry in the Everglades, Florida-a characterization with pyrolysis-gas chromatography–mass spectrometry. *Geoderma, 338*, 393-400.

Zhao, B., O'Connor, D., Zhang, J., Peng, T., Shen, Z., Tsang, D. C., & Hou, D. (2018). Effect of pyrolysis temperature, heating rate, and residence time on rapeseed stem derived biochar. *Journal of Cleaner Production, 174*, 977-987.

Part B: Publications

Chapter 2 – Heating up a cold case: Applications of analytical pyrolysis GC/MS to assess molecular biomarkers in peat

Authors, Kristy Klein[1,2*], Miriam Groβ-Schmölders[2], Christine Alewell[2], Jens Leifeld[1]

[1]Agroscope, Climate and Agriculture Group, Reckenholzstraße 191, CH-8046 Zürich

[2]Environmental Geosciences, University of Basel, Bernoullistrasse 32, CH-4056 Basel

Advances in Agronomy, Volume 165, pp. 115-159, 2021

https://doi.org/10.1016/bs.agron.2020.09.002

Abstract

Intact peatlands serve as a globally important carbon sink. However, impacts from climate change, extraction, and drainage increase aerobic decomposition in these ecosystems– shifting their carbon flux from sink to source. A variety of projects are ongoing to restore peatlands to their natural or near-natural states; however, for carbon sequestration, net accumulation of peat relative to decomposition is of primary importance. Molecular analysis techniques provide information on peat growth and degradation trends dating from centuries to millennia. Pyrolysis coupled to gas chromatography mass spectrometry (Py-GC/MS) has been proposed for the rapid characterization of molecular biomarkers in organic matter. This paper reviews plant and microbial biomarkers analyzable via Py-GC/MS for peatland ecosystems, associated challenges, and future applications of the technique. It is noted that far fewer organism-specific biomarkers have been identified via Py-GC/MS for microbial communities in comparison to plant-based studies, and as a topic remains an area greatly needing additional research. In the future, through improved Py-GC/MS-derived fingerprinting of peatland molecular components, periods of degradation and growth could be more precisely distinguished and described, even in profiles where changes in contributing source material are not macroscopically visible.

2.1 Introduction

Despite covering a relatively small percentage (3%) of the earth's surface, peatlands store around 600 gigatonnes (Gt) of organic carbon globally (Yu et al., 2010), and contribute as much as 20-25% of the total soil organic carbon stock (Scharlemann et al., 2014, Leifeld and Menichetti, 2018) or, correspondingly, the equivalent of almost two thirds current levels of atmospheric carbon (Clymo et al., 1998, IPCC, 2014). Due to slow rates of decomposition, net primary productivity generally exceeds organic matter (OM) decay in peatlands, leading to continuous OM accumulation in these ecosystems over millennia (Clymo, 1984). In addition to their important role in carbon cycling, peatland archives and changes in peat stratigraphy can provide information about previous palaeoclimatic events and their influence on regional palaeoecology and palaeohydrology (Blackford, 2000).

Impacts from climate change, extraction, and drainage for forestry and agriculture have affected approximately 10% of peatlands globally (Joosten, 2009), causing increased aerobic decomposition of large stores of OM. With a few noted exceptions (Lohila et al., 2011), this observed increase in aerobic decomposition causes the C flux in peat ecosystems to shift from sink to source, primarily through the loss pathways of carbon dioxide (CO_2), methane, and leaching of dissolved organic carbon (DOC) (IPCC, 2014). Global CO_2 emissions from degraded peat have been estimated at almost two Gt CO_2-eq annually, as well as substantial amounts of other greenhouse gases, such as nitrous oxide (Leifeld and Menichetti, 2018). Moreover, temperature sensitivity of peat OM stored at depth is not well understood (Davidson and Janssens, 2006). Temperature-induced peatland degradation could initiate positive warming feedback loops, where the loss of deeply sequestered OM generates an increase in global CO_2 emissions, further contributing to warming temperatures and the loss of more OM (Dorrepaal et al., 2009).

A variety of projects are ongoing to restore these ecosystems to natural or near-natural states. Restoration projects usually involve a multi-faceted approach targeting, for instance, the re-establishment of previous hydrology through rewetting, or the reintroduction of species biodiversity with high peat growth rates, such as *Sphagnum cuspidatum or S. magellanicum* (Schumann and Joosten, 2008). From a carbon sequestration perspective, net accumulation of peat relative to decomposition is of primary importance for successful rewetting, where growth of peat-producing vegetation must be substantially greater than OM decomposition (Glatzel et

al., 2004, Andersen et al., 2010). Accumulation can sometimes be seen visually in the profile as lighter-colored undecomposed material, whereas degraded peat typically appears darker and more oxidized, with less recognizable original plant material. However, changes in degradation status in peat profiles are not always easily visually delineated, and the continuum of changes in decomposition cannot always be observed macroscopically.

Analytical methods are needed that enable researchers to determine the degradative or restoration state of a peatland. Without effective tools that clearly correlate restoration efforts with net peat growth, it can be difficult to argue the effectiveness of a restoration program. In addition to the challenges of macroscopic assessments noted previously, other tools used to assess net peat growth generally involve long-term monitoring efforts, which often require expensive micrometeorological instruments, remote infrastructure, and extensive time commitments from staff. In particular, tools are needed to assess whether a peatland is growing (sequestering C), stable (with a net C budget of 0), or degrading (losing C).

2.2 Techniques for OM analysis

Molecular analysis methods offer an approach permitting one-time sampling events that can provide information on peatland development dating from years to millennia. The molecular components of a peat profile can be better understood with the use of molecular biomarkers: source-specific organic compounds that can be used as indicators for groups of organisms – or, in some cases - assigned to specific metabolism, genera or species. As an analytical tool coupled with other methods, biomarkers provide a useful way to link organic matter to paleo-environmental processes.

A variety of different biomarkers have been used to elucidate the impacts of environmental change on peatland ecosystems, including palaeo-environmental reconstruction (Chambers et al., 2012, Lopez-Dias et al., 2013), anthropogenic impacts (Dubois and Jacob, 2016), fire occurrence (Kaal et al., 2008b, Schellekens et al., 2009, Leifeld et al., 2018), changes in water table regime (Blackford, 2000, Laiho, 2006, Jaatinen et al., 2008), and as evidence for restoration of disturbed sites (Andersen et al., 2010). Further, organism-specific biomarkers (where “organism-specific” is loosely defined in this paper as a biomarker capable of distinguishing certain taxa and/or dominant metabolic pathways) can distinguish plant taxa present at the time of deposition, enabling researchers to identify changes in plant species

abundance as indicators of shifts in climate or hydrological conditions. Molecular biomarkers can also be used to distinguish contributing sources of microbial material. In the future, biomarkers could open the possibility of delineating periods of degradation and growth using ratios of microbial matter to undecomposed plant material, even in profiles where shifts in contributing source material cannot be visually assessed.

Examples of analytical techniques for characterization of peat OM include bulk (elemental analysis (Worrall et al., 2013)), spectroscopic (Fourier Transform Infrared spectroscopy (Artz et al., 2008, Chapman et al., 2001), solid-state ^{13}C nuclear magnetic resonance (NMR) spectroscopy (Preston et al., 1994, Baldock et al., 1997)), isotopic (isotope ratio mass spectrometry (IRMS) (Alewell et al., 2011, Krull and Retallack, 2000)), molecular (phospholipid fatty acid analysis (Frostegård and Bååth, 1996, Frostegård et al., 1993)), or compositional genomic studies (Wilmes and Bond, 2006, Tveit et al., 2013). Depending on the analytical goal, results obtained from these techniques range from a broad compositional overview (bulk EA) to a highly specific (molecular and genomic analyses) assessment of OM content. However, while precise and informative, many highly specific techniques often also involve time-consuming sample preparation and analysis times. Methods such as bulk stable isotopes and EA involve simpler analysis techniques but provide less specific information. More detailed techniques are needed to characterize the composition of SOM to obtain a better understanding of decomposition processes.

Pyrolysis coupled to gas chromatography mass spectrometry (Py-GC/MS) offers an alternative for the detailed characterization of molecular biomarkers in OM samples (Parsi and Górecki, 2006, Tolu et al., 2015, Summons, 2014). Py-GC/MS analysis combines a capacity to sample from a large window of different OM compound classes with a detailed analysis of their specific molecular composition. Through the thermal degradation of large complex organic compounds into smaller, more easily analyzable fragments, Py-GC/MS offers the specificity in chemical characterization that GC/MS analysis provides, while also permitting analysis of a larger range of high molecular weight compounds than traditional GC/MS techniques alone. In addition to its specificity and sensitivity, Py-GC/MS is a fairly rapid method of analysis, and generally does not require extensive pre-preparation beyond sample drying and homogenization. Further, emerging pyrolysis-driven compound specific isotopic analyses now offer an opportunity to apply isotopic ratio measurements directly to individual compounds obtained via this technique (**Section 2.8.1).** Despite these advantages, comparatively few studies incorporate Py-GC/MS

as a method of analysis in complex SOM systems such as peat, possibly due to limitations in data quantification or expertise required for the characterization of identified compounds (Derenne and Quénéa, 2015). However, for OM analysis where the relative rather than absolute abundance of compounds will be compared, Py-GC/MS is a fast and effective tool for assessing OM chemical composition.

For complex OM characterization in organic soils such as peat, a comprehensive compilation of Py/GC/MS-derived studies using the approach to identify biomarkers useful for characterizing the molecular composition of peat is needed. This paper provides a review of biomarkers analyzable through Py-GC/MS using an approach encompassing peatland community ecology (contributing plants and microbial organisms and their relationships to one another) and other important ecological influences (such as fire). In addition, information that can be obtained from this type of analysis is discussed, primarily with the larger goal of understanding peat OM formation and degradation and its relationship to climate processes (though in certain cases, other Py-GC/MS biomarker data sets are used in this review, where OM characterization studies with a peatland-focused aim are lacking). Furthermore, challenges associated with the technique and future applications of the science where research is particularly needed are presented.

2.3 The peatland ecosystem

Peatland OM has long been used as a proxy indicator for previous climatic and environmental conditions by providing a relatively continuous record of its growth and developmental history. The following section presents a broad "snapshot" of peatland communities (accumulation of botanical species, degradation by microbes, internal and external factors influencing the system), with the goal to clarify for readers the types of representative OM and ecological information sought via Py-GC/MS amenable molecular biomarkers (**Sections 2.4 and 2.5**).

Conditions suitable for peat formation can be found around the globe. The location of peatland ecosystems, hydrological characteristics, as well as mire type (e.g., fen, bog) (Lindsay, 2018) influence local botanical composition, leading to a variety of different peat "types." Regardless of peat type, water-saturated conditions in accumulating OM lead to increasingly anoxic conditions with depth. Decomposition dynamics are primarily driven by the interaction between

the water table and the dominant peat-forming plant serving as ecosystem engineer (Palozzi and Lindo, 2017).

Predominant peat-forming plants vary between ecosystems (blanket mires, raised bogs, tundra and palsa mires, tropical peat swamp forests, etc.), but include *Juncus* spp. (Yeloff et al., 2008), *Carex* spp. (Schellekens et al., 2012, Schellekens et al., 2015c), *Phragmites* spp. (Hughes and Dumayne-Peaty, 2002, Chapman, 1964), and *Sphagnum* spp. (McClymont et al., 2008, Schellekens et al., 2015a). Non-*Sphagnum* moss species (ex. *Ptilium* spp.), shrubs (ex. *Ericaceae* spp.), and a selection of tree species (*Pinus* spp., particularly in drier locations) can also be found geographically distributed across many higher-latitude mire ecosystems and serve as somewhat representative members of the boreal peatland community. *Sphagnum* spp. are especially important in the formation and accumulation of boreal peat, as abundant phenolic components in *Sphagnum* moss litter inhibit decomposition (Turetsky et al., 2008, Freeman et al., 2001). Similar to other moss species, *Sphagnum* spp. have a high cation exchange capacity that allow them to exchange hydrogen ions for nutrients in bog water, causing rapid acidification (Joosten and Clarke, 2002). *Sphagnum*-dominated bogs are unique in terms of their C storage capacity, which is increased due to the above-described conditions (Verhoeven and Liefveld, 1997, Hájek et al., 2011). *Sphagnum* spp. biomass growth in peatlands ranges from 19-1656 g m^{-2} yr^{-1} (Turetsky, 2003).

Regardless of the primary peat-forming plant, predominating vegetation creates a molecular signature in OM that can be used as a proxy for previous environmental conditions (McClymont et al., 2011). It is noted that while extensive reviews of peat-forming plant species and their ecology are available for temperate and boreal systems (Joosten and Clarke, 2002, Clymo, 1987), less information exists describing the vegetation in tropical peatland ecosystems, where considerable diversity in conditions for peat formation results in botanical biodiversity and zoned plant communities (Page and Baird, 2016, Page et al., 1999). Similar to the role of *Sphagnum* in boreal ecosystems, there may be botanical species characteristic of certain tropical peatland ecosystems that can identified in OM profiles using still undiscovered organism-specific molecular markers.

Micro-habitats within the landscape also play an important role in mire ecology, such as those formed in response to fluctuations in the water table. Peat generally consists of two hydrologic layers, the aerobic acrotelm, with higher rates of decomposition and hydraulic conductivity,

and the anaerobic catotelm, where decay processes are much slower (Belyea and Clymo, 2001). Dividing these two layers is the mesotelm, which occurs at the approximate depth of the minimum water table during the warm summer months (Joosten and Clarke, 2002). A diverse range of aerobic and anaerobic microbial communities populate these various regions, and their proportional role in decomposition varies with changes in water table levels (**Figure 1**). Changes in abundance of these different microbial communities have the potential to alter carbon dynamics and nutrient cycling.

Microbiota process the turnover of organic carbon and are instrumental for the mineralization of nutrients in peat (Andersen et al., 2013). A relationship has been demonstrated between microbial community composition and SOM formation at the molecular level in multiple studies (Snyder et al., 2004, Greenwood et al., 2006, Kallenbach et al., 2016) through the transformation of a wide range of plant-derived compounds into microbial biomass (Kögel-Knabner, 2002). Moreover, microbial communities can be linked to functional processes in these ecosystems. Specialized organisms tend to appear within peat as ecosystem mosaics in response to vegetation, physio-chemical and hydrological characteristics (Andersen et al., 2013,

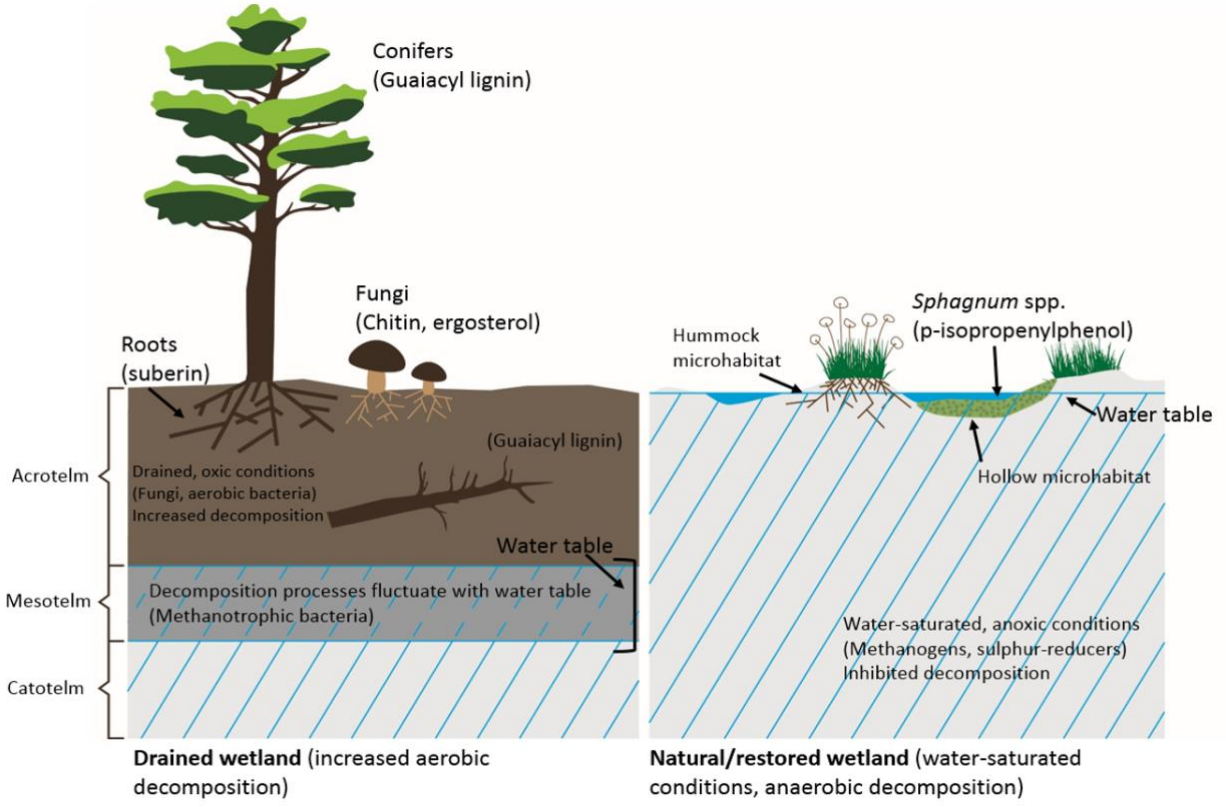

Figure 1. Schematic of typical observable community structure and example associated proxy biomarkers amenable to Py-GC/MS in boreal peatlands, with drained (left) and natural (right) ecosystems depicted.

Dedysh et al., 2006). The presence of fungal or bacterial residues in the profile can provide information about previous climate, above-ground plant communities, or hydrological conditions (Andersen et al., 2013, Peltoniemi et al., 2012, Gałka et al., 2018). For example, fungi play a primary functional role in decomposition in oxic upper layers (Andersen et al., 2013, Thormann et al., 2003). As conditions shift with depth from aerobic to anaerobic, microbial communities also change in composition, with bacterial communities increasing in abundance through the mesotelm and catotelm. Due to anoxic conditions and decreased availability of substrate, the role of bacteria in decomposition is thought to be less substantial compared to degradation initiated by fungi in the upper strata.

Changes in peat quality or composition also lead to changes in hydraulic conductivity, which can impact water table levels (Joosten and Clarke, 2002, Rezanezhad et al., 2016). This leads to shifts in the above-ground plant community, which creates further changes in the quality and composition of the peat (Wassen and Joosten, 1996), setting up a feedback mechanism that, depending on the direction of the vegetative shift, either encourages or discourages peatland degradation. Further, peatland ecosystems are also strongly influenced by natural and anthropogenic fires (**Section 2.6**). Boreal peat fires affect both soil formation processes and the future stability of C pools stored within, via the formation of pyrogenic carbon (Preston and Schmidt, 2006).

When peatlands are drained, a general succession pattern occurs from floating, submerged plants (*Sphagnum*), to emergent facultative aquatics (sedges), and an eventual transition towards that of forested habitats (Laiho et al., 2004, Strack et al., 2006, Neuhäusl, 1992). When restored, a reverse successional process can also occur (Klinger, 1996). These vegetation pattern shifts, whether due to climate variation (periods of drought) or drainage for agriculture, may be visible on the molecular level as shifts in OM chemical composition. Due to the importance of the predominating plant species as the driver in peatland community structure, shifts in the abundance of contributing plant material alone can communicate changes in paleo-environmental or climate conditions in a peat bog (Schellekens and Buurman, 2011). However, a more complete understanding of these ecosystem-wide changes can be obtained through systematic incorporation of microbial community data into existing plant community molecular analyses.

2.4 Plant biomarkers

For plant biomarkers, an important desired analytical distinction is the relative contribution of vascular plants (higher plants), and non-vascular plants, which are predominately represented in peat ecosystems as bryophyte mosses. Generally, in boreal ecosystems, increased cover of *Sphagnum* moss is an indicator for inundated conditions, whereas vascular plants (*Ericoid* spp., *Eriophorum* spp., *Pinus* spp.) tend to require drained conditions for roots to establish.

Table 1 provides a list of identified plant biomarkers amenable to analytical Py-GC/MS serving as useful plant indicators in peatland ecosystems, as well as typical observed pyrolysis products when applicable (categorized by compound class). Lipids are operationally defined in these classifications and are treated as a compound class in both plant and microbial biomarker tables in this review. A discussion follows of the most widely used biomarkers identifying plant components in current Py-GC/MS studies, as well as research areas requiring further attention in the field.

This survey is considered to be a broad overview of the available literature on the topic and may not include biomarker studies for lesser-known endemic plant species, or highly specific biomarkers for unique ecosystems. It is important to note that, depending on the predominant vegetation at the surface (ie., moss vs graminoid-dominated vegetation), markers may also demonstrate different decomposition kinetics throughout the depth of the profile. In addition, while an important part of the ecosystem, phreatophytic vascular plants have the potential to penetrate deeper peat layers via their root structures, changing decomposition dynamics and generating artificially "young" signals in otherwise older parts of the profile. If not removed prior to analysis (which is not always possible in highly degraded systems), the effect of these roots must be considered in the overall molecular analysis of the profile, particularly with regards to associated ^{14}C dating studies (**Section 2.8.2**).

Table 1. Example plant biomarkers obtainable by Py-GC/MS. Bold denotes peat studies.

	Compound class	Selected Example Biomarkers	Contributing organisms	Remarks	Relevant Py-GC/MS Studies
Lignin	Guaiacol and related guaiacyl derivatives	2-methoxy-Phenol (Guaiacol), p-methylguaiacol (Creosol), 4-ethyl-2-methoxy-Phenol (p-ethylguaiacol), 2-Methoxy-4-vinylphenol (p-vinylguaiacol), 2-methoxy-4-(2-propenyl)-Phenol (Eugenol), 2-methoxy-4-(1-propenyl)-Phenol (isoeugenol), 4-Hydroxy-3-methoxybenzaldehyde (vanillin), 3-hydroxy-4-methoxy-benzaldehyde (isovanillin)	Gymnosperms	Guaiacyl derivatives without presence of syringyl or p-hydroxyphenyl derivatives suggests coniferous species	(Saiz-Jimenez and De Leeuw, 1986, Martin et al., 1979)
	Syringol and related syringyl derivatives	2,6-dimethoxyphenol (Syringol), 1,2,3-Trimethoxybenzene (Methylsyringol)	Angiosperms	Syringyl derivatives in equal amounts to guaiacyl derivatives (absence of p-hydroxyphenyl) suggests angiosperms	**(Schellekens et al., 2009, Huang et al., 1998, Saiz-Jimenez and De Leeuw, 1986)**
	p-hydroxyphenyl derivatives	4-vinylphenol	Non-specific lignin indicator	Suggests grass (herbaceous non-woody) lignin when present in equal amounts to guaiacyl & syringyl	**(Kaal et al., 2017, Saiz-Jimenez and De Leeuw, 1986)**

Table 1. Example plant biomarkers obtainable by Py-GC/MS. Bold denotes peat studies.

	Compound class	Selected Example Biomarkers	Contributing organisms	Remarks	Relevant Py-GC/MS Studies
	Acids, Aldehydes, ketones of vanillyl, syringyl, and cinnamyl structures (Kögel-Knabner & Amelung, 2014)	4-hydroxy-3-methoxy-Benzoic acid (Vanillic acid), 1-(4-hydroxy-3-methoxyphenyl)-2-propanone (Vanillyl methyl ketone), 3-phenyl-2-Propenoic acid, (Cinnamic acid), 3-phenyl-2-Propenal, (Cinnamaldehyde)	Various vascular plant materials	Acid to Aldehyde ratio (Ac/Al) relative index for decomposition (Jex et al., 2014; Thevenot et al., 2010)	(Kisand et al., 2013)
Other polyphenols		4-isopropenylphenol	*Sphagnum* spp	Highly specific biomarker sensitive to changes in peat water table	**(Stankiewicz et al., 1997, Van der Heijden et al., 1997, McClymont et al., 2011, Schellekens et al., 2015a, Schellekens et al., 2009)**
Polysaccharides	Sum of polysaccharides	Pyrans, furans (examples: Furfural, 5-methyl-2-Furancarboxaldehyde, 4-Cyclopentene-1,3-dione, Ethanone, 1-(2-furanyl)-, 5-hydroxy-2-methyl-4H-Pyran-4-one, 5-hydroxymethylfurfural, 1,6-anhydro-β-D-glucopyranose, (levoglucosan))	Moss vegetation	In peat, may indicate high moss contribution & intact OM. **Not valid in aerobic systems**	**(Schellekens and Buurman, 2011, Schellekens et al., 2009)**
	Pentoses (arabinose and xylose)	Levoglucosan	Cellulose from fresh plant tissue		**(Fabbri and Helleur, 1999)**
Lipids/waxes	Aliphatic biopolymers	"Free" alkanes (C23-33) with no corresponding alkene	Leaf waxes of higher plants	Typically odd C predominance	**(Schellekens and Buurman, 2011)**
	Aliphatic biopolymers	n-C23-25 alkanes	Non-vascular plants (bryophytes)		**(Buurman et al., 2006, Schellekens**

Table 1. Example plant biomarkers obtainable by Py-GC/MS. Bold denotes peat studies.

	Compound class	Selected Example Biomarkers	Contributing organisms	Remarks	Relevant Py-GC/MS Studies
					and Buurman, 2011)
	Aliphatic biopolymers	n-C27-33 alkanes	Vascular plants		**(Schellekens and Buurman, 2011, Buurman et al., 2006)**
	Aliphatic biopolymers	mid-chain n-alkanes	Cutans & suberans (plant tissue)		**(Schellekens and Buurman, 2011, Nierop, 1998)**
	n-alkanols	n-C20, C22, C24 linear alcohols	Suberin in bark and roots		**(Buurman et al., 2006)**
	Ester-bound aliphatics	Suberin/cutin	Bark, rootlets		(Nip et al., 1986, Van Smeerdijk and Boon, 1987)
Terpenoids	Diterpenoids	Prist-1-ene/Prist-2-ene (from phytol)	Plant chlorophyll-a cleavage during pyrolysis (Ishiwatari et al., 1991)		(Ishiwatari et al., 1991, Carr et al., 2010)
	Triterpenoids	Taraxerol, taraxerone	Major constituent of cork in woody plants		(Van Smeerdijk and Boon, 1987, Killops and Frewin, 1994)
	Diterpenoid acids	Abietanoic acids, pimaric acid	Pine species		(Schellekens et al., 2013)

2.4.1 Non-vascular plants (*Sphagnum* mosses)

When using Py-GC/MS to screen for an overall contribution of non-vascular plants in peat, bryophytes can be identified through the presence of non-hydrolyzable aliphatic biopolymers in the C23-25 length range. However, for bogs dominated by *Sphagnum* spp., 4-isopropenylphenol is a well-tested and highly specific biomarker for the presence of *Sphagnum* moss and is highly amenable to Py-GC/MS analysis. (McClymont et al., 2011, Schellekens et al., 2009, Van der Heijden et al., 1997, Stankiewicz et al., 1997). This marker is useful not only due to its specificity to *Sphagnum* spp., but also because of the compound's apparent sensitivity to changes in the water table (Schellekens et al., 2015a), enabling its abundance to be used as an indicator of changes in hydrological regime and degradation status. (Schellekens et al., 2015a) measured 4-isopropenylphenol in *Sphagnum*-dominated peatlands, (with primary contributions from *S. centrale* and *S. subsecundum* and minor contributions from *S. palustre* and *S. magellanicum*). Due to the historical dominance of *Sphagnum* moss in the peat profile core, they concluded that observed variations (0.21-2.85% of the total ion current) in the biomarker abundance were unlikely to be caused by changes in the contribution of moss to the peat, but rather from variations in aerobic decomposition. As a result of their findings, these authors also concluded that inhibition of decomposition in *Sphagnum*-dominated ecosystems might not be due to the contribution of *Sphagnum*-contributed phenolics (such as 4-isopropenylphenol), as had been previously thought; but rather, that abundant presence of these phenolics suggested that water-logged conditions and anaerobic decomposition were already present in the peat profile.

In addition to climate/hydrological-derived shifts, 4-isopropenylphenol has also been used as a biomarker to reflect the influence of regional ecosystem events. 4-isopropenylphenol was used to confirm data demonstrating that airborne nutrient-depositing mineral dust corresponded with a seven-fold increase in net accumulation in Store Mosse (the "Great Bog"), a nutrient-limited ombrotrophic bog in southern Sweden (Kylander et al., 2018).

2.4.2 Vascular plants

2.4.2.1 Aliphatic biopolymers

In Py-GC/MS studies, non-hydrolyzable aliphatic biopolymers can be useful biomarkers for the differentiation of plant and microbial material. These biopolymers can include n-alkane/alkenes, alkanols, and alkanoic acid classes (Buurman et al., 2006). Long chain fatty acids are associated with higher plant leaf waxes (C27-33), whereas short chain fatty acids tend

to be associated with algal or microbial material (Buurman et al., 2006). Linear alcohols (C20, C22, C24) are also generally abundant and derived from cutan and suberan compounds in bark and root structures of higher plants (Buurman et al., 2006, Kögel-Knabner, 2002, Nierop, 1998, Nip et al., 1986, Van Smeerdijk and Boon, 1987).

N-alkane abundances can also be expressed in the form of lipid ratios. As examples, average chain length provides a reference index for higher plants (De la Rosa et al., 2012), whereas carbon preference index compares the abundance of odd (plant-derived) and even (microbial-derived) C-numbered *n*-alkanes to determine the degree of transformation of plant-based material (Zhou et al., 2005, Chambers et al., 2012, Schellekens and Buurman, 2011). Another widely applied proxy compares C_{23} alkanes, where high abundances have been shown to be dominant in *Sphagnum* spp.; to C_{29}, C_{31}, and C_{33} alkanes, which are dominant in vascular plants (Schellekens et al., 2009, Baas et al., 2000). When the distribution of these n-alkanes is compared as a "Sphagnum/vascular" ratio, they provide an indicator for surface moisture (Nichols et al., 2006).

Anaerobic conditions generally inhibit vascular plant growth, and lower plants (such as bryophytes) favor short or medium-chain n-alkane production. However, n-alkane chain length reduction has also been reported in aerobic decomposition of peat (Schellekens et al., 2009, Buurman et al., 2006), which can lead to confusing interpretations of the original vegetation source. N-alkane analysis may also present difficulties on certain instrumental Py-GC/MS configurations. Precise molecular interpretation of n-alkane signals via Py-GC/MS can be challenging. Low intensity molecular ion peaks (ions of the original neutral molecule used to determine molecular weight and probable elemental composition) are characteristic of straight and branched chain aliphatic mass spectra and can be difficult to distinguish from background noise (Sparkman et al., 2011). In addition, in the case of instrument configurations prone to cold spots or working in tandem with temperature-limited transfer lines, medium to long-chain aliphatics can be lost to analysis. Moreover, while n-alkane abundances between plant species may differ widely, they are not species-specific compounds (Schellekens and Buurman, 2011). For this reason, while aliphatic distributions remain a useful tool for correlating vegetation type, they may not always be the most reliable biomarkers for peat OM characterization where shifts in decomposition mechanisms have the potential to interfere with their chemistry.

2.4.2.2 Lignin-derived phenols

For the identification of vascular plants in peatland profiles, perhaps some of the most descriptive and informative biomarkers obtainable via Py-GC/MS are lignin-derived phenols (Martin et al., 1979). Lignin is formed almost exclusively in terrestrial vascular plants, where it forms the structural support material in cell walls and provides chemical resistance to biodegradation. It contributes a major OM component to plant litter, and is one of the most abundant known organic polymers in aboveground terrestrial ecosystems, second only in abundance to cellulose. Lignin is a class of highly complex organic polymers composed of aromatic subunits that are highly heterogeneous in structure. These polymers are derived chiefly from three main methoxylated alcohol monomers: coumaryl alcohol, coniferyl alcohol, and sinapyl alcohol, which are precursors to p-hydroxyphenyl (of lignin and non-lignin origin), guaiacyl (vanillyl) and syringyl phenylpropanoid subunits that are incorporated into the larger lignin polymer (Boerjan et al., 2003).

The amount and composition of each of these subunits varies by plant taxa and tissue origin, and can be used to classify contributing source material (Hedges and Mann, 1979, Kögel-Knabner and Amelung, 2014). For example, gymnosperms contain mostly guaiacol subunits; whereas angiosperms contain equal parts of guaiacol and syringol subunits (Saiz-Jimenez and De Leeuw, 1986). The sum of the relative abundance of all lignin subunits can be used to calculate the total vascular plant contribution (total lignin phenols). Alternatively, relative contribution of each of the three subunits can be determined, and can serve as a predictable method for distinguishing different contributing plant taxa in SOM. Lignin subunits such as syringyl (S), vanillyl (V), and cinnamyl (C) groups can be represented as ratios, which can be used to distinguish between gymnosperms (S/V=0) and angiosperms (S/V>0), or as an indicator for the degree of oxidative decomposition in soil, such as lignin-derived acid-aldehyde ratios (Thevenot et al., 2010, Jex et al., 2014, Kisand et al., 2013).

Py-GC/MS studies incorporating lignin analysis are ubiquitous in biogeochemistry literature and incorporate a variety of methods to investigate degradative changes in SOM. Molecular changes are dependent not only on the dominant contributing lignin source, but also the primary degradation mechanisms (aerobic vs anaerobic). For example, in a 23-year *Calluna vulgaris* peat study, (Huang et al., 1998) used Py-GC/MS to characterize changes in the molecular composition of decomposing plant litter with degradation. Consistent with other literature, (Jex et al., 2014), these authors found that syringyl subunit decomposition tended to be favored over

guaiacyl subunits, and that with increasing decomposition, lignin alcohol moieties oxidized to their corresponding aldehydes or ketones. In contrast, Schellekens and others used lignin biomarkers to explore the source and transformation of contributing vascular plants in graminoid-dominated peatland ecosystems (*Carex* spp., *Agrostis* spp. etc.), and conditions affecting their abundance (Schellekens et al., 2012, Schellekens et al., 2015c). They found preferred decomposition of guaiacyl over syringyl subunits through multiple stages of decomposition, and suggested that lignin decomposition mechanisms may be heavily dependent on plant-derived source chemistry.

Historically, lignin has been considered to be one of the most important proxies for vascular plant litter input. Guaiacyl lignin-derived pyrolysis products have been identified in Pliocene and Pleistocene aquifer sediments (Hartog et al., 2004). Unlike mineral soils, where organo-mineral associations and other stabilization mechanisms play an important role, chemical recalcitrance is a major factor for C stabilization in organic soils, where the slow process of anaerobic degradation and enzymatic inhibition are primary mechanisms for lignin preservation (Freeman et al., 2001).

While anaerobic conditions and enzymatic inhibition can result in the accumulation of lignin-derived compounds with depth in intact peatlands (Freeman et al., 2004), degraded peatlands undergoing increased aerobic decomposition can also be identified through their decreasing lignin content. For example, a decrease in the total lignin signal occurring with a corresponding increase in signals suggestive of fungi (such as chitin-derived biomarkers, see **Section 2.5.1**), could be considered a strong indicator for processes favoring aerobic decomposition. (Zhang et al., 2019) investigated shifts in the relative abundance of lignin and other compound classes to assess the impacts of changes in land use on OM chemistry in the Florida Everglades, demonstrating a substantial reduction of lignin fractions in the profile when peatlands were converted to agricultural use. This reduction in lignin content was considered evidence of SOC destabilization as soil microbial communities shifted in response to changing environmental conditions caused by ecosystem drainage and tilling (Ye et al., 2009). As field management activities introduced aerated conditions to the marshlands, they concluded that changes in the dominant microbiota led to increasing SOC mineralization and accelerated decomposition of otherwise "stable" lignin fractions, in agreement with the earlier findings of (Feng et al., 2008).

Frequently-used sample preparation techniques in SOM studies have been shown to release chemically similar organic phenols which might otherwise be attributed to lignin (such as tannins or suberins), thus potentially overestimating lignin's contribution (Jex et al., 2014). Ongoing research should work to further constrain lignin decomposition kinetics so that carbon modelling uncertainty can be improved (Wieder et al., 2018).

2.4.3 Other areas of peat plant biomarker research

5-n-alkylresorcinols are a useful biomarker for graminoids, and GC/MS studies have been conducted for this purpose (Avsejs et al., 2002, José et al., 2013, Żarnowski et al., 2002). However, with a few noted exceptions (Derenne et al., 1992), while cited as a specific biomarker for sedges in pyrolysis studies (McClymont et al., 2011, Buurman et al., 2006), other studies were not found using Py-GC/MS methodology to identify pyrolysates confirming the presence of this biomarker in peat OM at the time of this review. Future correlation of n-alkylresorcinol abundance with the presence of graminoids in peat is needed to determine its usefulness as a Py-GC/MS-amenable biomarker.

While not in the plant family *per se*, lichens are an important part of peatland ecosystems, and may be a strong indicator for limitations on peat growth, due to their occurrence in dry conditions in peatlands (Harris et al., 2018). In a study assessing the use of potential biomarkers identified via Py-GC/MS analysis, (Schellekens et al., 2015b) found that the phenolic compound 3-methoxy-5-methylphenol occurred exclusively in lichen species, though it was not ubiquitously present in every species tested. Continued Py-GC/MS work confirming the association of this compound with lichen species in peat could help to elucidate previous dry conditions in palaeo-ecological analysis, especially in cases where lichens are not visible in macroscopic analysis.

2.5 Microbial biomarkers

In comparison to plant biomarkers, far fewer studies directly explore the relative contribution of microbes and microbial residues in peatland profiles, particularly with respect to their role in decomposition and nutrient recycling (Andersen et al., 2013). Numerous studies have demonstrated the potential for biomarkers to distinguish pockets of microbial communities in the peatland profile, and to use this information to correlate changes in community composition with changes in the surrounding environment. Using different techniques, microbial biomarkers

have been used to estimate biomass (Wallander et al., 2013), track microbial community response to regional changes in hydrology or climate (Inglis et al., 2015, Jaatinen et al., 2008, Lopez-Dias et al., 2013, Pancost et al., 2007), and follow relationships between microbial communities and dominant peat-forming vegetation (Kip et al., 2010). The search is also underway for organism and process-specific biomarkers (Eglinton and Eglinton, 2008), which could be used to elucidate microbial functional roles in the palaeo-ecological profile.

Table 2 provides a list of identified microbial biomarkers (differentiated by specificity for fungi and bacteria) amenable to analytical Py-GC/MS, as well as typical observed pyrolysis products. While not necessarily specific to fungi or bacteria, some hexoses (galactose, mannose, fucose, rhamnose) are primarily produced by microbial organisms, and useful in general biomarker analyses seeking to estimate overall microbial contribution (Nierop et al., 2005, Huang et al., 1998). Similar to lipids, nitrogen (N)-containing compounds are considered to be operationally defined and are treated as a compound class. A discussion of the most widely used biomarkers denoting fungi and bacteria in current Py-GC/MS studies follows, as well as areas requiring further research. It is important to note that while Py-GC/MS studies exist assessing the molecular fingerprint of microbial organisms and analyzing the relative contribution of different chemical classes (Eudy et al., 1985), far fewer organism-specific biomarkers have been identified via Py-GC/MS for microbial communities in comparison to plant-based studies. This topic remains an unexplored area needing additional research. Areas where new Py-GC/MS amenable biomarkers will be particularly useful in assisting OM molecular characterization of important peatland microbial taxa are further discussed in **Section 2.5.3**.

Table 2. Example microbial biomarkers obtainable by Py-GC/MS. Bold denotes peat studies.

	Compound class	Selected Example Biomarkers	Contributing organisms	Remarks	Relevant Py-GC/MS Studies
Fungi					
N-containing Compounds	(N-acetylglucosamine)	Acetamide, acetylpyridones, acetamidofuran, 3-acetamideo-5-methylfuran, 3-acetamido-(2 and 4)-pyrones from chitin	Fungal biomass (living and non-living)	Can also derive from gram positive bacterial cell walls during pyrolysis (see discussion)	(Arthur Stankiewicz et al., 1996, Kaal et al., 2017)
Lipids	Sterols	Ergosterol	Living fungal biomass		(Parsi and Górecki, 2006)
Bacteria					
N-containing compounds	Amino sugars (Muramic acid, Galactosasmine)	2-pyridinecarboxamide	Gram positive bacteria		(Dworzanski et al., 2005)
Polysaccarides	Lipopolysaccharides	3-hydroxymyristic acid	Gram-negative bacteria	From cell wall structures	(Snyder et al., 2004, Dworzanski et al., 2005)
Lipids	Aliphatic biopolymers	Short chain n-alkanes (C14-C20)	Bacteria/algae	From cell wall compounds	**(Buurman et al., 2006)**
Terpenoids	Triterpenoids	Hopanes/Hopanoids (Pentacyclic triterpenoids)	Bacteria (gram-negative, methanotrophs, cyanobacteria, acetic acid bacteria, N-fixing, purple non-sulfur spp)		(Sugden et al., 2005, Greenwood et al., 2006, Carr et al., 2010)

2.5.1 Fungi

In fungi, chitin and ergosterol are two of the more commonly analyzed chemical markers in Py-GC/MS analysis. Chitin is generally considered a stable parameter for biomarker assessment of total fungal contribution to microbial tissue in soil (Kaal et al., 2017). Acetamide is a well-established pyrolysis product of chitin, and can be used as an indicator in Py-GC/MS analysis (Arthur Stankiewicz et al., 1996). However, it is noted that (Eudy et al., 1985) also identified acetamide as a pyrolysis product of glucosamine in bacterial cell walls in a comparative Py-GC/MS study of gram positive and gram negative bacteria. Both fungi and gram positive bacteria contain glucosamine; where fungi incorporate glucosamine in the form of chitin, and gram positive bacteria do so in the form of peptidoglycan. However, as fungal cell walls contain substantially larger amounts of glucosamine in the form of chitin than bacteria, they are considered to be the major contributor of this soil component.

Ergosterol, the primary sterol in fungal cell membranes, has also been described as a useful chemical biomarker for fungi (Madonna et al., 2001, West et al., 1987). Produced almost exclusively by fungal organisms, ergosterol becomes oxidized shortly after cell death and has been suggested as a proxy to estimate living fungal biomass in environmental samples (Stahl and Parkin, 1996). Ergosterol is a high molecular weight compound that may be prone to compound discrimination in Py-GC/MS instrument set-ups with cold spots or temperature-limited transfer lines. However, (Parsi and Górecki, 2006) used non-discriminating flash Py-GC/MS to detect the presence of ergosterol in different samples (including baker's yeast, indoor dust, and a leaf infected with a powdery mildew), and found that the compound was detectable in a variety of matrices with no sample pre-treatment. While ergosterol is currently one of the most useful known biomarkers for estimating living fungal biomass, inter- and intra-species specific variation in fungal ergosterol content has been reported (Joergensen and Wichern, 2018, Olsson et al., 2003). In addition to other methods for estimation of fungal biomass in environmental systems, (Wallander et al., 2013) has provided a thorough review of the advantages and limitations of the use of ergosterol and other microbial biomarkers.

2.5.2 Bacteria

All eubacterial cell walls contain peptidoglycan, a polymer consisting of alternating peptide and carbohydrate units. As much as 75% of bacterial biomass can be attributed to this compound, which has been used as a classic biomarker for microbial activity, particularly for gram positive species (Joergensen and Wichern, 2008, Killops and Killops, 2013, Schleifer and

Kandler, 1972). Attention has also been given to the glycan moiety of peptidoglycan, muramic acid, as a potential biomarker (Zhang and Amelung, 1996, Joergensen and Wichern, 2008). 2-furanmethanol (furfuryl alcohol) has been suggested as a specific pyrolysate biomarker attributable to the evolution of peptidoglycan (Eudy et al., 1985). However, as a chemical compound, 2-furanmethanol is fairly ubiquitous, and could be contributed to other sources (Morgan et al., 1990), including cellulose (Hassan et al., 2009).

Bacterial cell walls are also surrounded by lipid-based compounds, such as lipoproteins, lipopolysaccharides (LPS), and phospholipids. As a characteristic example of a bacterial LPS, Lipid A is present exclusively in gram-negative bacteria. At the time of this review, insufficient data exist to indicate the presence of organism-specific LPS biomarkers determined via Py-GC/MS analysis. While certain bacterial components such as 3-hydroxymystric acid contain large quantities of LPS, in a mixed matrix such as peat, these components can originate from multiple sources. LPS biomarkers may be useful for screening for the presence of gram positive or gram negative bacteria in a single-source matrix, but in complex organic matrices, their distinguishing power remains questionable.

Hopanoids are relatively stable lipids (Kip et al., 2010) generally attributed to aerobic bacteria (Lopez-Dias et al., 2013, Talbot et al., 2003). These compounds tend to be favored in acidic environments, and have been used as both a general marker for microbial biomass (Sugden et al., 2005), as well as for the more specific identification of methanotrophic bacteria across a variety of different analysis techniques (Greenwood et al., 2006, Pancost et al., 2007, Inglis et al., 2015). For anaerobic archaea, archaeol, sn-2-hydroxyarchaeol, and crenarchaeol have been used to provide a record for fossil biomass of methanogens in ombrotrophic bogs (Pancost et al., 2011, Lim et al., 2012, Eglinton and Eglinton, 2008), and are further discussed below.

2.5.3 Potential areas of peat microbial biomarker research

Organism-specific biomarkers amenable to Py-GC/MS are particularly needed to identify and distinguish aerobic and anaerobic microbiota, as these organisms serve different functional roles in global C cycling. In addition, biomarkers that clearly denote past microbial communities deeper in the profile are lacking (Pancost et al., 2011).

Obligate anaerobes in peatland communities can provide evidence for the current location of the catotelm, as well as an indication of former water table levels in the peat profile. Changes

in water table levels, such as re-inundating drained areas, could result in an initial increase in substrate for anaerobic organisms, and rewetting of drained peatlands can generate an increase in methane production via increased activity of anaerobic organisms (**Section 2.7.4**). Understanding the relationship between microbial communities and methane production in peatlands is crucial in order to assess methane's long-term atmospheric budget and its relationship to warming mitigation strategies, particularly as methanogens are highly temperature sensitive (Christensen et al., 2003, Høj et al., 2008). The glycerol dialkyl diether tetraether (GDGT) lipid archaeol has been suggested as a proxy able to assess and compare methanogenic biomass across different systems (Pancost et al., 2011, Lim et al., 2012). However, while GDGT lipids are a highly useful class of biomarkers for microbial analysis and may also be identifiable using Py-GC/MS techniques, at the time of this review, no studies investigating GDGT compounds via Py-GC/MS methods were identified. Characterizing pyrolysates of GDGT lipids may produce useful biomarker compounds that could be used in future Py-GC/MS studies, with the result of improving applicability and robustness of the Py-GC/MS method while also serving as an additional way to confirm GDGT lipid analysis results obtained via other methods.

2.6 Biomarkers as indicators of fire and pyrogenic carbon stores

Peatland fires have been linked to anthropogenic agro-pastoral activities since the Neolithic period (Rius et al., 2009). Peat biomass burns rapidly on both vertical and lateral gradients, and fires have long-term effects on OM decomposition in the ecosystem. Drainage activities permit ignition of material deeper in the peat profile, increasing the severity of smoldering combustion (Hu et al., 2018) and release of greenhouse gases (Rein et al., 2008). Boreal peatland fires initially result in a large release of CO_2 through the combustion of biomass, and heightened rates of OC loss are predicted through higher temperature profiles of burned soils (Allison and Treseder, 2011). Tropical peat swamp forests (such as those in Southeast Asia) are especially vulnerable to large-scale intense fires, as these ecosystems undergo widespread deforestation and drainage during conversion to oil palm and pulp tree plantations (Page et al., 2011, Hooijer et al., 2010).

Peatland fires result in the formation of pyrogenic carbon (PyC); C-enriched OM that is highly resistant to oxidation and degradation. PyC's degradation-resistant properties may serve as an important sink in the global C cycle (Seiler and Crutzen, 1980, Schmidt and Noack, 2000). PyC

conversion varies by contributing fuel components, but recent estimates of typical boreal forest fires have found that almost one-third (27.6%) of fire-affected C is converted to PyC (Santín et al., 2015). If translated into production for all boreal regions, this results in an annual production more than five times PyC production amounts reported previously, suggesting that this under-estimated C stock may be part of the missing sink in the global C balance (Santín et al., 2015).

Organic soils contain on average between 13-14 percent (PyC) of total SOC (Leifeld et al., 2018), very similar to average values (13.7 percent) reported for mineral soils (Reisser et al., 2016). However, due to the greater SOC storage capacity in organic soils, overall pyrogenic carbon stocks are much higher (5.8 kg C m^{-2})(Leifeld et al., 2018), and exceed values reported for mineral soils (0.014-0.02 kg C m^{-2}) (Czimczik et al., 2003) by as much as three orders of magnitude. Warming global temperatures are likely to result in increased incidence and intensity of peatland fires. Research elucidating the long-term response of microbial communities and subsequent soil respiration on decomposition of OM after burning events is vital to understanding the fire-derived feedback mechanisms most pertinent to climate change (Allison and Treseder, 2011).

Macroscopic charcoal analysis has typically been done to determine fire history; however, molecular analysis of extractable SOM using Py-GC/MS suggest that visual methods (similar to macroscopic analysis of plant remains) underestimate the PyC record (Kaal et al., 2008b). Fire biomarkers are needed to better understand the influence of fire occurrence in natural and degraded peatland profiles, as well as to better understand the mechanisms behind its preservation. Interpretation of PyC biomarkers obtained via Py-GC/MS can be challenging, as compounds indicative of combustion can also be produced as artifacts during the pyrolysis process. As an example, it has been argued that benzene and toluene are major PyC pyrolysis products (Kaal et al., 2008b, Rosa Arranz, 2007). However, benzene can also form as a secondary pyrolysis byproduct of components such as lignin, and toluene has been associated with pyrolysis of degraded proteins (Fuhrmann et al., 2004), as well as the breakdown of *Sphagnum*-derived phenols during microbial decomposition (Schellekens et al., 2009). As such, while a large contribution of these two aromatic compounds is indicative of a PyC origin, they should not be used solely as determinants of PyC content. However, if analyzed concurrently with the abundance of methoxyphenols or catechols, an inverse relationship is highly suggestive of aromatic PyC origin (Kaal et al., 2008b). Methoxyphenols and catechols are direct pyrolysis products of lignin, which decreases in abundance after peatland fires as fresh vegetation is

replaced by charred OM. Increasing abundance of benzofurans occurring concurrently with a decrease in abundance of polysaccharide compounds has also been suggested as a general indicator of fire occurrence (Schellekens et al., 2009, Kaal et al., 2008b).

Py-GC/MS amenable biomarkers have been identified that provide relatively confident characterization of PyC-derived material. Benzenepolycarboxylic acids (BPCAs) can serve as a biomarker for pyrogenic carbon in organic soils (Glaser et al., 1998), and have been investigated using Py-GC/MS (Kaal et al., 2008a). Heterocyclic N compounds such as pyrrole and indole have been shown to be produced upon heating of peat (Almendros et al., 2003), and may be a mechanistic step in the stabilization of pyrogenic carbon (Knicker, 2007). Other Py-GC/MS amenable compounds that have been reported to be of almost certain PyC origin include polyaromatic hydrocarbons (PAHs) (González-Pérez et al., 2014), benzonitrile, and isoquinoline (Kaal et al., 2008b). (González-Pérez et al., 2014) examined the reliability of Py-GC/MS analysis to identify the presence of PAHs in a variety of different environmental matrices, and found the method to be highly effective in characterizing not only incidents of fire, but also the intensity of the fire, depending on the type of PAH compounds present (for example, cata-condensed vs peri-condensed PAH structures).

Peat fires contribute different quality PyC depending on the temperature of the fire. Smoldering fires are especially problematic, as these fires can consume the pyrogenic char they produce, leading to an invisible fire record in the profile (Zaccone et al., 2014). As such, palaeofire events have been confused in previous analyses as atmospheric dust deposition or climate shifts (Zaccone et al., 2014). Improved molecular methods of palaeofire identification are needed to distinguish these events, and better constrain PyC's true contribution to the global C stock.

2.7 Challenges in interpreting biomarkers in peat

Palaeo-vegetation analysis operates on the assumption that the abundance of plant remains (whether reflected through molecular biomarkers or through macroscopic methods) provides a relatively accurate reflection of the surface vegetation at the time of deposition (Blackford, 2000). Despite the specificity Py-GC/MS analysis offers to determine the molecular components of a sample, some questions remain regarding how representative biomarker compounds are of the original peatland community. The following section presents an outlook on questions and limitations that should be considered when analyzing data obtained via Py-

GC/MS techniques. In some cases, targeted Py-GC/MS studies could be done to improve the knowledge gaps underlying these uncertainties, while in others, an integrated multi-disciplinary approach may be needed to better understand the overall system.

2.7.1 Variability in biomarker recalcitrance

While, like all analytical methods, potential areas of molecular discrimination exist (as previously discussed in this review), a major benefit of the Py-GC/MS method is its broad capacity to measure a wide range of chemical compounds typically present in complex soil organic matter samples. However, it is important to note that selective preservation of compounds within the SOM matrix can present challenges to researchers using Py-GC/MS in an attempt to, for example, reconstruct palaeo-ecological environmental conditions. Different compounds contributing to SOM have highly variable chemical composition, and subsequently, considerable variability in inherent chemical reactivity, i.e., recalcitrance, at the molecular level in soil systems. In addition to their microbial "palatability," compound reactivity can be influenced by abiotic factors such as temperature or soil chemistry (changes in pH, cation exchange capacity, etc.), as well as exposure to other organic compounds such as root exudates, and aggregation effects. Chemical interactions and their effect on OM stabilization are not as well constrained in organic soils compared to mineral soils. Due to mounting evidence that disturbance could result in a release of soil C from "old" OM stores in large stocks such as peat, understanding the factors affecting OM preservation is crucial (Moore et al., 2013).

Currently, there is no consistent method for comparing the recalcitrance of the variety of different compounds identified in complex OM. However, the recalcitrance of many compounds used as biomarkers, assuming identical environmental conditions, may be unequal due to basic differences in their molecular structure. When characterizing the chemical components of OM, it would be informative to incorporate a method normalizing for recalcitrance of identified compounds before comparing their relative abundances to one another or considering the external factors influencing their preservation. Indices for measuring recalcitrance have been developed and applied to other materials (such as biochar) to assess their stability against microbial decomposition (Harvey et al., 2012), but an index-based approach has not yet been widely used to compare the wider range of chemical compounds detected in peat. Simple indices, such as redox potential or carbon oxidation states, could be used as an estimated indicator of compound recalcitrance in organic soils (LaRowe and Van Cappellen, 2011). Applying such indices to compounds identified via OM characterization

techniques (such as Py-GC/MS), would permit a more appropriate comparison of observed biomarker abundance, and potentially assist researchers in gaining a more accurate understanding of the factors influencing OM preservation and turnover.

2.7.2 Natural seasonal, topographical, interspecies, and phenotypic variability

Due to the volatilization part of the pyrolysis process, Py-GC/MS offers an opportunity to assess differences in chemical composition of a wide variety OM structural materials with minimal preparation. These structural materials must be clearly classified and differentiated prior to analysis with respect to different seasons, micro-habitats, plant species, life-stages, morphological components (leaves, stems, roots), and natural genetic variations, as all generate variability in the relative contribution of vegetative input pathways into OM. For example, hummocks (areas typically above the water table) and hollows (areas typically below the water table) result in clusters of diverse plant communities in the same peat ecosystem with unique adaptations to their individual niches. Net primary productivity differs between these microhabitats, resulting in variations in deposition of accumulated plant material (Turetsky et al., 2008). In addition, the morphology of plant species adapted to hummocks and those adapted to hollows often differs in composition, resulting in variability in molecular components and potential differences in decomposition rates (Johnson and Damman, 1991).

Plant structural components (leaves, stems, root structures) also demonstrate both different CN content and molecular composition. These components can also exhibit different rates of decomposition, even from within the same plant (Machinet et al., 2011). This is particularly an issue when comparing above- vs belowground plant inputs, as root-derived OC is retained more efficiently than aboveground biomass (Schmidt et al., 2011, Rasse et al., 2005). In the case of peat, where preserved aboveground biomass mixes with belowground plant inputs in the profile, interpretation of the source of chemical components can be confusing.

Without cautious data interpretation, environmental effects can be confounded by the above-described natural variability in input of available OM. As not all plants and structural components originally present at the surface at the time of vegetative deposition will be equally incorporated into the peat mass with depth, biomarker abundance measurements can be skewed to reflect the source of certain contributing OM matter more than any climatic changes contributing to its presence, when it is not necessarily the intent of the study to do so (Jansen and Wiesenberg, 2017). Certain species that for various *in situ* reasons are more resistant to

degradation can generate a misleading "species signal" (Chambers et al., 2012). Thus, while Py-GC/MS can generate a robust molecular fingerprint representative of the chemical components of many different types of OM samples, it is important that botanical shifts in the peatland profile are analyzed in tandem with complementary methods assessing overall decomposition to determine whether the variation of a biomarker is due to its relative contribution from the source plant to the peat profile, or if its presence could have been influenced by other factors (Schellekens et al., 2015b).

2.7.3 Distinguishing living and dead microbial biomass

As the microbial fraction in a peatland profile consists of both living and dead biomass, some uncertainty exists when differentiating whether organisms present are representative of living biomass or are part of the palaeo-ecological record. Some biomarkers (such as ergosterol) are components of cellular membranes in living organisms and break down quickly after cell death, making them useful indicators for living biomass (see **Section 2.5.1**). However, while ergosterol has been shown to be amenable to Py-GC/MS analysis (Parsi and Górecki, 2006), studies specifically tracing changes in abundance of ergosterol in peat soils were not identified at the time of this review. Moreover, in addition to the challenges described above, the effect of changing environmental factors (pH, temperature, growth conditions) on generally environmentally labile compounds (such as ergosterol) has also not yet been determined.

Most microbial matter in soil profiles consists of necromass material, and dormant living microbial biomass and microbial necromass differ in their long-term turnover (Joergensen, 2018). To differentiate between the two, a combined biomarker approach using ergosterol and chitin has been used to compare living microbial biomass with total microbial matter (Ekblad et al., 1998). The ratio of ergosterol:chitin provides a reasonable estimate for active fungal decomposition (as opposed to previously deposited microbial necromass). Such an approach is expected to be amenable to Py-GC/MS techniques, and has thus far not yet been conducted for peat samples. Muramic acid from bacteria also tends to accumulate in SOM, and together these compounds constitute a major component of the total soil microbial residue fraction (Joergensen and Wichern, 2018, Amelung, 2001). While alternative methods are available to estimate overall microbial biomass (**Section 2.5**), additional Py-GC/MS-amendable biomarkers able to distinguish between living microbial organisms and total microbial matter, particularly within peatland profiles, will be useful – especially for the purpose of screening soil profiles for the presence of these organisms prior to more detailed analyses (Eglinton and Eglinton,

2008).

2.7.4 Rewetting and restoration of disturbed sites

Impacts on microbial decomposition processes are not well understood in rewetted or restored peatland ecosystems (Andersen et al., 2010), and these ecosystems can exhibit different effects after restoration. For example, for restored peatlands experiencing a transitional increase in growth of peat-forming plants and a renewed input of fresh OM, fluctuations in the water table regime (or plant growth that outpaces the water table) can result in periods where the aerobic layers extend deeper into the profile than would otherwise occur in a stable undisturbed ecosystem. As a result, bacterial and fungal activity have been observed to be greater in restored peatlands than for natural peatlands (Andersen et al., 2010, Andersen et al., 2013, Glatzel et al., 2004). On the other hand, restored peatlands in early stages of transition or with fluctuating water table levels can also generate a temporary source of methane (Waddington and Day, 2007). Further, most rewetted peatland ecosystems have been restored within the last 50 years, whereas anthropogenic peatland drainage has been occurring for hundreds, if not thousands of years (Erkens et al., 2016). Many restored organic soils have not yet stabilized sufficiently to establish a clear pattern regarding C flux "equilibrium" and GHG fluxes (Frolking and Roulet, 2007, Belyea and Baird, 2006, Hilbert et al., 2000). Organism-specific bacterial biomarkers (targeting methanogens, for instance) could help to address these uncertainties, as a comparison of their relative abundance could identify the dominating source of microbial activity in transitioning rewetted peat. However, as previously discussed (**Section 2.5.3**), Py-GC/MS-amenable microbial biomarkers specific to anaerobic communities are currently lacking.

This is important to consider, as warming-induced increases in wetland methane emissions could dominate anthropogenic emissions in the 21st century (Zhang et al., 2017). Peatland C emissions, whether from carbon dioxide or methane, can be correlated to the contributing microbial organisms, such as aerobic fungi or anaerobic bacteria (Yavitt et al., 2000). Increased availability and variety in organism-specific microbial biomarkers amenable to Py-GC/MS would allow researchers to estimate changes in C flux resulting from changes in dominance of these microbial communities. Moreover, using Py-GC/MS biomarkers to measure changes in microbial community abundance as rewetted/restored peatlands transition could allow researchers to better constrain the amount of time they require to establish equilibrium conditions, while still using economical one-time sampling event schedules. This, in turn, could

help to better estimate (and eventually parameterize) the changing C balance of rewetted/restored peatlands as they transition towards ecosystem equilibrium.

2.8 Applications of pyrolysis biomarker studies in future peat research

Within the SOC cycle, peatlands are considered to be "high value" ecosystems. This review provides a summary of information obtainable through molecular fingerprinting of OM characteristic of these ecosystems. However, despite a number of studies spanning over the past three decades, many questions remain, for the purposes of which Py-GC/MS analysis could be usefully applied.

2.8.1 Developments in compound specific ^{13}C isotope analysis

Bulk stable C isotope analysis is a long-used analytical technique for exploring the dominating isotopic fractionation mechanisms in OM profiles (plant vs microbial pathways), and is considered to be a highly robust method for the assessment of decomposition changes in peat (Alewell et al., 2011). This useful technique provides an assessment of the overall isotopic ratio abundance of bulk soils, but cannot supply more specific isotopic information about contributing individual OM compounds without the incorporation of additional analytical methods. Pyrolysis-compound specific isotopic analysis (CSIA) is an emerging pyrolysis-based technique where pyrolysis products are directed onto a IRMS in order to measure the isotopic ratio abundance ($\delta^{13}C$, $\delta^{15}N$, $\delta^{18}O$, and $\delta^{2}H$) of specific compounds evolving in the pyrolysate (Jiménez Morillo et al., 2015).

CSIA has been successfully applied in studies investigating the isotopic composition of major carbohydrate-derived compounds from C3 and C4 plants (González-Pérez et al., 2016), the chemical structure of polyethylene polymers (González-Pérez et al., 2015), and more recently, an isotopic investigation of the geographical origin of olive oils (Jiménez-Morillo et al., 2019). However, thus far, CSIA-based analysis techniques have yet to be conducted on peat. When combined with Py-GC/MS-derived biomarker analyses, the application of this technique to peat profiles will be highly beneficial in determining the specific molecular sources of changing bulk isotopic signals with depth.

2.8.2 Linking molecular biomarker data with radiocarbon dating

In order to better understand ecological processes occurring over time, the chronologies of these processes, (and the rate that they occur), must also be understood. Chronological dating methods have the potential to improve this knowledge. A variety of dating methods have been developed for applications in quaternary ecology, and include both continuous dating methods and stratigraphic methods, such as (Turetsky et al., 2004). To verify the chronology of samples originating in palaeo-ecological systems (<50,000 years old), radiocarbon (^{14}C) dating methods are often incorporated. When combined with ^{14}C measurements, molecular biomarkers can provide more specificity in degraded profiles where DNA extraction is no longer possible. Molecular biomarker analysis can now even be combined with compound specific ^{14}C measurements, enabling researchers to trace different turnover times of different carbon-based molecules (Mendez-Millan et al., 2014).

Complementing molecular biomarker data with the incorporation of ^{14}C measurements is particularly useful in peatland OM studies. While variability in recalcitrance of different chemical classes of biomarkers can stymie chronology estimates in peatland profiles, ^{14}C dating measurements can help to confirm the stratigraphic age of samples, allowing for a more accurate assessment of the fate of OM as it undergoes microbial transformation, and the rate that this process occurs. In addition to these inherent differences in molecular preservation, peatland profiles experiencing varying degrees of degradation are prone to erosion and subsidence (Leifeld et al., 2011). This results in peat with disturbed depth-age profiles which are themselves an indicator of peatland degradation. Care must be taken to avoid comparing corresponding depths in peat profiles if substantial differences in OC age are present (Kaal et al., 2008b). Depth-based ^{14}C dating can help to identify profiles with "old" carbon closer to the surface, so similar OC ages can be correlated to one another. Especially in drained or rewetted ecosystems where substantial subsidence has occurred at some point in the peat's history, correlating biomarker abundance with depth-based ^{14}C dating analysis should considerably improve net carbon balance estimates.

In addition to temporal studies, ^{14}C methods are useful in spatial analysis and can elucidate the origin of exported OC. In an international DO^{14}C pore water analysis comparison of drained and natural peatlands, (Evans et al., 2014) found that exported DOC originated largely from recently photosynthesized (post-bomb peak) material in intact peat ecosystems across both tropical and high latitude locations. However, drained peatlands experienced an increased

export of "old" carbon. Tropical locations appeared most susceptible to DOC loss, in agreement with the previous findings of (Moore et al., 2013). (Evans et al., 2014) also looked at the effects of rewetting on DOC transport. While the results were not found to be significant, an overall trend in the return to recent age of DO^{14}C export was observed, indicating progressive but incomplete recovery of drained systems. An improved understanding of not only the age, but also the OM source of DOC originating from peatlands would be useful to identify ecosystems most susceptible to DOC export via leaching or runoff.

Higher resolution ^{14}C measurements are needed to improve the calibration of existing dating models in peatland ecosystems. (Kołaczek et al., 2019) supplemented three age-depth models with new ^{14}C AMS dates in order to investigate their robustness. They found that the new dates did not conform to the previously published models. While they reported uncertainty regarding the explanation for these dating discrepancies, the authors argued that their results were evidence for the need for more high-resolution measurements, and suggested that improvements in the resolution of ^{14}C measurements could help to identify periods of disturbance (whether anthropogenic, atmospheric, or animal derived) in peat profiles. As AMS method sensitivities improve and sample cost decreases, Py-GC/MS biomarker data coupled to high resolution ^{14}C dated profiles will increase statistical confidence in the description of palaeo-ecological processes, similar to the current use of stable isotopes as a complement to OM characterization techniques (Alewell et al., 2011).

2.8.3 Latitudinal comparison of OM storage and composition in peatlands

Tropical peatlands are thought to comprise approximately 15-19 percent of global peat carbon pool (Page et al., 2011), though recent high-resolution geospatial work has indicated that tropical peatland inventory estimates are likely to be underestimated (Xu et al., 2018). While the total known tropical peatland area and volume comprises a smaller global percentage than Arctic and boreal peat, peat height accumulation rates in tropical ecosystems have been observed to reach 5-10 mm/ year, in comparison to temperate and boreal ecosystems, which generally accumulate less than 1 mm/year (Chimner and Ewel, 2005). Tropical peatlands are under increasing pressure from deforestation, burning and land use change from agriculture (Koh et al., 2009, Page and Hooijer, 2016), and are at greater risk for exploitation due to their location in often densely populated coastal regions.

In comparison to Arctic and boreal peatlands (Loisel et al., 2014), less is known about tropical peat SOC cycling, due to access challenges and spatial resolution issues from overlying tree

canopy cover. Additionally, impacts of land use changes in peatlands in tropical climates are poorly understood (Zhang et al., 2019). Moreover, peat systems in lower latitudinal areas often experience periodic drought cycles that could be exacerbated by climate change and drainage, leading to changes in OM composition, increased fire incidence, and carbon emissions.

Due to chemical composition differences in the dominating contributing vegetation, tropical peatlands may contain substantially different OM from boreal peat and may utilize different preservation mechanism pathways when compared to higher latitude locations. (Hodgkins et al., 2018) conducted an FTIR-based comparison of OM content in boreal and tropical peatland locations and found that lower latitude samples (south of 45°N) on average contained lower carbohydrate content and higher aromatic content than the higher latitude samples – suggesting that tropical peatlands may have inherent inhibitory decomposition mechanisms stemming from the higher lignin and phenolic content of the contributing shrub and tree vegetation. However, due to the small number of tropical latitude peatland sites sampled in this study, tropical peatland OM diversity here may not be wholly represented, and it remains unclear whether differences in OM chemical composition will render tropical peat more or less susceptible to substantial C loss. Latitudinal comparisons of carbon storage and molecular OM composition in peatlands will be useful to understand whether tropical peatlands might be affected to a greater (or lesser) degree than currently anticipated. These data could be further improved by using more sophisticated molecular analysis methods such as Py-GC/MS that will permit more detailed fingerprinting of highly biodiverse tropical sites.

2.8.4 Future Carbon Cycling Models

Our emerging understanding of soil ecosystem dynamics is used to update information in SOC geochemical cycling models (Wieder et al., 2018, Bailey et al., 2018). Environmental modelling is used to explore feedbacks between ecosystems and climate, as well as to evaluate potential environmental management strategies to mitigate future warming. However, experimental data depicting increasing temperature does not always display good correlation with model predictions, indicating that environmental parameters may not be well-constrained (Sulman et al., 2018). In addition, many of the standard C-cycling vegetation models cannot easily be applied to peatland ecosystems, which contain uniquely localized C-cycling dynamics and plant functional types (PFTs). For example, peatland simulations coupled with global SOC models typically describe C stocks and dynamics as conceptual C "pools," where each pool has a defined turnover rate (Ise et al., 2008). "Equilibrium" is reached in these models over an

accelerated time frame, generally a few centuries. This is problematic, as peatlands adapt over thousands of years to numerous shifts in climate and hydrology, resulting in the evolving layers of vegetation observed in their profiles (Heinemeyer et al., 2010).

Peatland C dynamics are currently summarized by relatively simple models for peat accumulation (Yu et al., 2001), most of which are largely based on the work of (Clymo, 1984). Peatland-adapted models generally depict peat formation with a distinctly layered stratigraphy that changes with long-term climate shifts, where each layer or "cohort" demonstrates different PFTs (Frolking et al., 2010, Kurnianto et al., 2015, Bauer, 2004, Heinemeyer et al., 2010). Peatland cohort markers could be identified locally or regionally, where shifts in climate (for example: using parameters of temperature and precipitation) could be tracked using a combination of ^{14}C dating techniques and Py-GC/MS OM characterization to identify re-occurring PFTs – enabling experimental and modelling data to be better constrained.

Models specific to peatland dynamics offer an opportunity to better understand the processes leading to the formation and C stabilization within these fragile ecosystems. Peat model parameters would greatly benefit from the inclusion of experimental data permitting a more accurate estimation of molecular OC content, as well as overall peat OM stoichiometry. Incorporation of molecular information obtained via Py-GC/MS-based OM fingerprinting can be used to improve peatland process-based models, which could be then incorporated into global models to increase our understanding of larger SOC dynamics (Schmidt et al., 2011). For example, this data could greatly improve the molecular stoichiometry used as an input to C and N stock measurements (Elser et al., 2010, Tipping et al., 2016). In the future, these developments could be further improved with the inclusion of molecular dynamic simulations of OM decomposition. Increased understanding of how decomposition dynamics in peatlands will affect carbon fluxes globally should improve accuracy and precision of experimental data-driven model parameters, which will also improve predictions for future carbon dynamics.

Acknowledgements

Robin Giger's assistance in the graphic design of **Figure 1** is greatly appreciated. This work was funded by the Swiss National Science Foundation, project number 200021_169556.

References

ALEWELL, C., GIESLER, R., KLAMINDER, J., LEIFELD, J. & ROLLOG, M. 2011. Stable carbon isotopes as indicators for environmental change in palsa peats. *Biogeosciences,* 8**,** 1769-1778.

ALLISON, S. D. & TRESEDER, K. K. 2011. Climate change feedbacks to microbial decomposition in boreal soils. *Fungal Ecology,* 4**,** 362-374.

ALMENDROS, G., KNICKER, H. & GONZÁLEZ-VILA, F. J. 2003. Rearrangement of carbon and nitrogen forms in peat after progressive thermal oxidation as determined by solid-state 13C- and 15N-NMR spectroscopy. *Organic Geochemistry,* 34**,** 1559-1568.

AMELUNG, W. 2001. Methods using amino sugars as markers for microbial residues in soil. *Assessment methods for soil carbon.* Lewis Publishers Boca Raton.

ANDERSEN, R., CHAPMAN, S. & ARTZ, R. 2013. Microbial communities in natural and disturbed peatlands: a review. *Soil Biology and Biochemistry,* 57**,** 979-994.

ANDERSEN, R., GRASSET, L., THORMANN, M. N., ROCHEFORT, L. & FRANCEZ, A.-J. 2010. Changes in microbial community structure and function following Sphagnum peatland restoration. *Soil Biology and Biochemistry,* 42**,** 291-301.

ARTHUR STANKIEWICZ, B., VAN BERGEN, P. F., DUNCAN, I. J., CARTER, J. F., BRIGGS, D. E. & EVERSHED, R. P. 1996. Recognition of chitin and proteins in invertebrate cuticles using analytical pyrolysis/gas chromatography and pyrolysis/gas chromatography/mass spectrometry. *Rapid Communications in Mass Spectrometry,* 10**,** 1747-1757.

ARTZ, R. R., CHAPMAN, S. J., ROBERTSON, A. J., POTTS, J. M., LAGGOUN-DÉFARGE, F., GOGO, S., COMONT, L., DISNAR, J.-R. & FRANCEZ, A.-J. 2008. FTIR spectroscopy can be used as a screening tool for organic matter quality in regenerating cutover peatlands. *Soil Biology and Biochemistry,* 40**,** 515-527.

AVSEJS, L. A., NOTT, C. J., XIE, S., MADDY, D., CHAMBERS, F. M. & EVERSHED, R. P. 2002. 5-n-Alkylresorcinols as biomarkers of sedges in an ombrotrophic peat section. *Organic Geochemistry,* 33**,** 861-867.

BAAS, M., PANCOST, R., VAN GEEL, B. & DAMSTÉ, J. S. S. 2000. A comparative study of lipids in Sphagnum species. *Organic Geochemistry,* 31**,** 535-541.

BAILEY, V. L., BOND-LAMBERTY, B., DEANGELIS, K., GRANDY, A. S., HAWKES, C. V., HECKMAN, K., LAJTHA, K., PHILLIPS, R. P., SULMAN, B. N. & TODD-BROWN, K. E. 2018. Soil carbon cycling proxies: Understanding their critical role in predicting climate change feedbacks. *Global change biology,* 24**,** 895-905.

BALDOCK, J., OADES, J., NELSON, P., SKENE, T., GOLCHIN, A. & CLARKE, P. 1997. Assessing the extent of decomposition of natural organic materials using solid-state 13C NMR spectroscopy. *Soil Research,* 35**,** 1061-1084.

BAUER, I. E. 2004. Modelling effects of litter quality and environment on peat accumulation over different time-scales. *Journal of Ecology,* 92**,** 661-674.

BELYEA, L. R. & BAIRD, A. J. 2006. Beyond "the limits to peat bog growth": Cross-scale feedback in peatland development. *Ecological Monographs,* 76**,** 299-322.

BELYEA, L. R. & CLYMO, R. 2001. Feedback control of the rate of peat formation. *Proceedings of the Royal Society of London B: Biological Sciences,* 268**,** 1315-1321.

BLACKFORD, J. 2000. Palaeoclimatic records from peat bogs. *Trends in Ecology & Evolution,* 15**,** 193-198.

BOERJAN, W., RALPH, J. & BAUCHER, M. 2003. Lignin biosynthesis. *Annual review of plant biology,* 54**,** 519-546.

BUURMAN, P., NIEROP, K. G. J., PONTEVEDRA-POMBAL, X. & MARTÍNEZ CORTIZAS, A. 2006. Chapter 10 Molecular chemistry by pyrolysis–GC/MS of selected samples of the Penido Vello peat deposit, Galicia, NW Spain. *In:* MARTINI, I. P., MARTÍNEZ CORTIZAS, A. & CHESWORTH, W. (eds.) *Developments in Earth Surface Processes.* Elsevier.

CARR, A. S., BOOM, A., CHASE, B. M., ROBERTS, D. L. & ROBERTS, Z. E. 2010. Molecular fingerprinting of wetland organic matter using pyrolysis-GC/MS: an example from the southern Cape coastline of South Africa. *Journal of Paleolimnology,* 44**,** 947-961.

CHAMBERS, F. M., BOOTH, R. K., DE VLEESCHOUWER, F., LAMENTOWICZ, M., LE ROUX, G., MAUQUOY, D., NICHOLS, J. E. & VAN GEEL, B. 2012. Development and refinement of proxy-climate indicators from peats. *Quaternary International,* 268**,** 21-33.

CHAPMAN, S. 1964. The ecology of Coom Rigg Moss, Northumberland: II. The chemistry of peat profiles and the development of the bog system. *The Journal of Ecology***,** 315-321.

CHAPMAN, S. J., CAMPBELL, C. D., FRASER, A. R. & PURI, G. 2001. FTIR spectroscopy of peat in and bordering Scots pine woodland: relationship with chemical and biological properties. *Soil Biology and Biochemistry,* 33**,** 1193-1200.

CHIMNER, R. A. & EWEL, K. C. 2005. A tropical freshwater wetland: II. Production, decomposition, and peat formation. *Wetlands Ecology and Management,* 13**,** 671-684.

CHRISTENSEN, T. R., EKBERG, A., STRÖM, L., MASTEPANOV, M., PANIKOV, N., ÖQUIST, M., SVENSSON, B. H., NYKÄNEN, H., MARTIKAINEN, P. J. & OSKARSSON, H. 2003. Factors controlling large scale variations in methane emissions from wetlands. *Geophysical Research Letters,* 30.

CLYMO, R. 1984. The limits to peat bog growth. *Philosophical Transactions of the Royal Society of London. B, Biological Sciences,* 303**,** 605-654.

CLYMO, R. 1987. The ecology of peatlands. *Science Progress (1933-)***,** 593-614.

CLYMO, R., TURUNEN, J. & TOLONEN, K. 1998. Carbon accumulation in peatland. *Oikos***,** 368-388.

CZIMCZIK, C. I., PRESTON, C. M., SCHMIDT, M. W. & SCHULZE, E. D. 2003. How surface fire in Siberian Scots pine forests affects soil organic carbon in the forest floor: Stocks, molecular structure, and conversion to black carbon (charcoal). *Global Biogeochemical Cycles,* 17.

DAVIDSON, E. A. & JANSSENS, I. A. 2006. Temperature sensitivity of soil carbon decomposition and feedbacks to climate change. *Nature,* 440**,** 165.

DE LA ROSA, J. M., FARIA, S. R., VARELA, M. E., KNICKER, H., GONZÁLEZ-VILA, F. J., GONZÁLEZ-PÉREZ, J. A. & KEIZER, J. 2012. Characterization of wildfire effects on soil organic matter using analytical pyrolysis. *Geoderma,* 191**,** 24-30.

DEDYSH, S. N., PANKRATOV, T. A., BELOVA, S. E., KULICHEVSKAYA, I. S. & LIESACK, W. 2006. Phylogenetic analysis and in situ identification of bacteria community composition in an acidic Sphagnum peat bog. *Applied and Environmental Microbiology,* 72**,** 2110-2117.

DERENNE, S., METZGER, P., LARGEAU, C., VAN BERGEN, P., GATELLIER, J., DAMSTÉ, J. S., DE LEEUW, J. & BERKALOFF, C. 1992. Similar morphological and chemical variations of Gloeocapsomorpha prisca in Ordovician sediments and cultured Botryococcus braunii as a response to changes in salinity. *Organic Geochemistry,* 19**,** 299-313.

DERENNE, S. & QUÉNÉA, K. 2015. Analytical pyrolysis as a tool to probe soil organic matter. *Journal of Analytical and Applied Pyrolysis,* 111**,** 108-120.

DORREPAAL, E., TOET, S., VAN LOGTESTIJN, R. S., SWART, E., VAN DE WEG, M. J., CALLAGHAN, T. V. & AERTS, R. 2009. Carbon respiration from subsurface peat accelerated by climate warming in the subarctic. *Nature,* 460**,** 616.

DUBOIS, N. & JACOB, J. 2016. Molecular biomarkers of anthropic impacts in natural archives: A review. *Frontiers in Ecology and Evolution,* 4**,** 92.

DWORZANSKI, J. P., TRIPATHI, A., SNYDER, A. P., MASWDEH, W. M. & WICK, C. H. 2005. Novel biomarkers for Gram-type differentiation of bacteria by pyrolysis–gas chromatography–mass spectrometry. *Journal of analytical and applied pyrolysis,* 73**,** 29-38.

EGLINTON, T. I. & EGLINTON, G. 2008. Molecular proxies for paleoclimatology. *Earth and Planetary Science Letters,* 275**,** 1-16.

EKBLAD, A., WALLANDER, H. & NÄSHOLM, T. 1998. Chitin and ergosterol combined to measure total and living fungal biomass in ectomycorrhizas. *The New Phytologist,* 138**,** 143-149.

ELSER, J., FAGAN, W., KERKHOFF, A., SWENSON, N. & ENQUIST, B. 2010. Biological stoichiometry of plant production: metabolism, scaling and ecological response to global change. *New Phytologist,* 186**,** 593-608.

ERKENS, G., VAN DER MEULEN, M. J. & MIDDELKOOP, H. 2016. Double trouble: subsidence and CO 2 respiration due to 1,000 years of Dutch coastal peatlands cultivation. *Hydrogeology Journal,* 24**,** 551-568.

EUDY, L. W., WALLA, M. D., HUDSON, J. R., MORGAN, S. L. & FOX, A. 1985. Gas chromatography—mass spectrometry studies on the occurrence of acetamide, propionamide, and furfuryl alcohol in pyrolyzates of bacteria, bacterial fractions, and model compounds. *Journal of analytical and applied pyrolysis,* 7**,** 231-247.

EVANS, C. D., PAGE, S. E., JONES, T., MOORE, S., GAUCI, V., LAIHO, R., HRUŠKA, J., ALLOTT, T. E., BILLETT, M. F. & TIPPING, E. 2014. Contrasting vulnerability of drained tropical and high-latitude peatlands to fluvial loss of stored carbon. *Global Biogeochemical Cycles,* 28**,** 1215-1234.

FABBRI, D. & HELLEUR, R. 1999. Characterization of the tetramethylammonium hydroxide thermochemolysis products of carbohydrates. *Journal of Analytical and Applied Pyrolysis,* 49**,** 277-293.

FENG, X., SIMPSON, A. J., WILSON, K. P., WILLIAMS, D. D. & SIMPSON, M. J. 2008. Increased cuticular carbon sequestration and lignin oxidation in response to soil warming. *Nature Geoscience,* 1**,** 836.

FREEMAN, C., OSTLE, N., FENNER, N. & KANG, H. 2004. A regulatory role for phenol oxidase during decomposition in peatlands. *Soil Biology and Biochemistry,* 36**,** 1663-1667.

FREEMAN, C., OSTLE, N. & KANG, H. 2001. An enzymic'latch'on a global carbon store. *Nature,* 409**,** 149.

FROLKING, S. & ROULET, N. T. 2007. Holocene radiative forcing impact of northern peatland carbon accumulation and methane emissions. *Global Change Biology,* 13**,** 1079-1088.

FROLKING, S., ROULET, N. T., TUITTILA, E.-S., BUBIER, J. L., QUILLET, A., TALBOT, J. & RICHARD, P. 2010. A new model of Holocene peatland net primary production, decomposition, water balance, and peat accumulation. *Earth System Dynamics*.

FROSTEGÅRD, Å. & BÅÅTH, E. 1996. The use of phospholipid fatty acid analysis to estimate bacterial and fungal biomass in soil. *Biology and Fertility of Soils,* 22**,** 59-65.

FROSTEGÅRD, Å., BÅÅTH, E. & TUNLIO, A. 1993. Shifts in the structure of soil microbial communities in limed forests as revealed by phospholipid fatty acid analysis. *Soil Biology and Biochemistry,* 25**,** 723-730.

FUHRMANN, A., FISCHER, T., LÜCKE, A., BRAUER, A., ZOLITSCHKA, B., HORSFIELD, B., NEGENDANK, J. F., SCHLESER, G. H. & WILKES, H. 2004. Late Quaternary environmental and climatic changes in central Europe as inferred from the composition of organic matter in annually laminated maar lake sediments. *Geochemistry, Geophysics, Geosystems,* 5.

GAŁKA, M., SWINDLES, G. T., SZAL, M., FULWEBER, R. & FEURDEAN, A. 2018. Response of plant communities to climate change during the late Holocene: Palaeoecological insights from peatlands in the Alaskan Arctic. *Ecological Indicators,* 85**,** 525-536.

GLASER, B., HAUMAIER, L., GUGGENBERGER, G. & ZECH, W. 1998. Black carbon in soils: the use of benzenecarboxylic acids as specific markers. *Organic geochemistry,* 29**,** 811-819.

GLATZEL, S., BASILIKO, N. & MOORE, T. 2004. Carbon dioxide and methane production potentials of peats from natural, harvested and restored sites, eastern Québec, Canada. *Wetlands,* 24**,** 261-267.

GONZÁLEZ-PÉREZ, J. A., ALMENDROS, G., DE LA ROSA, J. & GONZÁLEZ-VILA, F. J. 2014. Appraisal of polycyclic aromatic hydrocarbons (PAHs) in environmental matrices by analytical pyrolysis (Py–GC/MS). *Journal of Analytical and Applied Pyrolysis,* 109**,** 1-8.

GONZÁLEZ-PÉREZ, J. A., JIMÉNEZ-MORILLO, N., DE LA ROSA, J., ALMENDROS, G. & GONZÁLEZ-VILA, F. J. 2015. Pyrolysis-gas chromatography–isotope ratio mass spectrometry of polyethylene. *Journal of Chromatography A,* 1388**,** 236-243.

GONZÁLEZ-PÉREZ, J. A., JIMÉNEZ-MORILLO, N. T., DE LA ROSA, J. M., ALMENDROS, G. & GONZÁLEZ-VILA, F. J. 2016. Compound-specific stable carbon isotopic signature of carbohydrate pyrolysis products from C3 and C4 plants. *Journal of the Science of Food and Agriculture,* 96**,** 948-953.

GREENWOOD, P., LEENHEER, J., MCINTYRE, C., BERWICK, L. & FRANZMANN, P. 2006. Bacterial biomarkers thermally released from dissolved organic matter. *Organic Geochemistry,* 37**,** 597-609.

HÁJEK, T., BALLANCE, S., LIMPENS, J., ZIJLSTRA, M. & VERHOEVEN, J. T. A. 2011. Cell-wall polysaccharides play an important role in decay resistance of Sphagnum and actively depressed decomposition in vitro. *Biogeochemistry,* 103**,** 45-57.

HARRIS, L. I., MOORE, T. R., ROULET, N. T. & PINSONNEAULT, A. J. 2018. Lichens: A limit to peat growth? *Journal of Ecology,* 106**,** 2301-2319.

HARTOG, N., VAN BERGEN, P., DE LEEUW, J. & GRIFFIOEN, J. 2004. Reactivity of organic matter in aquifer sediments: geological and geochemical controls 1. *Geochimica et Cosmochimica Acta,* 68**,** 1281-1292.

HARVEY, O. R., KUO, L.-J., ZIMMERMAN, A. R., LOUCHOUARN, P., AMONETTE, J. E. & HERBERT, B. E. 2012. An index-based approach to assessing recalcitrance and soil carbon sequestration potential of engineered black carbons (biochars). *Environmental science & technology,* 46**,** 1415-1421.

HASSAN, E.-B. M., STEELE, P. H. & INGRAM, L. 2009. Characterization of fast pyrolysis bio-oils produced from pretreated pine wood. *Applied biochemistry and biotechnology,* 154**,** 3-13.

HEDGES, J. I. & MANN, D. C. 1979. The characterization of plant tissues by their lignin oxidation products. *Geochimica et Cosmochimica Acta,* 43**,** 1803-1807.

HEINEMEYER, A., CROFT, S., GARNETT, M. H., GLOOR, E., HOLDEN, J., LOMAS, M. R. & INESON, P. 2010. The MILLENNIA peat cohort model: predicting past, present and future

soil carbon budgets and fluxes under changing climates in peatlands. *Climate Research,* 45**,** 207-226.

HILBERT, D. W., ROULET, N. & MOORE, T. 2000. Modelling and analysis of peatlands as dynamical systems. *Journal of Ecology,* 88**,** 230-242.

HODGKINS, S. B., RICHARDSON, C. J., DOMMAIN, R., WANG, H., GLASER, P. H., VERBEKE, B., WINKLER, B. R., COBB, A. R., RICH, V. I. & MISSILMANI, M. 2018. Tropical peatland carbon storage linked to global latitudinal trends in peat recalcitrance. *Nature communications,* 9**,** 3640.

HØJ, L., OLSEN, R. A. & TORSVIK, V. L. 2008. Effects of temperature on the diversity and community structure of known methanogenic groups and other archaea in high Arctic peat. *The ISME journal,* 2**,** 37.

HOOIJER, A., PAGE, S., CANADELL, J., SILVIUS, M., KWADIJK, J., WOSTEN, H. & JAUHIAINEN, J. 2010. Current and future CO2 emissions from drained peatlands in Southeast Asia. *Biogeosciences*.

HU, Y., FERNANDEZ-ANEZ, N., SMITH, T. E. & REIN, G. 2018. Review of emissions from smouldering peat fires and their contribution to regional haze episodes. *International Journal of Wildland Fire,* 27**,** 293-312.

HUANG, Y., STANKIEWICZ, B., EGLINTON, G., SNAPE, C., EVANS, B., LATTER, P. & INESON, P. 1998. Monitoring biomacromolecular degradation of Calluna vulgaris in a 23 year field experiment using solid state 13C-NMR and pyrolysis-GC/MS. *Soil Biology and Biochemistry,* 30**,** 1517-1528.

HUGHES, P. & DUMAYNE-PEATY, L. 2002. Testing theories of mire development using multiple successions at Crymlyn Bog, West Glamorgan, South Wales, UK. *Journal of Ecology,* 90**,** 456-471.

INGLIS, G. N., COLLINSON, M. E., RIEGEL, W., WILDE, V., ROBSON, B. E., LENZ, O. K. & PANCOST, R. D. 2015. Ecological and biogeochemical change in an early Paleogene peat-forming environment: Linking biomarkers and palynology. *Palaeogeography, Palaeoclimatology, Palaeoecology,* 438**,** 245-255.

IPCC 2014. IPCC, 2014: climate change 2014: synthesis report. Contribution of Working Groups I. *II and III to the Fifth Assessment Report of the intergovernmental panel on Climate Change. IPCC, Geneva, Switzerland,* 151.

ISE, T., DUNN, A. L., WOFSY, S. C. & MOORCROFT, P. R. 2008. High sensitivity of peat decomposition to climate change through water-table feedback. *Nature Geoscience,* 1**,** 763.

ISHIWATARI, M., ISHIWATARI, R., SAKASHITA, H., TATSUMI, T. & TOMINAGA, H.-O. 1991. Pyrolysis of chlorophyll a after preliminary heating at a moderate temperature: implications for the origin of prist-1-ene on kerogen pyrolysis. *Journal of Analytical and Applied Pyrolysis,* 18**,** 207-218.

JAATINEN, K., LAIHO, R., VUORENMAA, A., DEL CASTILLO, U., MINKKINEN, K., PENNANEN, T., PENTTILÄ, T. & FRITZE, H. 2008. Responses of aerobic microbial communities and soil respiration to water-level drawdown in a northern boreal fen. *Environmental microbiology,* 10**,** 339-353.

JANSEN, B. & WIESENBERG, G. L. B. 2017. Opportunities and limitations related to the application of plant-derived lipid molecular proxies in soil science. *SOIL,* 3**,** 211-234.

JEX, C. N., PATE, G. H., BLYTH, A. J., SPENCER, R. G., HERNES, P. J., KHAN, S. J. & BAKER, A. 2014. Lignin biogeochemistry: from modern processes to Quaternary archives. *Quaternary Science Reviews,* 87**,** 46-59.

JIMÉNEZ-MORILLO, N. T., CABRITA, M. J., DIAS, C. B., GONZÁLEZ-VILA, F. J. & GONZÁLEZ-PÉREZ, J. A. 2019. Pyrolysis-compound-specific hydrogen isotope analysis (δ2H Py-CSIA) of Mediterranean olive oils. *Food Control***,** 107023.

JIMÉNEZ MORILLO, N. T., ROSA ARRANZ, J. M., GONZÁLEZ-VILA, F. J. & GONZÁLEZ-PÉREZ, J. A. 2015. Direct Compound Specific Isotopic Analysis (CHON) of complex samples using analytical pyrolysis (Py-CSIA).

JOERGENSEN, R. G. 2018. Amino sugars as specific indices for fungal and bacterial residues in soil. *Biology and Fertility of Soils***,** 1-10.

JOERGENSEN, R. G. & WICHERN, F. 2008. Quantitative assessment of the fungal contribution to microbial tissue in soil. *Soil Biology and Biochemistry,* 40**,** 2977-2991.

JOERGENSEN, R. G. & WICHERN, F. 2018. Alive and kicking: Why dormant soil microorganisms matter. *Soil Biology and Biochemistry,* 116**,** 419-430.

JOHNSON, L. C. & DAMMAN, A. W. 1991. Species-controlled Sphagnum decay on a south Swedish raised bog. *Oikos***,** 234-242.

JOOSTEN, H. 2009. The Global Peatland CO2 Picture: peatland status and drainage related emissions in all countries of the world. *The Global Peatland CO2 Picture: peatland status and drainage related emissions in all countries of the world.*

JOOSTEN, H. & CLARKE, D. 2002. Wise use of mires and peatlands. *International Mire Conservation Group and International Peat Society,* 304.

JOSÉ, C., PRINSEN, P. & GUTIÉRREZ, A. 2013. Chemical composition of lipids in brewer's spent grain: A promising source of valuable phytochemicals. *Journal of cereal science,* 58**,** 248-254.

KAAL, J., BRODOWSKI, S., BALDOCK, J. A., NIEROP, K. G. & CORTIZAS, A. M. 2008a. Characterisation of aged black carbon using pyrolysis-GC/MS, thermally assisted hydrolysis and methylation (THM), direct and cross-polarisation 13C nuclear magnetic resonance (DP/CP NMR) and the benzenepolycarboxylic acid (BPCA) method. *Organic Geochemistry,* 39**,** 1415-1426.

KAAL, J., CORTIZAS, A. M. & BIESTER, H. 2017. Downstream changes in molecular composition of DOM along a headwater stream in the Harz mountains (Central Germany) as determined by

FTIR, Pyrolysis-GC–MS and THM-GC–MS. *Journal of Analytical and Applied Pyrolysis,* 126**,** 50-61.

KAAL, J., CORTIZAS, A. M., ECKMEIER, E., CASAIS, M. C., ESTÉVEZ, M. S. & BOADO, F. C. 2008b. Holocene fire history of black colluvial soils revealed by pyrolysis-GC/MS: a case study from Campo Lameiro (NW Spain). *Journal of Archaeological Science,* 35**,** 2133-2143.

KALLENBACH, C. M., FREY, S. D. & GRANDY, A. S. 2016. Direct evidence for microbial-derived soil organic matter formation and its ecophysiological controls. *Nature communications,* 7**,** 13630.

KILLOPS, S. & FREWIN, N. 1994. Triterpenoid diagenesis and cuticular preservation. *Organic Geochemistry,* 21**,** 1193-1209.

KILLOPS, S. D. & KILLOPS, V. J. 2013. *Introduction to organic geochemistry*, John Wiley & Sons.

KIP, N., VAN WINDEN, J. F., PAN, Y., BODROSSY, L., REICHART, G.-J., SMOLDERS, A. J., JETTEN, M. S., DAMSTÉ, J. S. S. & DEN CAMP, H. J. O. 2010. Global prevalence of methane oxidation by symbiotic bacteria in peat-moss ecosystems. *Nature Geoscience,* 3**,** 617.

KISAND, V., GEBHARDT, S., RULLKÖTTER, J. & SIMON, M. 2013. Significant bacterial transformation of riverine humic matter detected by pyrolysis GC–MS in serial chemostat experiments. *Marine Chemistry,* 149**,** 23-31.

KLINGER, L. F. 1996. Coupling of soils and vegetation in peatland succession. *Arctic and Alpine Research,* 28**,** 380-387.

KNICKER, H. 2007. How does fire affect the nature and stability of soil organic nitrogen and carbon? A review. *Biogeochemistry,* 85**,** 91-118.

KÖGEL-KNABNER 2002. The macromolecular organic composition of plant and microbial residues as inputs to soil organic matter. *Soil Biology and Biochemistry,* 34**,** 139-162.

KÖGEL-KNABNER, I. & AMELUNG, W. 2014. Dynamics, chemistry, and preservation of organic matter in soils.

KOH, L. P., BUTLER, R. A. & BRADSHAW, C. J. 2009. Conversion of Indonesia's peatlands. *Frontiers in Ecology and the Environment,* 7**,** 238-238.

KOŁACZEK, P., GAŁKA, M., LAMENTOWICZ, M., MARCISZ, K., KAJUKAŁO-DRYGALSKA, K. & KARPIŃSKA-KOŁACZEK, M. 2019. Increased radiocarbon dating resolution of ombrotrophic peat profiles reveals periods of disturbance which were previously undetected. *Quaternary Geochronology,* 52**,** 21-28.

KRULL, E. S. & RETALLACK, G. J. 2000. δ13C depth profiles from paleosols across the Permian-Triassic boundary: Evidence for methane release. *Geological Society of America Bulletin,* 112**,** 1459-1472.

KURNIANTO, S., WARREN, M., TALBOT, J., KAUFFMAN, B., MURDIYARSO, D. & FROLKING, S. 2015. Carbon accumulation of tropical peatlands over millennia: a modeling approach. *Global change biology,* 21**,** 431-444.

KYLANDER, M. E., MARTÍNEZ-CORTIZAS, A., BINDLER, R., KAAL, J., SJÖSTRÖM, J. K., HANSSON, S. V., SILVA-SÁNCHEZ, N., GREENWOOD, S. L., GALLAGHER, K. & RYDBERG, J. 2018. Mineral dust as a driver of carbon accumulation in northern latitudes. *Scientific reports,* 8**,** 6876.

LAIHO, R. 2006. Decomposition in peatlands: Reconciling seemingly contrasting results on the impacts of lowered water levels. *Soil Biology and Biochemistry,* 38**,** 2011-2024.

LAIHO, R., LAINE, J., TRETTIN, C. C. & FINÉR, L. 2004. Scots pine litter decomposition along drainage succession and soil nutrient gradients in peatland forests, and the effects of inter-annual weather variation. *Soil Biology and Biochemistry,* 36**,** 1095-1109.

LAROWE, D. E. & VAN CAPPELLEN, P. 2011. Degradation of natural organic matter: a thermodynamic analysis. *Geochimica et Cosmochimica Acta,* 75**,** 2030-2042.

LEIFELD, J., ALEWELL, C., BADER, C., KRÜGER, J. P., MUELLER, C. W., SOMMER, M., STEFFENS, M. & SZIDAT, S. 2018. Pyrogenic carbon contributes substantially to carbon storage in intact and degraded northern peatlands. *Land degradation & development,* 29**,** 2082-2091.

LEIFELD, J. & MENICHETTI, L. 2018. The underappreciated potential of peatlands in global climate change mitigation strategies. *Nature communications,* 9**,** 1071.

LEIFELD, J., MÜLLER, M. & FUHRER, J. 2011. Peatland subsidence and carbon loss from drained temperate fens. *Soil Use and Management,* 27**,** 170-176.

LIM, K. L., PANCOST, R. D., HORNIBROOK, E. R., MAXFIELD, P. J. & EVERSHED, R. P. 2012. Archaeol: an indicator of methanogenesis in water-saturated soils. *Archaea,* 2012.

LINDSAY, R. 2018. Peatland (Mire Types): Based on Origin and Behavior of Water, Peat Genesis, Landscape Position, and Climate. *The Wetland Book: II: Distribution, Description, and Conservation***,** 251-273.

LOHILA, A., MINKKINEN, K., AURELA, M., TUOVINEN, J.-P., PENTTILÄ, T., OJANEN, P. & LAURILA, T. 2011. Greenhouse gas flux measurements in a forestry-drained peatland indicate a large carbon sink. *Biogeosciences*.

LOISEL, J., YU, Z., BEILMAN, D. W., CAMILL, P., ALM, J., AMESBURY, M. J., ANDERSON, D., ANDERSSON, S., BOCHICCHIO, C. & BARBER, K. 2014. A database and synthesis of northern peatland soil properties and Holocene carbon and nitrogen accumulation. *the Holocene,* 24**,** 1028-1042.

LOPEZ-DIAS, V., URBANCZYK, J., BLANCO, C. & BORREGO, A. 2013. Biomarkers as paleoclimate proxies in peatlands in coastal high plains in Asturias, N Spain. *International Journal of Coal Geology,* 116**,** 270-280.

MACHINET, G. E., BERTRAND, I., BARRIÈRE, Y., CHABBERT, B. & RECOUS, S. 2011. Impact of plant cell wall network on biodegradation in soil: role of lignin composition and phenolic acids in roots from 16 maize genotypes. *Soil biology and biochemistry,* 43**,** 1544-1552.

MADONNA, A. J., VOORHEES, K. J. & HADFIELD, T. L. 2001. Rapid detection of taxonomically important fatty acid methyl ester and steroid biomarkers using in situ thermal hydrolysis/methylation mass spectrometry (THM-MS): implications for bioaerosol detection. *Journal of Analytical and Applied Pyrolysis,* 61**,** 65-89.

MARTIN, F., SAIZ-JIMENEZ, C. & GONZALEZ-VILA, F. 1979. Pyrolysis-gas chromatography-mass spectrometry of lignins. *Holzforschung,* 33**,** 210-212.

MCCLYMONT, E. L., BINGHAM, E. M., NOTT, C. J., CHAMBERS, F. M., PANCOST, R. D. & EVERSHED, R. P. 2011. Pyrolysis GC–MS as a rapid screening tool for determination of peat-forming plant composition in cores from ombrotrophic peat. *Organic geochemistry,* 42**,** 1420-1435.

MCCLYMONT, E. L., MAUQUOY, D., YELOFF, D., BROEKENS, P., VAN GEEL, B., CHARMAN, D. J., PANCOST, R. D., CHAMBERS, F. M. & EVERSHED, R. P. 2008. The disappearance of Sphagnum imbricatum from Butterburn Flow, UK. *The Holocene,* 18**,** 991-1002.

MENDEZ-MILLAN, M., TU, T. N., BALESDENT, J., DERENNE, S., DERRIEN, D., EGASSE, C., M'BOU, A. T., ZELLER, B. & HATTÉ, C. 2014. Compound-specific 13 C and 14 C measurements improve the understanding of soil organic matter dynamics. *Biogeochemistry,* 118**,** 205-223.

MOORE, S., EVANS, C. D., PAGE, S. E., GARNETT, M. H., JONES, T. G., FREEMAN, C., HOOIJER, A., WILTSHIRE, A. J., LIMIN, S. H. & GAUCI, V. 2013. Deep instability of deforested tropical peatlands revealed by fluvial organic carbon fluxes. *Nature,* 493**,** 660.

MORGAN, S. L., WATT, B. E., UEDA, K. & FOX, A. 1990. Pyrolysis GC/MS profiling of chemical markers for microorganisms. *Analytical Microbiology Methods.* Springer.

NEUHÄUSL, R. 1992. Primary and secondary succession on wooded peat-bogs. *Acta Societatis Botanicorum Poloniae,* 61**,** 89-102.

NICHOLS, J. E., BOOTH, R. K., JACKSON, S. T., PENDALL, E. G. & HUANG, Y. 2006. Paleohydrologic reconstruction based on n-alkane distributions in ombrotrophic peat. *Organic Geochemistry,* 37**,** 1505-1513.

NIEROP, K. 1998. Origin of aliphatic compounds in a forest soil. *Organic geochemistry,* 29**,** 1009-1016.

NIEROP, K. G., VAN BERGEN, P. F., BUURMAN, P. & VAN LAGEN, B. 2005. NaOH and Na4P2O7 extractable organic matter in two allophanic volcanic ash soils of the Azores Islands—a pyrolysis GC/MS study. *Geoderma,* 127**,** 36-51.

NIP, M., TEGELAAR, E. W., BRINKHUIS, H., DE LEEUW, J. W., SCHENCK, P. A. & HOLLOWAY, P. J. 1986. Analysis of modern and fossil plant cuticles by Curie point Py-GC and Curie point Py-GC-MS: Recognition of a new, highly aliphatic and resistant biopolymer. *Organic Geochemistry,* 10**,** 769-778.

OLSSON, P. A., LARSSON, L., BAGO, B., WALLANDER, H. & VAN AARLE, I. M. 2003. Ergosterol and fatty acids for biomass estimation of mycorrhizal fungi. *New Phytologist,* 159**,** 7-10.

PAGE, S. & BAIRD, A. 2016. Peatlands and global change: response and resilience. *Annual Review of Environment and Resources,* 41**,** 35-57.

PAGE, S., RIELEY, J., SHOTYK, Ø. & WEISS, D. 1999. Interdependence of peat and vegetation in a tropical peat swamp forest. *Changes And Disturbance In Tropical Rainforest In South-East Asia.* World Scientific.

PAGE, S. E. & HOOIJER, A. 2016. In the line of fire: the peatlands of Southeast Asia. *Philosophical Transactions of the Royal Society B: Biological Sciences,* 371**,** 20150176.

PAGE, S. E., RIELEY, J. O. & BANKS, C. J. 2011. Global and regional importance of the tropical peatland carbon pool. *Global Change Biology,* 17**,** 798-818.

PALOZZI, J. E. & LINDO, Z. 2017. Boreal peat properties link to plant functional traits of ecosystem engineers. *Plant and Soil,* 418**,** 277-291.

PANCOST, R. D., MCCLYMONT, E. L., BINGHAM, E. M., ROBERTS, Z., CHARMAN, D. J., HORNIBROOK, E. R., BLUNDELL, A., CHAMBERS, F. M., LIM, K. L. & EVERSHED, R. P. 2011. Archaeol as a methanogen biomarker in ombrotrophic bogs. *Organic Geochemistry,* 42**,** 1279-1287.

PANCOST, R. D., STEART, D. S., HANDLEY, L., COLLINSON, M. E., HOOKER, J. J., SCOTT, A. C., GRASSINEAU, N. V. & GLASSPOOL, I. J. 2007. Increased terrestrial methane cycling at the Palaeocene–Eocene thermal maximum. *Nature,* 449**,** 332-335.

PARSI, Z. & GÓRECKI, T. 2006. Determination of ergosterol as an indicator of fungal biomass in various samples using non-discriminating flash pyrolysis. *Journal of Chromatography A,* 1130**,** 145-150.

PELTONIEMI, K., STRAKOVÁ, P., FRITZE, H., IRÁIZOZ, P. A., PENNANEN, T. & LAIHO, R. 2012. How water-level drawdown modifies litter-decomposing fungal and actinobacterial communities in boreal peatlands. *Soil Biology and Biochemistry,* 51**,** 20-34.

PRESTON, C., HEMPFLING, R., SCHULTEN, H.-R., SCHNITZER, M., TROFYMOW, J. & AXELSON, D. 1994. Characterization of organic matter in a forest soil of coastal British Columbia by NMR and pyrolysis-field ionization mass spectrometry. *Plant and Soil,* 158**,** 69-82.

PRESTON, C. & SCHMIDT, M. 2006. Black (pyrogenic) carbon: a synthesis of current knowledge and uncertainties with special consideration of boreal regions. Biogeoscience, 3, 397-420.

RASSE, D. P., RUMPEL, C. & DIGNAC, M.-F. 2005. Is soil carbon mostly root carbon? Mechanisms for a specific stabilisation. *Plant and soil,* 269**,** 341-356.

REIN, G., CLEAVER, N., ASHTON, C., PIRONI, P. & TORERO, J. L. 2008. The severity of smouldering peat fires and damage to the forest soil. *Catena,* 74**,** 304-309.

REISSER, M., PURVES, R. S., SCHMIDT, M. W. & ABIVEN, S. 2016. Pyrogenic carbon in soils: a literature-based inventory and a global estimation of its content in soil organic carbon and stocks. *Frontiers in Earth Science,* 4**,** 80.

REZANEZHAD, F., PRICE, J. S., QUINTON, W. L., LENNARTZ, B., MILOJEVIC, T. & VAN CAPPELLEN, P. 2016. Structure of peat soils and implications for water storage, flow and solute transport: A review update for geochemists. *Chemical Geology,* 429**,** 75-84.

RIUS, D., VANNIÈRE, B. & GALOP, D. 2009. Fire frequency and landscape management in the northwestern Pyrenean piedmont, France, since the early Neolithic (8000 cal. BP). *The Holocene,* 19**,** 847-859.

ROSA ARRANZ, J. M. D. L. 2007. Aislamiento y caracterización de formas de materia orgánica refractaria en sedimentos marinos. Implicaciones ambientales.

SAIZ-JIMENEZ, C. & DE LEEUW, J. W. 1986. Lignin pyrolysis products: Their structures and their significance as biomarkers. *Organic Geochemistry,* 10**,** 869-876.

SANTÍN, C., DOERR, S. H., PRESTON, C. M. & GONZÁLEZ-RODRÍGUEZ, G. 2015. Pyrogenic organic matter production from wildfires: a missing sink in the global carbon cycle. *Global Change Biology,* 21**,** 1621-1633.

SCHARLEMANN, J. P., TANNER, E. V., HIEDERER, R. & KAPOS, V. 2014. Global soil carbon: understanding and managing the largest terrestrial carbon pool. *Carbon Management,* 5**,** 81-91.

SCHELLEKENS, J., BARBERÁ, G. G. & BUURMAN, P. 2013. Potential vegetation markers–analytical pyrolysis of modern plant species representative of Neolithic SE Spain. *Journal of archaeological science,* 40**,** 365-379.

SCHELLEKENS, J., BINDLER, R., MARTÍNEZ-CORTIZAS, A., MCCLYMONT, E. L., ABBOTT, G. D., BIESTER, H., PONTEVEDRA-POMBAL, X. & BUURMAN, P. 2015a. Preferential degradation of polyphenols from Sphagnum – 4-Isopropenylphenol as a proxy for past hydrological conditions in Sphagnum-dominated peat. *Geochimica et Cosmochimica Acta,* 150**,** 74-89.

SCHELLEKENS, J., BRADLEY, J. A., KUYPER, T. W., FRAGA, I., PONTEVEDRA-POMBAL, X., VIDAL-TORRADO, P., ABBOTT, G. D. & BUURMAN, P. 2015b. The use of plant-specific pyrolysis products as biomarkers in peat deposits. *Quaternary Science Reviews,* 123**,** 254-264.

SCHELLEKENS, J. & BUURMAN, P. 2011. n-Alkane distributions as palaeoclimatic proxies in ombrotrophic peat: the role of decomposition and dominant vegetation. *Geoderma,* 164**,** 112-121.

SCHELLEKENS, J., BUURMAN, P. & KUYPER, T. W. 2012. Source and transformations of lignin in Carex-dominated peat. *Soil Biology and Biochemistry,* 53**,** 32-42.

SCHELLEKENS, J., BUURMAN, P., KUYPER, T. W., ABBOTT, G. D., PONTEVEDRA-POMBAL, X. & MARTÍNEZ-CORTIZAS, A. 2015c. Influence of source vegetation and redox conditions on lignin-based decomposition proxies in graminoid-dominated ombrotrophic peat (Penido Vello, NW Spain). *Geoderma,* 237**,** 270-282.

SCHELLEKENS, J., BUURMAN, P. & PONTEVEDRA-POMBAL, X. 2009. Selecting parameters for the environmental interpretation of peat molecular chemistry–a pyrolysis-GC/MS study. *Organic Geochemistry,* 40**,** 678-691.

SCHLEIFER, K. H. & KANDLER, O. 1972. Peptidoglycan types of bacterial cell walls and their taxonomic implications. *Bacteriological reviews,* 36**,** 407.

SCHMIDT, M. W. & NOACK, A. G. 2000. Black carbon in soils and sediments: analysis, distribution, implications, and current challenges. *Global biogeochemical cycles,* 14**,** 777-793.

SCHMIDT, M. W., TORN, M. S., ABIVEN, S., DITTMAR, T., GUGGENBERGER, G., JANSSENS, I. A., KLEBER, M., KÖGEL-KNABNER, I., LEHMANN, J. & MANNING, D. A. 2011. Persistence of soil organic matter as an ecosystem property. *Nature,* 478**,** 49.

SCHUMANN, M. & JOOSTEN, H. 2008. Global peatland restoration manual. *Institute of Botany and Landscape Ecology, Greifswald University, Germany,* 39**,** 103.

SEILER, W. & CRUTZEN, P. J. 1980. Estimates of gross and net fluxes of carbon between the biosphere and the atmosphere from biomass burning. *Climatic change,* 2**,** 207-247.

SNYDER, A. P., DWORZANSKI, J. P., TRIPATHI, A., MASWADEH, W. M. & WICK, C. H. 2004. Correlation of mass spectrometry identified bacterial biomarkers from a fielded pyrolysis-gas chromatography-ion mobility spectrometry biodetector with the microbiological gram stain classification scheme. *Analytical chemistry,* 76**,** 6492-6499.

SPARKMAN, O. D., PENTON, Z. & KITSON, F. G. 2011. *Gas chromatography and mass spectrometry: a practical guide*, Academic Press.

STAHL, P. D. & PARKIN, T. B. 1996. Relationship of soil ergosterol concentration and fungal biomass. *Soil Biology and Biochemistry,* 28**,** 847-855.

STANKIEWICZ, B. A., HUTCHINS, J. C., THOMSON, R., BRIGGS, D. E. & EVERSHED, R. P. 1997. Assessment of bog-body tissue preservation by pyrolysis-gas chromatography/mass spectrometry. *Rapid Communications in Mass Spectrometry,* 11**,** 1884-1890.

STRACK, M., WALLER, M. & WADDINGTON, J. 2006. Sedge succession and peatland methane dynamics: A potential feedback to climate change. *Ecosystems,* 9**,** 278-287.

SUGDEN, M. A., TALBOT, H. M. & FARRIMOND, P. 2005. Flash pyrolysis–a rapid method for screening bacterial species for the presence of bacteriohopanepolyols. *Organic geochemistry,* 36**,** 975-979.

SULMAN, B. N., MOORE, J. A., ABRAMOFF, R., AVERILL, C., KIVLIN, S., GEORGIOU, K., SRIDHAR, B., HARTMAN, M. D., WANG, G. & WIEDER, W. R. 2018. Multiple models

and experiments underscore large uncertainty in soil carbon dynamics. *Biogeochemistry,* 141**,** 109-123.

SUMMONS, R. E. 2014. The exceptional preservation of interesting and informative biomolecules. *The Paleontological Society Papers,* 20**,** 217-236.

TALBOT, H. M., SQUIER, A. H., KEELY, B. J. & FARRIMOND, P. 2003. Atmospheric pressure chemical ionisation reversed-phase liquid chromatography/ion trap mass spectrometry of intact bacteriohopanepolyols. *Rapid Communications in Mass Spectrometry,* 17**,** 728-737.

THEVENOT, M., DIGNAC, M.-F. & RUMPEL, C. 2010. Fate of lignins in soils: A review. *Soil Biology and Biochemistry,* 42**,** 1200-1211.

THORMANN, M. N., CURRAH, R. S. & BAYLEY, S. E. 2003. Succession of microfungal assemblages in decomposing peatland plants. *Plant and Soil,* 250**,** 323-333.

TIPPING, E., SOMERVILLE, C. J. & LUSTER, J. 2016. The C: N: P: S stoichiometry of soil organic matter. *Biogeochemistry,* 130**,** 117-131.

TOLU, J., GERBER, L., BOILY, J.-F. & BINDLER, R. 2015. High-throughput characterization of sediment organic matter by pyrolysis–gas chromatography/mass spectrometry and multivariate curve resolution: a promising analytical tool in (paleo) limnology. *Analytica chimica acta,* 880**,** 93-102.

TURETSKY, M. R. 2003. The role of bryophytes in carbon and nitrogen cycling. *The Bryologist,* 106**,** 395-409.

TURETSKY, M. R., CROW, S. E., EVANS, R. J., VITT, D. H. & WIEDER, R. K. 2008. Trade-offs in resource allocation among moss species control decomposition in boreal peatlands. *Journal of ecology,* 96**,** 1297-1305.

TURETSKY, M. R., MANNING, S. W. & WIEDER, R. K. 2004. Dating recent peat deposits. *Wetlands,* 24**,** 324-356.

TVEIT, A., SCHWACKE, R., SVENNING, M. M. & URICH, T. 2013. Organic carbon transformations in high-Arctic peat soils: key functions and microorganisms. *The ISME journal,* 7**,** 299.

VAN DER HEIJDEN, E., BOON, J., RASMUSSEN, S. & RUDOLPH, H. 1997. Sphagnum acid and its decarboxylation product isopropenylphenol as biomarkers for fossilised Sphagnum in peats. *Ancient Biomolecules,* 1**,** 93-107.

VAN SMEERDIJK, D. G. & BOON, J. J. 1987. Characterisation of subfossil Sphagnum leaves, rootlets of Ericaceae and their peat by pyrolysis-high-resolution gas chromatography-mass spectrometry. *Journal of Analytical and Applied Pyrolysis,* 11**,** 377-402.

VERHOEVEN, J. & LIEFVELD, W. 1997. The ecological significance of organochemical compounds in Sphagnum. *Acta Botanica Neerlandica,* 46**,** 117-130.

WADDINGTON, J. & DAY, S. 2007. Methane emissions from a peatland following restoration. *Journal of Geophysical Research: Biogeosciences,* 112.

WALLANDER, H., EKBLAD, A., GODBOLD, D. L., JOHNSON, D., BAHR, A., BALDRIAN, P., BJÖRK, R. G., KIELISZEWSKA-ROKICKA, B., KJØLLER, R., KRAIGHER, H., PLASSARD, C. & RUDAWSKA, M. 2013. Evaluation of methods to estimate production, biomass and turnover of ectomycorrhizal mycelium in forests soils – A review. *Soil Biology and Biochemistry,* 57**,** 1034-1047.

WASSEN, M. & JOOSTEN, J. 1996. In search of a hydrological explanation for vegetation changes along a fen gradient in the Biebrza Upper Basin (Poland). *Vegetatio,* 124**,** 191-209.

WEST, A., GRANT, W. & SPARLING, G. 1987. Use of ergosterol, diaminopimelic acid and glucosamine contents of soils to monitor changes in microbial populations. *Soil Biology and Biochemistry,* 19**,** 607-612.

WIEDER, W. R., HARTMAN, M. D., SULMAN, B. N., WANG, Y. P., KOVEN, C. D. & BONAN, G. B. 2018. Carbon cycle confidence and uncertainty: Exploring variation among soil biogeochemical models. *Global Change Biology,* 24**,** 1563-1579.

WILMES, P. & BOND, P. L. 2006. Metaproteomics: studying functional gene expression in microbial ecosystems. *Trends in Microbiology,* 14**,** 92-97.

WORRALL, F., CLAY, G. D., MASIELLO, C. A. & MYNHEER, G. 2013. Estimating the oxidative ratio of the global terrestrial biosphere carbon. *Biogeochemistry,* 115**,** 23-32.

XU, J., MORRIS, P. J., LIU, J. & HOLDEN, J. 2018. PEATMAP: Refining estimates of global peatland distribution based on a meta-analysis. *Catena,* 160**,** 134-140.

YAVITT, J. B., WILLIAMS, C. J. & WIEDER, R. K. 2000. Controls on microbial production of methane and carbon dioxide in three Sphagnum-dominated peatland ecosystems as revealed by a reciprocal field peat transplant experiment. *Geomicrobiology Journal,* 17**,** 61-88.

YE, R., WRIGHT, A. L., INGLETT, K., WANG, Y., OGRAM, A. V. & REDDY, K. 2009. Land-Use Effects on Soil Nutrient Cycling and Microbial Community Dynamics in the Everglades Agricultural Area, Florida. *Communications in soil science and plant analysis,* 40**,** 2725-2742.

YELOFF, D., BLOKKER, P., BARTLETT, S. A., MAUQUOY, D., ROZEMA, J. & VAN GEEL, B. 2008. Decomposition of Juncus seeds in a valley mire (Faroe Islands) over a 900 year period. *Organic Geochemistry,* 39**,** 329-341.

YU, Z., CAMPBELL, I. D., VITT, D. H. & APPS, M. J. 2001. Modelling long-term peatland dynamics. I. Concepts, review, and proposed design. *Ecological Modelling,* 145**,** 197-210.

YU, Z., LOISEL, J., BROSSEAU, D. P., BEILMAN, D. W. & HUNT, S. J. 2010. Global peatland dynamics since the Last Glacial Maximum. *Geophysical Research Letters,* 37.

ZACCONE, C., REIN, G., D'ORAZIO, V., HADDEN, R. M., BELCHER, C. M. & MIANO, T. M. 2014. Smouldering fire signatures in peat and their implications for palaeoenvironmental reconstructions. *Geochimica et Cosmochimica Acta,* 137**,** 134-146.

ŻARNOWSKI, R., SUZUKI, Y., YAMAGUCHI, I. & PIETR, S. J. 2002. Alkylresorcinols in barley (Hordeum vulgare L. distichon) grains. *Zeitschrift für Naturforschung C,* 57**,** 57-62.

ZHANG, X. & AMELUNG, W. 1996. Gas chromatographic determination of muramic acid, glucosamine, mannosamine, and galactosamine in soils. *Soil Biology and Biochemistry,* 28**,** 1201-1206.

ZHANG, Z., WANG, J. J., LYU, X., JIANG, M., BHADHA, J. & WRIGHT, A. 2019. Impacts of land use change on soil organic matter chemistry in the Everglades, Florida-a characterization with pyrolysis-gas chromatography–mass spectrometry. *Geoderma,* 338**,** 393-400.

ZHANG, Z., ZIMMERMANN, N. E., STENKE, A., LI, X., HODSON, E. L., ZHU, G., HUANG, C. & POULTER, B. 2017. Emerging role of wetland methane emissions in driving 21st century climate change. *Proceedings of the National Academy of Sciences,* 114**,** 9647-9652.

ZHOU, W., XIE, S., MEYERS, P. A. & ZHENG, Y. 2005. Reconstruction of late glacial and Holocene climate evolution in southern China from geolipids and pollen in the Dingnan peat sequence. *Organic Geochemistry,* 36**,** 1272-1284.

Chapter 3 – Investigating the influence of instrumental parameters and chemical composition on pyrolysis efficiency of peat

Authors, Kristy Klein[1,2*], Miriam Groß-Schmölders[2], Jose Maria De la Rosa[3], Christine Alewell[2], Jens Leifeld[1]

[1]Climate and Agriculture Group, Agroscope, Reckenholzstraße 191, 8046 Zürich, Switzerland

[2]Environmental Geosciences, University of Basel, Bernoullistrasse 32, 4056 Basel, Switzerland

[3]Instituto de Recursos Naturales y Agrobiología de Sevilla, Consejo Superior de Investigaciones Cientifícas (IRNAS-CSIC). Reina Mercedes Av. 10, 41012 Seville, Spain

Communications in Soil Science and Plant Analysis, Volume 51(12), pp. 1572-1581, 2020
https://doi.org/10.1080/00103624.2020.1784916

Abstract

To track changes in organic matter (OM) in peat soils, analytical techniques are needed that effectively characterize their chemical components. Pyrolysis-gas chromatography/mass spectrometry is a useful method for obtaining a chemical "fingerprint" of OM. To obtain representative fingerprints, the pyrolysis process should be highly reproducible and representative of the original sample; however, these key indicators for successful volatilization are underreported in the literature. We investigated the influence of instrumental parameters (temperatures, heating rates, sample mass), original organic C and nitrogen (N) content, and instrument type ("slow" vs "flash"), on volatilization of different peat samples by monitoring sample mass loss and changes in organic C and N content before and after pyrolysis. Average percent C by mass volatilized ("C pyrolysis efficiency") across all pyrolysis experiments conducted (mass, instrument types, and settings) was 47.8±1.8 %. Sample mass was not a major driver; however, instrument temperatures, heating rate and original N content had a significant influence on pyrolysis efficiency. N pyrolysis efficiency occurred at significantly higher rates (56.7 – 75.8 %) than C pyrolysis efficiency (45.1 – 51.6 %). N pyrolysis efficiency was also negatively influenced by decreasing concentrations of original sample N, suggesting that N-containing compounds may undergo preferential volatilization in high pyrolysis temperatures. Our data suggest that C pyrolysis efficiency is relatively insensitive to instrumental parameters; whereas when seeking to identify N-containing compounds, appropriate temperatures and heating rates must be chosen. These results provide an expected range for pyrolysis efficiency as a reference for peat samples analyzed with this technique.

3.1 Introduction

Soil organic matter (SOM) is a crucial store for terrestrial organic carbon (OC), and is considered to be an integral part of greenhouse gas emission mitigation (Paustian et al. 2016). Because of their huge OC store, peatlands play a special role in this context (Leifeld, Wüst-Galley, and Page 2019). Furthermore, peatlands are usually areas of great ecological and environmental value and have been used as a record of environmental changes. To this end, analysis methods are needed that can accurately identify and characterize organic matter (OM) composition, in order to track how these components change with decomposition and diagenesis processes. Differentiating changing conditions in peat using macroscopic methods presents a challenge, as the continuum of progressively decomposing OM can be difficult to distinguish visually. Characterizing the molecular components of an OM profile can distinguish periods with prevalence of degradation (decomposition) and growth (accumulation), through the use of molecular biomarkers. This, in turn, offers an opportunity to improve flux estimates and to potentially assess restoration efforts using ratios of microbial matter to undecomposed plant material.

Numerous analysis techniques have been applied for the characterization of OM in peat, such as Fourier Transform Infrared spectroscopy (Artz et al. 2008, Chapman et al. 2001), isotope-ratio mass spectrometry (IR/MS) (Alewell et al. 2011, Krull and Retallack 2000), or solid-state ^{13}C nuclear magnetic resonance (NMR) spectroscopy (Preston et al. 1994, Baldock et al. 1997). Due to the molecular heterogeneity of OM and difficulty in obtaining a representative "snapshot" of such complex material, many studies combine multiple complementary analytical techniques (De la Rosa et al. 2011, Lu, Hanna, and Johnson 2000, Krüger et al. 2016).

Analytical pyrolysis has been identified as an especially effective tool for the molecular characterization of complex OM, eliminating the need for time-consuming wet chemistry pretreatment techniques (Parsi et al. 2007, Schellekens, Buurman, and Pontevedra-Pombal 2009, Derenne and Quénéa 2015). The volatile products released during pyrolysis of peat often correspond to well-known components from plant and microbial origin (Boon, Dupont, and De Leeuw 1986). In particular, pyrolysis is an analytical tool especially responsive to the presence and composition of lignins (Martin, Saiz-Jimenez, and Gonzalez-Vila 1979), n-alkanes, and nitrogen (N)-containing compounds (De la Rosa et al. 2012). Much of SOM is composed of high molecular weight compounds (>600 Daltons) that are too large to be easily volatilized

using standard gas chromatography-mass spectrometry techniques (White et al. 2004). To extract this material, chemical separation techniques are often required that can lead to both a modification of the original extracted compounds, and a large component of remaining un-extractable OM material. Through thermal degradation of these large compounds into smaller molecular fragments (Saiz-Jimenez 1994), analytical pyrolysis permits the volatilization and identification of complex high molecular weight compounds which might not otherwise be detectable (White et al. 2004). Moreover, analytical pyrolysis coupled with gas chromatography-mass spectrometry (Py-GC/MS) provides enhanced structural detail, and when combined as part of a multi-proxy approach with other techniques, contributes high-resolution molecular data to OM component analysis.

While Py-GC/MS is a useful tool, some uncertainty exists regarding the representativeness of the pyrolyzed sample of the original OM. During the pyrolysis process, secondary reactions can occur from cleavage of larger macromolecules, resulting in the formation of novel compounds and inhibiting fragmentation of others (Saiz-Jimenez 1994). OM can also be modified via secondary reactions into compounds that are more thermally stable and resistant to pyrolysis than those originally present (Saiz-Jimenez 1994). Different instrument set-ups can create "cold spots," or areas of slower flushing of pyrolysates from the pyrolyzer to the detection system, potentially creating an environment for condensation of higher molecular weight compounds and preferential representation of smaller compounds in analysis (Parsi et al. 2007, Górecki and Poerschmann 2001).

In addition, the pyrolysis process typically leaves behind a carbonaceous residue (char) of unknown quantity and composition (Uden 1993). OM content in a sample is not necessarily proportionate to the amount of material pyrolyzed, and may be influenced by instrument parameters, sample mass, type and origin of OM represented (Preston et al. 1994), or the presence of minerals or metal cations in the original sample (Schulten and Leinweber 1996). Adjustments in temperature or heating rates may be needed for compounds of varying molecular weight and polarity, or to release OM bound to a mineral matrix.

As pyrolysate-derived chromatograms reflect only the material that was readily volatilized and transferred onto the GC column, variations in Py-GC/MS total ion intensities (TII) have been observed across different analytical techniques (Huang et al. 1998). Moreover, "standard approaches" for analytical measurements using pyrolysis-based techniques are lacking. Due to

the versatility of pyrolysis-driven methods when used to enhance volatilization of OM, researchers employ a variety of different temperatures, heating rates, instrumental configurations (offline pyrolysis, Curie-point pyrolysis, pyrolysis methods used in tandem with GC/MS or field ionization mass spectrometry (Py-FIMS), etc), OM pre-treatment and/or extraction approaches. These differences are driven both by specific needs of labs and the type of OM studied. Each configuration and technique results in differences in OM volatilization and potential chemical selectivity. Therefore, it can be difficult to compare separation and detection studies using pyrolysis to one another, as no two method approaches are exactly the same. As a result of this variability in volatilization efficiency and other above-described challenges, direct quantitative Py-GC/MS analysis has not been considered feasible to date. For estimation purposes, chromatographic peak areas have been related to the quantity contained in the original sample to compare the effects of temperature and time on pyrolysis product formation (Lu et al. 2011), or by normalizing pyrogram peaks by measuring sample weight before and after pyrolysis (Biller and Ross 2014, Sorge et al. 1993). Measurements for pyrolysis efficiency as well as changes in carbon (C) and N content have been obtained for mineral soils and SOM extractions (Leinweber and Schulten 1995, Schulten, Leinweber, and Theng 1996, Sorge et al. 1993). However, studies specifically and systematically addressing pyrolysis efficiency have not yet been conducted for peat.

Pyrolysis-derived sample weight loss and OM volatilization (changes in C and N content before and after pyrolysis) are not typically reported currently in analytical Py-GC/MS research as a systematic practice, despite the need for improved knowledge regarding expected ranges of volatilization across different OM types and pyrolysis instrument set-ups. Moreover, as Py-GC/MS analysis is becoming a more frequently used tool to investigate the chemical composition of peat, a frame of reference of expected volatilization of OM is particularly needed for studying organic soils.

3.2 Aims of current study

To explore the physical and chemical mechanisms influencing the reliability of analytical pyrolysis techniques for peat soil samples, this study aimed to investigate the effect of instrumental parameters and original sample composition (OC and total N) on the amount of OM material successfully volatilized (hereby referred to as pyrolysis efficiency). To approach

this aim, peat sample masses and OC and N content were monitored before and after pyrolysis to investigate pyrolysis-driven changes in OM content.

3.3 Materials and methods

3.3.1 Peat sample preparation

Ten peat samples were selected representing a range of different peatland types (fen, bog), climate (temperate, boreal), land uses, sampling depths, degradation status, and C and N content. The selected samples have also been previously analyzed via other instrumental techniques and are discussed further by (Leifeld et al. 2018). An overview of the selected sampling locations is provided in **Table 1.** All peat samples were collected in the field using peatland corers, stored at 2 °C until sample preparation, then oven-dried and homogenized with a mixer mill (Retsch MM 400) for three minutes at 25 Hz. No other pretreatment preparation of peat samples was applied prior to analysis. Due to insufficient sample quantity, sample S-7 was not measured in the Frontier pyrolysis efficiency analysis. All other peat samples used in the pyrolysis instrument comparison study were identical**.**

Table 1. Overview of sampling sites, including peatland type, current land use, sample depths, original OC and N content, soil pH, and degradation status.

Sample		Site	Coordinates	Peatland type*	Current land use	Sample depth (cm)	OC %	N %	Soil pH**	Status
S-1	P4a 83-85	Paulinenaue	52·69°N, 12·72°E	fen	GL	83-85	10.52	0.6	5.8	Degraded
S-2	Seeboden-Alp5	Seeboden-Alp	47·06°N, 8·46°E	bog	N	32-36	55.67	1.53	3.1	Degraded
S-3	P247D 83-86	Paulinenaue	52·69°N, 12·72°E	fen	GL	83-86	46.57	2.6	5.8	Degraded
S-4	GRC 186-189	Gruyere	47·24°N, 7·05°E	bog	N	186-189	55.49	1.42	4.5	Intact
S-5	HMC 180-183	Hagenmoos	47·24°N, 8·52°E	bog	FL	180-183	56.96	1.56	5.3	Degraded
S-6	Staatswald 80-95	Witzwil	46·98°N, 7·05°E	fen	FL	80-95	50.6	1.96	4	Degraded
S-7	GE1 80-82 BE-1734	Ahlen-Falkenberg	53·41°N, 8·49°E	bog	GL	80-82	50.08	0.9	3.4	Intact
S-8	P33 5-15	Witzwil	46·98°N, 7·05°E	fen	CL	Mai.15	28.13	1.89	6.8	Degraded
S-9	GI-1 80-82 BE-1743	Ahlen-Falkenberg	53·41°N, 8·49°E	bog	GL	80-82	52.38	1.53	3.3	Intact
S-10	Parzelle Spring	Witzwil	46·98°N, 7·05°E	fen	CL	45-55	40.33	2.4	5.1	Degraded

*before drainage
CL=cropland; GL=grassland;
FL=forest; N=natural;
** **0.01**
M CaCl2

3.3.2 Pyrolysis instruments and parameter settings

Instrumental parameters tested were temperature, heating rate, mass, and instrument set-up. Pyrolysis efficiency was monitored for changes by analyzing sample mass loss, as well as C and N content before and after pyrolysis.

C and N pyrolysis efficiency were calculated as percent volatilization:

$$PyE\ (\%) = (M_{original} - M_{final})/M_{original} * 100,$$

where $M_{original}$ represents the elemental mass of the original pre-pyrolysis sample (mg C or N, calculated from percentage C or N obtained from elemental analysis), and M_{final} represents the elemental mass of the post-pyrolysis sample (mg C and N contained in char, calculated using percentage C or N obtained from post-pyrolysis elemental analysis).

"Slow" pyrolysis analysis was conducted using an "offline" Netzsch Simultaneous Thermal Analyzer STA 449 F3 equipped with a TG-DSC sample carrier (Type S) in inert Helium atmosphere. Samples were analyzed at 600, 800, and 990 °C, and at heating rates of 10K/min., 20K/min., and 50K/min. At 50K/min, the highest temperature measurement was reduced to 950 °C due to instrumental limitations. To investigate the effect of sample mass on pyrolysis efficiency, peat samples were measured in 20 mg, 10 mg, and 5 mg mass ranges. Reproducibility of C pyrolysis efficiency was conducted using one peat sample (S-6) measured five times under identical conditions and similar approximate mass (20 mg). The relationship between OC and N content and pyrolysis efficiency was investigated with a ten-part sample dilution study. For the dilution experiments, two pure samples (S2 and S6) were mixed with powdered aluminum oxide Al_2O_3 to achieve 75, 66, 50, 33, 25, 10, 5, 2.5, and 1 percent of the original sample OC concentration, then homogenized in a mixer mill for two minutes at 21 Hz. Peat samples used to investigate sample mass, original OC and total N (dilution measurements), and reproducibility were analyzed at 800 °C and a heating rate of 20K/min. Mass loss was calculated via integration of the thermogravimetric curve obtained for each sample.

"Flash" pyrolysis was conducted using a double-shot pyrolyzer (Frontier Laboratories, model 2020i) operating in single shot mode. Approximately 20 mg of sample was introduced for one minute into a preheated (600 °C) micro-furnace with an inert He atmosphere. For "flash"

pyrolysis measurements, sample mass loss was calculated through the mass difference of the sample capsules before and after pyrolysis.

Bulk OC and N analysis was conducted on all samples using a EuroEA3000 Elemental Analyzer by dry combustion.

3.3.3 Statistical analysis

Analytical pyrolysis instruments and parameter settings were statistically tested for differences in pyrolysis efficiency. Pyrolysis efficiency was correlated to sample C/N mass ratios and original C and N content via regression analyses. Differences in C and N pyrolysis efficiencies for the different instrument parameters including the different instruments were determined using a one-way analysis of variance (ANOVA), where factors (mass, heating rate, and temperature) were tested. In cases where significant differences were identified, factors were tested individually by paired T-test. Differences between overall C and N pyrolysis efficiency across all samples was determined by paired T-test. Statistical significance for all tests was set as $p<0.05$. Results are given as mean ± standard deviation of the mean.

3.4 Results

3.4.1 C and N pyrolysis efficiency

Average C and N pyrolysis efficiency for the different instrumental parameters (temperatures, heating rate, and instrument) is provided in **Table 2.** Average C and N pyrolysis efficiency for different sample masses is provided in **Table 3**. While the "flash" pyrolysis instrument obtained a tendency towards higher efficiency measurements overall than those obtained from the "slow" pyrolysis instrument, they were not significantly different between the two instruments for C or N.

Mean C pyrolysis efficiency across all instrumental parameters (including different masses) was 47.8±1.8 %, and ranged from 45.1-51.6%. Analytical error was 1.1 %, and was determined from the average C pyrolysis efficiency obtained in the reproducibility study (36.4±0.4 %). C pyrolysis efficiency was not significantly influenced by increases in temperature or mass. Significant increases in C pyrolysis efficiency were observed for samples pyrolyzed at 600 °C when the heating rate was increased from 10K/min to 20K/min (***p*<0.01**), and from 10K/min to 50K/min (***p*<0.01**), but no differences were observed when the heating rate was increased from

20K/min to 50K/min. Significant increases in C pyrolysis efficiency were also observed for samples pyrolyzed at the highest temperature (990 °C) when the heating rate was increased from 10K/min to 50 K/min (***p*<0.01**) and from 20K/min to 50K/min (***p*<0.01**).

Mean N pyrolysis efficiency across all instrumental parameters was 67.3±6.1 % and ranged from 56.7-75.8 %. N pyrolysis efficiency was significantly higher than C pyrolysis efficiency in across all samples (***p*<0.01).** This suggests that N-containing compounds are preferentially volatilized during pyrolysis. Average reproducibility of N pyrolysis efficiency was determined using the same sample as measured for C reproducibility and was 80.1±0.8 %. N pyrolysis efficiency was not significantly different for different sample mass. High variability was observed for N pyrolysis efficiencies, possibly due to N concentrations of post-pyrolysis residues approaching the detection limit for the Elemental Analyzer.

Table 2. Average ± standard deviation of C and N pyrolysis efficiency for instrumental parameters (in units of percent C or N by mass volatilized). "Flash" pyrolysis efficiency measurements were conducted using the Frontier pyrolysis instrument. All other parameters were measured on the Netzsch pyrolysis instrument.

	Temperature 600 °C			Temperature 800 °C			Temperature 950/990 °C			"Flash"
	10K/min	20K/min	50K/min	10K/min	20K/min	50K/min	10K/min	20K/min	50K/min	600
C	46.6±3.8	48.6±3.4	50.0±3.4	46.2±5.3	47.9±4.6	48.7±3.6	45.3±5.8	45.1±5.1	48.7±4.3	51.6±5.5
N	58.4±3.4	56.7±3.5	60.9±3.2	67.7±6.5	69.3±6.7	70.5±7.6	72.5±14.9	75.8±12.4	75.5±12.2	63.4±8.4

Table 3. Average ± standard deviation of C and N pyrolysis efficiency using varied original sample mass (in units of percent C or N by mass volatilized). Measured on Netzsch pyrolysis instrument at 800 °C and 20K/min.

	Mass (mg)		
	20	10	5
C	48.6±4.8	46.6±5.1	47.4±5.5
N	69.5±6.9	69.9±7.7	65.0±11.6

N pyrolysis efficiency was significantly higher for temperatures of 800 °C and 900 °C than for 600 °C across all heating rates (***p*<0.01**). Significant differences in N pyrolysis efficiency were observed between 800 °C and 900 °C for heating rates at 20K/min (***p*<0.05**) and 50K/min (***p*<0.05**), but not for 10K/min. All N pyrolysis efficiencies measured from all temperature comparisons were statistically significant when the rate was increased from 10k/min to 50K/min, indicating that heating rate was an important factor for the volatilization of N-containing compounds (***p*<0.05**). A significant effect was also observed for heating rate at 600

°C, where N pyrolysis efficiency increased when the heating rate was increased from 20K/min to 50K/min (***p*<0.01**).

3.4.2 Original OC and N content and pyrolysis efficiency – sample dilutions

Dilution measurements showed only a weak correlation between C pyrolysis efficiency and original OC content **(r=0.25, *p*>0.05),** suggesting that initial concentrations of OC did not influence the successful pyrolysis of the material. However, a strong logarithmic relationship was observed between N pyrolysis efficiency and original N content (**Figure 1, r=0.83, *p*<0.01**). At low initial N concentration, pyrolysis efficiency sharply decreased.

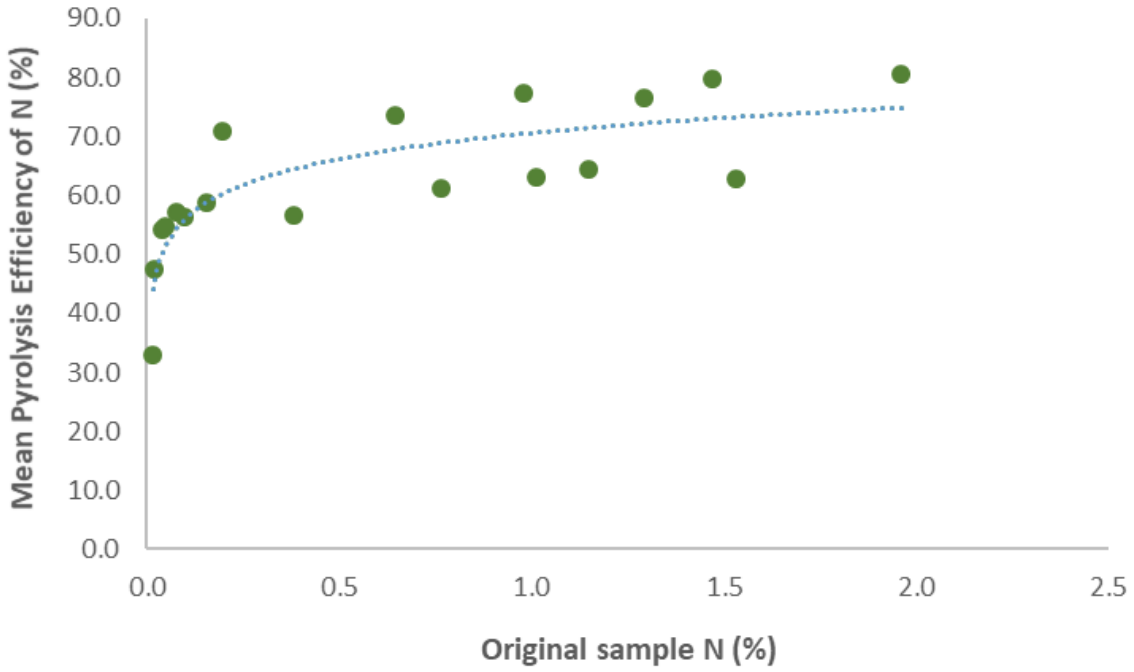

Figure 1. Average N pyrolysis efficiency and original sample N content (percent). The equation of the regression line is y = 6.3295ln(x) + 70.585.

3.4.3 Correlation to sample C/N

Original sample C/N ratios (pre-pyrolysis) were correlated to C pyrolysis efficiency. The C/N mass ratio had a strong positive linear correlation with pyrolysis efficiency on the "flash" Frontier instrument (**r=0.73, *p*<0.05**). However, a correlation was not observed with the "slow" Netzsch instrument, even across the highest temperatures and heating rates.

3.5 Discussion

The lack of significant difference in pyrolysis efficiency for C and N between the two instrument set-ups suggests that different pyrolysis instrument configurations can be expected to produce similar results, at least in terms of representativeness of the volatilized sample. Despite increasing trends with heating rate, the range for C pyrolysis efficiency (45.1-51.6 %) was relatively narrow, suggesting that C-derived compounds may be somewhat less sensitive to adjustments to the pyrolysis method. The range for N pyrolysis efficiency, however, was larger (56.7-75.8 %), suggesting a greater potential to adjust analytical instruments to improve N volatilization with increased temperature and heating rates. In addition, the significantly higher rates of N pyrolysis efficiency compared to C pyrolysis efficiency indicate that N-containing compounds may be preferentially volatilized during the pyrolysis process. The mechanism behind this stoichiometric preference is unclear, and should be investigated in future pyrolytic kinetic studies.

N-containing compounds were more likely to be influenced by decreasing concentrations, particularly at very low original concentrations. Our data suggest that if peat samples contain original N content of at least 0.5 %, an acceptable efficiency in pyrolyzed N-compounds (above 65 %) is likely. As N-containing compounds serve an important role in nutrient-limited ombrotrophic peatlands (Larmola et al. 2013), it is important to consider this potential for stoichiometric selectivity in Py-GC/MS studies seeking to investigate the molecular composition of N-containing SOM. Care must be taken to use N-appropriate temperature and heating rate parameters (ie., higher temperatures and heating rates than what might otherwise be appropriate for C compounds) in studies focused on N. This issue will also be of particular importance when characterizing N-containing compounds in OM, as amide and amine-derived compounds can be transformed into heterocyclic pyrols and pyridines in pyrolysis conditions at lower temperatures (e.g. 350 °C), resulting in more stable compounds that subsequently require higher temperatures (greater than 600 °C) for further volatilization (De la Rosa et al. 2008). Further, it may be advisable to seek out the assistance of different instrument set-ups in other labs to improve results.

It is important to note that due to the versatility of the method, variety of approaches used, and lack of available pyrolysis efficiency data in the literature, it is difficult to compare different pyrolysis-based studies to one another. Nevertheless, a cautious comparison of findings is

provided here. The ranges of C and N percent volatilization in this study (45.1-51.6 and 56.7-75.8, respectively) were slightly less than volatilization rates reported in previous studies on soil materials other than peat. While using pyrolysis-field ionization mass spectrometry (Py-FIMS) to investigate differences in clay-associated surfaces and interlayer OM volatility, (Schulten, Leinweber, and Theng 1996) reported that mineral soil samples volatilized 64 % C and 76 % N, and 86 % C and 91 % N for the same samples pre-treated with H_2O_2. It was also noted that before Py-GC/MS analysis, samples in that study were additionally pre-treated with tetramethylammonium hydroxide (TMAH). Further, (Leinweber and Schulten 1995) found an average volatilization of 57 % C and 79 % N from a wide range of OM samples when investigating soil-mineral associations in mineral soils of agricultural origin. While their findings were slightly higher than our values, we still consider them in agreement with the results of this study. (Sorge et al. 1993) used Py-FIMS to investigate method reproducibility and to explore the influence of sample organic C concentration on the percentages of volatilized matter. After determining the percentage of volatilized matter across a range of bulk soils, litter samples, and humic substances, they found that percent residue indicated that an average of only 24.6 % of the initial sample was volatilized, with as little as 4.7 % volatilization rate reported for whole soils. Volatilization of litter and humic substances in that study were 54.4 %, similar to the findings of this research (Sorge et al. 1993). It was also noted that, in agreement with this study, these authors reported higher N pyrolysis volatilization relative to C volatilization.

(Leinweber and Schulten 1995) and (Sorge et al. 1993) also reported a positive correlation of the proportion of OM volatilized to the initial sample C concentration, in contrast to the findings of this study. However, in addition to the TMAH thermochemolysis used by (Schulten, Leinweber, and Theng 1996), each of these previous studies included results that relied on a combination of chemical pre-treatments and/or extractions as a part of their analyses, which may have the potential to introduce chemical changes to the original sample material(Leinweber and Schulten 1995, Sorge et al. 1993). Although chemical pre-treatments and OM extractions can be beneficial in assisting in demineralization of OM-poor samples (such as from clayey soils), and may improve pyrolytic volatilization of OM, reliable results for molecular compounds can also be obtained using untreated samples (Grandy et al. 2009). Moreover, there is also compelling evidence that some pre-treatment and extraction methods can result in the selective loss of some OM compounds, thus skewing the interpretation of results (Schmidt et

al. 2011, Derenne and Quénéa 2015). Thus, it is beneficial to obtain measurements for pyrolysis efficiency for untreated samples.

3.6 Conclusions

Analytical pyrolysis is a highly reproducible technique for the volatilization and detection of organic constituents of peat samples. Sample heating rate were found to significantly influence both C and N pyrolysis efficiency, however the effect was stronger for N. N pyrolysis efficiency was also significantly influenced by increasing maximum temperatures, whereas C pyrolysis efficiency was not driven by this factor. Sample mass was not a major driver of pyrolysis efficiency for either C or N.

Overall pyrolysis efficiency was found to be affected by original N content, suggesting that successful OM volatilization may be influenced by original sample OM chemistry. For analytical pyrolysis measurements, this also suggests that original OM sample chemistry is more influential for complete volatilization than instrumental parameters used (assuming minimal combustion). It remains generally unknown whether certain classes of compounds (ie., polysaccharides, N-containing compounds) might be over or under-represented in peat Py-GC/MS studies when using different temperatures, heating rates, or instruments.

The results of this study are of interest for the development of quantitative applications of analytical pyrolysis in the near future. As most instrumental analysis methods present the potential for some degree of selectivity, combining Py-GC/MS techniques with complementary methods is recommended for robust analysis – particularly for the interpretation for complex OM. In addition, while analytical pyrolysis instruments are generally unable to achieve total sample volatilization, these data provide reasonable prediction for molecular recovery for peat OM samples when using pyrolysis analytical techniques. These estimates may also serve as an important check on method quality control prior to subsequent chemical characterization analysis.

Acknowledgments

The authors would like to thank the anonymous reviewer for their constructive comments and suggestions. Robin Giger conducted elemental analysis for all peat samples and maintenance

on the Netzsch pyrolyzer instrument. Markus Jocher assisted with maintenance for the Frontier pyrolyzer instrument. Their assistance with this work was invaluable and greatly appreciated. This study was funded by the Swiss National Science Foundation, project number 200021_169556. J.M. De la Rosa thanks the Spanish Ministry of Economy and Competitiveness (MINECO) and AEI for funding his "Ramón y Cajal" post-doctoral contract (RYC2014-16338).

References

Alewell, C, Reiner Giesler, Jonatan Klaminder, J Leifeld, and M Rollog. 2011. "Stable carbon isotopes as indicators for environmental change in palsa peats." *Biogeosciences* no. 8 (7):1769-1778.

Artz, Rebekka RE, Stephen J Chapman, AH Jean Robertson, Jacqueline M Potts, Fatima Laggoun-Défarge, Sébastien Gogo, Laure Comont, Jean-Robert Disnar, and Andre-Jean Francez. 2008. "FTIR spectroscopy can be used as a screening tool for organic matter quality in regenerating cutover peatlands." *Soil Biology and Biochemistry* no. 40 (2):515-527.

Baldock, JA, JM Oades, PN Nelson, TM Skene, A Golchin, and P Clarke. 1997. "Assessing the extent of decomposition of natural organic materials using solid-state 13C NMR spectroscopy." *Soil Research* no. 35 (5):1061-1084.

Biller, P, and AB Ross. 2014. "Pyrolysis GC–MS as a novel analysis technique to determine the biochemical composition of microalgae." *Algal Research* no. 6:91-97.

Boon, JJ, L Dupont, and JW De Leeuw. 1986. "Characterization of a peat bog profile by Curie point pyrolysis-mass spectrometry combined with multivariant analysis and by pyrolysis gas chromatography-mass spectrometry." *Peat and Water*:215-239.

Chapman, S. J., C. D. Campbell, A. R. Fraser, and G. Puri. 2001. "FTIR spectroscopy of peat in and bordering Scots pine woodland: relationship with chemical and biological properties." *Soil Biology and Biochemistry* no. 33 (9):1193-1200. doi: https://doi.org/10.1016/S0038-0717(01)00023-2.

De la Rosa, J. M., J. A. González-Pérez, F. J. González-Vila, H. Knicker, and M. F. Araújo. 2011. "Molecular composition of sedimentary humic acids from South West Iberian Peninsula: A multi-proxy approach." *Organic Geochemistry* no. 42 (7):791-802. doi: 10.1016/j.orggeochem.2011.05.004.

De la Rosa, JM, JA González-Pérez, R González-Vázquez, H Knicker, E López-Capel, DAC Manning, and FJ González-Vila. 2008. "Use of pyrolysis/GC–MS combined with thermal analysis to monitor C and N changes in soil organic matter from a Mediterranean fire affected forest." *Catena* no. 74 (3):296-303.

De la Rosa, José María, Silvia Regina Faria, María Eufemia Varela, Heike Knicker, Francisco Javier González-Vila, José Antonio González-Pérez, and Jakob Keizer. 2012. "Characterization of wildfire effects on soil organic matter using analytical pyrolysis." *Geoderma* no. 191:24-30.

Derenne, Sylvie, and Katell Quénéa. 2015. "Analytical pyrolysis as a tool to probe soil organic matter." *Journal of Analytical and Applied Pyrolysis* no. 111:108-120. doi: http://dx.doi.org/10.1016/j.jaap.2014.12.001.

Górecki, T, and J Poerschmann. 2001. "In-column pyrolysis: A new approach to an old problem." *Analytical chemistry* no. 73 (9):2012-2017.

Grandy, A Stuart, Michael S Strickland, Christian L Lauber, Mark A Bradford, and Noah Fierer. 2009. "The influence of microbial communities, management, and soil texture on soil organic matter chemistry." *Geoderma* no. 150 (3-4):278-286.

Huang, Y, G Eglinton, ERE Van der Hage, JJ Boon, R Bol, and Phil Ineson. 1998. "Dissolved organic matter and its parent organic matter in grass upland soil horizons studied by analytical pyrolysis techniques." *European Journal of Soil Science* no. 49 (1):1-15.

Krüger, Jan Paul, Christine Alewell, Kari Minkkinen, Sönke Szidat, and Jens Leifeld. 2016. "Calculating carbon changes in peat soils drained for forestry with four different profile-based methods." *Forest Ecology and Management* no. 381:29-36.

Krull, Evelyn S, and Gregory J Retallack. 2000. "δ13C depth profiles from paleosols across the Permian-Triassic boundary: Evidence for methane release." *Geological Society of America Bulletin* no. 112 (9):1459-1472.

Larmola, Tuula, Jill L Bubier, Christine Kobyljanec, Nathan Basiliko, Sari Juutinen, Elyn Humphreys, Michael Preston, and Tim R Moore. 2013. "Vegetation feedbacks of nutrient addition lead to a weaker carbon sink in an ombrotrophic bog." *Global Change Biology* no. 19 (12):3729-3739.

Leifeld, Jens, Christine Alewell, Cédric Bader, Jan Paul Krüger, Carsten W Mueller, Michael Sommer, Markus Steffens, and Sönke Szidat. 2018. "Pyrogenic carbon contributes substantially to carbon storage in intact and degraded northern peatlands." *Land degradation & development* no. 29 (7):2082-2091.

Leifeld, Jens, Chloé Wüst-Galley, and Susan Page. 2019. "Intact and managed peatland soils as a source and sink of GHGs from 1850 to 2100." *Nature Climate Change*:1-3.

Leinweber, P, and H-R Schulten. 1995. "Composition, stability and turnover of soil organic matter: investigations by off-line pyrolysis and direct pyrolysis-mass spectrometry." *Journal of Analytical and Applied Pyrolysis* no. 32:91-110.

Lu, Qiang, Xiao-chu Yang, Chang-qing Dong, Zhi-fei Zhang, Xu-ming Zhang, and Xi-feng Zhu. 2011. "Influence of pyrolysis temperature and time on the cellulose fast pyrolysis products: Analytical Py-GC/MS study." *Journal of Analytical and Applied Pyrolysis* no. 92 (2):430-438.

Lu, X. Q., J. V. Hanna, and W. D. Johnson. 2000. "Source indicators of humic substances: an elemental composition, solid state 13C CP/MAS NMR and Py-GC/MS Study." *Applied Geochemistry* no. 15 (7):1019-1033. doi: https://doi.org/10.1016/S0883-2927(99)00103-1.

Martin, F, C Saiz-Jimenez, and FJ Gonzalez-Vila. 1979. "Pyrolysis-gas chromatography-mass spectrometry of lignins." *Holzforschung* no. 33 (6):210-212.

Parsi, Z, N Hartog, T Górecki, and J Poerschmann. 2007. "Analytical pyrolysis as a tool for the characterization of natural organic matter—A comparison of different approaches." *Journal of analytical and applied pyrolysis* no. 79 (1):9-15.

Paustian, Keith, Johannes Lehmann, Stephen Ogle, David Reay, G Philip Robertson, and Pete Smith. 2016. "Climate-smart soils." *Nature* no. 532 (7597):49.

Preston, CM, R Hempfling, H-R Schulten, M Schnitzer, JA Trofymow, and DE Axelson. 1994. "Characterization of organic matter in a forest soil of coastal British Columbia by NMR and pyrolysis-field ionization mass spectrometry." *Plant and Soil* no. 158 (1):69-82.

Saiz-Jimenez, C. 1994. "Analytical pyrolysis of humic substances: pitfalls, limitations, and possible solutions." *Environmental science & technology* no. 28 (11):1773-1780.

Schellekens, Judith, Peter Buurman, and Xabier Pontevedra-Pombal. 2009. "Selecting parameters for the environmental interpretation of peat molecular chemistry–a pyrolysis-GC/MS study." *Organic Geochemistry* no. 40 (6):678-691.

Schmidt, Michael WI, Margaret S Torn, Samuel Abiven, Thorsten Dittmar, Georg Guggenberger, Ivan A Janssens, Markus Kleber, Ingrid Kögel-Knabner, Johannes Lehmann, and David AC Manning. 2011. "Persistence of soil organic matter as an ecosystem property." *Nature* no. 478 (7367):49.

Schulten, H-R, P Leinweber, and BKG Theng. 1996. "Characterization of organic matter in an interlayer clay-organic complex from soil by pyrolysis methylation-mass spectrometry." *Geoderma* no. 69 (1-2):105-118.

Schulten, Hans-Rolf, and Peter Leinweber. 1996. "Characterization of humic and soil particles by analytical pyrolysis and computer modeling." *Journal of analytical and applied pyrolysis* no. 38 (1-2):1-53.

Sorge, C, R Müller, P Leinweber, and H-R Schulten. 1993. "Pyrolysis-mass spectrometry of whole soils, soil particle-size fractions, litter materials and humic substances: statistical evaluation of sample weight, residue, volatilized matter and total ion intensity." *Fresenius' journal of analytical chemistry* no. 346 (6):697-703.

Uden, Peter C. 1993. "Nomenclature and terminology for analytical pyrolysis (IUPAC Recommendations 1993)." *Pure and applied chemistry* no. 65 (11):2405-2409.

White, Daniel M, D Sarah Garland, Lothar Beyer, and Kenji Yoshikawa. 2004. "Pyrolysis-GC/MS fingerprinting of environmental samples." *Journal of Analytical and Applied Pyrolysis* no. 71 (1):107-118.

Chapter 4 - Characterizing ecosystem-driven chemical composition differences in natural and drained Finnish bogs using Pyrolysis-GC/MS

Authors, Kristy Klein[1,2*], Judith Schellekens[3], Miriam Groβ-Schmölders[2], Pascal von Sengbusch[4], Christine Alewell[2], Jens Leifeld[1]

[1]Agroscope, Climate and Agriculture Group, Reckenholzstrasse 191, CH-8046 Zürich

[2]Environmental Geosciences, University of Basel, Bernoullistrasse 32, CH-4056 Basel

[3]Forest, Nature and Landscape, KU Leuven, Celestijnenlaan 200e – box 2411, BE -3001 Leuven

[4]Office for ecological reports, Fuchsrain 10, GER-79400 Kandern

In press, Organic Geochemistry, Volume 165, 2022

https://doi.org/10.1016/j.orggeochem.2021.104351

Abstract

Aerobic decomposition increases in drained peatlands; releasing stored organic matter (OM) and shifting greenhouse gas fluxes from sink to source. This study explored how drainage influenced peat OM chemical composition by investigating paired sites from a *Sphagnum*-dominated ombrotrophic Finnish bog undergoing contrasting hydrological management (natural and drained). Peat OM was investigated in replicate cores using analytical pyrolysis, compared with observed vegetation, elemental analysis (O:C, N:C), stable isotopes ($\delta^{13}C$, $\delta^{15}N$), and fraction radiocarbon. Principal component analysis of quantified pyrolysis products separated four primary components: vascular plants vs *Sphagnum*, aerobic degradation of fresh plant biomass, anaerobic processes in water-saturated depths, and pine vs *Eriophorum*. The largest influence of drainage on peat chemistry was via aerobic decomposition (decreased abundance of *Sphagnum* phenols and simple polysaccharides; accumulation of macromolecular polysaccharides) (***p*<0.05,** 0-2 cm). Drainage-induced shifts in vegetation (from *Sphagnum* to *Pinus sylvestris* (***p*<0.01,** 0-2 cm) were reflected by increased abundance in lignin, N-compounds, and lipids, and decreased abundance in phenols and polysaccharides. Anaerobic processes also differentiated the natural and drained sites and primarily affected polysaccharides (***p*<0.05,** 0-2, 8-10 cm). Vegetation shifts and aerobic decomposition similarly affected many of the same compounds upon drainage – demonstrating the simultaneous influence of different processes on the same OM. Pre-drainage inter-core variation illustrated the importance of replicate cores in disentangling anthropogenic changes from natural biodiversity. These findings suggest that even short-term and moderate alterations in peatland hydrology strongly influence the chemical composition of peat OM, and that its chemistry serves as an effective indicator to assess decomposition status.

4.1 Introduction

Due to the low rate of decomposition relative to net primary productivity (NPP), organic matter (OM) accumulates in intact peatlands, resulting in a carbon (C) store of approximately 600 gigatonnes (Gt) globally (Yu et al., 2010). Degradation stemming from drainage, agriculture, forestry, burning, and extraction have impacted roughly 10 percent of these fragile ecosystems worldwide (Joosten, 2009). As peatlands are degraded and exposed to increasingly oxic conditions, aerobic decomposition increases, releasing carbon dioxide estimated at two Gt annually (Leifeld & Menichetti, 2018), and shifting these C-dense ecosystems from C sink to source (IPCC, 2014; Humpenöder et al., 2020). To restore their numerous vital ecosystem services, peatland restoration projects are increasingly employed (Andersen et al., 2017; Dohong et al., 2018). In terms of C sequestration, peatland restoration is considered a success when NPP exceeds decomposition (Andersen et al., 2010), which results in a net increase of C storage. In order to target ecosystems that will most benefit from restoration (i.e., ecosystems susceptible to high C emissions), it is vital to improve our understanding of the factors influencing peat OM decomposition and C mineralization.

In chemically complex matrices such as peat, gas chromatography-mass spectrometry techniques can be coupled with pyrolysis (Py-GC/MS) for the chemical characterization of OM. The pyrolysis process breaks up complex macromolecules into smaller, more easily analyzed fragments prior to GC/MS analysis, preventing discriminative loss of high molecular weight organic compounds and providing a "fingerprint" of the OM's overall chemical composition (White et al., 2004; Klein et al., 2021). Peat OM composition analyzed via Py-GC/MS provides detailed molecular information on (past) peatland vegetation composition and decomposition processes. A number of source-specific pyrolysis products have been identified, such as the *Sphagnum* spp. biomarker *p*-isopropenylphenol (Stankiewicz et al., 1997; Van der Heijden et al., 1997; Schellekens et al., 2009; McClymont et al., 2011), and lignin from vascular plants (Hedges & Mann, 1979). Pyrolysis-GC/MS has large potential to identify different peat decomposition pathways. For example, degradation of lignocellulose in graminoid-dominated peat results in preferential loss of polysaccharides over lignin, while for *Sphagnum*-dominated peat the reverse is true and structural polysaccharides are preferentially preserved over phenols (Schellekens, Bindler, et al., 2015). In addition, chemical classes (phenols, polysaccharides, N compounds, lipids, etc.) can be compared to investigate broader land-use shifts (Zhang et al., 2019). Due to its complexity, it is useful to compare peatland OM chemical composition with other complementary methods as part of a multi-proxy analysis. In example, molar ratios can

be used as an overall measure of degradation, as (carbon, hydrogen, nitrogen, and oxygen) stoichiometric ratios vary in peat according to OM origin and decomposition (Wang et al., 2014; Moore et al., 2018; Leifeld et al., 2020). Further, radiocarbon ($F^{14}C$) measurements are generally used in calibrated peat age assessments (Trumbore, 2000; Wang et al., 2021), but can also be used in raw form as a rapid screening tool to assess the presence of subsidence (and thus whether depth comparisons are valid measurements).

Studies conducting depth-based comparisons of natural and drained sites within the same peatland ecosystem are relatively scarce. To study the effect of peatland drainage on OM composition, core samples have often been obtained from different peat locations (and sometimes ecosystems) out of necessity (Kuder et al., 1998; Heller et al., 2015; Harris et al., 2020), as few research sites offer an opportunity for paired comparisons from the same location due to the general worldwide long-term degradation of peat. To explore how drainage impacts the composition of peat OM, this study aimed to identify differences in the chemical composition of natural and drained peatland sites from the same ecosystem – both by hydrological management and with depth.

4.2 Materials and Methods

4.2.1 Location and sampling

The Lakkasuo peatland (61°48'N, 24°19'E) is an ombrotrophic bog in Finland that has been accumulating peat for the past 3,000-6,000 years, with a maximum reported peat depth of 3.7 m (Laine et al., 2004). Mean annual air temperature in the study area is 3 °C and mean annual precipitation is 700 mm (Minkkinen et al., 1999). In 1961, ditches were installed (70 cm depth, with spacing of 40 m – 60 m) for forestry purposes. Approximately 50 percent of the peatland was affected by this drainage (Minkkinen et al., 1999). An extensive survey of Lakkasuo ecology has been previously conducted (Laine et al., 2004).

Three peat core replicates were collected in June 2017 from the ombrotrophic natural/un-drained (ON) and drainage-affected locations (OD) to a depth of 1 m, using a Russian peat corer (Eijkelkamp, Netherlands). The water table levels were based on measurements obtained in a previous study and were approximately 6-7 cm below ground surface (bgs) in ON, and 15 cm bgs in OD (Jaatinen et al., 2007). ON and OD sampling sites were separated by a distance of approximately 15 m, and hydrologically separated by a drainage ditch (Murphy et al., 2009). Lateral distance between the replicate cores was measured with GPS and was approximately

1.3 m. The sampling depth was based on findings by (Krüger et al., 2016), who reported that the main effects of management in these two sites were primarily found in the upper 40 cm of the core depth profiles.

Surface vegetation in the area surrounding the OD sample site was described during the onsite assessment as a combination of *Oxycocco quadripetali-Pinetum silvestris*. Vegetation surrounding the ON sample site (which was restricted to hollow system areas) was described as a moist association of an *Empetrum-Sphagnum fuscum* bog with adjacent *S. fuscum* hummocks. Plant macrofossil assessments were conducted on sample cores ON1 and OD2 in 2017 and are provided in (**Supplementary Tables 4&5**).

After collection, the cores were stored at 2 °C until sample processing, where they were sliced into 2 cm sections, oven-dried at 40 °C for 72 hours, and then homogenized in a mixer mill (Retsch MM 400) for three minutes at 25 Hz. Each core was analyzed to a four cm resolution in two cm sections (0-2, 4-6, 8-10, etc.), down to a depth of 70 cm, for a total of 108 samples across the six cores. Samples were denoted by their site source (ON or OD), followed by core number (1-3), and profile section depth in cm (for example, ON1 0-2).

4.2.2 Py-GC/MS

Pyrolysis-gas chromatography/mass spectrometry (Py–GC/MS) was performed using a double shot pyrolyzer (Frontier Laboratories, model 2020i) operating in single shot mode, attached to an Agilent 7890 Series GC. As the focus of this study was to conduct a broad chromatographic survey where unintentional derivatization of the larger peat matrix could be disadvantageous, chemical pre-treatments (such as tetramethylammonium hydroxide) were not applied prior to analysis. Approximately one mg of sample was introduced for one minute into the preheated (600 °C) micro-furnace. Samples were flushed with Helium (He) for one minute prior to furnace introduction. The pyrolyzer interface with the GC unit was held at 320 °C. Pyrolyzed compounds were swept from the pyrolysis furnace to the GC column in inert He. Since the Py-GC/MS method was the same for all samples, it was assumed that any preferential pyrolytic efficiency for different compound classes was consistent (Klein et al., 2020).

The GC was equipped with a 30 m column (5xi-5sil, equivalent to HP-5ms) X 240 µm, 0.25 µm film thickness. In order to improve the chromatographic separation of abundant low molecular weight compounds, the GC oven temperature was held at 40 °C for 1 min and 50 °C

for one minute at the start of each run (with a ramped increase of 3 °C min^{-1} between each hold time). The oven temperature was then increased to 165 °C at 3 °C min^{-1}, followed by a second increase from 165 °C to 310 °C at 5 °C min^{-1}, and then stabilized at 310 °C for 10 min. The inlet was set to 280 °C in split mode (100:1). He was used as a carrier gas at a controlled flow of 1 ml min^{-1}. The GC was coupled to an Agilent 5977B series mass selective detector. Spectra were acquired at 70 eV ionizing energy in the 50-600 mass to charge ratio (*m/z*) range.

Pyrolysis product identification and integration were performed using Agilent ChemStation software. 108 compounds were selected as representative of the peat matrix (dominant peaks), and plant species and decomposition processes (specific compounds). These 108 compounds were quantified in all samples and assigned per their relative abundance using the peak area of their characteristic ion fragments (**Supplementary Table 1**). All peaks were checked manually to prevent mischaracterization stemming from slight shifts in retention times. For compound assignment, mass spectra were compared with published data as reported in the NIST 2014 mass spectral digital library, as well as to available literature. Results are provided in relative rather than absolute abundances. The sums of all peak areas were set as 100 percent, and individual peak abundance was calculated in relative proportion to the total quantified peak area (as relative percent abundance).

Assigned compounds were grouped by compound class and probable origin. These groupings were phenols, polysaccharides, lignin (guaiacyl-derived and syringyl-derived), benzenes, N compounds, and lipids (aliphatics, *n*-alkanes, methylketones, fatty acids, and terpenoids). The chemical classification groupings were further considered by their broader peatland ecological origin and/or association (Schellekens et al., 2009; Schellekens & Buurman, 2011; Schellekens, Bindler, et al., 2015; Kaal et al., 2017).

4.2.3 Elemental Analysis

Elemental analysis was conducted on all samples and used for the calculation of molar ratios (N:C, O:C) and C and N stocks (**Section 4.3.4**). Bulk C, H and N analysis was conducted by dry combustion using a EuroEA3000 Elemental Analyzer, and for organic O by pyrolysis at 1000 °C followed by GC-TCD quantification (Hekatech, Germany). Samples measured for pH from both ON and OD were pH<4.2, and were thus assumed to be free of carbonate. Therefore, bulk C concentrations were considered to be equivalent to organic C concentrations. In addition

to elemental analysis data, bulk density measurements obtained from the University of Basel were also used to calculate C and N stocks (Groß-Schmölders et al., 2020).

4.2.4 Radiocarbon isotope analysis

Fraction ^{14}C ($F^{14}C$) abundances were determined for three depths in each of the six cores (8-10, 48-50, 80-82 cm) using accelerator mass spectrometry (Oeschger Centre for Climate Change Research, Department of Chemistry and Biochemistry, University of Bern) in order to match the cores by $F^{14}C$ and not only by depth **(Section 3.4)**.

4.2.5 Statistics

To separate the multi-dimensional influence of ecosystem-driven processes (i.e., hydrological status, vegetation type, decomposition processes, etc.) on chemical composition, principal component analysis (PCA) was applied to the 108 quantified pyrolysis products using a correlation matrix. PCA pyrolysis product loadings take into account the shared variation of all pyrolysis products, and were used to interpret the processes reflected by individual PCs. PCA scores reflect the relative effect of the processes (PCs) in the samples and were used to evaluate the effects of drainage by assessing their variation with depth and between cores. Small compound abundances have the ability to introduce analytical error in PCA correlation matrices, and were encountered in some pyrolysis products in this study. However, such pyrolysis products can also be particularly informative about the processes they reflect; therefore, their inclusion was maintained. PCA loadings and scores show weight of variance, but are not quantitative metrics. Pyrolysis product depth profiles are presented as a quantitative measure of the processes reflected by individual PCs, and were selected based on their explained variance (>0.5 loadings on each PC) (Schellekens, Buurman, et al., 2015; Lopes-Mazzetto et al., 2018).

Correlation analyses were conducted using regression analysis and Pearson correlation. Differences between ON and OD in mean relative abundance of pyrolysis products (i.e., for summed chemical classes and for pyrolysis products with PC loadings >|0.5|) were tested by independent T-test. Unless otherwise specified, significance for all statistical tests was set at $\boldsymbol{p<0.05}$. Results presenting average values are given as mean±standard deviation of the mean. Statistical analyses and related depth plots were done using Python (version 3.8.2).

4.3 Results

4.3.1 General composition of peat pyrolysis products

A complete list of the pyrolysis products identified, including mean abundance of individual products, is provided in **Supplementary Table 1**. Across the investigated samples (all sites and depths), the contribution of primary chemical classes to all quantified pyrolysis products was: phenols 10.40%, lignin (guaiacyl- and syringyl-derived) 1.79%, benzenes 1.34%, N compounds 0.38%, polysaccharides 85.09%, and lipids (aliphatics and terpenoids) 1.00%. Depth profiles of the relative abundance of summed chemical classes (%) are given in **Fig 1**. Average and standard deviation of the relative abundance of each summed compound class is provided in **Supplementary Table 2**.

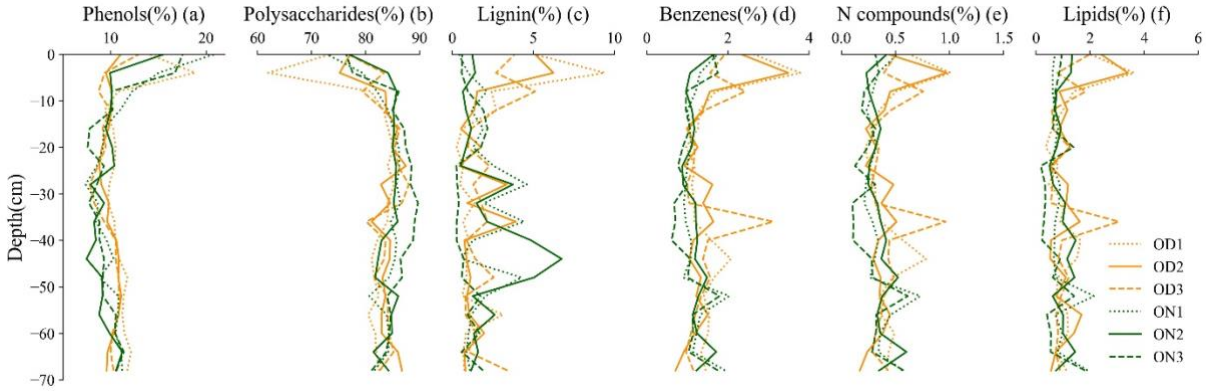

Fig 1(a-f). Relative abundance (%) of pyrolysis products summed by compound class for ON (green) and OD (orange).

Depth profiles of the summed compound classes (**Fig 1(a-f)**) demonstrated the largest differences in abundance in the surface peat (0-10 cm), with significantly higher abundances observed in OD for summed lignin (0-2 cm, ***p*<0.01)**, benzenes (0-2, 8-10, 12-14 cm, ***p*<0.05)** and summed lipids (0-2 cm, ***p*<0.01)**. While not significantly different in surface samples (0-4 cm), summed N compound relative abundance increased rapidly through the acrotelm of OD, where it was significantly higher in OD from 8-14 cm (***p*<0.05)** – reaching maximum abundance between 4-10 cm before decreasing with depth and approaching similar abundance between sites at 16-18 cm. Summed phenols and polysaccharides were not significantly different in surface samples, but trended higher in ON than OD, with continued increased abundance in ON until approximately 8-10 cm. Levoglucosan was a highly dominant pyrolysis product (average 44% abundance across all cores and depths) in the summed polysaccharides, and demonstrated through its outsized influence on the polysaccharide depth profile that individual pyrolysis products do not contribute similar influence in terms of abundance to their respective summed

compound class. When investigated separately from levoglucosan, the average relative abundance of the polysaccharides class was significantly higher in ON in surface samples (0-2 cm) (***p*<0.001**), and decreased from the surface before generally stabilizing with depth. Below 12-14 cm, the relative abundances of all summed compound classes followed generally similar trends; however, differences in individual core chemistry were apparent in certain depths (i.e., benzenes, N compounds, and lipids from 32-42 cm, and lignin from 36-52 cm).

4.3.2 Application of principal component analysis to quantified pyrolysis products

Principal components (PC) 1 to 4 explained 68.7% of the variance in all pyrolysis products. Pyrolysis product loadings for PC1-4 are provided in **Supplementary Table 3**. Depth profiles of scores for PC1-4 are shown in **Fig 2(a)** and summed relative abundance of pyrolysis products (%) with loadings (>|0.5|) representative of each PC are shown in **Fig 2(b-c)**. Loading projections of PC1 vs PC2, and PC3 vs PC4, which were used to identify the processes (**Section 4.1**) are provided in **Fig 3**.

PC1 scores (29.4% explained variance) were significantly different between ON and OD in surface samples, with high positive scores in OD and scores close to 0 in ON (0-2 cm) (**Fig 2(a),** ***p*<0.01**). With the exception of OD2, PC1 OD scores maximized at 4-6 cm before decreasing and approaching ON scores around 12-14 cm. Below 12-14 cm, both ON and OD scores remained near zero in PC1 - with the exception of OD1, which demonstrated mostly negative scores, and ON2, which demonstrated sustained positive scores – particularly in the depths between 40-52 cm. PC2 (19.0% explained variance) demonstrated high positive scores in both sites in surface samples (0-2 cm) that rapidly decreased with depth. OD scores approached zero at approximately 4-6 cm, whereas ON scores approached zero (with the exception of ON2) at approximately 8-10 cm. ON demonstrated significantly higher positive scores than OD at the surface (0-2 cm) (***p*<0.05**). Below 8-10 cm, PC2 scores remained near zero - with the exception of OD1, which demonstrated consistently positive scores with depth, and ON2, which demonstrated consistently negative scores. PC3 (12.2% explained variance) scores showed more variation through the depth profile, and were generally characterized by high positive scores in surface samples that decreased with depth; rapidly in the surface samples, then more gradually through the remainder of the cores. ON demonstrated significantly higher positive PC3 scores in surface samples (0-2, 8-10 cm) (***p*<0.05**). PC4 (8.5% explained variance) was separated by high positive scores in OD and low negative scores in ON in surface samples (0-2 cm) (***p*<0.05**). PC4 scores approached zero in all cores at

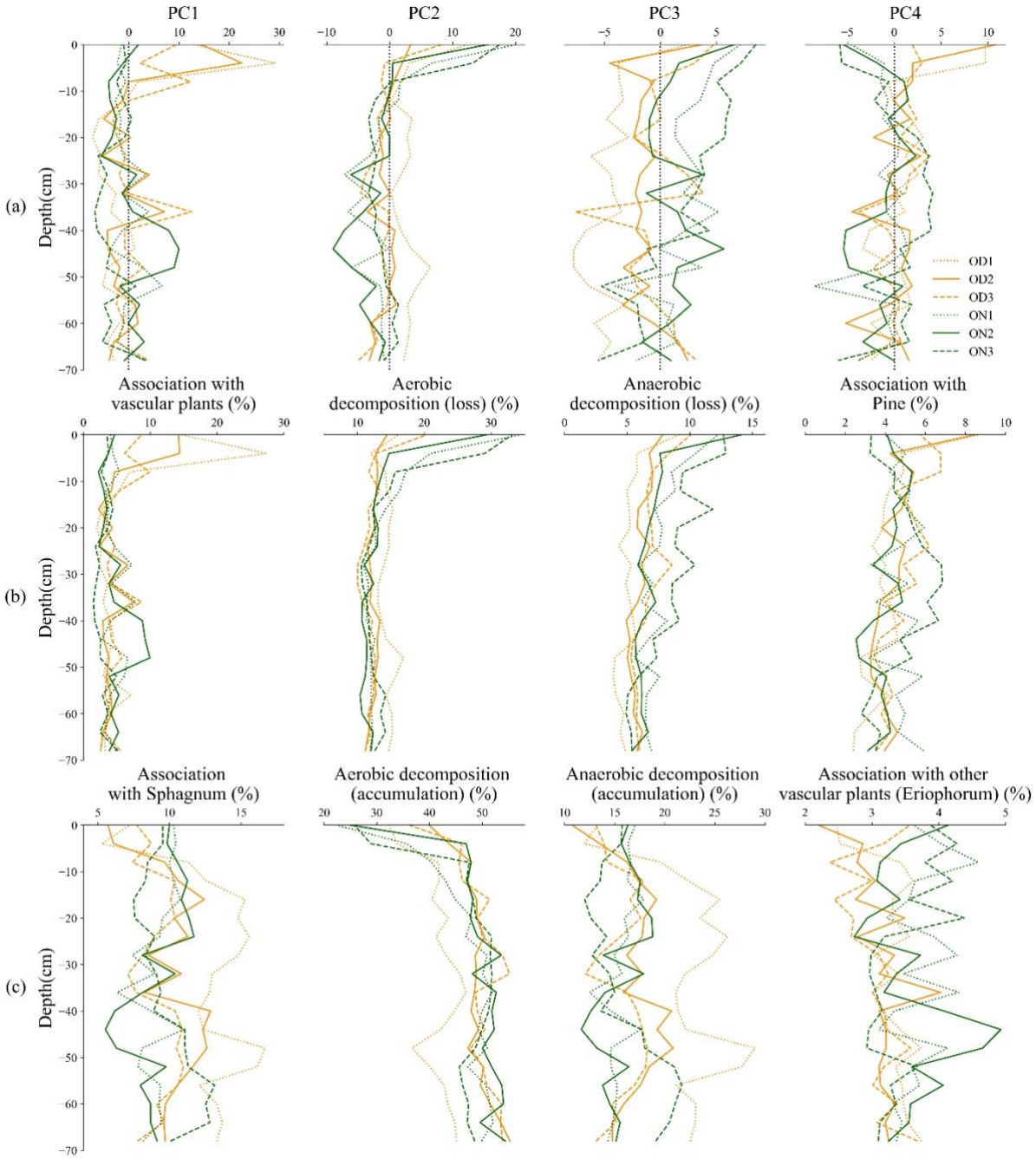

Fig 2(a-c). Interpretation of environmental processes driving chemical differences in Lakkasuo OM as reflected by PC1-PC4 (from left to right); demonstrated by (a) score projections with depth, (b) relative abundance (%) of associated pyrolysis products with PC positive loadings (>0.5), and (c) relative abundance (%) of associated pyrolysis products with PC negative loadings (<-0.5). ON is depicted in green, OD is depicted in orange.

approximately 8-10 cm. Below this depth, PC4 scores remained near zero through the remainder of the profile, with the exception of ON1-2, which both demonstrated negative scores.

4.3.3 Pyrolysis products reflective of processes (PCs)

PC1 was characterized by high positive loadings (>|0.5|) of pyrolysis products guaiacyl-derived lignin (19-27), catechols (10, 12) benzenes (1,2), C-29 sterols (59, 62, 63), sesquiterpenes (103-108), and N compounds (34, 36-39); and high negative loadings of phenols (17, 18) and polysaccharides (69, 71, 82, 86, 88, 90, 91) (**Fig 3**). Pyrolysis products with positive loadings on PC1 were in significantly greater abundance in OD in surface samples (0-2 cm) (***p*<0.05**); whereas products with negative loadings were in significantly higher abundance in ON (0-2 cm) (***p*<0.05**) (**Fig 2 (b-c)**). Below 8-10 cm depth, relative abundance stabilized in pyrolysis products with positive loadings - with the exception of ON2, which demonstrated higher relative abundances between 40-50 cm. While greater variability was observed in the pyrolysis products associated with negative PC1 loadings, abundances also stabilized below 8-10 cm - with the exception of OD1, which demonstrated consistently higher abundance through the remainder of the profile.

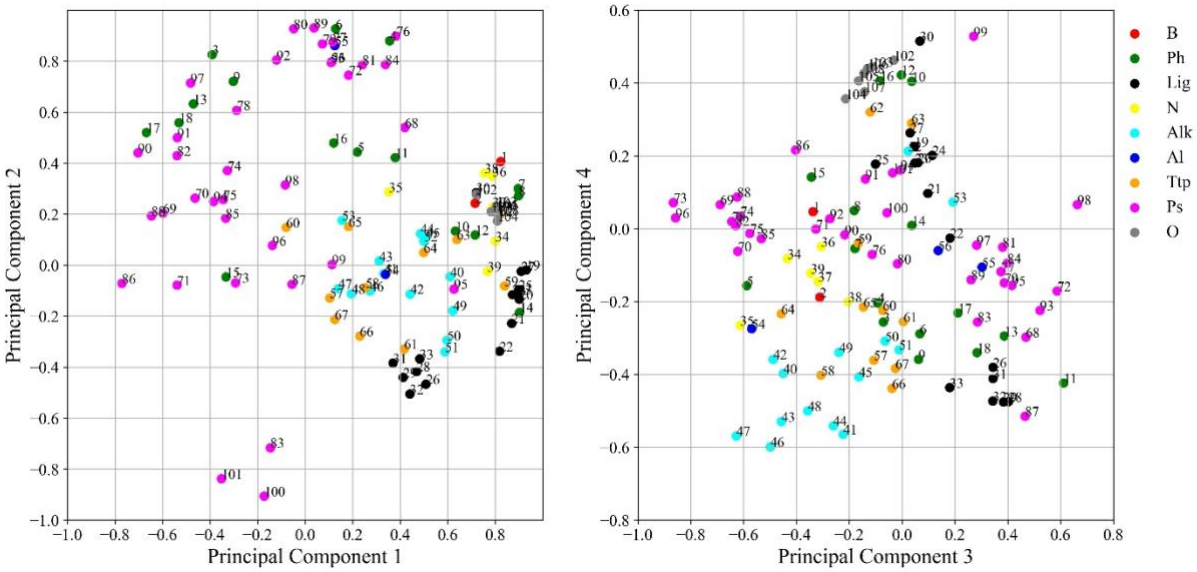

Fig 3. Principal component loadings of (left) PC1-PC2 projections, and (right) PC3-PC4 projections. PC1-4 explained 68.7% of the variance in all pyrolysis products (PC1=29.4%, PC2=19.0%, PC3=12.2%, PC4=8.5%). B, benzenes; Ph, phenols; Lig, lignin (all); N, nitrogen compounds; Alk, *n*-alkanes, *n*-alkenes, and *n*-methylketones; Al, other aliphatic hydrocarbons; Ttp, triterpenoids; Ps, polysaccharides; O, other terpenoids (mono- and sesquiterpenes).

PC2 demonstrated high positive loadings of polysaccharides (68, 72, 76-81, 84, 89, 92, 93, 97), unsaturated aliphatics (55, 56) and phenols (3, 4, 6, 9, 13, 17, 18); and high negative loadings of levoglucosan (100), 1,6-anhydro-β-D-glucofuranose (101), and an unknown (likely polysaccharide) compound (83). Pyrolysis products with positive loadings on PC2 displayed significantly higher abundance in ON in surface samples (0-2 cm) (***p*<0.01**); whereupon all products rapidly decreased in relative abundance from the surface before stabilizing at

approximately 8-10 cm. Products with negative loadings displayed significantly higher abundance in OD in surface samples (0-2 cm) (***p*<0.01**), and rapidly increased from the surface to the same depth as the compounds with positive loadings on PC2.

PC3 was characterized by high positive loadings of levogalactosan (98), 4-vinylphenol (11), 2-furanmethanol (72), and dihydro-6-methyl-2*H*-pyran-3(4*H*)-one (93); and negative loadings of polysaccharides (69, 70, 73, 74, 75, 78, 82, 85, 88, 96), the N compound 3-hydroxypyridine monoacetate (35), pristene (54), *p*-cresol (5), and the C-27 methylketone (47). PC3 associated pyrolysis products were in significantly higher abundance in ON in surface samples (0-2 cm) for both products with positive loadings (***p*<0.01**), and negative loadings (***p*<0.05**). Products associated with positive loadings on PC3 decreased rapidly in surface samples, and maintained a decreasing trend through the remainder of the profile. Products associated with negative loadings on PC3 demonstrated a slight increase in relative abundance with depth; however, the trend was less robust.

PC4 was characterized by positive loadings of levomannosan (99) and 4-vinylsyringol (30), as well as guaiacyl-derived lignin, C-29 sterols, catechols, and sesquiterpenoids; and negative loadings of *n*-alkanes and *n*-alkenes (41, 43, 44), methylketones (46, 47), and the polysaccharide 4-hydroxy-5,6-dihydro-(2*H*)-pyran-2-one (87). Syringyl-derived lignin also demonstrated almost exclusively negative loadings on PC4. Pyrolysis products with high positive loadings on PC4 displayed significantly higher abundance in OD (0-2 cm) (***p*<0.05**). Products with negative loadings were not significantly different in surface samples, but were significantly higher in ON at 4-6 cm (***p*<0.05**).

4.3.4 Elemental and radiocarbon analysis

Molar ratios were calculated from bulk peat samples for C, H, N, and O. Average O:C molar ratios were significantly higher in ON than OD in the upper 6 cm of the profile (***p*<0.05**) (**Fig 4**). N:C molar

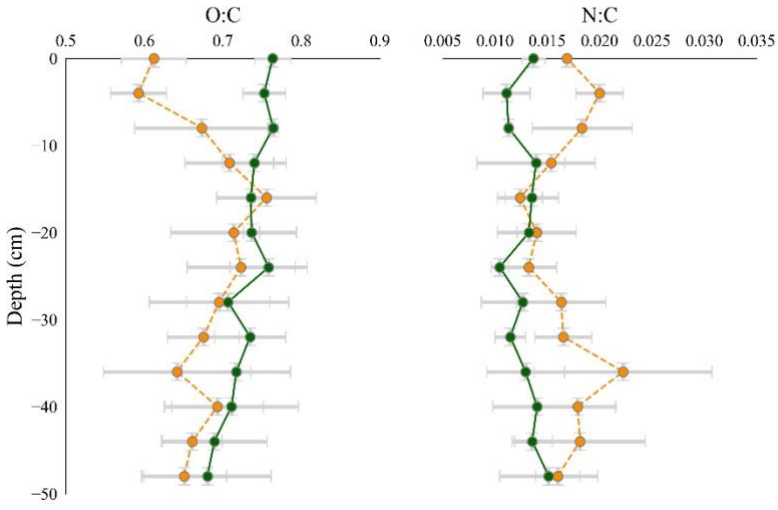

Fig 4. O:C (left) and N:C (right) depth profile molar ratios in ON and OD. Solid green lines indicate ON, and dashed orange lines indicate OD. Standard deviation was calculated through the average molar ratios of the three replicate cores.

ratios were significantly higher in OD than ON to the same depth. Differences between ON and OD were observed to approximately the same depth as those observed via Py-GC/MS analysis. Average C and N stocks were calculated to 82 cm depth in both ON and OD (kg/m^3). Average C and N stocks (respectively) were 17.97±2.72 and 0.30±0.05 in ON, and 28.33±2.98 and 0.51±0.07 in OD. C stocks were significantly higher in OD than ON **($p<0.05$).**

To improve the peat core depth correlations by identifying possible subsidence-caused depth shifts in the profile, drained and natural cores from the Lakkasuo site were matched by fraction radiocarbon abundance ($F^{14}C$) (**Supplementary Table 6**). No significant difference was observed in $F^{14}C$ abundance between ON and OD samples measured to 82 cm depth.

4.3.5 Correlation with complementary analyses (C/N ratio & bulk isotopes)

PC scores were correlated with bulk stable isotope values ($\delta^{13}C$ and $\delta^{15}N$) measured in a study conducted on the same peat cores (Groß-Schmölders et al., 2020), as well as C/N ratios determined using elemental analysis data obtained in this study (**Table 1, Supplementary Fig 1**). Significant moderate negative correlations were identified between PC1 and CN, and PC3 and $\delta^{15}N$ (**$p<0.01$**), with significant relationships also observed between PC4 and $\delta^{13}C$ (negative correlation), and PC3 and C/N (positive correlation).

Table 1. Correlation of PC scores 1-4 with corresponding $\delta^{15}N$, $\delta^{13}C$, CN ratios, and a summary of the processes reflected by each PC. Bold indicates significance at $p<0.01$. Signs (±) depict the direction of influence of the processes, interpreted by the loadings on each PC.

PC	$\delta^{15}N$	$\delta^{13}C$	C/N	Process
PC1	0.09	-0.16	**-0.55**	Vegetation shift: vascular plants (Pine) (+) vs *Sphagnum* (-)
PC2	-0.17	-0.27	-0.05	Aerobic decomposition processes: "fresh" plant material (+) vs increasing aerobic decomposition (-)
PC3	**-0.50**	0.24	**0.33**	Anaerobic decomposition processes: degradation of "palatable" compounds (+) vs relative accumulation (-)
PC4	0.06	**-0.43**	0.21	Vegetation shift: Pine (+) vs other vascular plants (*Eriophorum*) (-)

4.4 Discussion

4.4.1 Interpretation of the main processes by PCA loadings

The positive loadings on PC1 for guaiacyl-derived lignin, benzenes, C-29 sterols, sesquiterpenes, and N compounds are indicative of vascular plant growth, whereas negative loadings of phenols and polysaccharides are indicative of *Sphagnum* (**Fig 3**). PC1 therefore reflects vegetation origin. The negative loadings for most phenol pyrolysis products (with the

exception of the catechols (10, 12)) are in agreement with the negative loadings of the *Sphagnum* biomarker *p*-isopropenylphenol (13), and suggest that at the studied sites, most phenols can be primarily attributed to *Sphagnum*-derived OM rather than lignin-derived OM regardless of hydrological conditions (Zeh et al., 2020). *Sphagnum* spp. produce a pectin-like structural polysaccharide (sphagnan) in their cell walls that is the most likely source of the majority of the polysaccharides with negative loadings on PC1 (Hájek et al., 2011). The highest negative loadings on PC1 were observed for the polysaccharide α-acetobutyrolactone (86), which is associated with "fresh" plant material in peat (Tolu et al., 2015). In contrast, the high positive loadings of guaiacyl-derived lignin (relative to syringyl) are consistent with contribution from gymnosperms (Hedges & Mann, 1979). The high positive loadings of N are in agreement with the higher rhizospheric nutrient demand of vascular plants compared to *Sphagnum*; who have been shown to thrive in the nutrient-poor ombrotrophic conditions such as those occurring in this bog (Limpens et al., 2003; Malmer et al., 2003). Further, while both mosses and higher plants contain C-29 sterols, vascular plants generally display higher abundance (Ronkainen et al., 2013), and their positive loadings on PC1 support the argument that they can largely be attributed to pine litter in this ecosystem.

For PC2, the decrease in relative abundance of *Sphagnum* phenols (positive loadings), corresponding with increasing relative abundance of levoglucosan and 1,6-anhydro-β-D-glucofuranose (negative loadings) is consistent with preferential aerobic degradation of phenols over polysaccharides in *Sphagnum* peat (Schellekens, Bindler, et al., 2015), resulting in the relative accumulation of more "recalcitrant" compounds associated with cellulose (such as levoglucosan). PC2 thus reflects aerobic decomposition. The high positive loadings of phenols and polysaccharides that also had positive loadings on PC1 (associated with vascular plant material) likely indicate "fresh" plant material, and reflect preferential loss of polysaccharides over lignin in peat (Schellekens & Buurman, 2011).

PC3 separates polysaccharide pyrolysis products by positive and negative loadings, which combined with the observed decrease in relative abundance over the entire depth profile (**PC3, Fig 2(b)),** (suggesting "palatability" of these compounds) is consistent with anaerobic processes in the deeper water-saturated depths. 2-Furanmethanol has been previously proposed as a potential pyrolysate biomarker for bacteria (Eudy et al., 1985; Klein et al., 2021), and its high positive loadings here combined with its rapid decrease in abundance from the surface in both sites supports this argument. 1,4:3,6-Dianhydro-D-glucopyranose and the phenol *p*-cresol

(negative loadings) are both ubiquitous pyrolysis products in peat (Hatcher et al., 1988), and are likely artifacts of poorly decomposed OM preserved in anaerobic conditions. Further, the negative loadings of the polysaccharides here likely indicate inhibited decomposition of the sphagnan polysaccharide complex, as it is resistant to degradation in anaerobic conditions (Painter, 1991; Hájek et al., 2011). The particularly high negative loadings of the small polysaccharide 2-propylfuran (73) on PC3 are also notable, as its similarity in abundance between sites in surface samples together with its increase in relative abundance in the water-saturated depths in all cores suggests a possible origin from microbial residue.

The separation of lignin compounds on PC4 – with guaiacyl-derived compounds generally displaying positive loadings and syringyl-derived compounds displaying negative loadings - suggest that PC4 reflects the separation of pine from the contribution of another vascular (likely angiosperm-derived) source. The positive loadings of C-29 sterols, catechols, and sesquiterpenoids further indicate the influence of pine; whereas the 4-hydroxy-5,6-dihydro-(2*H*)-pyran-2-one (negative loadings) is a pyrolysis product of xylose, a hemicellulose-derived compound highly abundant in grass and sedge species (Pouwels et al., 1989; Schellekens, Buurman, et al., 2015). While the compound is also abundant in wood, its high negative loadings in association with syringyl-derived lignin suggest that 4-hydroxy-5,6-dihydro-(2*H*)-pyran-2-one is likely contributed by *Eriophorum* spp. in this bog, which corresponds with findings from macrofossil assessments conducted on two of the cores in 2017 (**Supplementary Tables 4&5**). Debate exists over whether *n*-alkan-2-ones are contributed directly by peat-forming vegetation (Nichols & Huang, 2007; Zhang et al., 2020) or by microbial sources via oxidation of *n*-alkanes or *n*-fatty acids (Lopez-Dias et al., 2013). The high positive loadings of the methylketones on PC4 combined with their negative loadings on PC3 in association with anaerobic processes suggest a multiple-source origin.

4.4.2 Effects of drainage on OM chemistry in Lakkasuo by PCA scores

In PC1, the clear separation of scores (**Fig 2(a**)) in ON and OD demonstrate the difference in chemical composition between *Sphagnum* and vascular plants in the surface peat. The higher positive scores observed in OD surface samples for PC1 (associated with vascular plants) is consistent with the positive higher scores in OD surface samples for PC4 (associated with Pine), and indicates that the majority of the vascular plant OM contribution in the upper acrotelm depths can be attributed to the *Pinus silvestris* onsite. The convergence of PC1 scores between 8-12 cm suggests that beneath these depths, the overall ecosystem was not substantially

different between the two sites (however, see **Section 4.3**). PC1 scores suggest that prior to the drainage activities onsite, OD1 and ON3 maintained the most consistent *Sphagnum* cover, whereas ON1 and ON2 experienced intermittent periods with more vascular plant growth.

The PC2 scores trace the shift in chemistry occurring via aerobic decomposition processes with depth. In surface samples, the higher positive scores in ON (as well as the slower decreases with depth in ON1 and ON3) is consistent with "fresh" *Sphagnum*, in contrast to the more rapidly degraded OM deposited in the drained horizons of OD. The convergence of the scores between 8-10 cm coincide with the convergence in PC1 scores reflecting changes in botanical composition, and reflect that both sites were generally water-saturated prior to drainage. Individually, ON2's rapid decrease (compared to the other two ON cores) in surface samples is consistent with observations from PC1 indicating increased vascular plant abundance in that core, and suggest that while it may be water-saturated presently, ON2 experienced the most consistent aerobic conditions of the six cores prior to the drainage activities. In contrast, OD1's consistently positive PC2 scores with depth suggest that before drainage activities, it was likely the most water-saturated of the six core sampling sites.

PC3 reflects anaerobic degradation in the deeper water saturated zone - particularly by the separation of source-dependent polysaccharides. Positive scores on PC3 likely show "fresh" plant material, whereas negative scores indicate increasingly anaerobically processed OM. While more variability was observed with depth in the PC3 scores, they generally trend higher in ON than OD through the entire profile depths, and suggest that ON experienced less microbial activity under anaerobic conditions compared to OD. In contrast, OD1 demonstrated the lowest PC3 scores of the six cores with depth, in addition to its scores consistent with increased *Sphagnum* cover (PC1) and water-saturated conditions (PC2). This suggests that OD1 may have experienced the most consistent anaerobic conditions of the six cores prior to the drainage activities.

The shift from high positive scores to low or negative scores observed in PC4 below 8-10 cm shows that before the drainage and forestry activities, *Pinus sylvestris* played little to no role in the ecosystem. However, the intermittent negative scores observed, particularly in the case of ON1 and ON2, indicate previous abundance of *Eriophorum* in addition to *Sphagnum* cover (as indicated by PC1 scores). Moreover, the vacillating shifts between zero and negative scores observed in each core with depth suggest that dominant vegetative cover may also have been

somewhat cyclical – perhaps with regular transitions from wet hollows and *Sphagnum* to drier hummocks and *Eriophorum*.

4.4.3 Representation of environmental processes

PCA illustrated that peat OM in the profile was often influenced by multiple processes (PCs) simultaneously. In example, many of the same pyrolysis products (i.e., polysaccharides and phenols) with high negative loadings on PC1 (**Fig 2(c)**, *Sphagnum*-associated) also demonstrated high positive loadings on PC2 (**Fig 2(b),** association with OM loss via aerobic decomposition). This demonstrates the simultaneous influence of multiple environmental processes on the same OM, and indicates the presence of multiple concurrent chemical signals driven by *Sphagnum*, vascular plants, and aerobic (and to a lesser degree, anaerobic) decomposition processes that must be disentangled.

While the PC scores best reflect the processes demonstrating the net effect of drainage (**Fig 2(a**)), the pyrolysis product depth profiles provide a quantitative approach that permits visualization of the relative amount of OM affected by each process (**Fig 2(b-c))**. Moreover, comparison of pyrolysis products allows for targeted abundance-driven comparisons as a method of clarifying unclear origins in peat OM.

4.4.4 Other proxies (molar ratios, C stocks, stable isotopes)

In stoichiometric assessments, higher O:C molar ratios tend to indicate less decomposed material, whereas higher N:C ratios suggest a greater abundance of proteinaceous material (Leifeld et al., 2020). In the surface sample depths, the lower O:C and higher N:C molar ratios in OD compared to ON are in agreement with these expectations and overall findings from the Py-GC/MS analysis.

In **Table 1**, the negative correlation between PC1 scores and C/N ratios was in agreement with higher positive loadings of N compounds on PC1. The negative correlations between PC2 and both stable isotopes is consistent with enrichment of $\delta^{13}C$ and $\delta^{15}N$ with increased aerobic decomposition, due to preferential microbial utilization of ^{12}C and ^{14}N during the decomposition process (Ågren et al., 1996; Nadelhoffer et al., 1996; Alewell et al., 2011; Krüger et al., 2015). However, the weak correlations also suggest that they also have been influenced by other factors in this peat. For PC3, the positive correlation with C/N combined with the negative correlation to $\delta^{15}N$ suggested links to increasingly anaerobic microbial

processes with depth (Krüger et al., 2015). The stronger $\delta^{15}N$ trend here is not necessarily unique to anaerobic decomposition, as relative $\delta^{15}N$ enrichment with depth is also typical in peat horizons governed by aerobic decomposition (Drollinger et al., 2019). However, our findings also correspond with data obtained from a bulk stable isotope study on the same peat cores, where initially depleted $\delta^{15}N$ values became more enriched with depth through the acrotelm and mesotelm before stabilizing in the catotelm, reflecting increased microbial contribution and transitioning decomposition communities in shallower peat regions (Krüger et al., 2015; Groß-Schmölders et al., 2020). For PC4, the increasing enrichment of $\delta^{13}C$ as scores are increasingly associated with *Eriophorum* is likely due to increased plant input in the historical samples where *Eriophorum* was more abundant (**Section 4.2**). The observed weak positive relationship between PC4 scores and C/N ratios also suggests a difference in the "quality" of deposited OM, depending on the dominant contributing vascular source. The lower C/N ratios and enriched ^{13}C ratios in samples associated with *Eriophorum* are consistent with other studies that reported lower C/N and enriched ^{13}C ratios for sedge species compared to woody shrubs (Biester et al., 2014; Zeh et al., 2020).

The lack of difference in $F^{14}C$ abundance with depth between the sites suggests either that OD OM has been compensated somewhat by higher litter inputs, or that subsidence has not yet played a large role at the sampling site. As the drainage activities at Lakkasuo were both non-intensive and comparatively recent (less than 60 years), insufficient time may have passed to permit substantial peat subsidence. Cross-referencing of cores by depth were thus considered to be valid comparisons.

The higher C stocks in OD compared to ON correspond with findings of previous researchers that pine tree stands can play an important role in bulk C density and C stocks of drained peat - due to an increase in primary productivity through input of new C from fine tree root material (Minkkinen & Laine, 1998; Minkkinen et al., 1999; Hommeltenberg et al., 2014; Minkkinen et al., 2018). The potentially outsized role of pine tree stands is also consistent with the higher abundance of guaiacyl-derived lignin observed in OD surface peat. Higher C stocks in OD were therefore considered evidence of increased contribution from pine-derived biomass, rather than subsidence stemming from peat oxidation.

4.4.5 Spatial variability

The depth profiles in Lakkasuo indicate that the changes in hydrology in the "modern" peatland (and its drainage activities) are preserved in the upper 10 cm of the cores. Below this depth, there is evidence of preservation of previous ecosystem conditions that were present prior to the drainage. Individual deviations from overall trends can be observed in single cores indicative of small-scale spatial biodiversity typical of hummock-hollow ecosystems and representative of natural variation in the peatland environment. Due to the close proximity of the Lakkasuo drained and natural sites and the similarity in ^{14}C abundance, it was assumed that the ecosystem was not significantly different between the two sampling locations prior to the drainage activities. The intra-site spatial variation apparent in the replicate cores partially overrides inter-site differences and thereby clearly demonstrates the effect of natural biodiversity on peat chemical composition. The effect of biodiversity can also be observed through the separation of PC4 scores between sample cores with depth, and provides some information about the history of the Lakkasuo sample site through the increased abundance in pyrolysis products reflective of *Eriophorum* cover – particularly in the ON1-2 cores. This seems to provide some evidence that historically, ON may generally have been the "drier" of the two sites prior to the drainage activities (relatively speaking in the context of an intact peat ecosystem), and underscores the importance that wherever possible, peatland OM comparisons should ideally be based on more than one field replicate.

4.5 Conclusions

Our findings confirm that peat hydrology is a strong driver for changes in peat chemical composition. PCA applied to a high resolution Py-GC/MS analysis of natural and drained peat core replicates from the same ecosystem allowed separation of concurrent environmental processes into individual components (changes in vegetation (PC1, PC4), aerobic decomposition processes (PC2), and anaerobic decomposition processes (PC3)). Aerobic conditions displayed the strongest drainage-induced influence on peat chemistry in terms of the relative percentage of OM affected, through large reductions in phenols and simple polysaccharides and relative accumulation of macromolecular polysaccharides levoglucosan and 1,6-anhydro-β-D-glucofuranose. The influence of drainage was also reflected by the changing botanical composition, through large reductions in phenols and polysaccharides indicative of the decreased *Sphagnum* cover at OD, and increased abundance of guaiacyl-derived lignin, benzenes, C-29 sterols, and sesquiterpenes representing the contribution from

the onsite *Pinus silvestris*. Changing botanical composition (*Sphagnum* vs Pine) influenced the abundance of many of the same pyrolysis products that were also influenced by aerobic conditions, suggesting that concurrent chemical signals (*Sphagnum*, vascular plants, degradative processes) were present and distinguishable in the same OM - particularly in peat polysaccharides, but also in the phenol compound class. Anaerobic decomposition played a comparatively minor role in overall degradative processes; however, its effects were increasingly visible in the cores with depth.

Overall, these results indicate that even "short-term" (<60 years) and "moderate" (<30 cm decrease in water table in OD) changes in peat hydrology result in directly traceable changes in chemical composition. Moreover, OM chemical composition can be used as an effective tool to assess degradative status with depth in peatlands, particularly when core replicates can be taken. As land use shifts have recently been shown to have long-term impacts on peat OM composition and its overall susceptibility to degradation (Schimmel et al., 2021), the extent to which degradation-driven changes in OM composition are reflective of changes in C emissions is an area urgently requiring further study.

Acknowledgments

The authors would like to thank the editor and anonymous reviewers for their time and efforts. Kari Minkkinen provided access to the Lakkasuo site for core sampling. Robin Giger conducted elemental analysis for all peat samples. Markus Jocher assisted with maintenance of the Py-GC/MS instrument. Their assistance with this work is invaluable and is greatly appreciated. This study was funded by the Swiss National Science Foundation, project number 200021_169556.

References

Ågren, G. I., Bosatta, E., & Balesdent, J. 1996. Isotope discrimination during decomposition of organic matter: a theoretical analysis. Soil Science Society of America Journal, 60(4), 1121-1126.

Alewell, C., Giesler, R., Klaminder, J., Leifeld, J., & Rollog, M. 2011. Stable carbon isotopes as indicators for environmental change in palsa peats. Biogeosciences, 8(7), 1769-1778.

Andersen, R., Farrell, C., Graf, M., Muller, F., Calvar, E., Frankard, P., Caporn, S., & Anderson, P. 2017. An overview of the progress and challenges of peatland restoration in Western Europe. Restoration Ecology, 25(2), 271-282.

Andersen, R., Grasset, L., Thormann, M. N., Rochefort, L., & Francez, A.-J. 2010. Changes in microbial community structure and function following Sphagnum peatland restoration. Soil Biology and Biochemistry, 42(2), 291-301.
Biester, H., Knorr, K.-H., Schellekens, J., Basler, A., & Hermanns, Y.-M. 2014. Comparison of different methods to determine the degree of peat decomposition in peat bogs. Biogeosciences, 11(10), 2691-2707.
Dohong, A., Aziz, A. A., & Dargusch, P. 2018. A review of techniques for effective tropical peatland restoration. Wetlands, 38(2), 275-292.
Drollinger, S., Kuzyakov, Y., & Glatzel, S. 2019. Effects of peat decomposition on δ13C and δ15N depth profiles of Alpine bogs. Catena, 178, 1-10.
Eudy, L. W., Walla, M. D., Hudson, J. R., Morgan, S. L., & Fox, A. 1985. Gas chromatography—mass spectrometry studies on the occurrence of acetamide, propionamide, and furfuryl alcohol in pyrolyzates of bacteria, bacterial fractions, and model compounds. Journal of Analytical and Applied Pyrolysis, 7(3), 231-247.
Groß-Schmölders, M., Sengbusch, P. v., Krüger, J. P., Klein, K., Birkholz, A., Leifeld, J., & Alewell, C. 2020. Switch of fungal to bacterial degradation in natural, drained and rewetted oligotrophic peatlands reflected in δ 15 N and fatty acid composition. SOIL, 6(2), 299-313.
Hájek, T., Ballance, S., Limpens, J., Zijlstra, M., & Verhoeven, J. T. A. 2011. Cell-wall polysaccharides play an important role in decay resistance of Sphagnum and actively depressed decomposition in vitro. Biogeochemistry, 103(1), 45-57.
Harris, L. I., Moore, T. R., Roulet, N. T., & Pinsonneault, A. J. 2020. Limited effect of drainage on peat properties, porewater chemistry, and peat decomposition proxies in a boreal peatland. Biogeochemistry, 151(1), 43-62.
Hatcher, P. G., Lerch III, H. E., Kotra, R. K., & Verheyen, T. V. 1988. Pyrolysis gc—ms of a series of degraded woods and coalified logs that increase in rank from peat to subbituminous coal. Fuel, 67(8), 1069-1075.
Hedges, J. I., & Mann, D. C. 1979. The characterization of plant tissues by their lignin oxidation products. Geochimica et Cosmochimica Acta, 43(11), 1803-1807.
Heller, C., Ellerbrock, R., Roßkopf, N., Klingenfuß, C., & Zeitz, J. 2015. Soil organic matter characterization of temperate peatland soil with FTIR-spectroscopy: effects of mire type and drainage intensity. European Journal of Soil Science, 66(5), 847-858.
Hommeltenberg, J., Schmid, H., Drösler, M., & Werle, P. 2014. Can a bog drained for forestry be a stronger carbon sink than a natural bog forest? Biogeosciences, 11(13), 3477-3493.
Humpenöder, F., Karstens, K., Lotze-Campen, H., Leifeld, J., Menichetti, L., Barthelmes, A., & Popp, A. 2020. Peatland protection and restoration are key for climate change mitigation. Environmental Research Letters, 15, 1-12.
IPCC. 2014. IPCC, 2014: climate change 2014: synthesis report. Contribution of Working Groups I. II and III to the Fifth Assessment Report of the intergovernmental panel on Climate Change. IPCC, Geneva, Switzerland, 151.
Jaatinen, K., Fritze, H., Laine, J., & Laiho, R. 2007. Effects of short-and long-term water-level drawdown on the populations and activity of aerobic decomposers in a boreal peatland. Global Change Biology, 13(2), 491-510.
Joosten, H. (2009). The Global Peatland CO2 Picture: peatland status and drainage related emissions in all countries of the world. Wageningen, The Netherlands: Wetlands International.
Kaal, J., Cortizas, A. M., & Biester, H. 2017. Downstream changes in molecular composition of DOM along a headwater stream in the Harz mountains (Central Germany) as determined by FTIR, Pyrolysis-GC–MS and THM-GC–MS. Journal of Analytical and Applied Pyrolysis, 126, 50-61.
Klein, K., Gross-Schmölders, M., Alewell, C., & Leifeld, J. 2021. Chapter Three - Heating up a cold case: Applications of analytical pyrolysis GC/MS to assess molecular biomarkers in peat. In D. L. Sparks (Ed.), Advances in agronomy (Vol. 165, pp. 115-159): Academic Press.

Klein, K., Gross-Schmölders, M., De la Rosa, J. M., Alewell, C., & Leifeld, J. 2020. Investigating the influence of instrumental parameters and chemical composition on pyrolysis efficiency of peat. Communications in soil science and plant analysis, 51(12), 1572-1581.
Krüger, Alewell, C., Minkkinen, K., Szidat, S., & Leifeld, J. 2016. Calculating carbon changes in peat soils drained for forestry with four different profile-based methods. Forest Ecology and Management, 381, 29-36.
Krüger, Leifeld, J., Glatzel, S., Szidat, S., & Alewell, C. 2015. Biogeochemical indicators of peatland degradation-a case study of a temperate bog in northern Germany. Biogeosciences, 12, 2861-2871.
Kuder, T., Kruge, M., Shearer, J., & Miller, S. 1998. Environmental and botanical controls on peatification—a comparative study of two New Zealand restiad bogs using Py-GC/MS, petrography and fungal analysis. International Journal of Coal Geology, 37(1-2), 3-27.
Laine, J., Komulainen, V., Laiho, R., Minkkinen, K., Rasinmäki, A., Sallantaus, T., Sarkkola, S., Silvan, N., Tolonen, K., & Tuittila, E. 2004. Lakkasuo: a guide to mire ecosystem. Lakkasuo: a guide to mire ecosystem.
Leifeld, J., Klein, K., & Wüst-Galley, C. 2020. Soil organic matter stoichiometry as indicator for peatland degradation. Scientific Reports, 10(1), 1-9.
Leifeld, J., & Menichetti, L. 2018. The underappreciated potential of peatlands in global climate change mitigation strategies. Nature communications, 9(1), 1071.
Limpens, J., Berendse, F., & Klees, H. 2003. N deposition affects N availability in interstitial water, growth of Sphagnum and invasion of vascular plants in bog vegetation. New Phytologist, 157(2), 339-347.
Lopes-Mazzetto, J. M., Schellekens, J., Vidal-Torrado, P., & Buurman, P. 2018. Impact of drainage and soil hydrology on sources and degradation of organic matter in tropical coastal podzols. Geoderma, 330, 79-90.
Lopez-Dias, V., Urbanczyk, J., Blanco, C., & Borrego, A. 2013. Biomarkers as paleoclimate proxies in peatlands in coastal high plains in Asturias, N Spain. International Journal of Coal Geology, 116, 270-280.
Malmer, N., Albinsson, C., Svensson, B. M., & Wallén, B. 2003. Interferences between Sphagnum and vascular plants: effects on plant community structure and peat formation. Oikos, 100(3), 469-482.
McClymont, E. L., Bingham, E. M., Nott, C. J., Chambers, F. M., Pancost, R. D., & Evershed, R. P. 2011. Pyrolysis GC–MS as a rapid screening tool for determination of peat-forming plant composition in cores from ombrotrophic peat. Organic Geochemistry, 42(11), 1420-1435.
Minkkinen, K., & Laine, J. 1998. Long-term effect of forest drainage on the peat carbon stores of pine mires in Finland. Canadian Journal of Forest Research, 28(9), 1267-1275.
Minkkinen, K., Ojanen, P., Penttilä, T., Aurela, M., Laurila, T., Tuovinen, J.-P., & Lohila, A. 2018. Persistent carbon sink at a boreal drained bog forest. Biogeosciences, 15(11), 3603-3624.
Minkkinen, K., Vasander, H., Jauhiainen, S., Karsisto, M., & Laine, J. 1999. Post-drainage changes in vegetation composition and carbon balance in Lakkasuo mire, Central Finland. Plant and Soil, 207(1), 107-120.
Moore, T. R., Large, D., Talbot, J., Wang, M., & Riley, J. L. 2018. The stoichiometry of carbon, hydrogen, and oxygen in peat. Journal of Geophysical Research: Biogeosciences, 123(10), 3101-3110.
Murphy, M., Laiho, R., & Moore, T. R. 2009. Effects of water table drawdown on root production and aboveground biomass in a boreal bog. Ecosystems, 12(8), 1268-1282.
Nadelhoffer, K., Shaver, G., Fry, B., Giblin, A., Johnson, L., & McKane, R. 1996. 15 N natural abundances and N use by tundra plants. Oecologia, 107(3), 386-394.
Nichols, J. E., & Huang, Y. 2007. C23–C31 n-alkan-2-ones are biomarkers for the genus Sphagnum in freshwater peatlands. Organic Geochemistry, 38(11), 1972-1976.

Painter, T. J. 1991. Lindow man, tollund man and other peat-bog bodies: the preservative and antimicrobial action of Sphagnan, a reactive glycuronoglycan with tanning and sequestering properties. Carbohydrate Polymers, 15(2), 123-142.
Pouwels, A. D., Eijkel, G. B., & Boon, J. J. 1989. Curie-point pyrolysis-capillary gas chromatography-high-resolution mass spectrometry of microcrystalline cellulose. Journal of Analytical and Applied Pyrolysis, 14(4), 237-280.
Ronkainen, T., McClymont, E. L., Väliranta, M., & Tuittila, E.-S. 2013. The n-alkane and sterol composition of living fen plants as a potential tool for palaeoecological studies. Organic Geochemistry, 59, 1-9.
Schellekens, J., Bindler, R., Martínez-Cortizas, A., McClymont, E. L., Abbott, G. D., Biester, H., Pontevedra-Pombal, X., & Buurman, P. 2015. Preferential degradation of polyphenols from Sphagnum – 4-Isopropenylphenol as a proxy for past hydrological conditions in Sphagnum-dominated peat. Geochimica et Cosmochimica Acta, 150, 74-89.
Schellekens, J., & Buurman, P. 2011. n-Alkane distributions as palaeoclimatic proxies in ombrotrophic peat: the role of decomposition and dominant vegetation. Geoderma, 164(3-4), 112-121.
Schellekens, J., Buurman, P., Kuyper, T. W., Abbott, G. D., Pontevedra-Pombal, X., & Martínez-Cortizas, A. 2015. Influence of source vegetation and redox conditions on lignin-based decomposition proxies in graminoid-dominated ombrotrophic peat (Penido Vello, NW Spain). Geoderma, 237, 270-282.
Schellekens, J., Buurman, P., & Pontevedra-Pombal, X. 2009. Selecting parameters for the environmental interpretation of peat molecular chemistry–a pyrolysis-GC/MS study. Organic Geochemistry, 40(6), 678-691.
Schimmel, H., Braun, M., Subke, J.-A., Amelung, W., & Bol, R. 2021. Carbon stability in a Scottish lowland raised bog: potential legacy effects of historical land use and implications for global change. Soil Biology and Biochemistry, 154, 108124.
Stankiewicz, B. A., Hutchins, J. C., Thomson, R., Briggs, D. E., & Evershed, R. P. 1997. Assessment of bog-body tissue preservation by pyrolysis-gas chromatography/mass spectrometry. Rapid Communications in Mass Spectrometry, 11(17), 1884-1890.
Tolu, J., Gerber, L., Boily, J.-F., & Bindler, R. 2015. High-throughput characterization of sediment organic matter by pyrolysis–gas chromatography/mass spectrometry and multivariate curve resolution: a promising analytical tool in (paleo) limnology. Analytica chimica acta, 880, 93-102.
Trumbore, S. 2000. Age of soil organic matter and soil respiration: radiocarbon constraints on belowground C dynamics. Ecological applications, 10(2), 399-411.
Van der Heijden, E., Boon, J., Rasmussen, S., & Rudolph, H. 1997. Sphagnum acid and its decarboxylation product isopropenylphenol as biomarkers for fossilised Sphagnum in peats. Ancient Biomolecules, 1(2), 93-107.
Wang, M., Moore, T. R., Talbot, J., & Richard, P. J. 2014. The cascade of C: N: P stoichiometry in an ombrotrophic peatland: from plants to peat. Environmental Research Letters, 9(2), 024003.
Wang, Y., Paul, S. M., Jocher, M., Espic, C., Alewell, C., Szidat, S., & Leifeld, J. 2021. Soil carbon loss from drained agricultural peatland after coverage with mineral soil. Science of the Total Environment, 800, 1-10.
White, D. M., Garland, D. S., Beyer, L., & Yoshikawa, K. 2004. Pyrolysis-GC/MS fingerprinting of environmental samples. Journal of Analytical and Applied Pyrolysis, 71(1), 107-118.
Yu, Z., Loisel, J., Brosseau, D. P., Beilman, D. W., & Hunt, S. J. 2010. Global peatland dynamics since the Last Glacial Maximum. Geophysical Research Letters, 37(13).
Zeh, L., Igel, M. T., Schellekens, J., Limpens, J., Bragazza, L., & Kalbitz, K. 2020. Vascular plants affect properties and decomposition of moss-dominated peat, particularly at elevated temperatures. Biogeosciences, 17(19), 4797-4813.
Zhang, Y., Huang, X., Wang, R., & Naafs, B. D. A. 2020. The distribution of long-chain n-alkan-2-ones in peat can be used to infer past changes in pH. Chemical Geology, 119622.

Zhang, Z., Wang, J., Lyu, X., Jiang, M., Bhadha, J., & Wright, A. 2019. Impacts of land use change on soil organic matter chemistry in the Everglades, Florida-a characterization with pyrolysis-gas chromatography–mass spectrometry. Geoderma, 338, 393-400.

Chapter 4 - Supplementary Data

Supplementary Table 1. **Quantified pyrolysis products with corresponding compound class (Group), molecular weight (MW, in atomic mass units), chemical formula, ion fragment (*m/z*) used for quantification, retention time (R.T. minutes), and mean relative abundance across all samples (%). Grouping: B= Benzenes, Lig=Lignin (guaiacyl (G) and syringyl (S) origin), N=N compound, Al=aliphatic (*n*-alkanes, *n*-alkenes, *n*-methylketones, *n*-fatty acids, and other aliphatics) Ph = Phenols, Ps = Polysaccharides, Ttp = triterpenoids, Mtp=monoterpenes, Stp = sesquiterpenes.**

Code	Pyrolysis product	Group	MW	Formula	*m/z*	RT	Mean abundance
1	Toluene	B	92	C7H8	91	4.624	1.18
2	Styrene	B	104	C8H8	104	9.007	0.15
3	Phenol	Ph	94	C6H6O	94	13.693	4.37
4	2-Methylphenol (o-cresol)	Ph	108	C7H8O	107	17.296	0.29
5	4-Methylphenol (p-cresol)	Ph	108	C7H8O	107	18.410	1.87
6	3-Ethylphenol	Ph	122	C8H10O	107	21.415	0.04
7	2,4-Dimethylphenol	Ph	122	C8H10O	107	21.931	0.13
8	2,5-Dimethylphenol	Ph	122	C8H10O	107	22.032	0.04
9	4-Ethylphenol	Ph	122	C8H10O	107	22.850	0.73
10	Catechol	Ph	110	C6H6O2	110	24.620	0.23
11	4-Vinylphenol	Ph	120	C8H8O	120	25.452	1.61
12	Methylcatechol	Ph	124	C7H8O2	124	28.859	0.05
13	*p*-Isopropenylphenol	Ph	134	C9H10O	134	29.256	0.46
14	3-Methoxy-5-methylphenol	Ph	138	C8H10O2	138	30.018	0.02
15	4-Formylphenol	Ph	122	C7H6O2	121	32.146	0.07
16	4-Acetylphenol	Ph	136	C8H8O2	121	35.365	0.28
17	4-Hydroxybiphenyl	Ph	170	C12H10O	170	45.492	0.15
18	C_1-Hydroxybiphenyl	Ph	184	C13H12O	184	48.697	0.06
19	Guaiacol	Lig, G	124	C7H8O2	109	18.618	0.23
20	4-Methylguaiacol	Lig, G	138	C8H10O2	138	23.701	0.22
21	4-Ethylguaiacol	Lig, G	152	C9H12O2	137	27.687	0.11
22	4-Vinylguaiacol	Lig, G	150	C9H10O2	135	29.356	0.51
23	4-Formylguaiacol	Lig, G	152	C8H8O3	151	33.053	0.13
24	4-(Prop-2-enyl)guaiacol, *trans*	Lig, G	164	C10H12O2	164	35.232	0.13
25	4-Acetylguaiacol	Lig, G	166	C9H10O3	151	36.637	0.15
26	4-(Propan-2-one)guaiacol	Lig, G	180	C10H12O3	137	38.287	0.03
27	4-(Propan-1-one)guaiacol	Lig, G	182	C9H10O4	137	42.941	0.08
28	Syringol	Lig,S	154	C8H10O3	154	30.969	0.04
29	4-Methylsyringol	Lig,S	168	C8H8O4	153	34.999	0.08
30	4-Vinylsyringol	Lig,S	180	C10H12O3	180	39.742	0.01
31	4-Formylsyringol	Lig,S	182	C9H10O4	181	43.325	0.01
32	4-(Prop-2-enyl)syringol, *trans*	Lig,S	194	C11H14O3	194	44.912	0.05
33	4-Acetylsyringol	Lig,S	196	C10H12O4	181	45.920	0.04
34	Pyridine	N	79	C5H5N	52	4.139	0.08
35	3-Hydroxypyridine monoacetate	N	137	C7H7NO2	95	20.174	0.12
36	Benzylnitrile	N	117	C8H7N	117	21.232	0.03
37	Indole	N	117	C8H7N	117	28.531	0.08
38	C1-indole	N	131	C9H9N	130	32.562	0.04
39	Diketodipyrrole	N	186		186	44.831	0.04
40	n-C23 alkane	Al	324	C23H48	57	59.020	0.02
41	n-C25 alkane	Al	352	C25H52	57	62.307	0.04
42	n-C29 alkane	Al	408	C29H60	57	68.108	0.02
43	n-C31 alkane	Al	436	C31H64	57	70.696	0.04
44	n-C23 alkene	Al	322	C23H46	55	58.919	0.04

Code	Pyrolysis product	Group	MW	Formula	*m/z*	RT	Mean abundance
45	n-C25 alkene	Al	350	C25H50	55	62.219	0.10
46	n-C25 methylketone	Al	366	C25H50O	59	65.519	0.01
47	n-C27 methylketone	Al	394	C27H54O	59	68.334	0.05
48	n-C29 methylketone	Al	422	C29H58O	59	70.948	0.02
49	n-C31 methylketone	Al	450	C31H62O	59	73.348	0.01
50	n-C33 methylketone	Al	478	C33H66O	59	75.772	0.02
51	n-C35 methylketone	Al	506	C35H70O	59	78.965	0.00
52	n-C14 fatty acid	Al	228	C14H28O2	60	47.243	0.01
53	n-C16 fatty acid	Al	256	C16H32O2	60	52.489	0.04
54	Pristene	Al	266	C19H38	56	46.015	0.17
55	C20 unsaturated aliphatic	Al	278	C20H38	68	49.283	0.01
56	Unsaturated aliphatic	Al	278	?	82	50.398	0.01
57	D-Friedoolean-14-ene	Ttp	410	C30H50	218	69.871	0.01
58	Urs-12-ene	Ttp	410	C30H50	218	70.117	0.02
59	Stigmasta-3,5-diene	Ttp	396	C29H48	396	70.520	0.04
60	Stigmasterol	Ttp	412	C29H48O	55	72.554	0.02
61	β-Sitosterol	Ttp	414	C29H50O	55	73.297	0.05
62	Stigmasta-3,5-dien-7-one	Ttp	410	C29H46O	174	74.368	0.04
63	γ-Sitostenone	Ttp	412	C29H48O	124	74.840	0.04
64	α-Tocopherol	Ttp	430	C29H50O2	165	71.011	0.04
65	α-Amyrin (Urs-12-en-3-ol, (3β)-)	Ttp	426	C30H50O	218	74.362	0.01
66	C30 hopanoid	Ttp	410	C30H50	191	71.759	0.01
67	C30 hopanoid isomer	Ttp	410	C30H50	191	71.887	0.01
68	Acetic acid	Ps	60	C2H4O2	60	2.483	2.65
69	(2H)-furan-3-one	Ps		C4H4O2	84	5.512	4.58
70	2-Furaldehyde	Ps	96	C5H4O2	96	6.583	6.04
71	4-Cyclopentene-1,3-dione	Ps	96	C5H4O2	96	6.816	0.60
72	2-Furanmethanol	Ps	98	C5H6O2	98	7.559	0.12
73	2-Propylfuran	Ps	110	C7H10O	81	7.943	0.23
74	4-Cyclopentene-1,3-dione	Ps	96	C5H4O2	96	8.623	0.18
75	4-Cyclopentene-1,3-dione	Ps	96	C5H4O2	96	8.806	0.08
76	2-methyl-2-Cyclopenten-1-one	Ps	96	C6H8O	67	9.606	0.10
77	2(5H)-Furanone	Ps	84	C4H4O2	55	9.858	0.40
78	Acetylfuran	Ps	110	C6H6O2	95	9.845	0.29
79	1,2-Cyclopentanedione	Ps	98	C5H6O2	98	10.670	1.03
80	5-Methyl-2(5H)-furanone	Ps	98	C5H6O2	55	11.161	0.11
81	3-Methyl-2,5-furandione	Ps	112	C5H4O3	68	11.508	0.13
82	5-Methyl-2-furaldehyde	Ps	110	C6H6O2	110	12.383	2.44
83	Unidentified carbohydrate with m/z 55, 86	Ps			55	12.534	1.16
84	3-Methyl-2(5H)-furanone	Ps	98	C5H6O2	69	12.975	0.04
85	Isomaltol	Ps	126	C6H6O3	111	13.234	0.08
86	3-Acetyl-2(3H)-furanone (α-Acetobutyrolactone)	Ps	128	C6H8O3	86	14.134	0.47
87	4-Hydroxy-5,6-dihydro-(2H)-pyran-2-one	Ps	114	C5H6O3	114	14.298	3.19
88	Tetrahydro-3,6-dimethyl-2H-pyran-2-one	Ps	128	C7H12O2	56	14.644	0.22
89	2-Hydroxy-3-methyl-2-cyclopenten-1-one	Ps	112	C6H8O2	112	15.646	0.34
90	Dianhydrorhamnose	Ps	128	C6H8O3	113	16.609	0.87
91	2,5-Dimethyl-4-hydroxy-3(2H)-furanone (Furaneol)	Ps	128	C6H8O3	128	18.618	0.70
92	Maltol	Ps	126	C6H6O3	126	19.853	0.50

Code	Pyrolysis product	Group	MW	Formula	*m/z*	RT	Mean abundance
93	Dihydro-6-methyl-2H-Pyran-3(4H)-one	Ps	114	C6H10O2	56	20.854	0.12
94	2,3-Dihydro-3,5-dihydroxy-6-methyl-4H-pyran-4-one (Pyranone)	Ps	144	C6H8O4	144	21.578	0.15
95	3,5-dihydroxy-2-methyl-4H-pyran-4-one	Ps	142	C6H6O4	142	23.676	0.71
96	1,4:3,6-Dianhydro-α-d-glucopyranose	Ps	144	C6H8O4	69	24.967	0.69
97	5-Hydroxymethylfurfural	Ps	126	C6H6O3	97	25.855	1.60
98	Levogalactosan	Ps	180	C6H12O6	60	32.965	4.98
99	Levomannosan	Ps	162	C6H10O5	60	36.536	4.48
100	Levoglucosan	Ps	162	C6H10O5	60	39.395	43.78
101	1,6-Anhydro-β-D-glucofuranose	Ps	162	C6H10O5	73	42.651	2.03
102	Limonene	Mtp	136	C10H16	68	15.721	0.02
103	Sesquiterpene with m/z 161, 176, 119, 105	Stp	176		161	29.275	0.01
104	Sesquiterpene with m/z 159, 177, 192	Stp	192		159	31.183	0.02
105	Sesquiterpene with m/z 177, 192	Stp	192		109	31.687	0.01
106	Sesquiterpene with m/z 105, 175, 190	Stp	190		175	33.475	0.01
107	Sesquiterpene with m/z 121, 191, 206	Stp	206		121	37.204	0.02
108	Sesquiterpene with m/z 105, 119, 204, 161, 133	Stp	204		105	37.682	0.03

Supplementary Table 2. **Average and standard deviation relative abundance (%) of ON and OD peat core replicates for summed compound classes.**

	Depth	Summed Phenols		Summed Polysaccharides		Summed Lignin		Summed Benzenes		Summed N compounds		Summed Lipids	
		Mean	Stdev	Mean	Stdev	Mean	Stdev	Mean	Stdev	Mean	Stdev	Mean	Stdev
Drained	0	12.69	1.49	75.82	1.99	4.69	0.72	2.30	0.36	0.52	0.10	2.13	0.24
	-4	12.58	5.43	73.53	10.81	6.12	3.35	2.95	1.21	0.79	0.35	2.61	1.58
	-8	9.89	1.03	81.36	2.17	3.04	1.86	1.90	0.47	0.57	0.16	1.36	0.49
	-12	9.81	0.38	83.51	0.25	2.26	0.78	1.37	0.07	0.40	0.05	0.92	0.29
	-16	9.74	0.56	85.44	1.12	0.78	0.35	1.09	0.15	0.27	0.04	0.69	0.15
	-20	9.71	0.74	85.12	0.27	1.01	0.75	1.14	0.15	0.30	0.07	0.95	0.52
	-24	9.31	0.95	85.85	1.70	1.14	1.01	1.09	0.14	0.27	0.05	0.65	0.16
	-28	8.91	1.03	85.37	2.58	1.71	1.49	1.24	0.33	0.36	0.11	0.76	0.38
	-32	9.29	0.86	85.13	1.39	1.37	0.43	1.20	0.17	0.33	0.03	0.92	0.32
	-36	9.80	0.56	81.77	2.01	2.26	1.62	1.98	1.01	0.61	0.31	1.86	1.11
	-40	10.55	0.07	83.47	1.20	0.88	0.13	1.42	0.23	0.45	0.11	1.05	0.56
	-44	10.77	0.20	83.01	1.72	1.06	0.31	1.51	0.52	0.50	0.25	0.96	0.50
	-48	11.14	0.53	82.11	0.88	1.53	0.90	1.52	0.17	0.44	0.07	1.04	0.21
	-52	11.14	0.24	83.35	0.83	0.79	0.14	1.33	0.09	0.37	0.02	0.81	0.10
	-56	10.97	0.23	82.50	1.85	1.67	1.27	1.42	0.19	0.39	0.05	1.20	0.47
	-60	10.66	0.70	83.02	1.26	1.45	0.56	1.26	0.22	0.40	0.09	1.14	0.29
	-64	10.62	1.33	84.38	2.10	0.80	0.16	1.08	0.23	0.32	0.10	0.73	0.00
	-68	10.56	1.10	83.95	2.40	1.66	1.52	1.11	0.37	0.34	0.15	0.86	0.28
Natural	0	18.01	2.67	75.38	2.20	0.76	0.43	1.68	0.06	0.42	0.10	1.00	0.32
	-4	13.91	3.54	80.39	3.37	1.00	0.42	1.38	0.35	0.31	0.06	0.92	0.34
	-8	10.83	1.24	84.67	2.21	1.26	0.78	1.05	0.14	0.25	0.04	0.70	0.08
	-12	10.40	0.53	84.76	0.51	1.32	0.55	1.03	0.08	0.25	0.06	0.69	0.01
	-16	8.86	0.93	85.82	1.12	1.76	0.52	1.11	0.06	0.32	0.04	0.79	0.15

Depth	Summed Phenols		Summed Polysaccharides		Summed Lignin			Summed Benzenes		Summed N compounds		Summed Lipids
	Mean	Stdev	Mean	Stdev	Mean	Stdev		Mean	Stdev	Mean	Stdev	Mean
-20	9.00	1.30	86.18	1.22	1.31	0.46	1.03	0.12	0.30	0.04	0.95	0.38
-24	9.42	0.92	86.77	1.49	1.11	1.25	0.89	0.12	0.22	0.08	0.43	0.22
-28	7.96	0.59	86.54	1.55	2.89	2.27	0.95	0.05	0.26	0.04	0.62	0.27
-32	8.58	0.80	87.10	2.32	1.29	0.79	0.94	0.26	0.22	0.11	0.76	0.38
-36	8.53	0.29	86.54	2.28	2.29	2.08	0.96	0.25	0.25	0.13	0.66	0.35
-40	8.97	0.57	85.82	2.92	2.13	2.41	0.98	0.33	0.29	0.16	0.79	0.63
-44	9.04	1.44	84.73	2.15	2.69	3.52	1.12	0.06	0.32	0.04	0.90	0.24
-48	9.05	0.19	84.28	2.49	3.31	2.39	1.13	0.31	0.36	0.14	0.92	0.44
-52	9.74	0.95	83.57	2.72	1.68	0.39	1.70	0.39	0.57	0.18	1.39	0.76
-56	10.05	1.08	84.41	0.48	1.59	0.91	1.20	0.11	0.37	0.07	0.71	0.30
-60	10.29	0.34	84.53	0.31	1.34	0.34	1.20	0.05	0.35	0.02	0.84	0.25
-64	11.26	0.11	83.16	1.50	1.03	0.52	1.30	0.37	0.41	0.17	0.93	0.47
-68	10.80	0.35	82.33	1.66	1.39	0.46	1.64	0.37	0.50	0.13	1.49	0.65

Supplementary Table 3. **Quantified pyrolysis products with associated PCA code and loadings for principal component analysis investigated to 95% explained variance. PC1-4 explained 68.7% of the variance in all pyrolysis products (PC1=29.4%, PC2=19.0%, PC3=12.2%, PC4=8.5%).**

Compound	ID	PC1	PC2	PC3	PC4	PC5	PC6	PC7	PC8	PC9	PC10	PC11	PC12	PC13	PC14	PC15	PC16	PC17	PC18	PC19
Toluene	1	0.82	0.41	-0.34	0.05	0.13	-0.05	0.03	0.07	0.02	0.01	-0.03	-0.08	-0.08	0.03	-0.01	0.03	-0.03	0.04	0.00
Styrene	2	0.71	0.24	-0.31	-0.19	0.27	-0.02	0.01	0.18	0.04	0.04	-0.01	-0.09	-0.16	0.02	0.06	0.01	-0.05	-0.04	0.00
Phenol	3	-0.39	0.83	-0.07	-0.26	0.12	-0.12	-0.06	-0.12	0.18	0.01	0.08	0.03	0.01	-0.02	-0.02	0.06	0.06	0.00	0.03
2-Methylphenol (o-cresol)	4	0.36	0.88	-0.09	-0.20	-0.03	-0.12	-0.02	-0.07	0.09	-0.02	0.08	-0.01	-0.06	-0.05	0.03	0.02	0.08	-0.02	0.02
4-Methylphenol (p-cresol)	5	0.22	0.44	-0.59	-0.16	0.36	-0.21	-0.18	-0.21	0.21	-0.05	0.15	0.07	-0.03	-0.05	-0.08	0.16	0.08	-0.02	0.05
3-Ethylphenol	6	0.13	0.93	0.07	-0.29	0.00	-0.10	0.02	0.04	0.08	-0.03	0.05	-0.02	0.02	-0.01	0.05	0.01	0.03	0.01	-0.01
2,4-Dimethylphenol	7	0.90	0.30	-0.18	-0.05	-0.07	-0.12	-0.04	-0.05	0.02	-0.07	0.12	0.02	-0.04	-0.08	0.02	0.02	0.10	-0.04	0.05
2,5-Dimethylphenol	8	0.90	0.27	-0.18	0.05	-0.19	-0.09	0.10	-0.04	0.03	-0.05	0.06	-0.01	-0.07	-0.07	0.01	0.01	0.07	-0.02	0.02
4-Ethylphenol	9	-0.30	0.72	0.06	-0.36	0.32	-0.23	-0.05	-0.08	0.19	0.04	-0.04	-0.01	-0.03	-0.01	-0.01	0.00	0.15	-0.03	0.05
Catechol	10	0.63	0.13	0.04	0.40	-0.16	0.17	-0.13	-0.14	0.26	0.12	-0.14	0.18	0.01	0.06	0.34	0.04	-0.01	0.01	-0.13
4-Vinylphenol	11	0.38	0.42	0.61	-0.42	-0.02	-0.22	-0.04	0.03	0.10	-0.04	-0.10	-0.02	0.02	0.03	-0.04	-0.02	-0.03	-0.06	0.11
Methylcatechol	12	0.71	0.12	0.00	0.42	-0.10	0.13	-0.10	-0.11	0.25	0.09	-0.18	0.17	0.07	0.03	0.25	0.02	-0.02	0.02	-0.08
p-Isopropenylphenol	13	-0.47	0.63	0.39	-0.29	0.20	-0.11	0.06	-0.01	0.22	0.06	-0.01	-0.02	0.05	0.04	0.05	-0.06	0.10	0.03	-0.01
3-Methoxy-5-methylphenol	14	0.90	-0.19	0.04	0.01	-0.29	-0.02	0.04	-0.07	0.05	0.00	0.12	-0.03	-0.02	-0.06	0.01	-0.07	0.06	-0.02	0.03
4-Formylphenol	15	-0.33	-0.05	-0.34	0.14	-0.43	0.15	-0.20	-0.08	0.06	-0.20	0.32	0.13	0.31	0.07	-0.06	0.20	0.13	-0.03	-0.15
4-Acetylphenol	16	0.12	0.48	-0.08	0.41	-0.03	0.31	-0.40	-0.15	-0.42	-0.05	-0.01	-0.11	-0.09	0.03	-0.11	0.04	0.11	-0.03	-0.18
p-Hydroxybiphenyl	17	-0.67	0.52	0.21	-0.23	0.20	-0.07	0.13	-0.03	0.26	0.07	0.06	-0.02	0.01	0.05	0.00	-0.06	0.11	-0.01	0.01
p-Benzylphenol	18	-0.53	0.56	0.28	-0.34	0.33	-0.10	0.06	-0.06	0.21	0.03	0.11	-0.01	0.02	0.00	0.01	-0.03	0.08	-0.03	0.01
Guaiacol	19	0.93	-0.02	0.05	0.23	-0.25	0.03	-0.02	-0.08	0.03	-0.02	0.02	0.02	-0.07	-0.03	0.05	0.01	0.06	-0.02	0.03
4-Methylguaiacol	20	0.90	-0.13	0.06	0.18	-0.30	0.00	-0.01	-0.07	0.07	-0.03	0.05	0.05	-0.06	-0.04	0.10	-0.01	0.09	-0.02	0.05
4-Ethylguaiacol	21	0.87	-0.23	0.10	0.10	-0.31	-0.02	-0.03	-0.06	0.03	-0.06	0.09	0.04	0.03	-0.08	0.10	0.02	0.05	0.04	0.01
4-Vinylguaiacol	22	0.82	-0.34	0.18	-0.03	-0.37	-0.07	-0.12	0.03	-0.03	-0.03	-0.01	0.05	-0.01	-0.06	0.09	0.04	0.01	-0.03	0.04
4-Formylguaiacol	23	0.90	-0.12	0.05	0.18	-0.33	0.02	0.00	-0.05	0.02	-0.03	0.08	0.01	-0.08	-0.05	0.08	-0.03	0.08	-0.04	0.05
4-(Prop-2-enyl)guaiacol, *trans*	24	0.87	-0.12	0.11	0.20	-0.36	0.04	-0.01	-0.02	0.05	-0.06	0.06	0.07	-0.04	-0.04	0.07	-0.04	0.10	-0.03	0.01
4-Acetylguaiacol	25	0.90	-0.10	-0.10	0.18	-0.23	0.03	0.11	-0.05	0.07	-0.03	0.12	-0.05	-0.10	-0.03	0.07	-0.04	0.08	-0.01	0.01
4-(Propan-2-one)guaiacol	26	0.51	-0.47	0.34	-0.38	-0.43	-0.06	-0.09	-0.09	0.08	-0.02	0.07	-0.02	-0.03	0.07	-0.11	-0.05	-0.06	-0.01	-0.10

Compound	ID	PC1	PC2	PC3	PC4	PC5	PC6	PC7	PC8	PC9	PC10	PC11	PC12	PC13	PC14	PC15	PC16	PC17	PC18	PC19
4-(Propan-1-one)guaiacol	27	0.91	-0.02	0.03	0.26	-0.26	0.05	0.05	-0.07	0.05	-0.03	0.06	0.01	-0.08	-0.02	0.05	-0.02	0.07	-0.04	0.04
Syringol	28	0.47	-0.42	0.40	-0.47	-0.40	-0.07	-0.02	-0.15	0.02	0.06	0.05	-0.06	-0.03	0.05	-0.09	-0.02	-0.07	0.02	-0.03
4-Methylsyringol	29	0.41	-0.44	0.38	-0.48	-0.35	-0.06	-0.01	-0.22	0.04	0.16	0.01	-0.09	-0.05	0.08	-0.16	-0.03	-0.08	0.03	-0.06
4-Vinylsyringol	30	0.72	0.29	0.07	0.52	-0.10	0.22	-0.10	-0.12	-0.10	0.05	-0.05	-0.04	-0.04	0.01	-0.05	-0.05	0.09	-0.04	0.02
4-Formylsyringol	31	0.37	-0.38	0.34	-0.41	-0.52	0.07	0.12	-0.20	0.08	0.12	0.08	-0.10	-0.02	0.11	-0.13	-0.06	-0.04	0.02	-0.07
4-(Prop-2-enyl)syringol, *trans*	32	0.44	-0.51	0.34	-0.47	-0.40	-0.01	-0.05	-0.11	0.03	0.07	0.02	-0.06	-0.02	0.06	-0.07	-0.02	-0.04	0.01	-0.05
4-Acetylsyringol	33	0.48	-0.37	0.18	-0.44	-0.24	-0.07	0.23	-0.30	-0.01	0.22	0.12	-0.25	-0.07	0.03	-0.17	-0.05	-0.04	0.05	-0.05
Pyridine	34	0.80	0.09	-0.43	-0.08	0.19	-0.04	0.03	0.09	0.04	0.00	0.03	-0.10	-0.14	0.07	0.00	0.15	-0.05	0.09	0.01
3-Hydroxypyridine monoacetate	35	0.35	0.29	-0.61	-0.27	0.17	-0.09	-0.16	0.03	-0.15	-0.02	0.25	-0.12	-0.18	0.00	-0.05	0.12	0.00	-0.06	0.17
Benzylnitrile	36	0.79	0.35	-0.31	-0.05	0.09	0.01	0.05	0.19	0.16	0.02	0.03	-0.09	-0.07	0.06	0.05	0.15	-0.11	0.13	-0.04
Indole	37	0.79	0.23	-0.32	-0.15	0.27	-0.04	-0.08	0.17	0.13	0.02	-0.03	-0.13	-0.05	0.07	0.03	0.14	-0.07	0.13	-0.05
C1-indole	38	0.75	0.36	-0.20	-0.20	0.29	-0.03	-0.19	0.14	0.03	0.02	-0.03	-0.13	-0.07	0.04	0.05	0.15	-0.04	0.11	-0.05
Diketodipyrrole	39	0.77	-0.02	-0.35	-0.12	-0.08	0.13	0.23	-0.04	0.28	0.00	0.09	-0.02	-0.09	-0.04	-0.13	-0.02	-0.04	0.08	-0.14
n-C23 alkane	40	0.61	-0.05	-0.45	-0.40	0.03	0.02	-0.15	0.19	-0.03	-0.15	0.15	0.15	0.11	0.21	0.10	-0.12	-0.03	0.05	0.01
n-C25 alkane	41	0.33	-0.03	-0.22	-0.56	0.49	-0.25	-0.23	0.09	-0.07	0.11	-0.17	-0.01	-0.08	0.04	0.10	-0.15	0.02	-0.08	-0.09
n-C29 alkane	42	0.44	-0.11	-0.49	-0.36	0.01	0.10	-0.33	0.05	-0.13	-0.12	0.20	0.15	0.22	0.15	0.07	-0.12	-0.10	-0.02	0.07
n-C31 alkane	43	0.31	0.02	-0.46	-0.53	0.37	-0.28	-0.31	-0.04	-0.05	0.09	-0.13	0.08	-0.04	-0.01	0.03	-0.03	0.05	-0.09	-0.06
n-C23 alkene	44	0.48	0.12	-0.26	-0.54	0.21	-0.03	0.35	-0.11	-0.19	0.02	-0.22	0.13	0.09	0.12	-0.01	0.03	-0.04	-0.14	-0.08
n-C25 alkene	45	0.51	0.11	-0.16	-0.41	0.18	-0.07	0.49	0.02	-0.28	-0.04	-0.31	0.06	0.10	0.10	0.05	0.09	-0.06	-0.11	-0.04
n-C25 methylketone	46	0.27	-0.10	-0.50	-0.60	0.33	0.24	-0.19	-0.01	-0.10	0.15	0.02	-0.04	0.05	0.08	0.04	-0.09	0.08	0.05	-0.01
n-C27 methylketone	47	0.14	-0.09	-0.63	-0.57	0.11	0.30	-0.13	-0.03	0.03	0.07	0.09	0.06	0.01	0.03	-0.01	-0.20	0.11	-0.02	0.01
n-C29 methylketone	48	0.19	-0.11	-0.36	-0.50	0.08	0.19	0.16	-0.41	-0.17	0.33	0.02	-0.05	0.19	-0.06	-0.04	0.01	0.20	0.14	0.01
n-C31 methylketone	49	0.62	-0.18	-0.24	-0.34	-0.03	-0.20	0.30	0.11	-0.17	-0.26	-0.09	0.10	0.08	-0.05	-0.18	-0.02	0.19	0.16	0.00
n-C33 methylketone	50	0.60	-0.29	-0.06	-0.31	-0.17	-0.33	0.15	0.25	-0.21	-0.31	-0.11	0.02	0.06	0.05	-0.03	0.05	0.20	0.02	0.03
n-C35 methylketone	51	0.59	-0.34	-0.01	-0.33	-0.25	-0.26	0.09	0.22	-0.19	-0.32	-0.06	0.00	0.07	0.04	-0.01	0.04	0.19	0.02	0.02
n-C14 fatty acid	52	0.50	0.09	0.02	0.21	0.08	0.01	0.14	0.48	-0.17	0.47	0.21	0.26	0.02	-0.05	-0.21	0.04	-0.03	0.00	0.00
n-C16 fatty acid	53	0.15	0.18	0.19	0.07	0.03	0.03	0.08	0.48	-0.20	0.55	0.25	0.42	-0.09	-0.18	-0.08	0.03	0.12	0.01	-0.08
Pristene	54	0.34	-0.04	-0.57	-0.27	0.14	0.27	0.28	0.04	-0.02	-0.06	0.18	0.02	-0.14	0.09	0.16	-0.19	-0.12	-0.17	-0.04
C20 unsaturated aliphatic	55	0.12	0.86	0.30	-0.11	-0.05	0.13	-0.08	0.01	-0.10	-0.11	0.03	0.05	0.18	-0.01	0.02	0.02	-0.06	0.06	-0.10
Unsaturated aliphatic	56	0.11	0.80	0.14	-0.06	-0.13	0.13	-0.10	0.11	-0.14	-0.09	0.15	-0.12	0.27	0.03	-0.06	0.02	-0.08	0.06	-0.10
D-Friedoolean-14-ene	57	0.10	-0.13	-0.11	-0.36	-0.10	0.65	-0.22	0.30	0.25	-0.01	-0.05	0.06	0.20	-0.12	-0.03	0.04	-0.08	0.15	0.12

Compound	ID	PC1	PC2	PC3	PC4	PC5	PC6	PC7	PC8	PC9	PC10	PC11	PC12	PC13	PC14	PC15	PC16	PC17	PC18	PC19
Urs-12-ene	58	0.25	-0.09	-0.31	-0.40	-0.04	0.55	0.36	-0.07	0.07	-0.09	-0.10	0.18	-0.01	-0.10	0.01	0.18	0.04	-0.26	-0.01
Stigmasta-3,5-diene	59	0.84	-0.08	-0.17	-0.04	0.16	-0.20	-0.27	-0.03	-0.06	0.12	-0.12	0.03	0.00	-0.12	-0.07	0.06	0.01	-0.02	-0.08
Stigmasterol	60	-0.08	0.15	-0.07	-0.22	0.16	0.23	0.11	-0.25	-0.12	-0.32	-0.15	0.46	-0.29	-0.27	-0.03	-0.25	-0.13	0.36	0.05
β-Sitosterol	61	0.42	-0.33	0.00	-0.25	0.17	-0.11	-0.65	-0.20	-0.04	0.03	-0.11	0.07	0.14	-0.11	0.01	0.12	-0.18	0.01	-0.02
Stigmasta-3,5-dien-7-one	62	0.82	0.19	-0.12	0.32	0.17	-0.01	-0.17	-0.17	0.06	0.09	-0.12	0.05	-0.01	0.05	0.02	0.01	0.03	-0.02	-0.07
γ-Sitostenone	63	0.64	0.10	0.04	0.29	0.13	0.05	-0.35	-0.19	-0.24	0.13	-0.14	-0.07	0.16	-0.10	-0.09	-0.13	-0.11	-0.18	0.26
α-Tocopherol	64	0.50	0.05	-0.46	-0.23	0.14	0.42	0.04	-0.05	0.12	0.05	0.17	0.07	0.07	0.29	-0.03	-0.18	-0.01	-0.04	0.08
α-Amyrin (Urs-12-en-3-ol, (3β)-)	65	0.18	0.15	-0.15	-0.22	0.04	0.21	0.56	-0.54	-0.19	0.17	-0.03	0.17	0.08	-0.06	0.11	0.26	-0.09	0.00	0.05
C30 hopanoid	66	0.23	-0.28	-0.04	-0.44	-0.06	0.61	-0.15	0.21	0.18	-0.05	-0.26	-0.15	-0.04	-0.20	-0.12	0.06	0.08	-0.05	-0.02
C30 hopanoid isomer	67	0.12	-0.21	-0.03	-0.38	-0.05	0.64	-0.11	0.24	0.28	0.00	-0.30	-0.16	-0.01	-0.14	-0.19	0.06	0.13	-0.04	0.06
Acetic acid	68	0.42	0.54	0.47	-0.30	-0.27	-0.06	0.20	0.15	0.05	-0.01	0.03	0.04	0.06	-0.03	0.04	-0.08	-0.10	-0.07	0.16
(2H)-furan-3-one	69	-0.60	0.20	-0.69	0.07	-0.30	-0.08	-0.02	-0.03	0.03	0.03	-0.03	0.00	0.00	-0.02	-0.08	0.03	-0.06	-0.03	0.02
2-Furaldehyde	70	-0.46	0.26	-0.62	-0.06	-0.55	-0.08	-0.02	0.07	0.01	0.04	-0.03	0.00	0.00	0.03	0.00	-0.02	-0.06	0.01	0.03
4-Cyclopentene-1,3-dione	71	-0.54	-0.08	-0.33	0.00	-0.65	-0.15	0.05	0.13	0.00	0.11	-0.18	0.06	-0.08	0.05	-0.08	0.07	-0.12	-0.04	0.08
2-Furanmethanol	72	0.18	0.75	0.59	-0.17	0.01	0.07	0.00	0.04	-0.10	-0.06	0.02	-0.01	0.01	0.00	0.03	0.02	-0.04	-0.02	-0.04
2-Propylfuran	73	-0.29	-0.07	-0.87	0.07	-0.11	0.02	0.18	0.11	-0.11	-0.10	0.06	-0.12	-0.03	-0.06	0.04	0.02	-0.12	-0.05	-0.03
4-Cyclopentene-1,3-dione	74	-0.33	0.37	-0.61	0.03	-0.58	-0.03	-0.02	0.11	-0.02	0.03	-0.01	-0.07	0.06	-0.04	0.02	-0.04	-0.05	0.01	-0.08
4-Cyclopentene-1,3-dione	75	-0.35	0.26	-0.58	-0.01	-0.58	-0.13	0.01	0.06	0.00	0.10	-0.08	-0.10	-0.05	-0.18	0.03	-0.06	0.03	-0.04	0.00
2-methyl-2-Cyclopenten-1-one	76	0.38	0.90	-0.11	-0.07	-0.10	0.01	-0.05	-0.03	-0.09	-0.01	0.00	-0.05	-0.04	-0.02	0.01	0.02	0.00	0.00	-0.03
2(5H)-Furanone	77	0.12	0.88	0.37	-0.12	-0.15	0.07	-0.04	0.00	-0.07	-0.05	0.01	-0.04	0.05	-0.06	-0.01	0.00	-0.02	0.00	-0.03
Acetylfuran	78	-0.29	0.61	-0.64	0.02	-0.31	-0.02	-0.07	0.03	-0.06	0.04	-0.02	-0.06	-0.02	-0.02	0.01	-0.01	-0.03	0.03	-0.02
1,2-Cyclopentanedione	79	0.07	0.87	0.39	-0.15	-0.16	0.03	0.01	0.00	-0.07	0.02	-0.03	0.00	-0.01	-0.04	0.01	-0.02	0.02	-0.03	-0.01
5-methyl-2(5H)-furanone	80	-0.05	0.93	-0.02	-0.10	-0.22	-0.01	0.04	0.01	-0.08	-0.05	0.01	-0.10	0.05	-0.14	-0.03	-0.03	-0.07	-0.06	0.01
3-methyl-2,5-furandione	81	0.24	0.79	0.38	-0.05	-0.14	0.22	0.09	-0.06	-0.07	-0.11	0.10	0.06	0.08	0.02	-0.03	0.10	-0.11	0.04	0.04
5-methyl-2-furaldehyde	82	-0.54	0.43	-0.63	0.01	-0.30	-0.08	-0.05	-0.07	0.04	0.05	0.03	0.02	0.02	0.04	-0.05	0.00	-0.01	0.02	0.04

Compound	ID	PC1	PC2	PC3	PC4	PC5	PC6	PC7	PC8	PC9	PC10	PC11	PC12	PC13	PC14	PC15	PC16	PC17	PC18	PC19
Unidentified carbohydrate with m/z 55, 86	83	-0.15	-0.72	0.29	-0.26	-0.37	-0.11	-0.11	0.16	0.00	0.01	0.00	0.07	-0.01	0.17	0.10	0.15	0.02	0.02	0.10
3-methyl-2(5H)-furanone	84	0.34	0.79	0.40	-0.09	-0.14	0.11	-0.06	-0.03	-0.08	-0.09	-0.01	-0.03	-0.02	-0.02	-0.06	-0.04	-0.02	-0.04	0.04
Isomaltol	85	-0.33	0.18	-0.53	-0.03	-0.29	-0.05	0.08	-0.08	-0.16	0.30	-0.16	-0.22	0.13	-0.03	0.24	-0.03	0.13	0.22	0.16
3-acetyl-2(3H)-furanone (α-Acetobutyrolactone)	86	-0.77	-0.07	-0.40	0.22	0.10	0.02	0.08	-0.18	0.13	-0.11	0.10	0.06	0.00	0.05	-0.11	0.10	0.01	0.00	0.08
4-Hydroxy-5,6-dihydro-(2H)-pyran-2-one	87	-0.06	-0.08	0.46	-0.51	-0.51	-0.14	-0.17	0.21	0.02	0.11	-0.08	0.22	-0.04	0.10	0.05	0.09	-0.06	-0.01	0.08
Tetrahydro-3,6-dimethyl-2H-pyran-2-one	88	-0.65	0.19	-0.62	0.09	-0.30	-0.05	-0.02	0.01	0.06	0.08	-0.09	0.01	0.05	0.07	-0.04	0.01	0.00	0.02	0.05
2-hydroxy-3-methyl-2-cyclopenten-1-one	89	0.04	0.93	0.26	-0.14	0.00	0.01	-0.06	-0.08	-0.12	-0.01	-0.02	-0.03	-0.05	-0.05	-0.01	0.03	0.04	-0.02	-0.05
Dianhydrorhamnose	90	-0.70	0.44	-0.22	-0.02	0.15	0.02	0.03	-0.25	0.12	-0.11	0.14	0.17	-0.05	-0.03	-0.18	0.08	-0.02	-0.04	0.07
2,5-Dimethyl-4-hydroxy-3(2H)-furanone (Furaneol)	91	-0.54	0.50	-0.14	0.14	-0.22	0.03	-0.16	0.09	0.13	-0.11	-0.16	0.24	-0.20	0.16	-0.20	-0.12	0.02	-0.12	-0.11
Maltol	92	-0.12	0.80	-0.27	0.03	-0.43	0.09	0.00	0.02	-0.08	0.06	-0.08	-0.06	-0.14	0.05	0.04	-0.03	0.04	0.04	-0.01
Dihydro-6-methyl-2H-Pyran-3(4H)-one	93	0.11	0.79	0.52	-0.22	-0.03	0.02	0.01	0.01	-0.05	-0.02	0.01	-0.01	0.03	-0.05	0.04	-0.02	0.00	0.00	0.00
2,3-dihydro-3,5-dihydroxy-6-methyl-4H-pyran-4-one (Pyranone)	94	-0.39	0.25	-0.01	0.16	-0.22	0.30	-0.22	-0.17	-0.20	0.03	-0.19	0.12	-0.28	0.49	-0.11	0.16	0.12	0.10	0.09
3,5-dihydroxy-2-methyl-4H-pyran-4-one	95	0.63	-0.09	0.42	-0.16	0.28	-0.02	-0.22	-0.06	-0.11	-0.07	0.16	-0.04	-0.21	-0.05	-0.06	0.10	-0.15	0.04	0.06
1,4:3,6-Dianhydro-α-d-glucopyranose	96	-0.14	0.08	-0.86	0.03	-0.26	-0.02	0.18	0.09	-0.08	-0.10	0.02	-0.13	-0.07	-0.12	0.02	-0.03	-0.13	0.00	-0.10
5-Hydroxymethylfurfural	97	-0.48	0.71	0.28	-0.05	-0.30	0.03	-0.02	0.01	0.01	0.05	-0.10	0.02	0.06	0.09	0.03	-0.15	0.06	0.05	-0.09
Levogalactosan	98	-0.08	0.31	0.66	0.07	0.30	0.27	0.37	0.23	-0.07	0.01	-0.05	-0.13	-0.04	0.15	0.07	0.04	-0.02	0.05	0.00
Levomannosan	99	0.11	0.00	0.27	0.53	0.40	0.48	0.16	0.13	-0.18	-0.01	0.15	-0.23	-0.06	0.13	0.04	-0.05	0.05	0.01	0.08

Compound	ID	PC1	PC2	PC3	PC4	PC5	PC6	PC7	PC8	PC9	PC10	PC11	PC12	PC13	PC14	PC15	PC16	PC17	PC18	PC19
Levoglucosan	100	-0.17	-0.91	-0.06	0.04	0.29	-0.09	-0.10	-0.08	-0.08	-0.04	0.00	0.00	0.03	-0.09	-0.08	-0.01	0.02	0.01	-0.06
1,6-Anhydro-β-D-glucofuranose	101	-0.35	-0.84	-0.04	0.15	0.29	0.03	0.09	0.03	-0.02	-0.08	0.03	-0.09	0.08	-0.02	0.03	-0.03	0.03	0.01	-0.09
Limonene	102	0.72	0.28	-0.03	0.46	-0.01	0.18	-0.20	-0.07	-0.25	-0.03	-0.05	0.00	0.05	-0.01	-0.10	-0.08	0.03	-0.03	-0.01
Sesquiterpene with m/z 161, 176, 119, 105	103	0.80	0.23	-0.11	0.44	0.09	-0.10	0.10	-0.01	0.08	0.02	-0.10	0.02	0.12	0.06	-0.16	-0.04	-0.04	0.00	0.06
Sesquiterpene with m/z 107, 159, 177, 192	104	0.81	0.17	-0.21	0.36	0.13	-0.17	0.16	0.04	0.15	0.01	-0.10	0.02	0.10	0.07	-0.13	-0.03	-0.03	0.04	-0.02
Ssquiterpene with m/z 109, 177, 192	105	0.81	0.22	-0.16	0.41	0.11	-0.12	0.13	0.02	0.14	0.02	-0.09	0.02	0.11	0.08	-0.12	-0.03	-0.04	0.03	0.00
Sesquiterpene with m/z 105, 175, 190	106	0.80	0.21	-0.13	0.44	0.09	-0.12	0.11	0.00	0.12	0.04	-0.09	0.03	0.13	0.05	-0.13	-0.06	-0.04	0.00	0.07
Sesquiterpene with m/z 121, 191, 206	107	0.78	0.21	-0.14	0.38	0.17	-0.17	0.18	0.03	0.15	0.01	-0.11	-0.01	0.08	0.04	-0.18	-0.06	0.00	0.06	0.01
Sesquiterpene with m/z 105, 119, 204, 161, 133	108	0.81	0.20	-0.15	0.43	0.10	-0.12	0.12	0.00	0.14	0.02	-0.09	0.03	0.11	0.07	-0.12	-0.04	-0.03	0.02	0.02

Supplementary Table 4. **Assessment of plant macroscopic remains with depth (cm) analyzed from Lakkasuo core ON1, with humification index (Von Post scale), and dominant species reported per horizon depth.**

Humification	Horizon (cm)	Dominant species	Macroscopic remains
	0-4	Sph.angustifolium	Living moss, *Sphagnum angustifolium*, *Kurzia pauciflora*, *Andromeda* leaves, 1 *Andromeda* stalk, 1 *Oxycoccus* leaf
H2-3	4 - 7	Sph.angustifolium	Sphagnum peat: *S. angustifolium, S. fuscum, S. balticum*, some *Kurzia pauciflora*, at 5-6 cm a few living dwarf shrub fine roots
H3 (H2)	8 -16	Sph. balticum	Mixed peat *S. fuscum/S. balticum*, from here dead dwarf shrub fine roots, individual dark fungal hyphae, at 10 cm a dwarf shrub root, at 12 cm cottongrass leaf sheath (*Eriophorum*), at 14 cm *Andromeda* leaves
H3 (H2)	16 -19	Sph. balticum	Transition, Sphagnum peat = *S. balticum, S. fuscum* interspersed, peat moss still quite intact, cottongrass leaves interspersed, 1 *Andromeda* stem
H3-4	19 - 25.5	Sph. balticum	*S. balticum* peat, some *S. fuscum* mixed in (not confirmed), individual cottongrass roots, 1 thinnish cottongrass fiber tuft, fine network of dwarf shrub fine roots, peat moss remains from here visibly decomposed and leaflets detached from the stem, at 19-22 cm two sturdy stems, probably *Andromeda*
H4	25.5 - 36	Sph. balticum	Light *S. balticum* peat, individual *Cymbifolia* leaflets, individual dark Sphagnum axes=*Cymbifolia* or *S. fuscum*, peat fiber-rich similar to above: cottongrass leaves, individual cottongrass roots, 2 living cottongrass roots!, more dwarf shrub stems, 1 cottongrass fiber bundle, mesh of dwarf shrub fine roots, from here some fine-grained substance (=amorphous peat substance), 1 *Andromeda* leaf > probably transported here from above
H4-5	36 - 38.5	Sph. balticum	Mixed peat, at the edge, a cottongrass fiber bundle, *S. balticum* peat beneath it, cottongrass roots, individual cottongrass leaves, more dwarf shrub stems, 1 *Andromeda* stem, scattered dwarf shrub fine roots
	38.5 - 44	Sph. balticum	S. balticum peat and a few *Cymbifolia* leaves, 1 *S. fuscum* leaf blade, narrow branch leaf from *S. cuspidatum*? (unconfirmed), some fine-grained amorphous matrix as well, cottongrass roots and leaves, individual rotted dwarf shrub stem, network of dwarf shrub fine roots
H4	44 - 52	Sph. balticum	Light *S. balticum* peat with mixture >> individual *S. fuscum*-stem and branch leaves, 1 *S. fuscum* capitulum, several *Cymbifolia* leaves (=*S. magellanicum* confirmed), 1 *Oxycoccus* leaf, cottongrass leaves and roots, individual rotted dwarf shrub axes
H4	52 - 54	Cymbifolia?	Sphagnum peat with approximately 20% cottongrass fiber, fibers also between the peat moss, several Cymbifolia leaves, some cottongrass roots and leaves, network of dwarf shrub fine roots, 1 dwarf shrub axes
H4	54 - 63	Sph. balticum	Light *S. balticum* peat, approximately 20% Cymbifolia leaves, individual *S. fuscum*-little stems (not confirmed)
H4-H5	63 - 75	Cymbifolia	Predominantly *Cymbifolia* peat, only a few fine-leaved peat moss, some *S. balticum*, some fine-grained amorphous matrix, 1 *S. fuscum* stem leaves and probably more *S.fuscum* leaflets (not confirmed), many cottongrass roots and leaves, faint network of dwarf shrub fine roots

Humification	Horizon (cm)	Dominant species	Macroscopic remains
H4 (3)	75 - 82.5	Cymbifolia	*S. cymbifolia* peat (light Sphagnum remains), approximately 10% fine-leaved peat moss, some fine-grained amorphous material, clearly more ragged peat moss remains, fewer dwarf shrub fine roots, locally many cottongrass roots and individual cottongrass leaves, at 81 cm thin cottongrass fiber, many dark little stems with hyalodermis (probably Sph. mag.), only a few small branch leaves > partly *Acutifolia* leaves (*S. fuscum/rubellum*), partly *cuspidata* (*S. balticum/S. angustifolium*), 1 *S. angustifolium* leaf blade
H4	82.5 - 86	Cymbifolia/Sph. balticum	Mixed peat *Cymbifolia-S. balticum* (approximately 1:1), with many cottongrass roots, a few dwarf shrub roots, many *Cymbifolia* leaf blades, no *Acutifolia* or *Cuspidata* leaf blades found!
H4	86 - 94	Cymbifolia	*Cymbifolia* peat, individual *Cymbifolia* leaf blades, two *S. balticum* leaf blades, approximately 30% small branch leaves >> probably *S. angustifolium* (large membrane gaps) and *S. balticum*, three Sphagnum little stems without hyalodermis = *S. angustifolium*, scattered cottongrass leaves and roots, a few dwarf shrub fine roots
H4	94 - 102	Cymbifolia	*Cymbifolia* peat, one leafy *S. magellicanicum* little stems (not confirmed), more *S. angustifolium*-little stems , individual *S. balticum* stems and leaves, some cottongrass roots and leaves

Supplementary Table 5. **Assessment of plant macroscopic remains with depth (cm) analyzed from Lakkasuo core OD2, with humification index (Von Post scale), and dominant species reported per horizon depth. Diagnostic species are defined as species that indicate by their presence a hydrological regime change or shift in habitat conditions.**

Humification	Horizon (cm)	Dominant species	Diagnostic species	Macroscopic remains
no hydromorphic horizon	0 - 2	Pleurozium	Aulacomnium	Extant moss (*Pleurozium schreberi, Aulacomnium palustre*), slightly disturbed through core, pine needles, 1 *Oxycoccus* stem
no hydromorphic horizon	1.5 - 3.5	Pleurozium	cap./rubellum	Bleached *Pleurozium* remains, fragment from *Oxycoccus* leaf, no macrocopically discernable fungal growth, however very fine dark brown fungal hyphae are present, in places nests with broken up needles/leaves, no woody roots, many pine needles, very small amount of amorphous substance, very little *S. capillifolium/rubellum* leaves
no hydromorphic horizon	3.5 - 5.5	rubellum	Pleurozium	Phase with dying *Sphagnum rubellum/capillifolium*-peat, only a little *Sphagnum* leaves, 1 staminate pine cone, many dead Pinus fine roots, pine needle remains, 1 small cottongrass leaf sheath, more *Oxycoccus*leaves, 1 *Oxycoccus* fine roots, individual cottongrass roots, more *Pleurozium* leaves
crumbly, squeezing impossible	5.5 - 8.5	rubellum	rubellum	Transition horizon to light Sphagnum peat, quite heterogenous, *Sph. rubellum*-peat, individual shredded leaves from *Cymbifolia*, 1 cottongrass leaf sheath, dead *Pinus* fine roots, brown nests with amorphous material,. *Sph*. shredded leaves between light *Sph.* peat, 1 partially rotten cottongrass root
H3	8.5-13	rubellum	Ledum?	Quite homogenous light *Sph. Rubellum* peat, scattered *Pinus* fine roots, 1 *Oxycoccus* stem, 1 brown capsule with red seeds (*Ledum palustre*)
H3 (cottongr.H4)	13 - 18	rubellum	Pleurozium	yellow-orange-brown *Sph. rubellum* peat, 1 small cottongrass leaf sheath, more cottongrass roots, more *Pinus* fine roots, 1 *Pleurozium* leaf, small amount of fine-grained substance
H3-4	18 - 23	rubellum	balticum	yellow-orange *Sph. rubellum* peat, more cottongrass roots, *Pinus* roots with fine roots, very small amount of fine-grained amorphous material, a few dwarf shrub fine roots
H3	23 - 28	rubellum	balticum	yellow-orange *S. rubellum* peat, individual narrow cottongrass leaf sheath, more cottongrass fine roots and leaves, 1 *Andromeda* stem, a few dwarf shrub fine roots (heaped in places), individual *S. balticum* leaves, individual Cymbifolia leaves

Humification	Horizon (cm)	Dominant species	Diagnostic species	Macroscopic remains
H4	28 - 30		cymbifolia	Transition from yellow *Sph* peat in brown peat, from above the first appearance of Cymbifolia leaves, light *Sphagnum* peat
H4-5	30 - 34.5	rubellum		Light brown to brown S. rubellum peat with S. balticum, Sphagnum leaves more strongly decomposed than above, approximately 80% Sphagnum leaves shredded, approximately 15% fine-grained amorphous substance, individual cottongrass leaves, below 1 sturdy cottongrass leaf sheath, 1 dwarf shrub stem
H5-6	34.5 - 39.5	rubellum/balticum	Eriophorum, Ledum?	Brown-dark brown Sphagnum/cottongrass peat, *S. rubellum* + *S. balticum*, cottongrass leaf sheath, Sphagnum remains strongly decomposed, interspersed cottongrass leaves, elliptical fruits (*Ledum palustre*?), very few dwarf shrub fine roots
H4	39.5 - 44.5	rubellum	Eriophorum, S. balticum	gold-brown *S. rubellum* peat with *S. balticum*, many cottongrass roots and leaves, some cottongrass leaf sheaths, spots with more strongly decomposed Sphagnum leaves
H4	44.5 - 50	rubellum		gold-brown S. rubellum peat, individual Sph.cymbifolia leaves, scattered cottongrass leaves and roots, 1 long dwarf shrub stem, more fine-grained substance than above, approximately 20% ragged Sphagnum leaves
H4	50 - 55	rubellum/balticum	Ledum?	medium brown to dark brown *S. rubellum/balticum* mixed peat, individual Cymbifolia leaves, Sphagnum remains mushy, scattered dwarf shrub fine roots, brown fruits (*Ledum palustre*), approximately 20-30% ragged Sphagnum remains, approximately 10 -20% amorphous substance
H4	55 - 60	rubellum	balticum	medium-brown *S. rubellum* peat with *S. balticum*, light patches (*S. balticum*?), scattered cottongrass roots and leaves, coralloid *Pinus* fine roots, many dwarf shrub fine roots, many leafy Sphagnum branches, 1 Sphagnum spore capsule
H8 at 60-62cm	60 - 65	rubellum	balticum	medium-brown *S. rubellum* peat with dark band at 60-62 cm, scattered *S. balticum* leaves, individual Cymbifolia leaves, scattered dwarf shrub fine roots., coralloid *Pinus* fine roots, quite a lot of fine-grained substance and shredded Sphagnum leaves
H4	65 - 70	cymbifolia	balticum	medium-brown *S. cymbifolia* peat (*S. magellanicum* confirmed!), *S. balticum* and small amount of *S. rubellum* mixed in, scattered cottongrass roots and leaves, individual *Pinus* fine roots

Humification	Horizon (cm)	Dominant species	Diagnostic species	Macroscopic remains
H4	70 - 76	cymbifolia	Scheuchzeria	medium-brown *Cymbifolia* peat, with *S. balticum* and *S. rubellum*, in places many scattered Sphagnum leaves, well preserved Cymbifolia leaves, 1 *Scheuchzeria* rhizome, scattered cottongrass roots and leaves
H4	76 - 81	cymbifolia	balticum, rubellum	heterogenous Cymbifolia peat with *S. balticum* and *S. rubellum*, individual dwarf shrub fine roots, spotty gold-yellow Cymbifolia leaves, spotty fine-grained substrance and scattered Sphagnum remains
H4	81 - 87	balticum/magell.	balticum	medium-brown Sphagnum peat *S. cymbifolia/S. balticum* 1:1. with dark strips (amorphous substance), many cottongrass roots and leaves, scattered dwarf shrub fine roots
H4-5	87 - 93	balticum/magell.	Scheuchzeria	medium-brown Sphagnum mixed peat: *S. cymbifolia-balticum*, shredded *S. balticum* leaves, 1 *Scheuchzeria* rhizome, scattered dwarf shrub fine roots
H4-5	93 - 100	balticum/magell.	balticum	medium-brown to browner Sphagnum mixed peat, *Cymbifolia : balticum* 1 : 1, with cottongrass leaf sheaths, scattered *S. rubellum*, many shredded S. balticum leaflets and also fine-grained substance, dwarf shrub fine roots, individual dwarf shrub stem

Supplementary Table 6. **Measured fraction of 14C ($F^{14}C$) for selected samples from the Lakkasuo cores ± instrumental analytical error.**

Depth	Sample	$F^{14}C$	Sample	$F^{14}C$
8-10	ON1	1.0614±0.003	OD1	1.0788±0.003
	ON2	1.1687±0.003	OD2	1.1903±0.003
	ON3	1.0585±0.003	OD3	1.1304±0.003
48-50	ON1	1.0063±0.003	OD1	0.9765±0.003
	ON2	0.9955±0.003	OD2	0.9994±0.003
	ON3	1.0150±0.003	OD3	0.9691±0.002
80-82	ON1	0.9274±0.002	OD1	0.9135±0.002
	ON2	0.9232±0.002	OD2	0.9191±0.002
	ON3	0.9121±0.002	OD3	0.8949±0.002

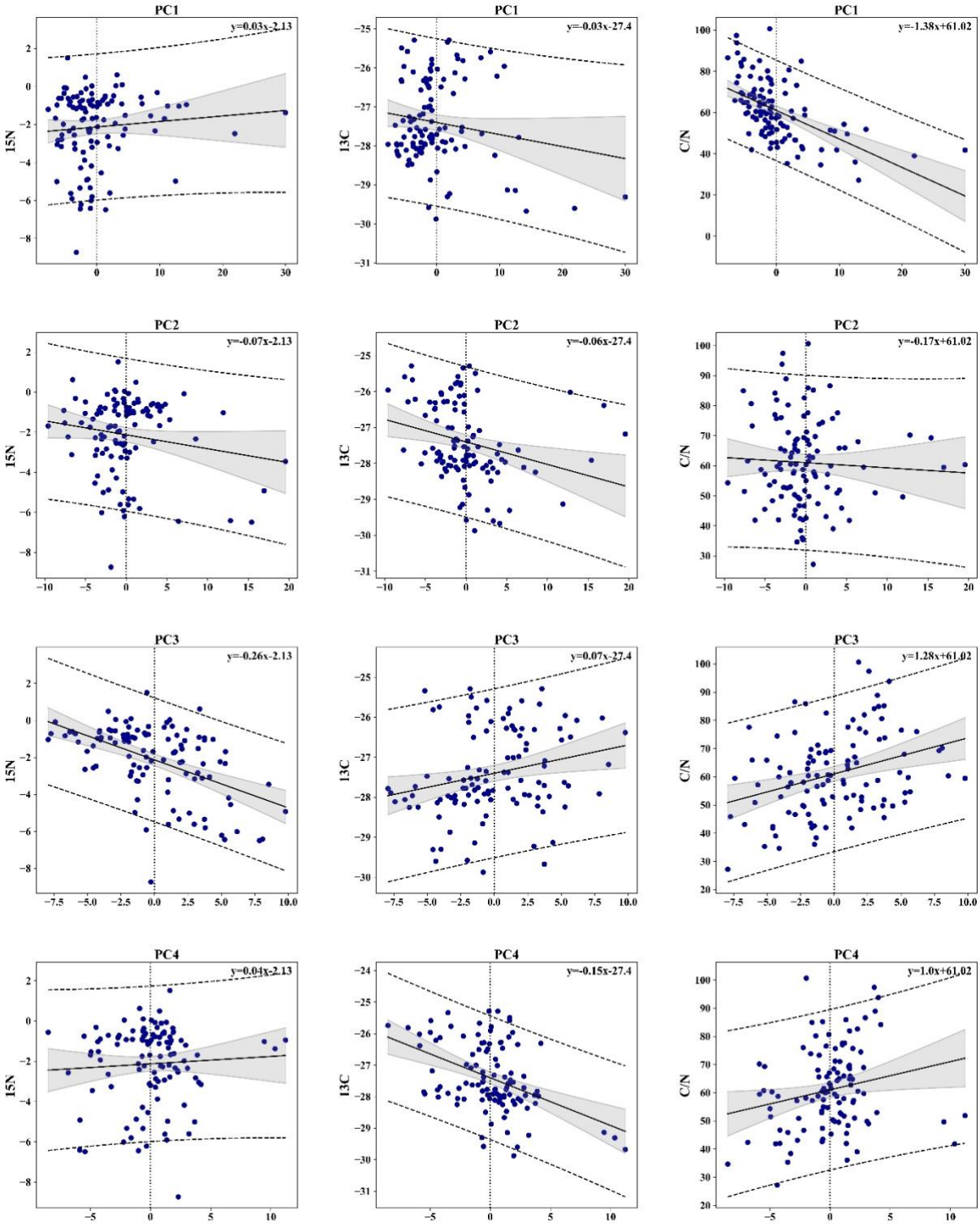

Supplementary Figure 1. **Linear correlations (Pearson) for PC1-4 with $\delta^{15}N$ (left) & $\delta^{13}C$ (middle) isotope abundance, and CN ratios (right).**

Chapter 5 - Chemical composition as an early indicator of rewetting in a Swedish minerogenic boreal mire – a Py-GC/MS study

Authors, Kristy Klein[1,2*], Judith Schellekens[3], Miriam Groβ-Schmölders[2], Pascal von Sengbusch[4], Christine Alewell[2], Jens Leifeld[1]

[1]Agroscope, Climate and Agriculture Group, Reckenholzstrasse 191, CH-8046 Zürich

[2]Environmental Geosciences, University of Basel, Bernoullistrasse 32, CH-4056 Basel

[3]Forest, Nature and Landscape, KU Leuven, Celestijnenlaan 200e – box 2411, BE -3001 Leuven

[4]Office for ecological reports, Fuchsrain 10, GER-79400 Kandern

In preparation

Abstract

Increased focus has been placed on rewetting drained peatlands to restore C sequestration function. To demonstrate successful rewetting in transitioning drained peatlands, initial changes in chemical composition that can serve as chemical indicators reflecting rewetted conditions are needed. This research aimed to investigate chemical differences between paired natural and rewetted peat sites in a minerotrophic boreal mire in northern Sweden for early chemical indicators of peatland OM response following rewetting. Peatland chemistry was traced by site and depth using 105 quantified pyrolysis products in three replicate cores per site using pyrolysis-gas chromatography mass spectrometry (Py-GC/MS). Py-GC/MS results were compared with elemental composition (C/N, H:C/O:C atomic ratios) measured by bulk elemental analysis on the same samples.

Principal component analysis (PCA) separated environmentally-driven influences on peat chemical composition, which differentiated both the natural and rewetted sites from one another as well as the present rewetted vs historical drainage periods. Differences in chemical composition and peat hydrological status were demonstrated by Py-GC/MS summed compound classes, PCA scores, and elemental composition to the same depth. *Sphagnum* phenols were abundant in both natural and rewetted surface samples - suggesting that these phenol compounds may serve as an early indicator of rewetted conditions in *Sphagnum* peatlands. However, compound classes typically more abundant in vascular plants were slower to respond to the changes in hydrological conditions (higher lignin, N compounds, benzenes, lipids, polyaromatic hydrocarbons), and reflected effects of drainage through differences in chemical composition between the natural and rewetted sites throughout the entire profile.

These findings suggest that rewetted peat continues to demonstrate different chemical characteristics from drained peat that remain visible in the OM composition through the entire profile depth, underscoring the importance of maintaining rewetted conditions in restored peatland ecosystems. However, the robust recovery observed in the *Sphagnum*-derived phenols serves as a strong early indicator that even after >80 years of drainage, initial OM chemical responses to rewetting are rapid in surface peat.

5.1 Introduction

Drainage for extraction, agriculture, and forestry disturbs the sensitive carbon (C) balance of peatland ecosystems, tipping them towards stronger aerobic decomposition and increased release of greenhouse gases contributing to global warming. In Europe alone, more than half of the original peatlands have already been drained (Andersen et al., 2017). Due to their sheer size, this change in C balance is substantial: without a dedicated focus on peatland restoration and protection, terrestrial systems are currently projected to remain a global net source of CO_2 throughout the 21st century, despite implementation of other mitigation measures such as afforestation (Humpenöder et al., 2020).

To restore the C sequestration function of peatlands, an increased focus has been placed on the rewetting of formerly drained ecosystems (Andersen et al., 2017). However, the response of peatlands to rewetting after previous drainage is not well understood – particularly in terms of changes to organic matter (OM). While the re-establishment of water-saturated conditions in peatlands mitigates the release of CO_2 originating from aerobic mineralization, rewetting activities are also associated with hot spots for methane (Wilson et al., 2009). For successful rewetting projects, the extent of previous degradation may also be a factor: (Emsens et al., 2020) estimated that for sufficient microbial recovery on a functional biochemical level, at least 70% percent minimum OM content would be required as a baseline for the rewetted ecosystem – thereby limiting the capacity for recovery of more severely degraded ecosystems. Depending on the nature of their former usage (drainage for forestry, agriculture, extraction, etc.), rewetted peatlands may continue to exhibit impacts to substrate stemming from the previous increased decomposition rates, rendering the remaining OM more (or less) vulnerable (Clymo, 1984; Schimmel, Braun, Subke, Amelung, & Bol, 2021).

Peatland greenhouse gas emissions originate from stored OM, and to understand the influences upon these emissions, it is essential to understand the chemical forces driving them. For example, changes in rewetted peat OM content following drainage have been shown to be dependent on the ecosystem type (fen, mire, forest, coastal, etc.), suggesting that degradation extent (and C loss) in many peatlands is largely dependent on regional ecological OM chemistry (Negassa, Acksel, Eckhardt, Regier, & Leinweber, 2019). Vulnerable peatlands could therefore be targeted for restoration with these criteria in mind. In order to create restoration programs where peatland ecosystems with the highest C loss potential are selected (as well as to assess

the effectiveness of these programs), analysis methods able to detect chemical differences in OM are needed to assess decomposition status changes in natural, degraded, and transitioning rewetted peat.

Pyrolysis coupled with gas chromatography tandem mass spectrometry (Py-GC/MS) is particularly useful for the disentanglement of complex chemical changes occurring in peatland OM (Klein, Gross-Schmölders, Alewell, & Leifeld, 2021; Schellekens, Bradley, et al., 2015; Zeh et al., 2020). Thermal degradation breaks the bonds of large organic macromolecules into smaller, more easily analyzed fragments, thus permitting subsequent chemical characterization of complex organic matter otherwise not easily analyzable without time-consuming chemical pre-treatment techniques (White, Garland, Beyer, & Yoshikawa, 2004). Chemical classes (phenols, polysaccharides, N compounds, lipids, etc.) demonstrate a summarized response in OM to hyrological changes, and for a more targeted investigation of chemical differences, individual biomarkers specific to vegetation can also be traced. For example, lignin syringyl-guaiacyl (S/G) ratios estimate vascular plant source, as angiosperms generally demonstrate higher S/G ratios and gymnosperms demonstrate lower ratios (Hedges & Mann, 1979). The biomarker *p*-isopropenylphenol is highly specific to *Sphagnum* moss, and provides a rapid indicator for peat hydrological conditions (McClymont et al., 2011; Stankiewicz, Hutchins, Thomson, Briggs, & Evershed, 1997; Van der Heijden, Boon, Rasmussen, & Rudolph, 1997). Further, levoglucosan is an abundant pyrolysis product in peat, and can provide an estimate for the increase in relative abundance of more stable OM left behind after more labile compounds have been consumed via aerobic decomposition (Schellekens, Bindler, et al., 2015). In the case of such complex OM matrices, multi-proxy analyses are useful in preventing over-interpretation of findings (Biester, Knorr, Schellekens, Basler, & Hermanns, 2014). As a complementary method, elemental composition can be used to determine C/N and H:C/O:C (van Krevelen) ratios (Preston & Schmidt, 2006), which provide a general indicator for the amount and composition of OM and can be compared with chemical characterizations obtained via Py-GC/MS.

Differences in OM composition have been previously demonstrated in natural and drained peatlands (Klein et al., 2021)*;* however, a similar high-resolution chemical composition comparison has not yet been conducted for natural and rewetted sites from the same ecosystem. This study aimed to use Py-GC/MS techniques to identify early chemical indicators of rewetting by comparing undrained "natural" and rewetted peat that experienced at least 80 years of

previous drainage from the same boreal ecosystem. Findings from Py-GC/MS are also compared with elemental composition measurements (C/N, Van Krevelen analysis) conducted on the same samples.

5.2 Materials and Methods

5.2.1 Site description and sampling

Degerö Stormyr (64°11'N, 19°33'E) is an acidic mire with minerogenic conditions (poor fen) located in northern Sweden in the Kulbäcksliden Experimental Forest. The deepest layers of peat (generally between 3-4 m, but as deep as 8 m in places) correspond to an age of roughly 8000 years (Nilsson et al., 2008). Drainage ditches were installed at Degerö in the beginning of the 20th century (Malmström, 1923), with continued drainage conditions for at least 80 years afterwards. The ditches at the sampling site were allowed to refill naturally starting as early as the late 1970s.

The natural (NM) site was characterized by established *Sphagnum cuspidata* in the carpet horizon, with occurrences of cloudberry (*Rubus chamaemorus*), bog rosemary (*Andromeda polifolia*), and cranberry (*Vaccinium oxycoccos*), and wet flark areas containing peat moss carpets with *Sphagnum majus* and bladder rush (*Scheuchzeria palustris*). Due to the surface wetness at the rewetted site (DC), cores were collected in the transition area near the edge of the former drainage channel to access solid peat. At the time of the June 2017 sampling event, the former drainage channel ditches were well-established with young *Sphagnum riparium*, a strong indicator for wet minerotrophic conditions. To the southwest of the drainage channel, *Ledum palustre, Empetrum nigrum, Betula nana, and Vaccinium spp.* were present. Tree encroachment was also present southwest of the trench; however, high mortality was observed, likely due to the high water table (WT). While both sites were water-saturated during sampling in 2017, previous WT measurements in the rewetted site collected during the drainage period were between 10-15 cm below ground surface (bgs) (Groß-Schmölders et al., 2020; Nilsson et al., 2008).

Three peat cores each were collected in 50 cm sections to one meter depth from the NM and DC sites, for a total of six cores, using a Russian peat corer (Eijkelkamp, Netherlands). The cores were stored at 2°C prior to processing, cut into 2 cm sections, oven dried at 40°C for 72 hours, then homogenized in a mixer mill (Retsch MM 400) for three minutes at 25 Hz. Cores

were analyzed to a mixed 2-4 cm resolution to 52 cm, with a total of 82 samples measured across the six cores. Samples were denoted by site source (NM or DC), core number (1-3), and profile depth in cm (for example, NM1 0-2).

5.2.2 Py-GC/MS

Py–GC/MS was performed using a double shot pyrolyzer (Frontier Laboratories, model 2020i) operating in single shot mode, in tandem with an Agilent 7890 Series gas chromatograph (GC) coupled with an Agilent 5977B series mass selective detector (MS). Py-GC/MS equipment, instrument settings, and chromatographic analysis were conducted according to the methodology previously described in (Klein et al., 2021). Samples (approximately 1 ml) were flushed with Helium (He) for one minute directly before pyrolysis, then introduced to the pre-heated (600 °C) pyrolyzer micro-furnace. Pyrolysis products were swept from the pyrolyzer unit in inert He to the GC, which was equipped with a 30 m column (5xi-5sil, equivalent to HP-5ms) X 240 µm, 0.25 µm film thickness. The pyrolyzer-GC interface was maintained at 320 °C. He was used as the GC carrier gas at a controlled flow of 1 ml min^{-1}. The GC oven was held at 40 °C for 1 min and 50 °C for 1 min at the beginning of every run (with a ramped increase of 3 °C min^{-1} between hold times). The oven temperature was then increased to 165 °C at 3 °C min^{-1}, followed by a second increase from 165 °C to 310 °C at 5 °C min^{-1}, and stabilized afterwards at 310 °C for 10 min. The inlet was set to 280 °C in split mode (100:1). Mass spectra were acquired at 70 eV ionizing energy in the 50-600 mass to charge ratio (*m/z*) range, and compared with published data reported in the NIST 2014 digital library – as well as to available literature.

Pyrolysis product identification and quantification were done using Agilent ChemStation software. 105 pyrolysis products spanning seven different compound classes (benzenes, polyaromatic hydrocarbons (PAHs), phenols, polysaccharides, lignin, N-containing compounds, and lipids) were quantified in each sample as representative of vegetation and degradative processes, and assigned per their relative abundance by the peak area of characteristic ion fragments. Integrations were checked manually to ensure correct assignment in the event of slight retention time shifts. The sum of all integrated chromatographic peak areas was set to 100 percent, and individual pyrolysis product abundances were determined in relative proportion to the total quantified peak area (relative percent abundance).

5.2.3 Elemental analysis

Elemental analysis was conducted on all samples. Bulk C, H and N analysis was conducted by dry combustion using a EuroEA3000 Elemental Analyzer, and for organic O by pyrolysis at 1000 °C followed by GC-TCD quantification (Hekatech, Germany).

5.2.4 Statistics

Principal component analysis (PCA) was applied to the 105 quantified pyrolysis products to separate the influences of differing environmental factors. Principal components (PCs) were identified using the largest explained variance of all pyrolysis products on each PC. Pyrolysis product loadings were used to interpret the processes reflected by individual PCs; whereas scores reflect the relative effect of each PC in the samples, and were used to evaluate the influence of each PC with depth, by site, and in individual cores.

Correlations between PCA scores and C/N ratios were determined by regression analysis (Pearson). Differences in mean relative abundance of selected pyrolysis products between NM and DC sites were tested by independent t-test. For the t-tests, mean relative abundance for depths NM 0-2 and NM 12-14 were calculated using the mean relative abundance from only two cores (NM2 and 3 and NM 1 and 2, respectively), due to insufficient sample material. Statistical analyses and related plots were done using Python (version 3.8.2). Significance for all statistical tests was set at $p<0.05$.

5.3 Results

5.3.1 Abundance of summed compound classes and targeted biomarkers

A complete list of pyrolysis products investigated and the loadings used to identify the processes (PCs) is provided in **Supplementary Table 1**. Depth profiles of the summed relative abundance (%) of the seven investigated chemical classes are provided in **Figure 1(a-g)**. Across all samples, the relative contribution of each primary chemical class to all summed pyrolysis products was: benzenes 1.33%, lignin 1.13%, PAHs 0.10%, phenols 11.20%, polysaccharides 84.86%, N compounds 0.49%, and lipids 0.90%. Levoglucosan was a highly dominant polysaccharide pyrolysis product, and contributed an average of 38.02% of the average summed

polysaccharide abundance. Depth profiles for targeted S/G ratios, *p*-isopropenylphenol, and levoglucosan (%) are shown in **Figure 2(a-c)**.

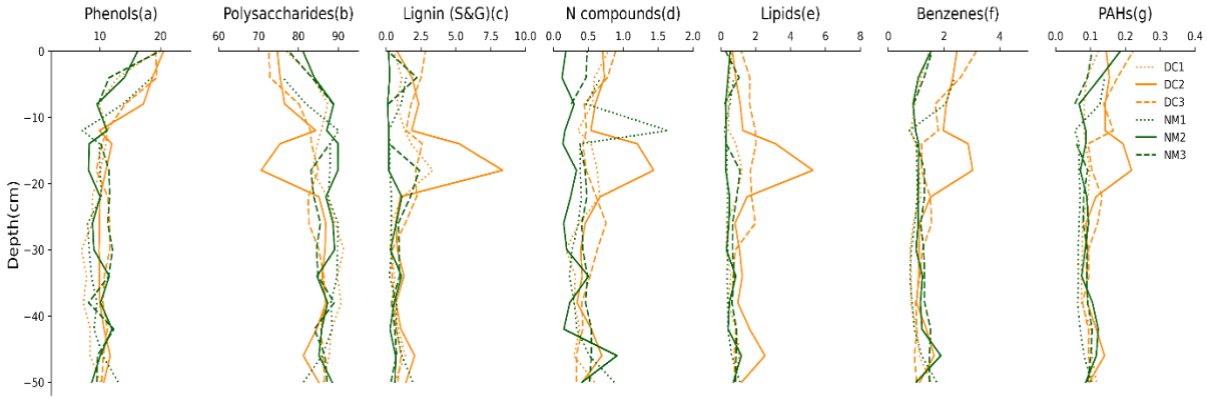

Figure 1(a-g). Relative abundance (%) of summed pyrolysis products by compound class, quantified by Py-GC/MS. DC cores are depicted in orange, NM cores are depicted in green.

The relative abundance of summed phenols, polysaccharides, lipids, benzenes, and PAHs were not significantly different between NM and DC through the depth of the profile; however, the abundance of all chemical classes investigated (with the exception of the polysaccharides) trended higher in DC surface samples (0-12 cm). Summed lignin (syringyl and guaiacyl-derived pyrolysis products) demonstrated significantly higher abundance in DC from 12-16 cm (***p*<0.05**); whereas N compounds demonstrated significantly higher abundance in DC in surface samples (0-2 cm) and at 22-24 cm (***p*<0.05)**. Phenols demonstrated higher abundance in both sites (with DC trending higher than NM) from the surface to 12 cm, and remained relatively stable with depth thereafter through the remainder of the profile; whereas summed polysaccharides demonstrated lower abundance (with NM trending higher than DC) to the same depth, before stabilizing in abundance at approximately 12 cm (with the exception of the DC2 core, which demonstrated a sharp decrease in relative polysaccharide abundance between 12-22 cm). Summed lignin, N compounds, lipids, benzenes, and PAHs all maintained relatively stable abundance in the deeper peat samples (>12 cm), again with the exception of DC2, which displayed a sharp increase in abundance between 12-22 cm.

With the exception of 46-52 cm (NM>DC, ***p*<0.05**), *p*-isopropenylphenol was not significantly different between NM and DC; however, abundances trended slightly higher in DC surface samples (0-6 cm). S/G lignin ratios were not significantly different in NM and DC surface samples (0-10 cm). Below 12 cm, S/G ratios were more strongly separated according to site, and with the exception of 34-36 cm, were significantly lower in DC from 12-40 cm (***p*<0.05**). It was noted that the S/G ratio was poorly correlated to summed lignin abundance. Levoglucosan abundance did not demonstrate significant differences between sites at the surface (but trended lower in DC in surface samples (0-6 cm)), but was signifantly lower in DC at 14-16 cm (***p*<0.05).**

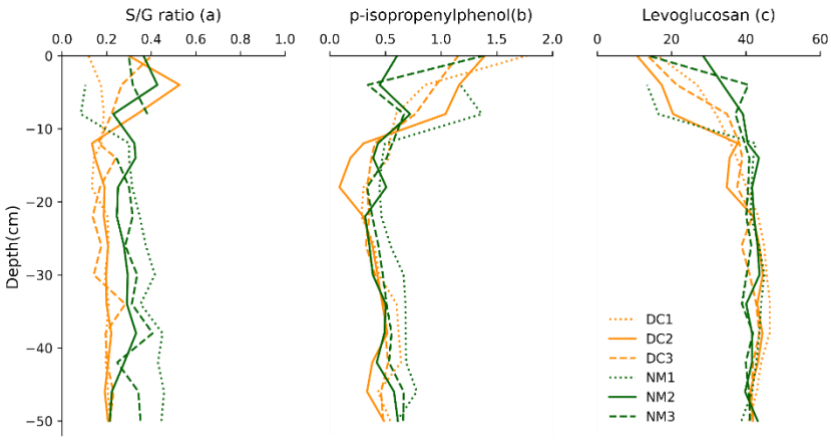

Figure 2(a-c). Relative abundance (%) of targeted molecular biomarkers in NM and DC for S/G ratio (a), *p*-isopropenylphenol (b), levoglucosan (c).

5.3.2 PCA of quantified pyrolysis products

Principal components (PC) 1 to 4 explained 77.8% of the variance in all pyrolysis products. PCA score projections with depth for PC1-4 are provided in **Figure 3**. PCA biplots depicting scores distinguished by site and loading vectors are given in **Figure 4(a-d)**.

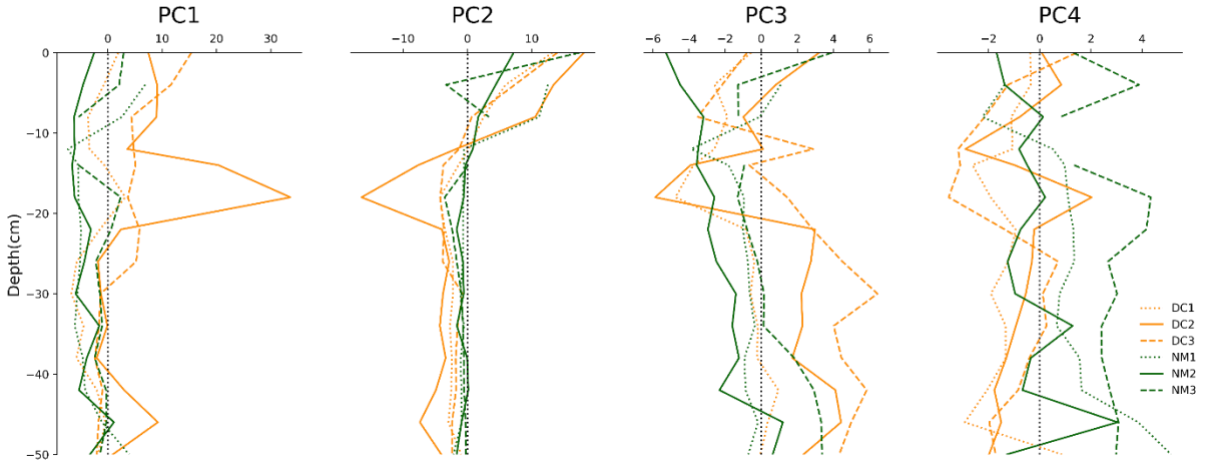

Figure 3. Processes driving chemical differences in Degerö Stormyr peat reflected by PCA score projections with depth.

PC1 scores (38.8% explained variance) were not significantly different between sites through the depth of the profile. Core DC2 demonstrated substantially higher positive scores from 8-20 cm depth than the other five cores. Below 20 cm, PC1 scores generally remained near zero through the remainder of the depth profile, with DC scores trending slightly more positive than NM scores. PC2 scores (28.5% explained variance) were generally characterized by positive scores in surface samples that decreased rapidly with depth - transitioning to low negative scores from approximately 8-10 cm through the remainder of the profile. PC2 scores were not significantly different between NM and DC in surface samples (though DC trended slightly higher). Below 8 cm, DC displayed more negative scores than NM, and was significantly lower between 26-28 cm and 38-40 cm, (***p*<0.05**). PC3 scores (7.0% explained variance) were not significantly different between NM and DC through the depth of the profile. PC3 scores demonstrated an increasing trend from negative scores in surface samples to positive scores with depth in all cores. PC4 scores (3.5% explained variance) were significantly lower in DC compared to NM at 14-16 cm (***p*<0.05**), 34-36 cm (***p*<0.05),** and 46-48 cm (***p*<0.001**).

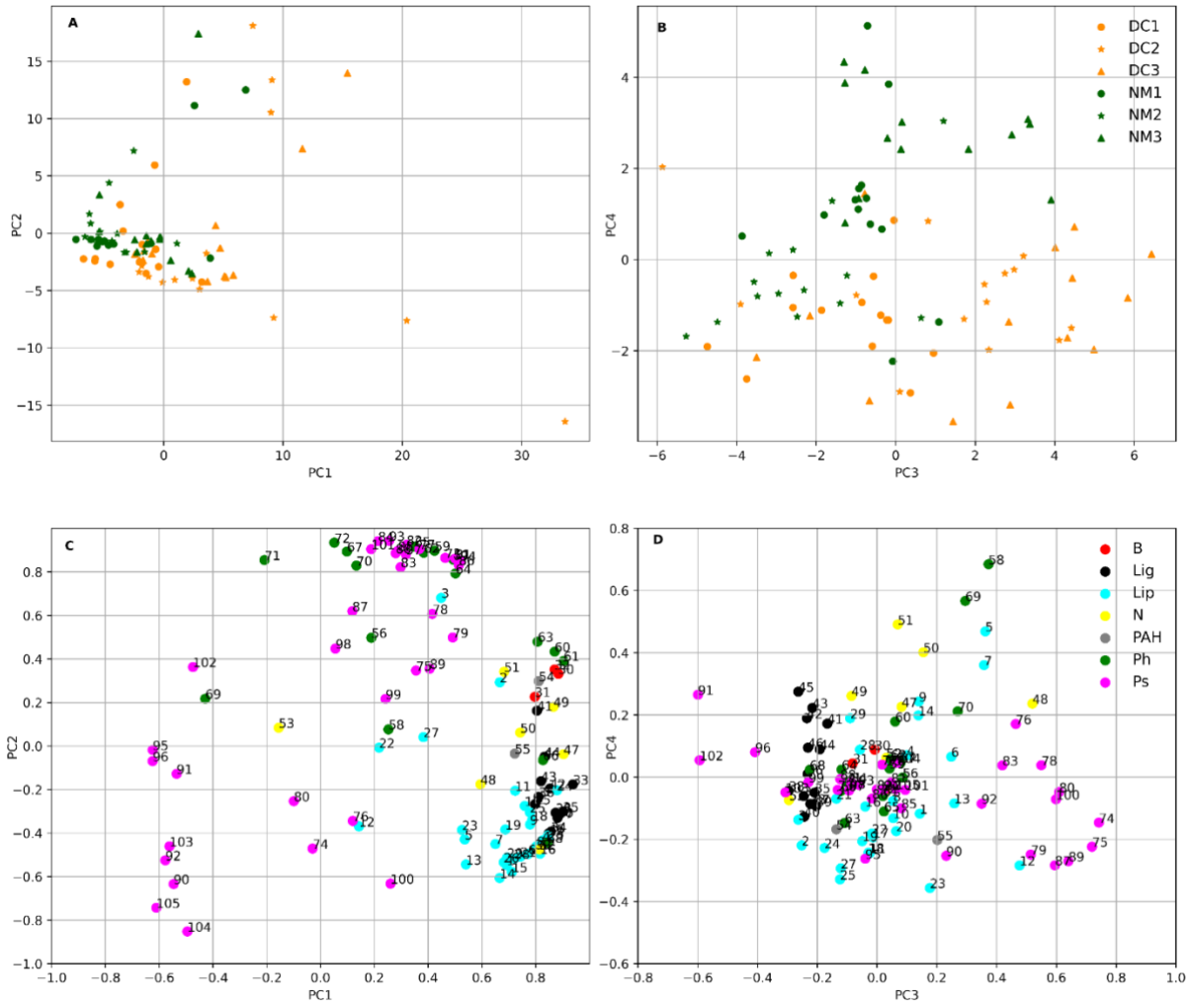

Figure 4. PCA scores (a,b) and loadings (c,d) for PC1-PC2 (left), and PC3-PC4 (right).

Throughout the depth of the profile, PC4 scores trended positive for NM (with the exception of NM2, which demonstrated intermittent negative scores), and negative for DC (with the exception of DC2, which demonstrated positive scores between 14-22 cm).

PC1 loadings were characterized by positive loadings of both guaiacyl and syringyl-derived lignin, benzenes and PAHs, catechols and xylenol phenols (60, 61, 63, 66), N compounds (except 53), and lipids. Pyrolysis products with high negative loadings on PC1 included a number of polysaccharide pyrolysis products (90-92, 95-96, 102-105). PC2 was characterized by positive loadings of phenols (57, 59, 62, 64, 65, 67, 70-72) including the *Sphagnum* biomarker *p*-isopropenylphenol (67), polysaccharides (73, 77, 78, 81-88, 93, 94, 97, 101), and the C-16 fatty acid (3). Pyrolysis products with negative loadings on PC2 included the polysaccharides with negative loadings on PC1 (except 102) - with particularly high negative loadings for levoglucosan (104), 1,6-anhydro-d-galactofuranose (105), and acetobutyrolactone (90). Lignin and lipid pyrolysis products with high loadings on PC1 generally had negative loadings on PC2. Benzenes, phenols, and N compounds with negative loadings on PC1 had positive loadings on PC2. PC3 positive loadings were characterized by primarily by polysaccharide pyrolysis products (74, 75, 78-80, 87, 89, 100) and the N compound 3-hydroxypyridine monoacetate (48). PC3 negative loadings were characterized by the polysaccharides 4-hydroxy-5,6-dihydro-(2*H*)-pyran-2-one (91), levogalactosan (102), and furaneol (96). All lignin pyrolysis products also demonstrated low negative loadings on PC3. Pyrolysis products with the highest positive loadings on PC4 included the phenols *p*-cresol (58), and 4-hydroxy-benzaldehyde (69); with syringyl-derived lignin, indoles (50-51), and C-23 and 25 *n*-alkanes (5, 7) also demonstrating positive loadings. Pyrolysis products with negative loadings on PC4 included guaiacyl-derived lignin, and sterols (except 28-29).

5.3.3 Complementary analyses (C/N ratios and van Krevelen plot)

Percent C, H, N, and O measured by elemental analysis for the bulk peat samples is given in **Supplementary Table 2**. The C/N depth profile and van Krevelen plot for Degerö are shown in **Figure 5** and **6**, respectively. Average C/N trended higher in NM than DC in the upper 12 cm of the profile, and was significantly higher at 8-10 cm (***p*<0.05**). Higher C/N ratios were generally observed in surface samples (0-10 cm) compared to deeper peat. A decrease in C/N was observed in DC2 between 12-22 cm; whereas an increase was present in DC1 from 12-18 cm.

C/N ratios were correlated with PC scores by depth. Significant negative correlations were observed between peat C/N and PC1 and PC4 (R=-0.47 and R=-0.46, respectively, ***p*<0.001**), and a significant positive correlation was observed between C/N and PC2 (R=0.30, ***p*<0.05**).

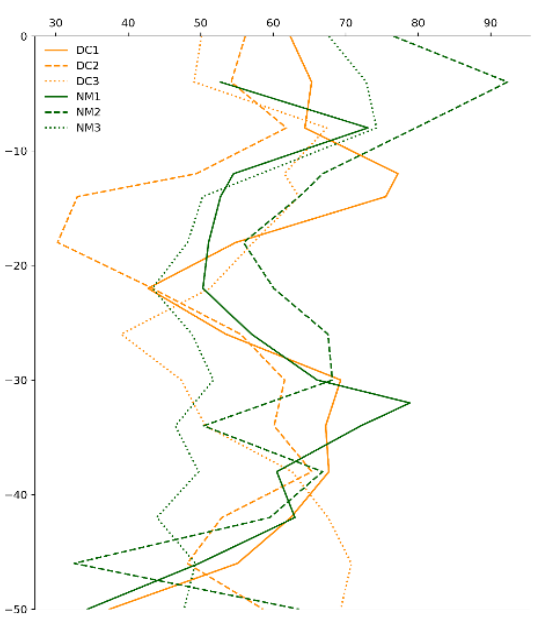

Figure 5. C/N ratios in NM and DC.

Van Krevelen plots calculated using the atomic ratios for H:C vs O:C for all samples demonstrated an increasing trend in H:C/O:C from the deepest peat to the surface samples (**Figure 6**). Surface samples from both sites demonstrated the highest H:C/O:C, with the highest ratios observed in DC2 0-2 (H:C=1.78; O:C=0.78). NM maintained consistently higher H:C/O:C compared to DC in mid-depth peat (approximately 10-40 cm); however these samples also demonstrated higher variability. In the deepest samples, NM and DC demonstrated relatively similar H:C/O:C ratios on the lower end of the van Krevelen plot range. DC2 samples (14-16 and 18-20 cm) demonstrated the lowest observed H:C/O:C ratios (H:C=1.55, O:C=0.59, and H:C=1.58, O:C=0.55, respectively).

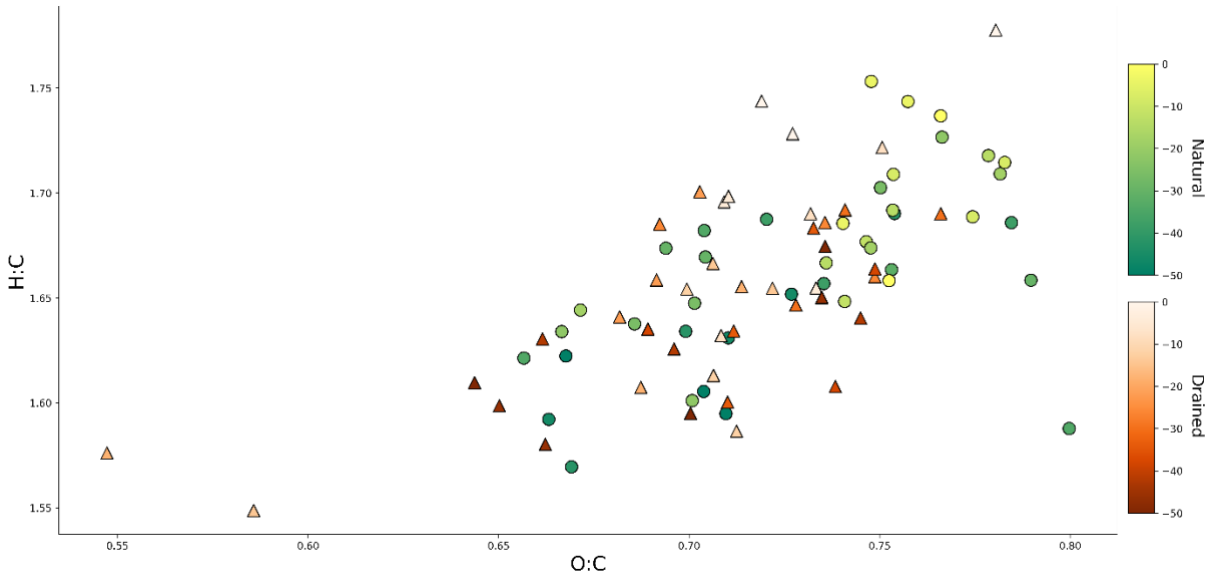

Figure 6. Van Krevelen plots of atomic H:C and O:C ratios determined by elemental analysis for NM (green color-mapped circles) and DC (red color-mapped triangles) at Degerö. Lighter colors indicate peat samples closer to the surface, whereas darker colors indicate deeper peat.

5.4 Discussion

5.4.1 Interpretation of environmental processes occurring at Degerö

The high positive loadings on PC1 for both guaiacyl- and syringyl-derived lignin and the negative loadings of polysaccharide products associated with (degraded) *Sphagnum* (Klein et al., 2021), suggest that PC1 reflects vascular plant influence on *Sphagnum* peat. Moreover, the sharp increase observed in DC2 scores between 8-22 cm is also demonstrated in the summed compound classes (except for the phenols; (**Figure 1**)), the *Sphagnum* biomarker *p*-isopropenylphenol (**Figure 2b**), and decreased C/N ratios (**Figure 5**) at the same peat depth - suggesting that the DC2 sample area was previously strongly impacted by vascular plant growth.

In PC2, the positive loadings of the *Sphagnum* biomarker, as well as other phenols and polysaccharides are associated with fresh *Sphagnum*; whereas the high negative loadings of levoglucosan and 1,6-anhydro-β-D-glucofuranose are associated with progressive accumulation of high molecular weight polysaccharides in degrading peat OM after preferential decomposition of *Sphagnum* phenols and polysaccharides (Klein et al., 2021, Schellekens, Bindler, et al., 2015). The lower scores (particularly in DC) are consistent with the more rapid initial decomposability of these *Sphagnum* phenols and polysaccharides in aerobic conditions, leaving the remaining OM in the consistently water-saturated deep catotelm with relatively stable abundance of these compounds (Schellekens, Bindler, et al., 2015). Therefore, PC2 primarily reflects aerobic degradation of *Sphagnum* peat. The lower scores in the deeper DC horizons (**Figure 3 & Figure 4a**) suggest that the effects of drainage were evident over the entire analyzed core depth, and also indicate relatively homogenous degradation of *Sphagnum* peat. Further, the comparatively minor variation in scores in deeper NM core samples suggest that "natural" variation in the water table (i.e., the loss of aforementioned PC2 phenols and polysaccharides due to aerobic decomposition) was likely relatively low. The strong separation in PC2 scores in the surface vs deeper peat clearly demarcate the depth to which the "new" *Sphagnum* influence extends (0-12 cm), suggesting that *Sphagnum*-derived phenols are an early indicator for OM chemical changes associated with recent peatland rewetting. In the DC2 core, the sharp decrease in PC2 scores combined with the increase in PC1 scores between approximately 12-22 cm (and at 46 cm) suggests that this core sample site previously experienced stronger drainage conditions than the other two DC sites.

For PC3, the positive loadings of polysaccharides (such as (2H)-furan-3-one, 2-furaldehyde, isomaltol, 4-cyclopentene-1,3-dione, 1,4:3,6-dianhydro-α-d-glucopyranose, 5-methyl-2-furaldehyde, and 2-propylfuran), combined with the increasingly positive trend in PC3 scores with depth are consistent with the relative accumulation of decomposition-resistant *Sphagnum*-derived "sphagnan" polysaccharides in anaerobic conditions (Hájek, Ballance, Limpens, Zijlstra, & Verhoeven, 2011; Painter, 1991), and suggest that PC3 mainly reflects anaerobic degradation processes. The negative loadings of 4-hydroxy-5,6-dihydro-(2*H*)-pyran-2-one and levogalactosan are in agreement with the findings from a previous study demonstrating microbial palatability of these compounds under anaerobic conditions (Klein et al., 2021).

The positive loadings on PC4 for *p*-cresol and 4-hydroxy-benzaldehyde along with indoles, and the C-23, 25, and 27 *n*-alkanes do not allow for a straightforward interpretation of PC4. However, PC4 strongly separates NM and DC consistently across the depth of the profiles across the four investigated PCs (**Figure 4b**). The separation of sites suggests a relationship between PC4 and drainage, and also supports observations from PC2 that drainage affected the entire profile depth, whereas rewetting primarily affected the surface layer. However, the strong correlations of PC1 and PC4 in the deeper peat in NM (14-50 cm), combined with the absence of a correlation in DC may also suggest that PC4 reflects an environmental process occurring in the peat prior to drainage (likely in NM). PC4 may therefore reflect "historical" conditions (>12 cm) that previously differentiated the two sample sites prior to the drainage activities.

5.4.2 Comparison with elemental analysis

C/N ratios can be considered a general indicator for decomposition, as lower C/N ratios reflect greater microbial transformation of OM (Leifeld, Klein, & Wüst-Galley, 2020). The lower C/N ratio in DC in the surface peat (0-10 cm) indicates that the newly formed OM may not yet have had sufficient time to respond to the effects of the rewetting, despite the renewed growth of *Sphagnum* on the DC site. However, it was also noted that the H:C/O:C ratios were generally similar in surface samples, with DC2 0-2 demonstrating one of the highest ratios of all samples (H:C=1.78; O:C=0.78). This indicates a strong increase in functional groups in the rewetted DC surface samples, in agreement with the findings of (Negassa et al., 2019), who observed stronger preservation in carboxyl functional groups in rewetted samples compared to drained, and suggested that newly rewetted peat OM may benefit not only from enriched input of vegetation at the surface, but also from a degree of protection provided to "original" carbohydrate and phenol content in the subsurface.

5.4.3 Chemical differences in compound classes after rewetting

Summed chemical classes provide a semi-quantitative measure for comparison of chemical differences between NM and DC, and clearly identify depth differences where the largest changes occur. The phenol relative abundance in DC surface samples was considered similar to that observed in NM, suggesting that the rewetted peat has recently become more similar (in terms of *Sphagnum*-influenced phenol chemistry) to the undrained "natural" conditions of NM. While *Sphagnum* phenols are vulnerable to decomposition in aerobic conditions (Schellekens, Bindler, et al., 2015), they are relatively resistant to decomposition in water-saturated (anaerobic) conditions (Christopher Freeman, Ostle, Fenner, & Kang, 2004; Chris Freeman, Ostle, & Kang, 2001). Therefore, an increase in *Sphagnum*-derived phenols in boreal surface peat may signal a transition to enhanced OM recovery in peatland ecosystems.

While phenol abundance accumulated rapidly in the rewetted peat surface samples in agreement with the changing hydrological conditions, not all chemical classes appeared to have responded to the rewetting in the same time-frame. The consistently higher abundance of summed lignin, N compounds, benzenes, lipids, and PAHs in DC surface samples was consistent with the lower C/N ratios observed to the same depth, and may indicate that the OM has had insufficient time to chemically respond to the rewetting (beyond the contribution from *Sphagnum* phenols) - despite the change in observed vegetation and hydrological conditions. In the deeper peat, it is likely that compounds associated with previous vascular plant-derived material (i.e., higher lignin, N compounds, benzenes, lipids) will remain as a permanent "fingerprint" of the historical drained conditions - as substantial decomposition of lignin generally necessitates aerobic conditions (Feng, Simpson, Wilson, Williams, & Simpson, 2008; Zhang et al., 2019). However, the increased abundance in these same compound classes in the surface peat (where *Sphagnum* is currently abundant) may reflect residual impacts on the more recently deposited rewetted OM originating from "older" peat below, suggesting that some chemical characteristics of "newer" OM may be slower to respond to changed hydrological conditions.

5.5 Conclusions

This analysis demonstrated that peatland rewetting activities result in rapid initial changes in OM chemical composition in surface peat, even after more than 80 years of previous drainage. The primary influences on the *Sphagnum*-dominated peatland chemistry were shifts in

vegetation, aerobic, and anaerobic decomposition processes. Differences were preserved between the natural and formerly drained conditions in the historical peat. Results (OM analyzed by chemical class, elemental analysis, and PCA scores) demonstrated shifts in OM composition occurring to the same depth, suggesting that the rewetting influence extended from the surface through approximately the first 12 cm of the peat; whereas deeper samples showed evidence of the previous drainage. Summed phenols (and more specifically, the *Sphagnum* biomarker *p*-isopropenylphenol) served as early indicators for changes in OM composition following rewetting. N compounds, lignin, benzenes, lipids, and PAHs responded more slowly to the rewetting.

Our results indicate that while the chemical composition of previously drained peat undergoes a rapid initial response to rewetting, and that these changes are likely to have a positive impact on the overall stability of both newly formed and historically drained and degraded peat, some OM could potentially demonstrate longer-term impacts. Recent findings have suggested that some micro-organisms may exhibit the capacity for adaptation to changing hydrology, and that historical environmental conditions could continue to alter rates of microbial transformation, even if current conditions change (Lehmann et al., 2020). As peatland C stability is largely determined by the availability of its OM to microbial transformation, determining the nature and rate of response of rewetted peat OM chemistry is an area requiring further research.

Acknowledgements

Mats Nilsson provided access to Degerö Stormyr for core sampling. Robin Giger conducted elemental analysis for all peat samples. Markus Jocher assisted with maintenance of the Py-GC/MS instrument. Their assistance with this work is invaluable and is greatly appreciated. This study was funded by the Swiss National Science Foundation, project number 200021_169556.

References

Andersen, R., Farrell, C., Graf, M., Muller, F., Calvar, E., Frankard, P., . . . Anderson, P. (2017). An overview of the progress and challenges of peatland restoration in Western Europe. *Restoration Ecology, 25*(2), 271-282.

Biester, H., Knorr, K.-H., Schellekens, J., Basler, A., & Hermanns, Y.-M. (2014). Comparison of different methods to determine the degree of peat decomposition in peat bogs. *Biogeosciences, 11*(10), 2691-2707.

Clymo, R. (1984). The limits to peat bog growth. *Philosophical Transactions of the Royal Society of London. B, Biological Sciences, 303*(1117), 605-654.

Emsens, W.-J., van Diggelen, R., Aggenbach, C. J., Cajthaml, T., Frouz, J., Klimkowska, A., . . . Seeber, E. (2020). Recovery of fen peatland microbiomes and predicted functional profiles after rewetting. *The ISME journal, 14*(7), 1701-1712.

Feng, X., Simpson, A. J., Wilson, K. P., Williams, D. D., & Simpson, M. J. (2008). Increased cuticular carbon sequestration and lignin oxidation in response to soil warming. *Nature Geoscience, 1*(12), 836.

Freeman, C., Ostle, N., Fenner, N., & Kang, H. (2004). A regulatory role for phenol oxidase during decomposition in peatlands. *Soil Biology and Biochemistry, 36*(10), 1663-1667.

Freeman, C., Ostle, N., & Kang, H. (2001). An enzymic'latch'on a global carbon store. *Nature, 409*(6817), 149.

Groß-Schmölders, M., Sengbusch, P. v., Krüger, J. P., Klein, K., Birkholz, A., Leifeld, J., & Alewell, C. (2020). Switch of fungal to bacterial degradation in natural, drained and rewetted oligotrophic peatlands reflected in δ 15 N and fatty acid composition. *SOIL, 6*(2), 299-313.

Hájek, T., Ballance, S., Limpens, J., Zijlstra, M., & Verhoeven, J. T. A. (2011). Cell-wall polysaccharides play an important role in decay resistance of Sphagnum and actively depressed decomposition in vitro. *Biogeochemistry, 103*(1), 45-57. doi: 10.1007/s10533-010-9444-3

Hedges, J. I., & Mann, D. C. (1979). The characterization of plant tissues by their lignin oxidation products. *Geochimica et Cosmochimica Acta, 43*(11), 1803-1807.

Humpenöder, F., Karstens, K., Lotze-Campen, H., Leifeld, J., Menichetti, L., Barthelmes, A., & Popp, A. (2020). Peatland protection and restoration are key for climate change mitigation. *Environmental Research Letters*.

Klein, K., Schellekens, J., Groβ-Schmölders, M., von Sengbusch, P., Alewell, C., & Leifeld, J. (2021). Characterizing ecosystem-driven chemical composition differences in natural and drained Finnish bogs using Pyrolysis-GC/MS. *Organic Geochemistry*, 104351.

Klein, K., Gross-Schmölders, M., Alewell, C., & Leifeld, J. (2021). Chapter Three - Heating up a cold case: Applications of analytical pyrolysis GC/MS to assess molecular biomarkers in peat. In D. L. Sparks (Ed.), *Advances in agronomy* (Vol. 165, pp. 115-159): Academic Press.

Lehmann, J., Hansel, C. M., Kaiser, C., Kleber, M., Maher, K., Manzoni, S., . . . Torn, M. S. (2020). Persistence of soil organic carbon caused by functional complexity. *Nature Geoscience, 13*(8), 529-534.

Leifeld J., Klein, K., & Wüst-Galley, C. (2020). Soil organic matter stoichiometry as indicator for peatland degradation. *Scientific Reports, 10*(1), 1-9.

Malmström, C. (1923). Degerö stormyr.

McClymont, E. L., Bingham, E. M., Nott, C. J., Chambers, F. M., Pancost, R. D., & Evershed, R. P. (2011). Pyrolysis GC–MS as a rapid screening tool for determination of peat-forming plant composition in cores from ombrotrophic peat. *Organic Geochemistry, 42*(11), 1420-1435.

Negassa, W., Acksel, A., Eckhardt, K.-U., Regier, T., & Leinweber, P. (2019). Soil organic matter characteristics in drained and rewetted peatlands of northern Germany: Chemical and spectroscopic analyses. *Geoderma, 353*, 468-481.

Nilsson, M., Sagerfors, J., Buffam, I., Laudon, H., Eriksson, T., Grelle, A., . . . Lindroth, A. (2008). Contemporary carbon accumulation in a boreal oligotrophic minerogenic mire–a significant sink after accounting for all C-fluxes. *Global Change Biology, 14*(10), 2317-2332.

Painter, T. J. (1991). Lindow man, tollund man and other peat-bog bodies: the preservative and antimicrobial action of Sphagnan, a reactive glycuronoglycan with tanning and sequestering properties. *Carbohydrate Polymers, 15*(2), 123-142.

Preston, C., & Schmidt, M. (2006). Black (pyrogenic) carbon: a synthesis of current knowledge and uncertainties with special consideration of boreal regions. Biogeoscience, 3, 397-420.

Schellekens, J., Bindler, R., Martínez-Cortizas, A., McClymont, E. L., Abbott, G. D., Biester, H., . . . Buurman, P. (2015). Preferential degradation of polyphenols from Sphagnum – 4-Isopropenylphenol as a proxy for past hydrological conditions in Sphagnum-dominated peat. *Geochimica et Cosmochimica Acta, 150*, 74-89. doi: https://doi.org/10.1016/j.gca.2014.12.003

Schellekens, J., Bradley, J. A., Kuyper, T. W., Fraga, I., Pontevedra-Pombal, X., Vidal-Torrado, P., . . . Buurman, P. (2015). The use of plant-specific pyrolysis products as biomarkers in peat deposits. *Quaternary Science Reviews, 123*, 254-264.

Schimmel, H., Braun, M., Subke, J.-A., Amelung, W., & Bol, R. (2021). Carbon stability in a Scottish lowland raised bog: potential legacy effects of historical land use and implications for global change. *Soil Biology and Biochemistry, 154*, 108124.

Stankiewicz, B. A., Hutchins, J. C., Thomson, R., Briggs, D. E., & Evershed, R. P. (1997). Assessment of bog-body tissue preservation by pyrolysis-gas chromatography/mass spectrometry. *Rapid Communications in Mass Spectrometry, 11*(17), 1884-1890.

Van der Heijden, E., Boon, J., Rasmussen, S., & Rudolph, H. (1997). Sphagnum acid and its decarboxylation product isopropenylphenol as biomarkers for fossilised Sphagnum in peats. *Ancient Biomolecules, 1*(2), 93-107.

White, D. M., Garland, D. S., Beyer, L., & Yoshikawa, K. (2004). Pyrolysis-GC/MS fingerprinting of environmental samples. *Journal of Analytical and Applied Pyrolysis, 71*(1), 107-118.

Wilson, D., Alm, J., Laine, J., Byrne, K. A., Farrell, E. P., & Tuittila, E. S. (2009). Rewetting of cutaway peatlands: are we re-creating hot spots of methane emissions? *Restoration Ecology, 17*(6), 796-806.

Zeh, L., Igel, M. T., Schellekens, J., Limpens, J., Bragazza, L., & Kalbitz, K. (2020). Vascular plants affect properties and decomposition of moss-dominated peat, particularly at elevated temperatures. *Biogeosciences, 17*(19), 4797-4813.

Zhang, Z., Wang, J. J., Lyu, X., Jiang, M., Bhadha, J., & Wright, A. (2019). Impacts of land use change on soil organic matter chemistry in the Everglades, Florida-a characterization with pyrolysis-gas chromatography–mass spectrometry. *Geoderma, 338*, 393-400.

Chapter 5 – Supplementary Data

Supplementary Table 1. **Quantified pyrolysis products with associated PCA code, compound class, retention time (RT, min), and loadings for principal component analysis investigated to 95% explained variance.**

PCA code	Compound	Compound class	Quant ion (*m/z*)	RT	PC1	PC2	PC3	PC4	PC5	PC6	PC7	PC8	PC9	PC10	PC11	PC12	PC13	PC14	PC15	PC16
1	Pristene	Lip	56	46.34	0.69	-0.55	0.14	-0.12	0.04	0.18	-0.17	0.02	-0.05	-0.07	-0.04	-0.01	-0.14	0.04	0.13	-0.02
2	n-C14 fatty acid	Lip	60	47.41	0.67	0.29	-0.25	-0.22	0.07	-0.13	0.00	0.19	-0.09	-0.09	0.42	0.15	0.06	-0.20	-0.05	-0.08
3	n-C16 fatty acid	Lip	60	52.66	0.45	0.68	-0.26	-0.14	-0.13	0.04	0.06	-0.06	-0.06	-0.08	0.34	0.04	-0.05	-0.10	0.06	-0.17
4	n-C23 alkene	Lip	55	59.18	0.83	-0.43	0.10	0.07	-0.20	0.10	-0.17	-0.03	-0.02	-0.07	-0.07	-0.01	0.00	-0.02	0.07	-0.01
5	n-C23 alkane	Lip	57	59.28	0.54	-0.43	0.36	0.47	0.01	0.10	0.11	-0.20	-0.02	0.08	-0.04	0.10	0.08	0.11	-0.02	-0.02
6	n-C25 alkene	Lip	55	62.45	0.77	-0.50	0.25	0.07	-0.12	0.12	-0.11	0.01	-0.05	0.00	-0.03	0.05	0.03	0.02	0.12	0.01
7	n-C25 alkane	Lip	57	62.58	0.65	-0.45	0.36	0.36	-0.05	0.15	0.05	-0.13	0.05	0.04	-0.07	0.06	0.06	0.07	-0.05	-0.05
8	n-C27 alkene	Lip	55	65.49	0.80	-0.46	0.05	-0.08	0.01	0.25	-0.12	0.06	0.04	-0.08	-0.01	-0.01	-0.11	0.02	0.02	-0.05
9	n-C27 alkane	Lip	57	65.55	0.78	-0.36	0.14	0.24	0.08	0.27	0.12	0.03	0.08	0.01	-0.07	-0.03	-0.05	0.04	-0.09	-0.02
10	n-C29 alkane	Lip	57	68.34	0.76	-0.28	0.05	-0.13	0.31	0.31	0.22	0.03	0.00	0.03	-0.16	0.08	-0.06	-0.14	-0.01	-0.01
11	n-C31 alkane	Lip	57	70.94	0.72	-0.21	-0.02	-0.24	0.31	0.24	0.29	0.01	0.01	0.08	-0.22	0.17	0.01	-0.20	-0.02	-0.01
12	n-C21 methylketone	Lip	59	59.35	0.14	-0.37	0.48	-0.28	-0.39	-0.23	0.33	-0.23	0.25	0.15	-0.07	0.13	-0.13	-0.02	-0.03	-0.04
13	n-C23 methylketone	Lip	59	62.69	0.54	-0.54	0.26	-0.08	-0.43	-0.10	0.18	-0.10	0.10	0.04	-0.06	0.10	-0.03	0.01	0.07	-0.09
14	n-C25 methylketone	Lip	59	65.74	0.67	-0.61	0.14	0.20	-0.13	0.17	-0.12	-0.07	-0.02	-0.05	0.00	0.01	0.05	0.05	0.08	-0.05
15	n-C27 methylketone	Lip	59	68.57	0.71	-0.58	0.03	0.04	-0.24	0.15	-0.21	0.02	-0.05	-0.15	-0.07	-0.02	0.01	-0.07	0.04	-0.03
16	n-C29 methylketone	Lip	59	71.21	0.82	-0.50	-0.04	-0.09	-0.10	0.14	-0.15	0.05	-0.05	-0.09	-0.05	0.00	-0.09	-0.05	-0.02	-0.01
17	n-C31 methylketone	Lip	59	73.66	0.85	-0.41	-0.01	-0.19	0.00	0.12	-0.04	0.04	0.01	-0.02	0.03	0.01	-0.18	-0.03	-0.08	0.00
18	n-C33 methylketone	Lip	59	76.18	0.79	-0.34	-0.03	-0.24	-0.25	-0.12	0.02	-0.12	0.11	-0.09	-0.01	0.05	-0.16	-0.07	-0.09	0.03
19	n-C35 methylketone	Lip	59	79.48	0.69	-0.38	-0.05	-0.21	-0.33	-0.13	0.01	-0.17	0.12	-0.09	-0.07	0.07	-0.21	-0.07	-0.13	0.07
20	Stigmasta-3,5-diene	Lip	396	70.80	0.85	-0.43	0.06	-0.17	-0.06	-0.12	0.03	-0.08	0.08	0.12	-0.01	0.04	0.07	0.03	-0.03	0.00
21	α-Tocopherol	Lip	165	71.24	0.74	-0.51	-0.14	-0.07	-0.07	0.06	-0.18	0.12	-0.04	-0.08	-0.02	0.02	0.11	-0.01	0.09	-0.02
22	Stigmasterol	Lip	55	72.83	0.22	-0.01	-0.02	-0.18	0.45	0.40	-0.21	-0.24	0.02	-0.16	0.00	-0.06	-0.59	0.22	-0.03	-0.12
23	β-Sitosterol	Lip	55	73.57	0.53	-0.39	0.18	-0.36	-0.08	-0.28	0.25	-0.24	0.28	0.18	0.09	0.08	-0.03	0.10	-0.09	-0.02
24	Stigmasta-3,5-dien-7-one	Lip	174	74.66	0.88	-0.20	-0.18	-0.23	-0.06	-0.09	0.01	0.07	0.07	0.05	0.19	0.09	0.04	-0.05	-0.12	-0.05
25	γ-Sitostenone	Lip	124	75.00	0.78	-0.30	-0.12	-0.33	0.08	-0.11	0.10	0.08	0.01	0.21	0.10	0.10	0.05	0.08	-0.15	0.03

PCA code	Compound	Compound class	Quant ion (*m/z*)	RT	PC1	PC2	PC3	PC4	PC5	PC6	PC7	PC8	PC9	PC10	PC11	PC12	PC13	PC14	PC15	PC16
26	C30 Pentacyclic Triterpenoid	Lip	204	70.14	0.68	-0.53	0.04	0.05	-0.37	0.01	-0.13	-0.06	-0.04	-0.12	-0.18	0.05	0.06	-0.11	0.04	-0.05
27	α-Amyrin (Urs-12-en-3-ol, (3β)-)	Lip	218	74.60	0.38	0.04	-0.12	-0.29	0.60	0.31	0.31	0.02	-0.01	0.05	-0.29	0.18	0.08	-0.22	0.03	-0.04
28	C30 hopanoid	Lip	191	72.01	0.72	-0.52	-0.06	0.09	-0.34	-0.03	-0.13	-0.05	-0.07	-0.07	-0.16	0.04	0.08	-0.10	-0.03	0.00
29	C30 hopanoid isomer	Lip	191	72.13	0.69	-0.51	-0.09	0.19	-0.34	-0.07	-0.13	-0.06	-0.09	-0.03	-0.14	0.03	0.07	-0.06	-0.04	-0.02
30	Toluene	B	91	4.73	0.88	0.33	-0.01	0.09	0.00	0.14	0.19	0.14	0.00	0.00	0.11	-0.06	0.03	0.05	-0.01	0.04
31	Styrene	B	104	9.16	0.80	0.23	-0.08	0.04	-0.16	0.34	0.17	0.07	-0.05	0.10	0.12	-0.11	0.04	0.22	0.00	0.04
32	Acetophenone	B	105	17.74	0.87	0.35	0.03	-0.04	0.05	0.09	0.11	0.16	0.05	0.03	0.08	-0.05	0.11	-0.02	0.04	0.05
33	Guaiacol	Lig	109	18.81	0.94	-0.18	-0.22	-0.09	0.05	-0.06	-0.08	0.06	0.05	0.02	-0.02	-0.07	0.08	0.03	-0.03	0.04
34	4-Methylguaiacol	Lig	138	23.91	0.86	-0.39	-0.25	-0.06	0.01	-0.06	-0.14	0.01	0.03	0.01	-0.06	-0.05	0.06	0.01	-0.04	0.06
35	4-Ethylguaiacol	Lig	137	27.85	0.90	-0.30	-0.21	-0.05	0.11	-0.12	-0.06	-0.05	0.02	0.00	-0.04	-0.02	0.10	0.05	0.01	0.03
36	4-Vinylguaiacol	Lig	135	29.53	0.81	-0.23	-0.23	0.01	0.20	-0.31	-0.03	-0.19	0.01	0.01	0.04	0.00	0.08	0.16	0.04	-0.05
37	4-Formylguaiacol	Lig	151	33.21	0.88	-0.33	-0.21	-0.09	0.11	-0.09	-0.15	0.03	0.00	0.00	0.04	0.00	0.01	0.06	-0.07	0.01
38	4-(Prop-2-enyl)guaiacol, *trans*	Lig	164	35.42	0.87	-0.31	-0.30	-0.04	0.03	-0.07	-0.13	0.00	0.05	0.02	-0.07	-0.09	0.04	0.02	-0.03	0.07
39	4-Acetylguaiacol	Lig	151	36.81	0.80	-0.47	-0.20	-0.09	-0.11	0.01	-0.22	0.10	-0.05	-0.01	0.03	-0.02	0.01	0.00	-0.09	0.05
40	4-(Propan-1-one)guaiacol	Lig	137	38.49	0.88	-0.33	-0.24	-0.13	0.06	-0.01	-0.12	0.07	0.01	0.03	-0.02	-0.03	0.05	0.01	-0.08	0.05
41	Syringol	Lig	154	31.13	0.80	0.16	-0.17	0.17	0.24	-0.26	0.14	-0.12	0.09	-0.15	0.12	-0.13	0.00	-0.07	0.14	-0.02
42	4-Methylsyringol	Lig	153	35.20	0.85	-0.19	-0.24	0.19	0.18	-0.20	0.06	-0.17	0.06	-0.12	0.00	-0.10	0.01	-0.04	0.07	0.00
43	4-Vinylsyringol	Lig	180	39.95	0.82	-0.16	-0.22	0.22	0.28	-0.21	0.10	-0.19	0.10	-0.10	0.01	-0.10	0.00	-0.04	0.07	-0.03
44	4-Formylsyringol	Lig	181	43.47	0.83	-0.05	-0.19	0.09	0.30	-0.23	0.00	-0.13	0.02	-0.19	0.12	-0.02	-0.07	-0.10	0.05	-0.08
45	4-(Prop-2-enyl)syringol, *trans*	Lig	194	45.11	0.80	-0.27	-0.26	0.27	0.11	-0.24	0.01	-0.20	0.03	-0.13	-0.03	-0.09	0.06	-0.01	0.08	-0.02
46	4-Acetylsyringol	Lig	181	46.05	0.85	-0.40	-0.23	0.09	0.03	-0.10	-0.13	-0.04	-0.01	-0.12	0.06	-0.03	-0.03	-0.03	-0.03	0.00
47	Pyridine	N	79	4.29	0.90	-0.04	0.08	0.23	0.01	0.07	0.02	0.28	0.06	0.09	0.04	0.01	-0.06	0.02	-0.06	-0.07
48	3-Hydroxypyridine monoacetate	N	95	20.34	0.59	-0.18	0.52	0.24	0.16	0.08	-0.09	0.25	0.08	0.19	0.11	0.00	-0.02	-0.02	0.11	-0.23
49	Benzylnitrile	N	117	21.35	0.87	0.18	-0.09	0.26	-0.06	0.19	0.10	0.15	-0.04	0.06	0.22	-0.03	-0.04	0.02	-0.01	0.03

PCA code	Compound	Compound class	Quant ion (*m/z*)	RT	PC1	PC2	PC3	PC4	PC5	PC6	PC7	PC8	PC9	PC10	PC11	PC12	PC13	PC14	PC15	PC16
50	Indole	N	117	28.67	0.74	0.06	0.15	0.40	-0.04	-0.06	0.03	0.35	0.19	0.13	0.01	0.04	-0.12	0.04	-0.05	-0.15
51	C1-indole	N	130	32.73	0.68	0.34	0.07	0.49	-0.05	0.00	0.14	0.24	0.15	0.07	0.05	-0.04	-0.10	0.09	0.00	-0.03
52	Diketodipyrrole	N	186	45.02	0.81	-0.47	0.03	0.06	-0.17	0.11	-0.14	0.08	-0.02	-0.01	-0.03	-0.02	0.07	-0.12	0.00	0.04
53	13-Docosenamide	N	59	66.66	-0.16	0.08	-0.29	-0.07	-0.09	-0.13	-0.21	0.28	0.26	0.08	-0.03	0.43	-0.15	0.08	0.59	0.19
54	Indene	PAH	116	16.55	0.81	0.30	-0.14	-0.17	-0.03	0.29	0.18	-0.06	-0.08	0.01	0.15	-0.07	0.05	-0.04	0.12	0.08
55	C14-polyaromatic hydrocarbon	PAH	178	47.59	0.72	-0.03	0.20	-0.20	-0.26	0.09	0.31	-0.17	0.03	0.09	0.12	-0.13	0.05	0.03	0.14	0.03
56	Phenol	Ph	94	13.74	0.19	0.50	0.09	0.00	-0.10	0.11	0.04	-0.26	-0.48	0.18	-0.07	0.21	0.18	0.09	0.11	-0.36
57	2-Methylphenol (o-cresol)	Ph	107	17.37	0.49	0.86	0.08	0.05	-0.10	-0.01	0.00	-0.02	0.01	-0.02	-0.04	-0.01	-0.02	-0.01	-0.03	0.00
58	4-Methylphenol (p-cresol)	Ph	107	18.51	0.25	0.08	0.37	0.68	-0.09	0.28	0.24	-0.14	0.21	0.01	0.10	-0.01	0.05	-0.12	-0.04	0.16
59	3-Ethylphenol	Ph	107	21.51	0.42	0.90	0.04	0.03	-0.07	-0.05	0.01	0.04	-0.03	-0.05	-0.05	-0.02	-0.03	0.00	0.00	0.00
60	2,4-Dimethylphenol	Ph	107	22.04	0.87	0.43	0.06	0.18	0.02	0.02	0.05	-0.01	0.04	0.03	0.01	-0.02	0.00	-0.01	-0.02	0.04
61	2,5-Dimethylphenol	Ph	107	22.15	0.90	0.39	0.02	-0.06	0.10	0.00	-0.06	0.04	-0.03	0.01	-0.06	-0.02	0.02	0.03	-0.04	0.06
62	4-Ethylphenol	Ph	107	22.94	0.38	0.89	0.05	0.06	-0.03	0.09	0.14	-0.09	0.06	0.00	-0.04	-0.01	0.02	-0.10	-0.02	0.00
63	Catechol	Ph	110	24.75	0.81	0.48	-0.11	-0.15	0.15	-0.03	0.11	0.00	0.01	0.07	0.08	-0.06	-0.01	-0.04	0.11	0.02
64	4-Vinylphenol	Ph	120	25.51	0.50	0.79	-0.12	0.02	0.06	-0.16	0.04	-0.15	0.15	0.06	0.05	-0.02	0.01	-0.04	0.05	-0.05
65	2-Acetylresorcinol	Ph	137	27.76	0.35	0.92	0.02	-0.11	-0.06	-0.06	-0.12	-0.02	0.02	-0.05	-0.06	-0.03	0.03	0.03	0.00	-0.02
66	Methylcatechol	Ph	124	28.98	0.83	-0.06	-0.12	-0.04	0.20	0.05	0.20	0.08	-0.02	0.15	-0.19	-0.12	0.01	0.01	0.12	0.21
67	*p*-Isopropenylphenol	Ph	134	29.36	0.10	0.89	0.07	0.05	-0.03	-0.04	-0.03	0.02	0.25	0.05	-0.20	-0.01	-0.09	-0.04	-0.09	-0.06
68	3-Methoxy-5-methylphenol	Ph	138	30.14	0.84	-0.44	-0.23	0.02	0.07	-0.06	-0.12	-0.05	0.00	-0.01	-0.02	-0.03	0.02	-0.02	-0.03	0.01
69	4-Formylphenol	Ph	121	32.23	-0.43	0.22	0.29	0.57	0.15	-0.26	-0.17	-0.13	0.06	-0.12	0.02	0.25	-0.11	-0.23	-0.03	0.04
70	4-Acetylphenol	Ph	121	35.33	0.13	0.83	0.27	0.21	-0.11	0.03	0.01	0.11	0.01	-0.18	0.02	0.06	-0.02	-0.19	-0.02	0.14
71	4-Hydroxybiphenyl	Ph	170	45.64	-0.21	0.85	-0.10	-0.01	-0.11	0.23	0.02	-0.20	0.14	0.03	-0.06	0.00	-0.06	-0.17	-0.01	0.02
72	C_1-Hydroxybiphenyl	Ph	184	48.84	0.05	0.93	0.01	-0.05	-0.12	0.13	0.04	-0.13	0.11	0.04	-0.05	0.01	-0.02	-0.11	0.02	-0.07
73	Acetic acid	Ps	60	2.55	0.46	0.86	-0.13	-0.04	-0.02	0.02	-0.04	-0.03	0.01	0.01	-0.10	-0.01	0.00	0.05	0.03	-0.04
74	(2H)-furan-3-one	Ps	84	5.64	-0.03	-0.47	0.74	-0.15	0.26	-0.16	-0.16	0.11	0.21	0.08	0.02	-0.03	0.08	0.00	-0.01	-0.03

PCA code	Compound	Compound class	Quant ion (*m/z*)	RT	PC1	PC2	PC3	PC4	PC5	PC6	PC7	PC8	PC9	PC10	PC11	PC12	PC13	PC14	PC15	PC16
75	2-Furaldehyde	Ps	96	6.70	0.36	0.35	0.72	-0.22	0.16	-0.06	-0.04	-0.10	-0.09	-0.22	0.02	-0.04	0.10	0.18	-0.01	0.10
76	4-Cyclopentene-1,3-dione	Ps	96	6.93	0.12	-0.34	0.46	0.17	0.49	-0.22	-0.19	0.01	0.21	-0.01	-0.08	0.16	0.15	0.15	-0.14	-0.03
77	2-Furanmethanol	Ps	98	7.67	0.37	0.91	0.02	0.04	0.00	-0.18	-0.05	0.06	-0.01	-0.06	-0.03	0.02	-0.04	-0.02	0.00	-0.04
78	2-Propylfuran	Ps	81	8.05	0.42	0.61	0.55	0.04	0.05	-0.19	-0.02	0.16	-0.10	-0.14	0.00	0.02	-0.08	0.09	-0.02	-0.01
79	4-Cyclopentene-1,3-dione	Ps	96	8.71	0.49	0.50	0.51	-0.25	-0.12	0.02	-0.21	-0.14	0.12	0.13	-0.01	-0.15	-0.01	0.09	0.10	0.01
80	4-Cyclopentene-1,3-dione	Ps	96	8.88	-0.10	-0.25	0.61	-0.05	0.13	0.13	-0.35	-0.30	-0.05	0.39	0.18	-0.08	-0.04	-0.02	0.00	0.24
81	2-methyl-2-Cyclopenten-1-one	Ps	67	9.74	0.50	0.86	0.05	-0.02	-0.01	0.01	-0.06	0.03	0.00	0.02	-0.05	-0.03	-0.01	0.01	-0.03	0.04
82	2(5H)-Furanone	Ps	55	9.96	0.32	0.92	0.00	-0.04	-0.07	-0.02	-0.15	-0.01	0.07	0.04	-0.07	-0.04	0.03	0.03	0.04	-0.03
83	Acetylfuran	Ps	95	9.98	0.30	0.82	0.42	0.04	-0.08	0.04	-0.13	0.00	-0.08	-0.08	0.07	-0.04	0.01	0.00	0.00	0.07
84	1,2-Cyclopentanedione	Ps	98	10.85	0.21	0.94	-0.09	-0.02	-0.03	-0.03	-0.17	-0.05	0.07	0.12	-0.05	-0.05	-0.04	0.01	-0.02	-0.02
85	5-methyl-2(5H)-furanone	Ps	55	11.26	0.29	0.90	0.08	-0.10	-0.01	0.07	-0.16	-0.02	0.04	0.07	-0.04	-0.06	0.16	0.01	0.07	0.00
86	3-methyl-2,5-furandione	Ps	68	11.56	0.51	0.83	-0.02	-0.07	0.10	-0.03	-0.01	0.02	0.05	-0.03	-0.02	0.00	0.05	-0.01	0.00	0.02
87	5-methyl-2-furaldehyde	Ps	110	12.52	0.12	0.62	0.59	-0.28	0.07	0.01	-0.15	0.10	0.07	-0.20	-0.01	0.00	0.14	-0.11	-0.07	0.05
88	3-methyl-2(5H)-furanone	Ps	69	13.08	0.28	0.89	-0.12	-0.01	-0.09	-0.01	-0.23	-0.08	0.11	0.18	-0.05	-0.01	0.01	0.04	0.01	0.02
89	Isomaltol	Ps	111	13.37	0.41	0.36	0.64	-0.27	-0.13	-0.02	0.09	-0.06	-0.01	-0.17	0.31	0.09	0.01	-0.05	0.03	-0.03
90	3-acetyl-2(3H)-furanone (α-Acetobutyrolactone)	Ps	86	14.29	-0.55	-0.63	0.23	-0.25	0.01	0.04	0.01	0.11	0.20	-0.20	0.01	-0.17	0.04	-0.07	0.08	-0.02
91	4-Hydroxy-5,6-dihydro-(2H)-pyran-2-one	Ps	114	14.56	-0.53	-0.13	-0.60	0.27	-0.02	0.11	-0.02	-0.35	0.20	-0.02	0.14	0.03	0.04	0.10	0.09	-0.03
92	Tetrahydro-3,6-dimethyl-2H-pyran-2-one	Ps	56	14.80	-0.58	-0.52	0.35	-0.09	0.10	0.11	-0.04	-0.04	0.27	-0.21	-0.03	-0.13	0.13	0.01	0.13	-0.10
93	2-hydroxy-3-methyl-2-cyclopenten-1-one	Ps	112	15.85	0.25	0.94	-0.06	-0.02	-0.08	0.03	-0.16	-0.06	0.02	0.04	-0.06	0.00	-0.03	0.01	-0.04	-0.01

PCA code	Compound	Compound class	Quant ion (*m/z*)	RT	PC1	PC2	PC3	PC4	PC5	PC6	PC7	PC8	PC9	PC10	PC11	PC12	PC13	PC14	PC15	PC16
94	2,3-Dimethyl-2-cyclopenten-1-one	Ps	67	16.22	0.52	0.85	0.02	-0.04	-0.01	-0.02	-0.01	0.04	-0.01	0.00	-0.04	-0.04	0.00	0.01	-0.01	0.02
95	Dianhydrorhamnose	Ps	113	16.78	-0.62	-0.02	-0.04	-0.26	-0.01	0.31	-0.13	0.04	0.48	-0.19	-0.02	-0.15	0.26	-0.06	0.04	-0.17
96	2,5-Dimethyl-4-hydroxy-3(2H)-furanone (Furaneol)	Ps	128	18.81	-0.62	-0.07	-0.41	0.08	-0.11	0.47	-0.06	-0.22	0.19	-0.11	0.13	-0.01	0.06	0.01	-0.08	0.09
97	Maltol	Ps	126	20.07	0.32	0.88	-0.09	-0.04	0.01	0.15	-0.19	-0.04	0.05	-0.05	0.05	0.10	-0.06	-0.11	-0.08	0.00
98	2,3-dihydro-3,5-dihydroxy-6-methyl-4H-pyran-4-one (Pyranone)	Ps	144	21.82	0.06	0.45	-0.09	-0.04	-0.21	0.02	0.49	0.19	0.07	-0.45	-0.16	0.03	0.00	0.38	-0.02	-0.01
99	3,5-dihydroxy-2-methyl-4H-pyran-4-one	Ps	142	23.91	0.24	0.22	-0.23	-0.02	0.10	0.33	-0.13	-0.10	0.16	-0.18	0.16	0.55	0.20	0.24	-0.13	0.14
100	1,4:3,6-Dianhydro-α-d-glucopyranose	Ps	69	25.21	0.26	-0.63	0.60	-0.07	0.06	0.17	-0.15	0.05	-0.09	-0.04	0.15	0.06	-0.03	-0.03	0.04	-0.07
101	5-Hydroxymethylfurfural	Ps	97	26.05	0.19	0.90	0.09	-0.04	-0.13	-0.13	0.00	0.07	-0.15	-0.15	-0.15	0.03	-0.04	0.06	-0.08	0.07
102	Levogalactosan	Ps	60	33.96	-0.47	0.36	-0.59	0.05	-0.04	0.12	-0.31	0.02	0.16	0.19	0.00	-0.02	0.03	0.04	-0.12	-0.13
103	Levomannosan	Ps	60	36.75	-0.56	-0.46	-0.31	-0.05	-0.26	-0.03	0.01	0.38	0.28	0.14	0.05	-0.04	-0.02	-0.04	-0.09	-0.06
104	Levoglucosan	Ps	60	36.88	-0.49	-0.85	0.07	0.05	0.04	-0.01	0.10	0.02	-0.04	-0.03	0.04	-0.02	-0.06	-0.06	0.01	0.07
105	1,6-Anhydro-β-D-glucofuranose	Ps	72	43.11	-0.61	-0.74	0.06	-0.04	-0.05	-0.04	0.11	0.05	-0.08	-0.03	0.11	-0.10	-0.05	-0.04	-0.02	0.06

Supplementary Table 2. **Elemental composition for carbon, hydrogen, and nitrogen measured in duplicated replicates (%), oxygen (%), mean±standard deviation abundance and C/N ratios, with corresponding core and depth.**

Core	Depth	(N) %	(C) %	(H) %	(N) %	(C) %	(H) %	(O) %	Mean N	% var. N	Mean C	% var. C	Mean H	% var. H	CN
DC1	0	0.79	49.85	7.17	0.71	43.61	6.29	45.31	0.75	0.06	46.73	4.41	6.73	0.62	62.35
DC1	-4	0.72	46.73	6.58	0.71	46.72	6.63	44.18	0.72	0.00	46.72	0.01	6.60	0.04	65.30
DC1	-8	0.71	46.18	6.54	0.72	46.24	6.48	45.09	0.72	0.01	46.21	0.05	6.51	0.05	64.36
DC1	-12	0.62	47.86	6.70	0.62	47.57	6.46	44.50	0.62	0.00	47.72	0.21	6.58	0.17	77.21
DC1	-14	0.62	46.35	6.32	0.61	46.64	6.50	44.75	0.62	0.01	46.50	0.21	6.41	0.12	75.54
DC1	-18	0.87	47.53	6.31	0.87	47.71	6.45	43.64	0.87	0.00	47.62	0.13	6.38	0.10	54.83
DC1	-22	1.05	45.51	6.26	1.11	46.78	6.37	41.95	1.08	0.05	46.14	0.90	6.31	0.08	42.73
DC1	-26	0.89	46.50	6.46	0.85	46.48	6.60	45.60	0.87	0.02	46.49	0.01	6.53	0.10	53.46
DC1	-30	0.67	46.65	6.57	0.68	46.64	6.58	46.08	0.67	0.01	46.65	0.00	6.58	0.01	69.31
DC1	-34	0.71	47.31	6.22	0.70	47.63	6.45	44.94	0.71	0.00	47.47	0.22	6.33	0.16	67.24
DC1	-38	0.71	47.36	6.46	0.70	48.07	6.55	43.85	0.71	0.01	47.72	0.50	6.50	0.07	67.68
DC1	-42	0.78	48.94	6.66	0.79	49.02	6.65	43.20	0.78	0.01	48.98	0.06	6.66	0.01	62.43
DC1	-46	0.90	49.14	6.32	0.89	49.38	6.65	43.50	0.89	0.01	49.26	0.17	6.49	0.24	55.07
DC1	-50	1.28	48.45	6.63	1.31	48.48	6.37	41.59	1.30	0.02	48.46	0.02	6.50	0.19	37.39
DC2	0	0.77	43.28	6.31	0.78	43.58	6.56	45.19	0.77	0.01	43.43	0.21	6.43	0.18	56.14
DC2	-4	0.81	44.16	5.86	0.82	44.19	6.32	43.19	0.82	0.00	44.17	0.02	6.09	0.32	54.20
DC2	-8	0.68	42.07	5.97	0.68	42.12	6.11	42.14	0.68	0.00	42.10	0.04	6.04	0.10	61.82
DC2	-12	0.93	45.73	6.20	0.92	45.79	6.10	43.10	0.93	0.00	45.76	0.04	6.15	0.07	49.39
DC2	-14	1.49	49.04	6.39	1.48	49.06	6.27	38.31	1.49	0.01	49.05	0.01	6.33	0.08	32.98
DC2	-18	1.63	49.48	6.51	1.64	49.57	6.50	36.14	1.64	0.01	49.53	0.06	6.50	0.01	30.25
DC2	-22	1.03	45.08	6.37	1.05	45.09	6.41	42.24	1.04	0.02	45.08	0.01	6.39	0.03	43.30
DC2	-26	0.86	44.50	6.06	0.75	44.79	6.29	44.57	0.80	0.08	44.64	0.20	6.18	0.16	55.49
DC2	-30	0.79	45.00	6.17	0.67	44.83	6.16	43.60	0.73	0.09	44.92	0.12	6.16	0.00	61.57
DC2	-34	0.71	45.31	6.19	0.80	45.36	6.16	43.02	0.75	0.06	45.33	0.04	6.17	0.02	60.12
DC2	-38	0.68	45.00	6.00	0.65	42.12	5.68	42.89	0.67	0.02	43.56	2.04	5.84	0.23	65.31
DC2	-42	0.93	45.89	6.17	0.81	46.30	6.32	42.78	0.87	0.08	46.10	0.29	6.24	0.11	52.92
DC2	-46	1.06	47.34	6.27	0.91	47.73	6.40	41.21	0.99	0.10	47.54	0.27	6.33	0.09	48.14
DC2	-50	0.77	45.33	5.88	0.78	45.82	6.24	42.56	0.78	0.01	45.58	0.34	6.06	0.25	58.62
DC3	0	0.91	45.32	6.58	0.91	45.83	6.66	43.69	0.91	0.00	45.58	0.36	6.62	0.06	50.11
DC3	-4	0.94	45.86	6.50	0.94	46.30	6.54	43.64	0.94	0.00	46.08	0.31	6.52	0.03	49.07
DC3	-8	0.67	45.06	6.10	0.66	44.58	6.09	42.33	0.67	0.00	44.82	0.33	6.10	0.00	67.40
DC3	-12	0.74	45.86	6.15	0.76	46.33	6.04	43.79	0.75	0.01	46.10	0.33	6.09	0.08	61.54

Core	Depth	(N) %	(C) %	(H) %	(N) %	(C) %	(H) %	(O) %	Mean N	% var. N	Mean C	% var. C	Mean H	% var. H	CN
DC3	-14	0.72	45.81	6.30	0.72	45.94	6.44	43.20	0.72	0.00	45.87	0.09	6.37	0.10	63.54
DC3	-18	0.80	45.52	6.28	0.79	45.72	6.31	43.42	0.80	0.01	45.62	0.14	6.29	0.02	57.24
DC3	-22	0.90	46.45	6.43	0.91	46.33	6.39	42.77	0.91	0.00	46.39	0.08	6.41	0.03	51.26
DC3	-26	1.17	45.99	6.42	1.19	45.76	6.47	42.35	1.18	0.01	45.88	0.16	6.44	0.03	39.03
DC3	-30	0.95	44.15	6.29	0.93	44.55	6.20	45.30	0.94	0.01	44.35	0.28	6.25	0.06	47.31
DC3	-34	0.88	44.99	6.25	0.90	44.98	6.37	43.94	0.89	0.01	44.99	0.01	6.31	0.09	50.66
DC3	-38	0.72	44.64	6.17	0.70	44.63	6.21	44.56	0.71	0.02	44.64	0.01	6.19	0.03	62.60
DC3	-42	0.66	45.00	6.10	0.67	45.09	6.22	44.74	0.67	0.01	45.04	0.06	6.16	0.09	67.58
DC3	-46	0.65	45.45	6.21	0.64	45.30	6.27	44.45	0.64	0.01	45.37	0.11	6.24	0.04	70.78
DC3	-50	0.64	44.77	6.31	0.65	44.84	6.20	43.95	0.65	0.00	44.81	0.05	6.25	0.07	69.31
NM1	-4	0.84	44.42	6.49	**	**	**	44.29	0.84	**	44.42	**	6.49	**	52.70
NM1	-8	0.60	44.41	6.28	0.62	44.58	6.39	44.71	0.61	0.01	44.49	0.12	6.34	0.07	73.06
NM1	-12	0.83	45.48	6.36	**	**	**	45.27	0.83	**	45.48	**	6.36	**	54.53
NM1	-14	0.82	42.99	6.09	0.81	42.96	6.22	44.61	0.82	0.01	42.98	0.02	6.15	0.09	52.73
NM1	-18	0.85	43.06	6.09	0.84	43.12	6.19	44.91	0.84	0.00	43.09	0.04	6.14	0.07	51.08
NM1	-22	0.86	43.09	6.26	0.86	43.13	6.14	44.05	0.86	0.00	43.11	0.03	6.20	0.08	50.30
NM1	-26	0.77	43.59	6.12	0.76	43.58	6.25	43.60	0.76	0.00	43.59	0.01	6.18	0.09	57.01
NM1	-30	0.64	42.58	5.84	0.65	42.63	5.94	44.86	0.65	0.01	42.60	0.03	5.89	0.07	66.05
NM1	-34	0.59	42.27	5.49	0.59	42.29	5.70	45.08	0.59	0.00	42.28	0.01	5.59	0.14	72.09
NM1	-38	0.70	42.62	6.03	0.71	42.67	5.96	44.61	0.71	0.01	42.65	0.04	5.99	0.05	60.49
NM1	-42	0.70	44.20	6.26	0.71	44.62	6.25	44.64	0.71	0.01	44.41	0.30	6.26	0.01	63.00
NM1	-46	0.89	44.66	6.13	0.91	44.64	6.16	43.27	0.90	0.02	44.65	0.01	6.15	0.02	49.78
NM1	-50	1.37	46.70	6.31	1.37	47.16	6.38	41.78	1.37	0.00	46.93	0.33	6.34	0.04	34.36
NM2	0	0.58	44.22	6.04	0.58	44.50	6.22	44.51	0.58	0.00	44.36	0.20	6.13	0.13	76.62
NM2	-4	0.47	43.25	6.28	0.47	43.45	6.31	43.78	0.47	0.00	43.35	0.14	6.30	0.02	92.34
NM2	-8	0.54	42.90	6.01	0.54	43.00	6.07	44.34	0.54	0.01	42.95	0.07	6.04	0.04	79.68
NM2	-12	0.68	45.26	6.29	0.66	44.70	6.06	44.43	0.67	0.02	44.98	0.40	6.18	0.16	66.83
NM2	-14	0.70	44.57	6.22	0.70	44.58	6.16	43.74	0.70	0.00	44.58	0.01	6.19	0.04	63.59
NM2	-18	0.78	44.19	6.12	0.82	45.04	6.33	44.48	0.80	0.03	44.61	0.60	6.22	0.15	55.91
NM2	-22	0.77	46.55	6.21	0.78	46.69	6.23	43.56	0.78	0.00	46.62	0.10	6.22	0.02	60.07
NM2	-26	0.72	47.00	6.50	0.68	47.03	6.33	42.99	0.70	0.03	47.02	0.02	6.42	0.12	67.55
NM2	-30	0.68	46.51	6.41	0.69	46.46	6.53	43.65	0.68	0.01	46.49	0.04	6.47	0.09	68.16
NM2	-34	0.95	48.01	6.34	0.95	47.78	6.61	41.93	0.95	0.00	47.90	0.16	6.47	0.19	50.39
NM2	-38	0.66	44.32	6.01	0.67	44.34	6.23	43.46	0.66	0.00	44.33	0.01	6.12	0.16	66.81

Core	Depth	(N) %	(C) %	(H) %	(N) %	(C) %	(H) %	(O) %	Mean N	% var. N	Mean C	% var. C	Mean H	% var. H	CN
NM2	-42	0.79	46.64	6.35	0.78	46.86	6.38	43.57	0.79	0.00	46.75	0.16	6.37	0.02	59.55
NM2	-46	1.44	46.82	6.26	1.39	44.98	5.93	40.59	1.41	0.04	45.90	1.30	6.09	0.23	32.53
NM2	-50	0.73	45.94	6.12	0.72	45.96	6.10	43.48	0.72	0.01	45.95	0.02	6.11	0.01	63.56
NM3	0	0.68	45.61	6.61	0.66	44.80	6.48	46.17	0.67	0.01	45.21	0.57	6.54	0.10	67.67
NM3	-4	0.63	44.94	6.24	0.62	45.61	6.48	44.69	0.62	0.01	45.28	0.47	6.36	0.16	72.85
NM3	-8	0.60	44.19	6.32	0.58	43.14	6.15	45.57	0.59	0.01	43.66	0.74	6.24	0.12	74.26
NM3	-14	0.89	44.40	6.10	0.88	44.46	6.43	44.63	0.88	0.01	44.43	0.04	6.26	0.23	50.26
NM3	-18	0.98	47.59	6.46	0.99	47.33	6.54	42.49	0.99	0.00	47.46	0.19	6.50	0.06	48.18
NM3	-22	1.12	48.32	6.56	1.09	47.63	6.51	42.64	1.11	0.02	47.98	0.49	6.53	0.03	43.34
NM3	-26	0.91	45.84	6.40	1.00	47.20	6.37	43.51	0.95	0.06	46.52	0.96	6.39	0.02	48.79
NM3	-30	0.90	47.11	6.59	0.93	47.19	6.57	43.62	0.91	0.02	47.15	0.05	6.58	0.02	51.76
NM3	-34	0.99	46.35	6.44	1.01	46.49	6.58	43.57	1.00	0.01	46.42	0.09	6.51	0.10	46.49
NM3	-38	0.92	45.66	6.38	0.93	46.25	6.55	44.14	0.92	0.01	45.95	0.41	6.46	0.12	49.71
NM3	-42	1.10	47.64	6.05	1.07	48.00	6.46	42.66	1.09	0.02	47.82	0.25	6.25	0.29	43.93
NM3	-46	0.92	45.71	6.23	0.94	45.97	6.23	43.41	0.93	0.01	45.84	0.18	6.23	0.00	49.26
NM3	-50	0.97	46.09	6.13	0.97	46.34	6.24	43.37	0.97	0.01	46.22	0.17	6.18	0.08	47.69

** insufficient sample for replicate measurement

Acknowledgments

We stand on the shoulders of giants in any big thing we achieve in life – and nowhere is this more true than in the world of science. There are so many who have helped me along this journey. I would first like to thank the Swiss National Science Foundation, for providing the funding that made my work possible.

There are those who provided huge stepping stones that have led me to this point. To Ehimare Aigbivbalu – you taught an evening class in your spare time at a local community college after a long workday. You didn't have to take more time to stop me as I left class one night, and ask the story of a non-traditional student taking an intro environmental science course. You went the extra mile for me – and our conversation that evening sparked this entire journey. To my advisor at the University of North Texas, Dr. Paul Hudak: I had two classical music degrees and no strong science background when we met. Thank you for taking a chance on me, and allowing me the academic freedom to explore and plan my research as you advised me during the course of my masters degree. You helped me learn to think like a scientist.

To Agroscope and the members of the Climate and Agriculture group: thank you for our many thought-provoking conversations over coffee (and aperó beers). To Robin Giger – thank you for your help with elemental analysis and introducing me to the Py-GC/MS. You got me started with my measurements. To Markus Jocher, the "machine whisperer," all the hours of help with maintenance on the Py-GC/MS (the beast) are so dearly appreciated. You kept me up and running on the instrument, and I couldn't have done it without you.

I would also like to thank my co-authors, Miriam Groβ-Schmölders, Dr. Pascal von Sengbusch, and Dr. Judith Schellekens for their expertise, feedback, and support. To Judith: thank you for our many enjoyable skype sessions, and for introducing me to the world of principal component analysis. I've so enjoyed our collaboration and have learned so much from you.

I would like to extend my thanks to my advisors. Dr. Christine Alewell – thank you so much for the time and helpful feedback you've given me over the past four years! I'm grateful for it. Dr. Tim Moore, we were introduced in strange circumstances – overseas e-mails, and during a raging pandemic. And yet….you decided to serve as an external advisor for some Texan living across the Atlantic. Thank you for jumping into this adventure with me. Finally, to Dr. Jens Leifeld: I couldn't have done any of this without you. You answered my endless questions, guided me through so many roadblocks, provided so much assistance both with administrative and academic issues, and served as a fountain of knowledge over the last four years – and yet somehow, you did it all while smiling and laughing about everything along the way. Thank you for your patience, for your kindness and generosity, and for your lightheartedness. You made the hard times much more manageable, and I'm so thankful for your guidance.

To Anne-Lena: when you got a new American office-mate in 2017, I imagine that you might have been nervous about what it would be like. I was a loud, out-of-place Texan, but that was all just fine by you. We laughed together every day, and you quickly became my first real friend here in Switzerland. Were it not for you, I don't know that I would have lasted through those first few very difficult months. It can be hard to settle into a new country so culturally different from your own. You opened your heart, your life, and your home to me. I remain forever grateful for your friendship.

To my friends and family back home: I've missed so many events while living overseas – weddings, births, birthdays, Thanksgivings, and Christmases. Thank you so much for your patience and understanding - I miss and love y'all so much. Santos, it can be hard to keep up with friends with a six-hour time zone difference – but you made a point of making sure we stayed connected and never lost touch with each other. You checked in on me regularly during the hard times, and showed up with your party hat to celebrate during the good times. From our time at UNT together to now - I'm so grateful for your friendship all these years. To Kathy – thank you for our zoom sessions and for listening as I droned on about my research. Every card you've sent us has brightened my day. I feel so loved whenever we talk, and I'm so glad you're in my life. To my mom – thank you for believing in me, and for your endless enthusiasm for this adventure. Your support has been invaluable, and I couldn't have done any of this without you. Thank you for our daily phone calls –you have no idea how important they were to me. I love you.

Finally, to Mark: without your steadfast easy-going patience, I don't know where I'd be today. I'm so grateful for the hours of coding tutorials, advice, pep talks, and warm meals you've given me over the past two years. You supported me endlessly – and lovingly - while I wrote….and rewrote….and wrote some more. Life in Switzerland is so much better with you and Paco dog by my side. I love you so much.